MARINE MACROALGAE AS A SOURCE FOR BIOFUEL PRODUCTION

A thesis submitted to Goa University for the Award of the

Degree of

Doctor of Philosophy

in

Biotechnology

by

ALISHA CLAUDIA FERNANDES

Goa University

Taleigao Plateau, Goa

October, 2020

MARINE MACROALGAE AS A SOURCE FOR BIOFUEL PRODUCTION

A thesis submitted to Goa University for the Award of

the Degree of

Doctor of Philosophy

in

Biotechnology

by

Alisha Claudia Fernandes

Research guide: Prof. Usha D. Muraleedharan

Goa University

Taleigao Plateau, Goa

October, 2020

गोंय विद्यापीठ
ताळगांव पठार,
गोंय - ४०३ २०६
फोन : +९१-८६६९६०९०४८
फॅक्स : +०९१-८३२-२४५११८४/२४५२८८९

Goa University
Taleigao Plateau, Goa-403 206
Tel : +91-8669609048
Fax : +091-832-2451184/2452889
E-mail : registrar@unigoa.ac.in
Website : www.unigoa.ac.in

15 YEARS OF CELEBRATING THE MAHATMA

(Accredited by NAAC with Grade 'A')

CERTIFICATE

This is to certify that the research work presented in this thesis entitled **"Marine macroalgae as a source for biofuel production"** submitted by Ms Alisha Claudia Fernandes for the award of the degree of Doctor of Philosophy in Biotechnology is based on original studies carried out by her under my guidance and supervision at the Department of Biotechnology, Goa University, in partial fulfillment of the requirements of the degree, and that no part thereof has been presented for the award of any degree, diploma, associateship or other similar titles or recognition.

Dr. Usha D. Muraleedharan

(Research Guide)
Professor, Department of Biotechnology
Goa University, 403 206
Goa, India

Place: Goa University
Date: 30/10/2020

STATEMENT

As required under the University ordinance OB-9A, I hereby state that the present thesis entitled **"Marine macroalgae as a source for biofuel production"** is my original contribution and that the same has not been submitted on any previous occasion for any degree. To the best of my knowledge, the present study is the first comprehensive work of its kind from the area mentioned. The literature related to the problem investigated has been cited. Due acknowledgements have been made wherever facilities and suggestions have been availed of.

Alisha Claudia Fernandes

Place: Goa University

Date: 30/10/2020

Acknowledgement

Undertaking this PhD has been a truly life-changing experience for me and it would not have been possible without the support and guidance that I received from many people.

I would like to express my deepest gratitude to my research guide **Prof. Usha D. Muraleedharan** for her valuable and constructive guidance during the planning and development of this research work. As it is rightly said, "strive for excellence, not perfection"; my supervisor, whose pleasing attention to detail drove me to make every effort to offer quality in my research and writing of this thesis.

I take this opportunity to acknowledge **Prof. Varun Sahni**, the Vice-Chancellor, Goa University and **Dr. Satish Shetye** (former Vice-Chancellor) of Goa University for providing the necessary infrastructure and permission to carry out my research.

I express my sincere gratitude to the present and former Deans of faculty of Life sciences, **Prof. P.K. Sharma**, **Prof. M. K. Janarthanam** and **Prof. Saroj Bhosle** for their valuable guidance and encouragement.

A very special thanks to **Prof. S.G. Tilve** for his advice and support in his capacity as the Vice Chancellor's nominee.

I gratefully acknowledge the financial assistance received from University Grants Commission, India through the UGC-Maulana Azad National Fellowship for Minorities (2014-19).

I would like to offer my special thanks to the entire faculty of the Department of Biotechnology; **Prof. Sanjeev Ghadi** (Head of the Department), **Prof. Savita Kerkar**, **Prof. Urmila Barros** for their insightful questions, enthusiastic encouragement and useful critiques for this research work. I would also like to thank **Dr. Abhishek Mishra**, **Dr. Dhermendra Tiwari**, **Dr. Sanika Samant**, **Dr. Trupti Asolkar** and **Dr. Meghanath Prabhu** for their encouragement and suggestions.

The valuable assistance provided by the non-teaching staff of our department, **Late. Mr. Martinho, Mr. Serrao, Mr. Tulsidas, Mr. Ulhas, Mrs. Ruby, Mrs. Neelima, Mr. Parijat, Mr. Sameer, Mr. Rahul, Dr. Sandhya, Ms. Jaya** and **Mr. Ashish** is greatly appreciated. I would like to thank them for their kind help, ever willing support and encouragement throughout the tenure of my research. I would also like to thank **Mrs. Gulabi, Mrs. Kunda** and **Mrs. Manda** for ensuring a clean atmosphere at the workplace. Also, they have been kind, caring and have always uttered words of encouragement.

My sincere gratitude to **Dr. Anjan Ray**, Director, Council of Scientific And Industrial Research - Indian Institute of Petroleum (CSIR-IIP) who provided me permission to access their laboratories and research facilities. I am particularly grateful to **Dr. Thallada Bhaskar,** Head, Material Resource Efficiency Division (MRED), CSIR-IIP for permitting me to carry out the experiments at the prestigious institute. Without his valuable support and his continuous guidance it would not have been possible to conduct a major part of this research. My sincere thanks are extended to **Mr. Bijoy Biswas** for all the help rendered while carrying out my analysis at CSIR-IIP.

In my daily work I have been blessed with a friendly and cheerful group of fellow students. I would like to thank all my PhD colleagues; **Surya, Amruta, Shuvanker, Kirti, Imran, Preethi, Michelle, Srijay, Judith, Delicia, Nicola, Priti, Noha** and **Deepti** for their practical suggestions, helpful advice, unwavering support and motivation during the entire tenure of this research. My earnest thanks to **Priyanka, Samantha, Ruchira, Manasi, Pingal, Sreekala** and **Perantho** with whom I have shared moments of anxiety as well as great excitement. They were of immense support in deliberating over my problems and findings and their presence was very important in a process that is often filled with tremendous solitude. I wish to acknowledge my seniors **Kanchana, Asha** and **Lillian**, for helping me in numerous ways during various stages of my Ph.D.

I wish to express my gratitude to SAIF - IIT, Bombay for providing the facility for elemental analysis; CSIR - IIP, Dehradun, Dept. of Biotechnology and Dept. of Zoology, Goa University, for providing GC-MS facility to carry out FAME analysis.

I am thankful to my colleagues from the Dept. of Zoology, **Kiran**, **Megal**, **Rajeshwari** and especially **Praveen** and **Avelyno** for all the help and advice provided. I also whole heartedly acknowledge my colleagues from the Dept. of Chemistry and Dept. of Microbiology for the valuable help rendered.

I would also like to thank former M.Sc. students **Deepak**, **Biki** and special thanks to **Rajesh** for his help in sample collection at Goa Univeristy and his hospitality during my stay at Dehradun.

I am very grateful to my hostel friends. Their support and encouragement was worth more than I can express on paper.

I would like to offer my sincere thanks to my family and friends, who were of tremendous support throughout my Ph.D duration. They have always been a happy distraction to rest my mind outside of my research. I am also grateful to all those who have directly or indirectly helped me through their prayers and good wishes for the completion of my research work.

I remember all my teachers, staff and colleagues from St. Aloysius College, Mangalore. They have played an important role in moulding me into the person that I am today.

Finally, I thank the Lord Almighty to whom I owe my very existence, for providing me this opportunity and granting me the capability to proceed successfully. My beloved parents, brother and sister in law for being my motivation and for supporting me spiritually throughout writing this thesis and my life in general.

------- Alisha Claudia Fernandes

TABLE OF CONTENTS

Chapter I

General Introduction

The global demand for energy is continuously on the rise in recent years, due to increasing human population, urbanization and industrialization (Demirbas, 2007; Sharma and Singh, 2017; Berardi, 2017). The basic sources of energy are petroleum, natural gas, coal, hydro- and nuclear power (Source: U.S. Energy Information Administration, June 2020). There is heavy dependence on fossil fuels to meet the ever increasing energy requirements. It is expected that the world energy demand will be rising to 41% by the year 2035 (Source: BP, 2014). Energy can be widely categorized into three types: fossil fuel, nuclear (uranium and thorium) and renewable, of which approximately 80% of the world's primary energy demands are met by fossil fuels such as coal, petroleum crude oil and natural gas (Asif and Muneer, 2007). Petroleum is the largest single source of energy across the world, exceeding coal, natural gas, nuclear, hydro and renewables. One needs to critically attend to energy security because of the uneven distribution of the fossil fuel resources on which a good number of countries presently rely on. The Middle East is the dominant oil region of the world, accounting for 64.5% of global reserves (https://www.opec.org/opecweb/en/datagraphs/330.htm). The Kingdom of Saudi Arabia is often cited as the world's largest oil producer. The country produces 12% of the oil consumed daily in the entire world (https://www.investopedia.com/investing/worlds-top-oil-producers/). If, however, one takes into account the production of biofuels and liquid fuel from natural gases as well as shale oil production, the United States would be the largest crude oil producer (18%), followed by Saudi Arabia, Russia, Canada and China (Nejat et al., 2015; Source: U.S. Energy Information Administration, April 2020). The demand from the transport sector, which has a share of 30% of the world's entire energy consumption, is only likely to increase further, with the rising demand for transportation of goods and people (Asif and Muneer, 2007).

1.1. ENERGY SCENARIO IN INDIA

India is no exception with respect to the energy consumption which is on a logarithmic rise due to population and modernisation (Tripathi et al., 2016). India accounted for 7.9 % of the world's primary energy consumption in 2018 (BP, 2019a) and her share of the total global primary energy demand is set to rise to ~11% by 2040, underpinned by strong population growth and economic development (BP, 2019b). Being the third largest energy consumer in the world after the United States and China (http://www.eia.gov/countries/analysisbriefs/India

/india.pdf), India depends heavily on imported crude oil, mostly from the Middle East. Further, India's oil imports are anticipated to ascend to 6 million barrels per day by 2030, which would make her the third largest importer of oil. As per Ravindranath et al. (2011), nearly 30% of India's energy needs are met by oil, and more than 60% of that oil is imported. The fuel consumption in India in the transportation sector alone is expected to double by 2030 (Leduc et al., 2009). Diesel remains the most-consumed oil product, accounting for 39% of petroleum product consumption in 2015 and is used basically for commercial transportation and, to a lesser degree, in the industrial, electric power, and agricultural sectors (Source: U.S. Energy Information Administration, September 2020).

1.2. THE NEED FOR RENEWABLE ENERGY

The prolonged and intensive use of fossil fuels has led to a decline in the fossil fuel reserves, besides causing emission of harmful air pollutants such as sulfur and nitrogen oxides, carbon monoxide and suspended particulate matter (Sudhakar et al., 2018). Fossil fuel combustion produces more amount of carbon dioxide (about 98%) than any other anthropogenic activity (Goldemberg, 2000). This leads to environmental degradation, a direct threat to human health and quality of life, while also affecting the ecological balance and biological diversity (Demirbas, 2008b; Jung et al., 2013). Fossil fuels are hence now considered unsustainable and the situation has provoked a need to reduce their use, look for new cleaner sources of energy, and develop alternative fuels which are renewable and inexhaustible. Such measures would also help in reducing greenhouse gases (GHGs), particularly carbon emissions stemmimg largely from fossil fuel combustion (Vassilev and Vassileva, 2016). Renewable energy being derived from natural sources such as biomass energy, solar energy, wind power and geothermal energy, is plentiful, unlimited and widely available. Being clean and environmentally secure, it is understandably widely accepted as a promising replacement to fossil fuels. The use of such sources can contribute to long term sustainable energy supplies, help mitigate pollution by decreasing atmospheric emissions of CO_2 and also generate employment opportunities (FAO, 2011). Renewable energy at present contributes to only 13.5% of the total energy needs but renewable resources are distributed more uniformly all over the globe than fossil and fissile energy sources; energy flows from renewable energy

sources are more than three times higher than the current energy use worldwide (Demirbas, 2008b; Gaurav et al., 2017).

1.2.1. Biomass as a Renewable Energy Source

The most prevalent source of renewable energy is biomass. Biomass (Greek, bio, life + maza or mass) is biological material derived from living or recently living organisms. It mostly refers to plants or plant-based materials which are exclusively called ligno-cellulosic biomass. Examples of biomass resources include firewood, wood chippings, agricultural residues, animal wastes, aquatic biomass, agricultural crops and their waste by-products and even municipal wastes. Biomass has been listed as the fourth largest available energy resource of the world, after coal, oil and natural gas (Hall et al., 1992; Ladanai and Vinterback, 2009). Biomass composition includes celluloses, hemicelluloses, lignin, lipids, proteins, simple sugars, starches, water, hydrocarbons, ash, *etc*. Extensive research has been carried out on the use of plant biomass as an alternate energy source, it being a renewable resource and fixing CO_2 in the atmosphere through photosynthesis (Moser, 2009; Ho et al., 2014). Aquatic biomass, which includes algae, is considered better in relation to terrestrial plants in terms of solar energy storage, nutrient assimilation and potential for biofuel production, on account of its higher photosynthetic efficiency, higher growth rate and productivity (Lardon et al., 2009). Biomass is known to contain only very small amounts of sulfur and nitrogen, which would result in lesser emission of their oxides compared to thermal power plants. Also, the use of biomass as an energy source is generally considered completely carbon neutral because the CO_2 released during combustion or conversion of biomass into chemicals merely replaces that removed from the environment by photosynthesis during the production of biomass (Goldemberg, 2000).

1.3. BIOFUELS

Biofuels are liquid or gaseous fuels chiefly produced from biomass. They are predominantly used in vehicles but can also be utilized in engines or fuel cells for generation of electricity. Being carbon neutral and renewable, they could serve as a replacement for petroleum fuels (Demirbas, 2010; John et al., 2011; Sirajunnisa and Surendhiran, 2016), with slight engine

modifications or even as they are. They promote sustainable development by virtue of being biodegradable and environmentally friendly.

Biofuels are generally categorized by source, type and generation. They are mainly categorized either as primary biofuels (firewood, agro-residues, organic material) that are made use of directly in an unprocessed form or as secondary biofuels (charcoal, ethanol, biodiesel, bio-oil, biogas) that are processed from biomass. They could be in solid form (wood, charcoal), liquid form (bioethanol, biodiesel, bio-oil) or gaseous form (biogas, syngas). In research, biofuels are additionally classified into first, second, third and fourth generations, based on the biomass feedstocks and the processing technology (Noraini, et al., 2014; Ullah, et al., 2015). Various sources of biomass are used for production of biofuels, the energy output after conversion being considerably dependent on the type of biomass used.

1.3.1. First Generation Biofuels

These are produced from edible crops such as sugarcane, rapeseed, soybean, corn, palm, *etc*. These crops are used for their starch, sugar, and/or oil content which is converted to biofuels using different processes. The largest amount of biofuel is produced in the form of ethanol, 80% of which has come from corn and sugarcane (Dutta et al., 2014). The use of food crops for biofuel is, however, debatable since it competes with food supply. Besides, food crops need large amount of land and water. Extensive cultivation of certain food crops also raises concerns regarding pollution of agricultural land and damage to the environment due to their requirement of fertilizers and pesticides (Chiu et al., 2009). Moreover, substitution of food crops as energy crops also results in an increase in food price, imposing a burden primarily on the economically backward sectors of the population. In the present scenario of a rapidly increasing population, the main query that rightly arises is whether to use food crops for the production of biofuels or rather to meet the nutritional demands of the increasing population (Hong et al., 2014). As much as a decade ago, Brennan and Owende (2010) had recorded that almost 1% (14 million hectares) of the world's available agricultural land was being used for the production of biofuels, providing 1% of global transport fuels.

1.3.2. Second Generation Biofuels

These are produced from feedstock comprising lignocellulosic biomass such as woody biomass, tall grasses (Swichgrass), *Jatropha*, *etc*. These biofuels exhibit advantages over the first-generation ones because they do not compete with food supplies and generally have higher yield and reduced land requirements. Transportation difficulties, high downstream processing costs, moderate reduction of the GHG and a low net energy yield would, however, restrict their use (Carriquiry et al., 2011). Most energy crops of the first and second generation not only threaten the availability of adequate food supply but also impinge on arable land for their cultivation, besides consuming quantities of water and fertilizer for their growth.

1.3.3. Third Generation Biofuels

These are produced from aquatic biomass such as algae (microalgae and macroalgae) and are widely researched as a potential workable alternative energy source that may overcome the major shortcomings associated with first and second generation biofuels. Algae are considered the only alternative to food crops for renewable fuel production as they contain energy rich lipids and carbohydrates (Sirajunnisa and Surendhiran, 2016). Various advantages of algae are notable, such as high biomass yields, low lignin content, high efficiency CO_2 mitigation, no requirement of any arable land (unlike land crops) and being amenable to cultivation in waste or salt water. One drawback of the third generation biofuels is that the biofuel produced from these sources has certain limitations in terms of ecological footprint, economic performance, dependence on environment (sunlight) and geographical location (latitude), which accounts for its research still being in its infancy (Pienkos and Darzins, 2009). Besides, due to high production costs the positive features of algae-based fuel production are far from adequate as of now, as a tenable alternative to replace fossil fuels.

1.3.4. Fourth Generation Biofuels

Metabolic engineering of algae for production of biofuel from oxygen producing photosynthetic microorganisms is considered as fourth generation biofuel and has great potential in providing sustainable and clean energy (Lu et al., 2011). These next-generation biofuels take a step further to create ultra-clean carbon-negative biofuels, together with carbon sequestration.

They are expected to be carbon negative both at the level of the raw material and of process technology (Vassilev and Vassileva, 2016; Ziolkowska, 2020).

1.3.5. Advantages of the Use of Biofuel

One main difference between biofuels and petroleum fuels lies in the oxygen content. Oxygen levels of biofuels are in the range of 10-45% while petroleum has virtually no oxygen. The chemical properties of biofuels are hence different when compared with petroleum fuels (Demirbas, 2009). The advantages of biofuels over petroleum fuels are that they can be converted from easily available biomass sources, are carbon neutral, biodegradable, sustainable and more environment friendly. As biofuel has its own merits towards an eco-friendly environment, its effective contribution in the transportation sector will lead to increase in its share in the automobile market and herald a rapid growth in the near future (Demirbas, 2008a). Biofuel has in a way been accepted as a potential alternate fuel in the future transportation development. 'Green' biofuel has already found its position in the economy of developing countries such as China and India, partly curtailing the rapid rise in oil prices of fossil fuels (Ullah et al., 2015).

1.4. THE NATIONAL POLICY ON BIOFUELS, 2018

The National Policy on Biofuels was created by the Ministry of New and Renewable Energy (Govt. of India) during the year 2009 in order to promote biofuels in India. Worldwide, biofuels have been gaining prominence in the last few years and it is necessary to keep up with the pace of development in this field. Biofuels in India are of strategic importance as they would provide good opportunities to generate employment, develop income for farmers, reduce imports, manage waste, *etc*. The Biofuels programme in India has been primarily affected due to the limited availability of domestic feedstock for biofuel production, which needs to be without delay.

The Union Cabinet headed by the Prime Minister Shri Narendra Modi approved the National Policy on Biofuels, 2018 ("Policy") on the 16th of May 2018. (http:// petroleum. nic.in /sites/ default/ files/biofuelpolicy2018_1.pdf). The Policy groups biofuels as "Basic Biofuels" *i.e.*, First Generation bioethanol & biodiesel and "Advanced Biofuels" *i.e.* Second Generation

ethanol, Municipal Solid Waste (MSW) to "drop-in" fuels, Third Generation biofuels, bio-CNG, *etc*, to permit extension of suitable financial and fiscal incentives under each group. The Policy expands the scope of raw material for ethanol production by allowing the use of sugarcane juice, sugar containing materials (such as sugar beet, sweet sorghum), starch containing materials (like corn and cassava), damaged food grains (like wheat, broken rice and rotten potatoes unfit for human consumption), for ethanol production. Farmers are at a risk of not getting appropriate price for their produce during the surplus production phase. Considering this, the Policy allows use of excess food grains for production of ethanol for blending with petrol, with the approval of the National Biofuel Coordination Committee. With a focus on Advanced Biofuels, the Policy indicates a viability gap funding scheme for 2G ethanol Bio refineries of Rs.5000 crore in 6 years, over and above additional tax incentives, and higher purchase price as compared to 1G biofuels. The Policy also encourages setting up of supply chain mechanisms for biodiesel production from non-edible oilseeds, used cooking oil and short gestation crops. Finally, the roles and responsibilities of all the concerned Ministries/Departments with respect to biofuels have been captured in the Policy document to synergize efforts. The expected benefits of the policy are to reduce import dependency, provide a cleaner environment, manage municipality solid waste and create infrastructural investment in rural areas. It would also provide health benefits in a way, such as by diverting the use of used cooking oil to produce biodiesel rather than reusing it in the food industry. Additionally, the policy would lead to employment generation and create additional income to farmers.

1.5. ALGAL BIOMASS AS A BIOFUEL SOURCE

In 1970, the Aquatic Species Program directed the focus of their research to producing biodiesel from high lipid content algae. The concept of using algae as a source of fuel is thus not new but is rather gaining prominence because of the increasing price of petroleum and more significantly, the emerging concern about global warming that is connected with combustion of fossil fuels. Algae have therefore received great attention as a novel resource to produce biofuels (Vassilev and Vassileva, 2016). They are aquatic photosynthetic organisms that grow rapidly on saline water, coastal seawater, municipal wastewater or on land unsuitable for agriculture and farming (Chen et al., 2015c; Pittman et al., 2012). Algae-based

fuels are considered the most sustainable, renewable, effective and environment friendly response to climate change and food security, besides being a promising renewable energy resource on the horizon, with the capacity to meet long-term global demand for fuels.

1.5.1. Biomass Conversion Technologies

The main routes for biofuel production from algae can be divided into two categories, *viz.*, biochemical and thermo-chemical conversion (TCC) technologies. Of the two, thermochemical conversions are generally much quicker (Gollakota et al., 2018) but not until recently have they been given attention in an effort to meet the rising energy demands worldwide as well as address the environmental problems due to conventional fossil energy production and utilization. The type of biofuel obtained and its mass fraction from the original feedstock is directly influenced by the conditions used in the thermochemical process (Tian et al., 2014).

The primary biomass TCC technologies are gasification, supercritical fluid extraction, pyrolysis and hydrothermal liquefaction:

a) Gasification

Gasification converts biomass into combustible gas mixture at elevated temperatures *i.e.*, above 700°C (Osada et al., 2006). The biomass reacts with oxygen and steam to generate syngas, a mixture of hydrogen, carbon monoxide, carbon dioxide and methane. Although it is considered a flexible process in relation to the types of biomass it can convert, syngas is a low calorific gas (typical 4-6 MJ m^{-3}) that can be burnt directly in gas engines and gas turbines (Brennan and Owende, 2010) or has to be converted to fuel *via* a secondary process such as Fischer-Tropsch synthesis (Dimitriadis and Bezergianni, 2017).

b) Supercritical Fluid Extraction (SFE)

This is a process for separating two components by using supercritical fluids as the extracting solvent. Applications of SFE include bioseparations, petroleum recovery, crude de-asphalting and dewaxing, coal processing, selective extraction of fragrances, oils and impurities from agricultural and food products, *etc*. (Sapkale et al., 2002). The use of high pressures, however, leads to high operational and capital costs for SFE plants.

c) Biomass pyrolysis

Pyrolysis is defined as thermal degradation of dry biomass by heat, in the absence of oxygen, resulting in the production of charcoal (solid), bio-oil (liquid), and fuel gas products. Pyrolysis technologies are often classified by their heating rate, with rates of 0.1-1 °C/s referred to as slow pyrolysis, 10-200 °C/s as fast pyrolysis, and >1000 °C/s as flash pyrolysis (Demirbas and Arin, 2002).

d) Hydrothermal liquefaction

Hydrothermal liquefaction (HTL) of biomass is the thermochemical conversion of biomass into liquid fuels, carried out in a hot, pressurized water environment in the absence of oxygen at high temperatures (280-370 °C) and operating pressures (5-25 MPa) (Behrendt et al., 2008; Anastasakis and Ross, 2011; Elliot et al., 2015; Gollakota et al., 2018). The HTL process produces a water-insoluble, hydrocarbon-rich liquid biocrude with a relatively elevated higher heating value (HHV) as the main product, besides aqueous, gaseous, and solid phase by-products. Reactors for thermochemical liquefaction are complex and therefore expensive, but have an important advantage in their ability to convert wet biomass into energy.

Pyrolysis and HTL are two widely researched comparable technologies, as they both render bio-based intermediate products (often referred to as bio-oils or biocrude). Dried feedstock is the most important requirement for the pyrolysis process, while it is not necessary in the case of liquefaction, such that the cost of fuel production is reduced to a large extent due to the wet nature of the selected feeds such as algae. Besides, the bio-oil produced through HTL appears to have lower oxygen and nitrogen content, higher energy value and better stability properties than that obtained by pyrolysis (Xu et al., 2014b; Barreiro et al., 2013). Finally, the lower operating temperature, high energy efficiency and low tar yield compared to pyrolysis are major parameters that render the HTL technology more competitive for biomass conversion to fuel products than pyrolysis (Gollakata et al., 2018).

1.6. TYPES OF ALGAL BIOFUELS : BIODIESEL AND BIO-OIL

The two main routes to produce liquid biofuels from algae are biodiesel *via* extraction and transesterification and bio-oil *via* pyrolysis or HTL. The reliance on lipid content in the

macroalgae is a major distinction in the production of macroalgal biodiesel as against HTL-based macroalgal bio-oil (Chisti, 2007; Brennan and Owende, 2010), and is a decisive parameter while screening suitable candidates for biodiesel production. During HTL, on the other hand, the entire algal biomass inclusive of all organic components gets converted to biocrude oil (Vardon et al., 2012), and it is an ideal process for converting wet biomass, including low-lipid algae, into biocrude oil. Solvent extraction is another key requirement in extracting out the lipids for biodiesel production whereas for HTL, water is majorly used as a solvent as well as a reactant (Akiya and Savage, 2002). High-lipid algae may however, require simpler processes for post-HTL oil upgrading and refining than other algal species (Tian et al., 2014).

1.6.1. Biodiesel

Biodiesel is a mixture of monoalkyl esters of fatty acids, produced from renewable biological sources such as vegetable oils or animal fats using a transesterification reaction in the presence of a catalyst (Marchetti et al., 2007; Vyas et al., 2010). Biodiesel is referred to as B100 or "neat" fuel. Pure biodiesel blended with petrodiesel is termed "biodiesel blend". Biodiesel blends are referred to as BXX; the XX designates the amount of biodiesel in the blend (*i.e.*, a B20 blend is 20% biodiesel and 80% petrodiesel). The most common biodiesel blends are B5 (upto 5% biodiesel blend), and B20 (upto 20% biodiesel blend). B100 is used as blendstock to produce lower blends and hardly used as a transportation fuel as such (Moser, 2009; Knothe, 2010).

1.6.1.1. Historical background of biodiesel

The famous German inventor Rudolph Diesel (1858-1913) designed the original diesel engine in the 1890s. The working of the diesel engine is based on the principle of compression ignition, in which fuel is introduced into the engine's cylinder by injection after air has been compressed to a high pressure and temperature. As the fuel enters the cylinder it self-ignites and burns quickly, forcing the piston back down and converting the chemical energy in the fuel into mechanical energy. Dr. Rudolph Diesel, after whom the engine is named, has the first patent for the compression ignition engine, issued in 1893. Diesel became known worldwide for his innovative engine which had an advantage over petrol engines in that it could run on

fuels derived from various sources including vegetable oils. The first public demonstration of vegetable oil based diesel fuel was at the Paris Exposition in 1900, where Diesel demonstrated a diesel engine running on peanut oil and this invention led to him winning the grand prix, the biggest prize at the Exposition (Backhaus, 2017). The French government had assigned the Otto Company to build a diesel engine to run on peanut oil as it was attracted to the use of vegetable oils as a domestic fuel for their African colonies. Rudolph Diesel later carried out intensive work on vegetable oil fuels and became a top promoter of such a concept, believing that diesel engines running on plant oils had strong potential and envisioned that these would be as important as petroleum-based fuels. In a speech as early as in 1912 he had stated that "the use of vegetable oils for engine fuels may seem not important today. But such oils may in the course of time become as important as petroleum and the coal products of present time." According to the history of biodiesel fuel, Rudolf Diesel's primary engine model worked on its own power for the first time in Germany in 1893. The 10th of August has therefore been announced as "International Biodiesel Day" to respect and remember this event (Knothe, 2005a).

In 1853 scientists E. Duffy and J. Patrick carried out transesterification of vegetable oils into methyl esters for the first time (Demirbas, 2008a). This was however, much before the first diesel engine even became functional. Despite the widespread use of petroleum fuels, scientists in many countries still continued to experiment during the 1930s and the World War II, trying to create workable diesel fuel for internal combustion engines. There were preliminary operational problems due to the high viscosity of vegetable oils as compared to petroleum diesel fuel. The concept of biodiesel was proposed for the first time in 1937 when a Belgian scientist G. Chavanne was granted a patent for a "*Procedure for the transformation of vegetable oils for their uses as fuels*" (Belgian Patent 422,877). This patent illustrates the alcoholysis of vegetable oil (palm oil) using ethanol (Knothe, 2005a). This almost certainly is the first case of the production of what is widely known as "biodiesel" today. The process of transesterification converts vegetable oil into alkyl esters which are much less viscous and easy to burn in a diesel engine. The transesterification reaction is the basis for the production of modern biodiesel, which has become the trade name for fatty acid methyl esters (FAMEs). More recently, in 1977 a Brazilian scientist Expedito Parente applied for the first patent for "industrial process for biodiesel". An Austrian company founded the first biodiesel pilot plant

and industrial scale plant, Gaskoks in 1987 and 1989, respectively (Mojifur et al., 2012). Shortly after, the first "biodiesel standard" was issued in 1991 and in 1997 a German standard (DIN 51606) was released. The first ASTM D6751 was published in the year 2002. In October 2003, a new biodiesel standard DIN EN14214 was published in Europe. In September 2004, the state of Minnesota in USA started the sales of diesel fuel that contained 2% biodiesel. The month of October 2008 saw the publication of the first biodiesel blend specification standard ASTM. The present version of the European standard EN 14214 was published in November 2008 (Mahmudul et al., 2017).

1.6.1.2. Benefits of biodiesel

Biodiesel is renewable, environmentally friendly, carbon neutral (Chisti, 2008) and an efficient, clean, 100% natural energy alternative to petroleum fuels (Mahmudul et al., 2017). It is superior to diesel in terms of sulfur content, flash point, aromatic content (Bala, 2005; Knothe et al., 2015), higher cetane number and higher biodegradability (Bozbas, 2008; Sharma et al., 2008). It has better lubricant properties than petrodiesel. Its oxygen content improves the combustion process, leading to a decreased level of tailpipe polluting emissions (Moser, 2009; Karmakar et al., 2017) and qualifying it as less polluting than conventional petroleum diesel fuel. The oxygen content also makes its degradation about four times quicker than petrodiesel (Demirbas, 2007). Biodiesel can be used in any compression ignition (diesel) engine and essentially requires little or no minor engine modifications because its properties are similar to those of mineral diesel (Aresta et al., 2005b). Its usage reduces GHG emissions. The risks of handling, transporting and storing biodiesel are much lower than those associated with fossil diesel. Taken as a whole, biodiesel would help to reduce a country's dependence on crude oil imports and also support agriculture by providing new opportunities for employment and market for domestic sources.

1.6.1.3. Problems associated with biodiesel

Certain disadvantages of biodiesel have also to be looked into, such as its slightly higher viscosity, higher cloud point and pour point, lower energy content, higher nitrogen oxide (NO_x) emissions, injector coking, engine compatibility, and greater engine wear. The industrial disadvantages of biodiesel blends include issues with freezing of fuel in cold

climates, reduced energy density, and fuel degradation under longer periods of storage. Engines which have used pure hydrocarbon fuels for a long time face problems when subjected to biodiesel use. Hydrocarbon fuels frequently form a layer of deposits on the inside of tanks. When biodiesel blends are used, it causes loosening of these deposits, causing them to block the fuel filters. However, proper filter maintenance following introduction of the biodiesel blend can ease this problem (Wardle, 2003).

1.6.1.4. Sources of biodiesel

Biodiesel is produced from a variety of sources (Karmakar et al., 2010). Edible crops (first generation crops) such as soybean (Santos et al., 2013), rapeseed (Mazanov et al., 2016), castor (Meneghetti et al., 2006), palm (Johari et al., 2015) and sunflower (Bastianoni et al., 2008; Lang et al., 2001) have been studied for biodiesel production. Non-edible crops (second generation crops) such as rubber seed (Morshed et al., 2011), cotton seed (Onukwuli et al., 2017), *Jatropha*, soapnut (Achten et al., 2008; Chhetri et al., 2008; Kartika et al., 2013) and *Pongamia* (Babu et al., 2009) have been identified as potential sources. Other feedstock *viz*., low cost oils and fats such as beef tallow (Taravus et al., 2009), restaurant waste frying oil (Encinar et al., 2007; Kulkarni and Dalai, 2006) and animal (poultry) fats (Moreira et al., 2010) can also be converted into biodiesel. Different countries have completely different potential biodiesel feedstock. For example, soybean is the primary source for biodiesel production in the US and Brazil whereas rapeseed is the most common source in Europe. Palm oil is a significant source of biodiesel in Indonesia while in India and Southeast Asia, *Jatropha* has been an important source. More recently, microalgae have gained attention to be among the third generation of biodiesel sources and species such as *Chlorella protothecoides* (Xu et al., 2006), *Nannochloropsis oculata* (Umdu et al., 2009), *Chlorella zofingienesis* (Liu et al., 2010), *Scenedesmus abundans* (Mandotra et al., 2014) and *Botryococcus braunii* (Hidalgo et al., 2016) have been researched on.

According to some estimates, the yield (per acre) of oil from algae is over 200 times that from the best-performing plant/vegetable oils (Sheehan et al., 1998). While the majority of algal biodiesel research to date has focused on strain selection and optimizing the productivity of microalgae (Demirbas, 2010; Halim et al., 2011; Beetul et al., 2014; Nelson and Viamajela,

2016), macroalgae also have been proposed both as feedstocks for diverse biomass applications and as targets for liquid and solid fuel production. Till date, a small number of studies have analyzed and reported the potential of marine macroalgae as a source for biodiesel. Earliest studies on biodiesel were reported by Aresta et al. (2005b), which focused on comparison of supercritical CO_2 extraction and thermochemical liquefaction for biodiesel production from a green alga *Chaetomorpha linum*. Attempts were made to produce biodiesel from brown macroalgae such as *Sargassum tenerrimum* (Khan et al., 2017; Kumari et al., 2011) and *P. tetrastromatica* (Ashokkumar et al., 2017). Red macroalgae such as *Chondrus crispus* (Cancela et al., 2012) and *Hypnea musciformis* (Martins et al., 2012) have been studied and the green macroalgae *Enteromorpha compressa* (Suganya et al., 2014a), *Ulva lactuca* and *Ulva intestinalis* (Abomohra et al., 2018) have been reported as potential macroalgal sources for biodiesel production. Studies had been carried out using freshwater macroalgae *Oedogonium* and *Spirogyra* (Hossain et al., 2008) for production of biodiesel but the yields were low. Khola and Ghozala (2012) found that *Cladophora* proved a better source than *Spirogyra* and *Oedogonium*. In yet another study by Ahmed et al. (2010), biodiesel was obtained from *Spirogyra, Cladophora* and the marine macroalga *Gracilaria*, and engine performance experiment results showed improved fuel consumption efficiency with increase in the percentage of biodiesel blend. Borghini et al. (2012) evaluated the lipid content for producing biodiesel from *Chaetomorpha linum*, *Gracilariopsis longissima* and *Ulva lactuca*, macroalgae hitherto considered a 'waste bio-mass'.

Several studies have been conducted on pretreatment of macroalgae for oil extraction. In a study carried out by Bharathiraja et al. (2016), ultrasonication emerged as the pretreatment of choice for improved yields from the macroalgae *Gracilaria edulis, Enteromorpha compressa* and *Ulva lactuca*. In another study on *Ulva lactuca* (Suganya and Renganathan, 2012), optimization of extraction parameters was performed and better oil yield obtained from sonicated samples with a maximum 5% moisture content, and using a solvent composite of 1% diethyl-ether and 10% methylene chloride in n-hexane. Optimization studies using a variety of polar and nonpolar solvent combinations have been carried out to enable maximal yield of lipids from macroalgae such as *Enteromorpha intestinalis* (Jeong and Park, 2015), *Ulva fasciata, Gracilaria corticata, Sargassum tenerrimum* (Kumari et al., 2011), *Cystoseira indica* and *Scinia hatei* (Khan et al., 2015).

Attempts have been made to optimize the time required for lipid extraction (Suganya and Renganathan, 2012). Cancela et al. (2012) attempted direct microwave-assisted extraction and transesterification and found it feasible for the production of biodiesel from *Chondrus crispus*, *Himanthalia elongata* and *Undaria pinnatifida*. In a study by Suganya et al. (2013) *Enteromorpha compressa* was used to produce biodiesel using a two-step acid-alkali transesterification method which provided a maximum yield of 90.6%. This work was further improved upon, wherein a rapid *in situ* transesterification was reported as a suitable technique to produce biodiesel from *Enteromorpha compressa* with a methyl ester yield of 98.89% (Suganya et al., 2014a). Ultrasonic-assisted acid-base transesterification was carried out on the oil of a green macroalga *Caulerpa peltata* (Suganya et al., 2014b). Alkali catalysis by NaOH has been used for transesterification of oil from marine macroalgae *Fucus spiralis* and *Pelvetia canaliculata* (Urrejola et al., 2012). Martins et al. (2012) compared various extraction and transesterification methods for fatty acid content of *Hypnea musciformis, Sargassum cymosum* C. Agardh and *Ulva lactuca* L. using the method of Bligh and Dyer (1959). The fatty acid content of the three species of seaweeds significantly varied when extracted and transesterified by different methods. Furthermore, the best method for one species was not the same for another species.

In a first study of its kind, Xu et al. (2014a) described an efficient system for lipid production by oleaginous yeast using carbon sources derived from a brown macroalga, *Laminaria japonica* to produce biodiesel, the maximum lipid content obtained being 48.3%. More recently, waste industrial products have been used as catalysts to produce biodiesel from *U. fasciata* (Khan et al., 2016), with noteworthy results. A study by Maceiras et al. (2016) reported the production of biodiesel from *Fucus spiralis* and *Pelvetia canaliculata* by direct transesterification, avoiding a prior step of oil extraction. Statistical tools such as Response Surface Methodology (RSM) have been used to optimize variables for predicting the best conditions for obtaining maximal lipid, biodiesel yield and storage characteristic, from macroalgae such as *Chara vulgaris* (Siddiqua et al., 2015) and *Sargassum myriocystum* (Renita et al., 2014). Some have reported the non-suitability of macroalgae as a major source of lipids as the yields are lower than from microalgae or other crops. Comparative study on oil production from macroalgae *Gracilariopsis longissima* and *Chaetomorpha linum vs* sunflower showed that the production of oil from sunflower seeds was more feasible than from

macroalgae (Bastianoni et al., 2008). Shalaby et al. (2010) carried out comparative studies on biodiesel production from different varieties of macroalgae: four rhodophytes, one chlorophyte and one phaeophyte, which gave very low yields in comparison to the green microalga *Dictyochloropsis splendida*. El Maghrabhy and Fakhry (2015) analyzed the lipid content and fatty acid composition of Mediterranean macroalgae *Jania rubens* (Rhodophyta), *Ulva linza* (Chlorophyta) and *Padina pavonica* (Phaeophyta) using chloroform/methanol solvent system and interpreted that seaweeds as a whole were not feasible for production of biodiesel.

Macroalgae are widely available but remain an underutilized biomass resource. There are few studies on macroalgal biofuel production in both academia and industry and based on the current knowledge it is not possible to make a full-scale assessment for producing economically efficient biofuels. Hence, more time and effort are required to explore this resource. Biofuel technologies would still require considerable research and development. The technologies used need to be evaluated for technical feasibility, economic efficiency as well as environmental impact and the byproducts has to be recycled. Macroalgal farming has the potential to generate added socio-economic benefits to coastal communities in tropical regions.

1.6.2. Bio-oil

The HTL process converts algal biomass to produce a dark and viscous, energy-dense liquid product called bio-oil along with gaseous, aqueous and solid phase by-products (Barreiro et al., 2013; Han et al., 2019). The physico-chemical properties of bio-oil depend on feedstocks and HTL parameters (Vardon et al., 2011). The HHV of the bio-crude oil is in the range of 30-38 MJ/kg (Muppaneni et al., 2017; Neveux et al., 2014b; Vardon et al., 2012). Bio-oil is known to have an energy content about 70-95% of that of petroleum crude (Tian et al., 2014; Brown et al., 2010). It constitutes a complex mixture of a large number of compounds with a wide range in molecular weight. Algal bio-oil obtained via HTL would need to be upgraded (Duan and Savage, 2011), mainly to remove oxygen and nitrogen, before it can be used as a transportation fuel. The HTL processing can be applied to various types of algae, without

restriction to high-lipid sources (Elliot et al., 2015). The overall aim in HTL is to generate a product with a higher energy density by removal of oxygen (Elliot et al., 2015).

1.6.2.1. Historical background of the HTL process

Direct biomass liquefaction was the terminology used for HTL in the 1970-1980s (Elliot, 2015). Research on HTL had already begun in the early 1940s using terrestrial biomass, but this technology gained significance only after the oil crisis of 1973, as an alternative for biofuel production. Pioneering work on HTL was done at the Pittsburgh Energy Research Center in the 1970s, by Appell and coworkers (Toor et al., 2011). The HTL process consisted of converting dried wood to an anthracene oil at 300-370 °C in the presence of a catalyst (Na_2CO_3) and reducing gas (CO/H_2). However, major technical problems were encountered during the running of the plant, due to feedstock feeding, undissolved solids and an increase of medium viscosity. These problems were then taken up by the Lawrence Berkeley Laboratories (LBL) (Schaleger et al., 1982; Thigpen et al.,1982) from Berkeley, California where they carried out a pretreatment by acid hydrolysis of the feedstock (wood) prior to its liquefaction. The pretreatment at 180 °C for 45 min weakened the lignocellulosic material. A water/wood slurry was then prepared and the pH adjusted to 8 using the catalyst Na_2CO_3. This must have required a large amount of catalyst due to the low pH of the substrate. The subsequent wood slurry liquefaction lasted for 10-60 min at a temperature of 340 °C (Bouvier et al., 1988; Stevens, 1994). Both processes were demonstrated in a pilot plant in Albany, Oregon. But again, due to the innumerable mechanical problems, the research was halted by the US Department of Energy in the early 1980s as the price of petroleum dropped and interests shifted to fuel additives, such as ethanol. In the 1980s, the Shell Laboratory in Amsterdam developed the Hydrothermal Upgrading (HTU®) process as a reaction to the oil crises of 1973 and 1980. The research was again halted soon due to unfavorable economic conditions in 1988. In 1997, with support from the Dutch Government, a consortium with Shell Netherlands and Stork Engineers & Contractors as the main partners started an R&D program and resumed the process. Again, the introduction of the feed in the reactor was a critical issue, as well as the heating of the reactants and the treating of the effluent water. A pilot plant had been erected, with the aim of producing sufficient technical and economic data to study the feasibility of a commercial demonstration plant, which is yet to see the light of the day (Toor

et al., 2011). In the HTU pilot plant a number of different biomasses (also with high moisture content) were liquefied under high-pressure (Feng et al., 2004). The biomass was suspended and pumped into the reactor using a high pressure pump. In the eighties, the US Environmental Protection Agency's (EPA) Water Engineering Research Laboratory at Ohio developed a prototype sludge-to-oil reactor system (STORS) capable of processing undigested municipal sewage sludge with 20% solids at a rate of 30 L/h. Approximately 73% of the energy content of the feedstock was recovered as combustible products (oil and char), suitable for use as a boiler fuel. Subsequently, several other applications of so-called STORS processes have emerged. In 2001, a STORS demonstration project sponsored by the US-EPA was successfully completed, converting raw sewage sludge to oil at a plant located in California. The technology was further developed by a company called Thermo Energy (Adams et al., 2004) but the updated status is unavailable. Currently, technology companies such as Licella/Ignite Energy Resources (Australia), Altaca Energy (Turkey), Steeper Energy (Denmark), and Nabros Energy (India) continue to explore the commercialization of HTL.

1.6.2.2. Sources for bio-oil production

A considerable number of studies on HTL of various biomasses have been carried out. Lignocellulosic biomass (also known as woody biomass) such as pinewood (Liu and Zhang, 2008), beechwood (Tekin et al., 2012) and swichgrass (Wei et al., 2014) have been examined for their suitability for bio-oil production, resulting in promising yields. Yin et al. (2010) used cattle manure and upon optimizing the HTL conditions, a maximum bio-oil yield of 38.49 wt.% was obtained at 310 ^{o}C. Sewage sludge from wastewater treatment plants (Zhai et al., 2014) and waste plastics (Williams et al., 2007) have been effectively tested as feedstock for biocrude production *via* HTL, with excellent results.

Several studies have investigated the characteristics of algal biomass as a feedstock (Xu et al., 2014b; Guo et al., 2015; Gollakota et al., 2018). Biller and Ross (2011) successfully used thermochemical liquefaction at 350 °C on the microalgae *Chlorella vulgaris*, *Nannochloropsis occulata* and *Porphyridium cruentum* and the cyanobacteria *Spirulina*, and the yields of biocrude were found 5-25 wt.% higher than the lipid content of the algae, depending upon their biochemical composition. Li et al. (2014a) demonstrated that algal composition greatly

influenced oil yield and quality, by HTL studies of a low-lipid, high-protein microalga (*Nannochloropsis* sp.) and a high-lipid, low-protein microalga (*Chlorella* sp.). The highest biocrude yield for *Nannochloropsis* sp. was 55 wt.% at 260 °C, 60 min and for *Chlorella* sp. was 82.9 wt.% at 220 °C, 90 min. A GC-MS analysis revealed varying distribution of chemical compounds in the biocrude. In particular, the highest hydrocarbon content was 29.8% and 17.9% for *Nannochloropsis* and *Chlorella* sp., respectively.

Comparative studies on HTL and pyrolysis were carried out by Jena and Das (2011) on the microalgae *S. platensis,* wherein HTL resulted in higher bio-oil yields and lower char yields. Besides, bio-oil obtained from HTL was found to have higher energy density and superior fuel properties such as thermal and storage stabilities.

Parameters of HTL such as temperature, pressure, retention time, catalysts and solvents have been studied to obtain maximum quantity and high quality of bio-oil. Muppanneni et al. (2017) investigated HTL of *Cyanidioschyzon merolae* under various reaction temperatures and catalysts. Maximum biocrude oil yield of 16.98 wt.% was obtained at 300° C with no catalyst, which increased to 22.67 wt.% with the introduction of KOH into the reaction mixture as a catalyst. Another optimization study conducted by Toor et al. (2013) on *N. salina* and *S. platensis* revealed that maximal bio-crude yield of 46 wt.% was obtained from *N. salina* at 350 °C whereas for *S. platensis* the optimal HTL condition was at 310 °C.

Experiments have been carried out to yield biocrude oil from various kinds of macroalgae using HTL. Li et al. (2012) reported the use of *Sargassum patens* C. Agardh biomass to generate bio-oil *via* HTL, at a yield of 32.1 wt.% and a calorific value of 27.1 MJ/kg. Elliott et al. (2013) reported a bio-oil yield between 8.7 wt.% and 27.7 wt.% from the brown algae *Saccharina* sp., dependent on the time of harvesting. Anastasakis and Ross (2015) performed HTL on four brown macroalgae *Laminaria digitata, L. saccharina, L. hyperborean* and *Alaria esculenta*, yielding bio-oil at 13 wt.%, 10 wt.%, 8 wt.% and 13 wt.%, respectively. Raikova et al. (2017) screened 13 macroalgae covering the three macroalgal groups and reported the highest bio-oil yield of 29.9 wt.% for *Ulva lactuca*. All biocrude oils produced were similar in elemental composition and HHV. Neveux et al. (2014a) conducted HTL experiments on four green marine macroalgae *Derbesia tenuissima, Ulva ohnoi, Chaetomorpha linum, Cladophora*

coelothrix and two freshwater green macroalgae *Cladophora vagabunda* and *Oedogonium* sp. The maximum biocrude yield was obtained from *Oedogonium* at 26.2 wt.% for the freshwater algae studied whereas *D. tenuissima* produced the highest (19.7 wt.%) among the marine species, followed by *U. ohnoi* (18.7 wt.%). In India, HTL studies have been carried out on the macroalgae *Sargassum tenerrimum*, *Enteromorpha flexuosa* and *Ulva fasciata*, with comparative yields (Singh et al., 2015a; Singh et al., 2015b; Biswas et al., 2018a).

In various studies, temperatures ranging from 280-350° C have been investigated for production of maximum bio-oil from macroalgae and calorific values were reported to be between 28-36 MJ/kg (Anastasakis and Ross, 2011; Bach et al., 2014; Parsa et al., 2018). Slightly higher temperatures of around 350-450 °C have also been tested for production of bio-oil in a comparative study on three macroalgae *Ulva lactuca*, *Laminaria japonica* and *Gelidium amansii* (Li et al., 2014b), to obtain bio-oil yields of 14.17 wt.%, 12.87 wt.% and 11.98 wt.%, respectively. Aresta et al. (2005b) carried out HTL on *Chaetomorpha linum* at 395° C to produce biodiesel. As reported by Xu et al. (2015), HTL of *Enteromorpha prolifera* at 370 °C for 60 min yielded bio-oil at 34.7 wt.%.

Most of the HTL experiments for production of bio-oil have been conducted using water, while studies have been carried out using solvents and co-solvents as well. Biswas et al. (2017a) studied the effect of two solvents methanol and ethanol on the bio-oil yield from *Sargassum tenerrimum*, which was 22.8 and 23.8 wt.%, respectively, whereas the bio-oil yield with water was 16.33 wt.%. He et al. (2016) examined the use of organic co-solvent (n-heptane, toluene and anisole, up to 10 wt.%) in the HTL of macroalgal biomass *Oedogonium* and observed that bio-oil produced with n-heptane had significantly reduced levels of nitrogen (1.1wt.%) and oxygen (12.5 wt.%) and was relatively less viscous. In a study carried out on *Enteromorpha prolifera,* Lu et al. (2017) observed that the addition of crude glycerol to the algal feed in HTL significantly improved biocrude production to 38.71% at 320 °C. A co-liquefaction study was carried out by Jin et al. (2013) to obtain bio-oil from the microalga *Spirulina platensis* and macroalga *Enteromorpha prolifera* by HTL. The HHV of bio-oil produced from the co-liquefaction was 35.3 MJ/kg. The energy recovery from the co-liquefaction was found to be higher than the average value from separate liquefactions of the

two algal types. Co-liquefaction did not affect the molecular composition but influenced the relative amount of each component in the bio-oil.

Various catalysts have been used to improve the yield of bio-oil in HTL studies. Zhou et al. (2010) conducted HTL on the green macroalga *Enteromorpha prolifera* using a catalyst Na_2CO_3 and obtained a yield of 23 wt.% bio-oil. In another study, Yan et al. (2019) employed three basic catalysts (KOH, NaOH and Na_2CO_3) during HTL of the green macroalga *Ulva prolifera,* and obtained a maximum bio-oil yield of 26.7% with KOH compared to the 12.0 wt.% from non-catalytic liquefaction.

Although high yields of bio-oil can be obtained from HTL of macroalgae, there are some limitations that hinder its use as feedstock. One of the major limitations is their high ash content which can reduce the quality and yield of the bio-oils generated (Bach et al., 2014; Neveux et al., 2014b). The high ash content of macroalgae is due to the presence of inorganic salts and metals and hence studies have been conducted to lower their ash content. Diaz-Vazquez et al. (2015) employed five demineralization treatments on *Sargassum* spp. with nanopure water, nitric acid, citric acid, sulfuric acid and acetic acid, wherein nitric acid was the most effective in reducing ash content. Also, the bio-oil yield increased for HTL of citric acid treated *Sargassum* spp in comparison with untreated algae. In another study, Neveux et al. (2014b) treated three species of macroalgae, *viz.*, *Derbesia tenuissima, Ulva ohnoi* and *Oedogonium* sp. prior to hydrothermal processing, to reduce nitrogen, sulfur and ash within the biomass. Nutrient starvation during culturing effectively reduced nitrogen and sulfur levels within the biomass, which led to a reduction in nitrogen by 51-59 wt.% and sulfur by 64-88 wt.% within the bio-oil. Also, washing of biomass after harvesting the algae reduced the ash content for all species by 7-83 wt.%. The removal of ash affected neither the quantity nor the quality of bio-oil produced.

1.7. ALGAE

Algae are varied group of photosynthetic organisms ranging from unicellular (microalgae or phytoplankton) to multicellular (macroalgae) living in both marine and freshwater environments (Demirbas, 2010; Bharathiraja et al., 2015; Raheem et al., 2015). An alga may range in size from micrometers to several tens of meters. Algae are the principal producers of

oxygen on earth. They can grow easily in both fresh and saline water and are not dependent on agriculturally productive or environmentally sensitive land, being able to grow even in agricultural, industrial or municipal waste waters and on wastelands. They have much higher photosynthetic efficiency (6-8%) compared to terrestrial biomass (1.8-2.2%), as reported by Aresta et al. (2005a) and can easily convert solar energy, water and CO_2 by photosynthesis to a wide range of metabolites and chemicals. Also, algae have greater capacity to generate and store carbon resources because they are more efficient CO_2 fixers (Vassilev and Vassileva, 2016) and have higher productivity rates than terrestrial plants. They pose little or no competition with foods and feeds. Algae are a non-toxic fuel resource (Noraini et al., 2014) and highly biodegradable (Chisti, 2007), with no requirement for herbicides or pesticides for their cultivation. Algae-based fuels can also bring social benefits by creating employment opportunities (Ullah et al., 2015).

1.7.1. Microalgae: Advantages and Disadvantages

Microalgae are energy and oil dense and their fuels can be rendered cost-effective with more effort. According to Chisti (2007), certain microalgae are rich in oils, and others can be grown under conditions that favor the accumulation of large quantities of oil to produce biofuels. Microalgal cultivation using sunlight energy can be carried out in open or covered ponds or closed photobioreactors, based on tubular, flat plate or other designs. The total lipid (neutral and polar) content of algal biomass varies from 1% to 75%, depending upon the microalgal strain and cultivation conditions, with values generally greater than 40% in nutrient stress conditions (Kumar et al., 2016). Microalgae have higher yield per hectare than macroalgae (Chen et al., 2015c). Microalgal cultivation consumes less water than land crops. Microalgal farming could be potentially more cost effective than conventional farming. On the other hand, one of the major disadvantages of microalgae for biofuel production is the low biomass concentration in the microalgal culture due to the limit of light penetration, which in combination with the small size of the algal cells makes the harvest of algal biomasses relatively costly (Demirbas, 2010).

1.7.2. Macroalgae

1.7.2.1. Classification, general structure, characteristics and composition

Larger marine algae are referred by a generic term "seaweeds" or a specific term "macroalgae" (Jung et al., 2013). Seaweeds or marine macroalgae are the large primary producers of the sea. They are comparatively large, diverse, multicellular and photoauxotrophic aquatic plants, able to grow up to 70m in length (Van Den Hoek, 1981; Raheem et al., 2015; https://www.americanscientist.org/article/the-science-of-seaweeds). Although more elaborate than unicellular algae, macroalgae lack the complex structures found in plants and consist of a leaf-like thallus instead of roots, stems and leaves.

Macroalgae are classified into three major groups according to their characteristic thallus color derived from photosynthetic pigmentation (Demirbas, 2010; Chen et al., 2015a). Besides, all of the groups contain chlorophyll granules. Green seaweeds contain similar proportion of chlorophyll *a* to *b* as herbaceous land plants (Wynne, 1981). The red color in seaweed is due to chlorophyll *a*, phycoerythrin and phycocyanin. Brown seaweeds possess the main photosynthetic pigments chlorophyll *a* and *c* and in addition, they have the accessory pigment fucoxanthin that gives the characteristic brown color. These accessory pigments hide chlorophyll in such a way that the green color is effectively masked (Bast, 2014; http://www.seaweed.ie/algae/phaeophyta.php). The type of pigments, extent of growth and chemical composition of macroalgae are significantly determined by their habitat conditions in the marine environment such as light (the principal contributor), temperature, salinity, nutrients, pollution and even waves and currents (Jung et al., 2013). Specific pigments present in diverse seaweeds absorb a specific wavelength of light.

Macroalgae normally grow on rocky substrates although in some cases they are attached to sand particles. Their structure is generally made up of three clearly identifiable parts. At the bottom there is a root-like structure called the holdfast which secures the organism to its habitat. It is joined by a stipe (or stem) to the leaf-like blades. The seaweed can have one or more blades, and the blades can have different shapes. In some algae, the blades have a distinct midrib. Photosynthesis primarily occurs in the blades and it is thus important that the stipe is long enough to place the blades close enough to the surface of the water to receive

light. Some species such as *Sargassum* spp. have air-filled bladders which ensure their access to light by holding them upright in the water (https://www.americanscientist.org/article/the-science-of-seaweeds). Some algae have fronds which are a combined part of the blade and stipe.

1.7.2.2. Economic uses of macroalgae

Macroalgae with their high resources have been explored as sources of food (Norziah et al., 2000; Sanchez-Machado et al., 2004; Dawczynski et al., 2007; Yaich et al., 2011; Miyashita et al., 2013; Kadam et al., 2017). They have been studied for their seasonal chemical and nutritional composition (Kamenarska et al., 2002; Khotimchenko et al., 2002; Khairy and El-Shafay, 2013; Polat and Ozogul, 2013). In addition, macroalgae are researched for their medicinal value (Nwosu et al., 2011; Pangestuti and Kim, 2012), experimented in cosmetic industry (Andrade et al., 2013; Wang et al., 2015), aquaculture and feed for animals (Viera et al., 2005; Soler-Vila et al., 2009), *etc*. Studies have been carried out to test their potential for production of biofuels such as bioethanol, biogas and biodiesel (Trivedi et al., 2013; Suganya et al., 2013).

1.7.2.3. Advantages of macroalgae

Macroalgae are significantly different from terrestrial plants in terms of their morphological and physiological features as well as chemical composition (Sudhakar et al., 2018). Firstly, macroalgae contain very low lignin content or no lignin at all because they do not need to stand rigidly in water (Wegeberg and Felby, 2010; Kraan et al., 2013), lignin being needed for the rigidity of terrestrial plants. They can hence provide many benefits for biorefinery since there is no need for the difficult lignin removal processes and detoxification of lignin-originated inhibiting compounds (Meinita et al., 2012).

Compared to terrestrial biomass, macroalgae have a high content of water (70-90% fresh wt.), 25-50% dry wt. carbohydrate, 7-15% dry wt. protein and 1-5% dry wt. lipid (Jensen,1993; Peralta-Garcia et al., 2016). The high photosynthetic ability of macroalgae offers them the potential to generate and store sufficient carbon resources needed for biorefinery. Macroalgae have higher productivity rates than terrestrial biomass such as corn and switchgrass (Chung et

al., 2011). Marine macroalgae thus exhibit high potential to replace terrestrial biomass and generate sustainable bioenergy and biomaterials (Jung et al., 2013). It should be noted that unlike microalgae, seaweeds can be cultivated more easily in an open sea rather than in a controlled environment system. Also, due to their low content of cellulose coupled with absence of lignin, brown macroalgal biomass may be easily converted into biofuels when compared to terrestrial plants (Kraan, 2013). Seaweed can be easily harvested and quantities of biomass could be obtained due to their larger size (Jung et al., 2013; Sudhakar et al., 2018). The current seaweed production normally comes from harvesting natural seaweeds directly from the ocean or collecting shore strewn seaweed. These practices are clearly unsustainable for seaweed fuel application on a very large scale. Therefore, for renewable energy production, growing macroalgae in a dedicated cultivation system would become inevitable.

1.7.2.4. Cultivation and harvesting of macroalgae

The cultivation and harvesting of seaweed is relatively easy and different from that of microalgae. Microalgae have to be cultivated in a system designed for that purpose whereas macroalgae can be grown in open seas and a considerable amount of biomass could be accumulated. Seaweed collection can be carried out in three ways: direct harvesting from the marine environment, collection of dead seaweed from the shore and culturing selected seaweed species. Harvesting techniques include manual (hand) harvesting and mechanical (dredge, moving boat, mesh conveyor) harvesting (Sudhakar et al., 2018). Continuous mechanical harvesting leads to unfavorable consequences on marine ecosystems and would significantly reduce the growth of macroalgal species. There are, however, areas where elimination of flourishing macroalgae growth is advantageous as it helps in removal of excessive nutrients from the environment. Seaweed cultivation methods include offshore, onshore and integrated seaweed cultivation**.** Offshore cultivation is the direct culturing in seawater through the use of anchored ropes. It can also be combined with onshore aquacultures and offshore wind farm sites (Langlois et al., 2012). Controlled conditions of growth and harvesting can be maintained, thus enabling higher efficiency and productivity than natural growth. Macroalgae can be favourably cultivated in lagoons or sheltered bays to obtain the nutrients directly from seawater.

1.7.2.5. Global distribution of macroalgae

Seaweeds are distributed throughout the world and are currently produced by 42 countries for various commercial purposes (Subba Rao et al., 2018). Seaweed production is dominant in Asia, China (62.8%) being the largest producer (Wei et al., 2013) since the 1980s, followed by Indonesia (13.7%), Philippines (10.6%), Korea (North and South, 8%), Japan (2.9%) and Malaysia (0.9%) (Khan and Satam, 2003; Sudhakar et al., 2018), while in Europe, the largest producers of seaweed are France, Norway, Ireland, Iceland, the Russian Federation and Spain (Mac Monagail et al., 2017). The rest of the world contributes only 1.1% of the global production (Chopin et al., 2014). Research shows that although there are about 9200 species of seaweeds, only 221 species are utilized commercially (Sirajunnisa and Surendhiran, 2016). Seaweed production from aquaculture is mainly prevalent in Asia, with China leading the market (72%), followed by minor contributions from the Philippines, Indonesia, and the Republic of Korea.

1.7.2.6. The Indian scenario on macroalgae production

India has a stretch of about 8085 km long coastline, 51,200 sq. km of continental shelf area, 2.02 million sq. km of Exclusive Economic Zone (EEZ) and nine maritime states (Kaladharan and Kaliaperumal, 1999). According to Reddy et al. (2014) of the total number of seaweed species recorded from the Indian coast, the majority belongs to the Rhodophyta (422) followed by the Chlorophyta (217) and finally the Phaeophyta (191). Cultivation and harvesting of seaweeds in India chiefly happens in the southeastern coastal region from Rameswaram to Kanyakumari (Kaladharan and Kaliaperumal, 1999). The state of Tamil Nadu ranks first in seaweed production among the nine coastal states and union territories (Subba Rao and Mantri, 2006). Since seaweed is not an important aspect of the Indian diet, seaweed resources are entirely used for the production of commercially and industrially important agar and alginates. The entire carrageenan requirement of India is met through imports. However, to make a beginning, pilot scale cultivation of seaweeds such as *Hypnea* species has been taken up by PepsiCo India Holdings Ltd., Gurgaon (Haryana state), with support from the Marine Algal Research Center, CSMCRI, Mandapam, Tamil Nadu, to mainly cultivate the seaweed all year round as well as to evaluate the carrageenan to begin indigenous production

in the country (Khan and Satam, 2003). Indian seaweeds are mostly harvested manually. Such harvesting is an important source of additional income to more than 10,000 coastal fisherfolk (Immanuel & Sathiadhas, 2004). Commercial cultivation of *Kappaphycus alvarezii* was started in 2001 along the southeast coast of Tamil Nadu by PepsiCo India Holdings (P) Ltd., after licensing cultivation technology from the CSIR-CSMCRI, Bhavnagar in the state of Gujarat. The commercial production has expanded to coastal districts in Tamil Nadu and expansion is in progress in Gujarat, where commercial activities have commenced in 2017 (Ganesan et al., 2019).

1.7.3. Challenges Associated with Algae and Algal Fuels

The major obstacle against the widespread utilization of algae is their high production costs and low cost efficiency. The cultivation, harvesting, transportation, storage and pre-treatment of algae and separation and processing of the final algae-based fuels are expensive (Bharatiraja et al., 2015). The precise quantity of algae that can be grown, harvested and processed in a sustainable manner appears unclear. Large-scale usage of macroalgae for biofuel production has been limited as compared to microalgae due to a more complex structure; slower growth rate and lower oil content (Ziolkowska et al., 2014). Harvesting of microalgae is but more difficult than that of macroalgae due to their microscopic size (Chen et al., 2015a; Ghosh et al., 2016). Very little research has been carried out on production of biofuels from algae. Many areas of research are now being focused to gain knowledge on the variability of composition and properties of algae, practical experience in biofuel production, technological problems during processing of algae, *etc*. The most important criteria for biofuel production are screening and selection of algae. Numerous algal species exist on earth but all cannot be used for biofuel production since crucial factors such as availability of algae, abundance, growth rate, photosynthetic yield, biomass productivity, carbohydrate and lipid content have to be taken into account.

1.8. Motivation for the present study

With the above background on algal biofuels, the present research was envisaged to focus on screening for suitable macroalgal sources for production of biofuels. Attempts have been made to maximize extraction of algal oils, convert them to biofuels and characterize the product obtained to assess its suitability.

In particular, the research presented in this thesis was initiated with the following objectives in perspective:

- Collection of macroalgal species from the Goan coastline and preliminary screening for lipid content.
- Standardization of extraction procedures and evaluation of the algal oils for biodiesel potential.
- Optimization of the transesterification of oil by acid / alkali / enzyme catalysis.
- Characterization of fatty acids by chromatographic procedures.
- Identification/evaluation of potential macroalgal sources in terms of yield and acceptable biodiesel quality.
- Hydrothermal liquefaction of brown, red and green macroalgal samples for bio-oil production.
- Evaluation of the bio-oil and biochar as biofuels.

Chapter II

Sampling and Processing of Macroalgae

Collection of macroalgal samples is carried out from the intertidal zone during low tide. It is advisable to reach the site an hour or two in advance of the low tide timing predicted by the tide tables. This would help to observe the macroalgae in their natural habitat and also provide added time for collection (Dhargalkar and Kavlekar, 2004). It is very important to handle the seaweed biomass carefully after harvesting since improper handling could lead to spoilage during transportation and storage. Impurities such as sand, stones, epiphytes, aquatic plants and animals can cause changes in biomass composition and have to be removed from the macroalgae by adequate washing with sea water, followed by fresh water. Appropriate drying of the sample is very important, the biomass being of almost 70-90% water and thereby susceptible to decay (Gallagher et al., 2018). Sun drying is currently the most convenient method of drying macroalgae but it is not as well-controlled as oven drying (Milledge and Harvey, 2016). The grinding of seaweed samples to a much smaller size enhances the surface area of the biomass for improved product extractions.

2.1. MATERIALS & METHODS

Marine macroalgae are seasonally available on the coastline of certain rocky beaches of Goa, India. Due to their high water content, large amount of algal biomass was needed to carry out continuous lipid extractions, which thus called for continual sampling. Various macroalgal samples available along a few beaches of Goa *viz*., Vagator, Anjuna and Vainguinnim were collected during low tide, guided by the tide table (www.nio.org; https://www.windfinder.com/tide/panaji_goa). The freshly collected samples were washed at site with sea water, transported to the laboratory and then washed thoroughly with tap water to remove attached debris and dirt. They were then rinsed with distilled water, blot dried by frequent turning over to prevent rotting and then quick dried in an oven for 2 - 3 h at 50 °C. The dried samples were coarsely crushed and powdered using an electric mixer-grinder (Fig. 2.1). Finally, the powdered samples were tightly packed and stored in disposable plastic bags until further analysis.

The inherent moisture content of the algae was calculated using the formula:

% Moisture content = (dry wt. of sample / wet wt. of sample) x 100

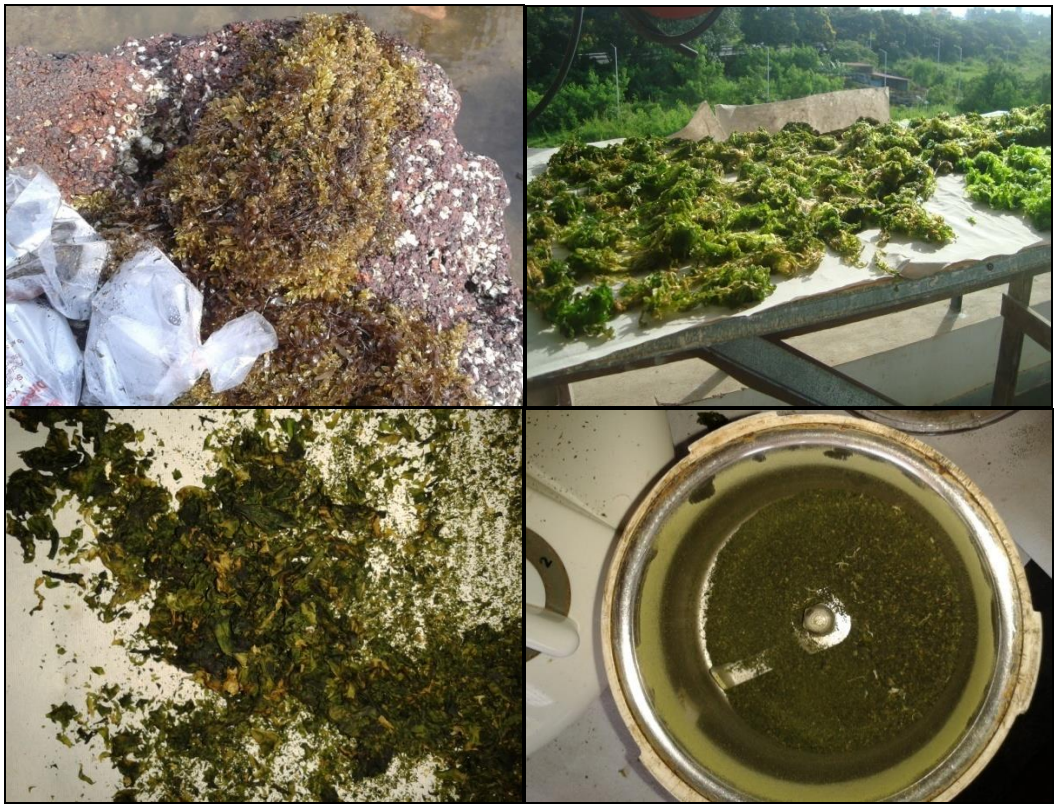

Fig. 2.1: Macroalgae being collected, dried and ground

2.2. RESULTS & DISCUSSION

Various macroalgae available along a few beaches of Goa were collected through repeated samplings during low tide (Table 2.1). Seven macroalgal samples were identified (kind courtesy, Prof. Vijaya Kerkar, Department of Botany, Goa University) and grouped as Brown macroalgae (class Phaeophyceae): *Sargassum tenerrimum, Padina tetrastromatica* and *Stoechospermum marginatum*, Green macroalgae (class Chlorophyceae): *Ulva fasciata*, *Enteromorpha flexuosa* and *Chaetomorpha media*, and Red macroalgae (class Rhodophyceae): *Gracilaria corticata*.

Table 2.1: Macroalgal sample collection

Sampling date	Sampling site	Tide level (m)	Sampling time (hours)	Samples collected
13 Feb 2014	Anjuna	0.51	16:09	*Padina tetrastromatica, Sargassum tenerrimum, Gracilaria corticata*
12 Mar 2014	Vainguinnim	0.75	14:16	*Sargassum tenerrimum*
13 Mar 2014	Vagator	0.69	15:03	*Amphiroa fragilissima*
10 Sept 2014	Anjuna	0.15	17:43	*Ulva fasciata, Enteromorpha flexuosa, Chaetomorpha media*
24 Oct 2014	Anjuna	0.21	16:51	*Ulva fasciata, Chaetomorpha media*
06 Nov 2014	Anjuna	0.07	16:12	*Padina tetrastromatica, Gracilaria corticata, Ahnfeltia plicata, Hypnea cervicornis, Dictyota dichotoma, Stoechospermum marginatum, Caulerpa sertuloides*
05 Dec 2014	Vainguinnim	0.16	15:55	*Sargassum tenerrimum*
17 Jan 2015	Anjuna	0.20	14:15	*Stoechospermum marginatum, Hypnea cervicornis*
27 Aug 2015	Anjuna, Vagator	0.7	14:55	*Ulva fasciata, Enteromorpha flexuosa*
24 Sept 2015	Anjuna	0.7	13:40	*Ulva fasciata*
14 Oct 2015	Anjuna	0.2	17:25	*Padina tetrastromatica,*

				Gracilaria corticata, Chaetomorpha media
22 Dec 2015	Anjuna	0.2	14:20	*Sargassum tenerrimum, Stoechospermum marginatum*
21 Jan 2016	Anjuna	0.23	14:50	*Sargassum tenerrimum*
31 Oct 2016	Anjuna	0.3	16:45	*Padina tetrastromatica, Gracilaria corticata*
25 Nov 2016	Vainguinnim	0.7	18.30	*Sargassum tenerrimum*
12 Jan 2017	Anjuna	-0.1	14:30	*Stoechospermum marginatum*
05 Oct 2017	Anjuna	0.4	15:45	*Ulva fasciata, Gracilaria corticata*
26 Sept 2018	Anjuna	0.2	17:34	*Gracilaria corticata, Ulva fasciata*
09Jan 2019	Vainguinnim	0.2	18:30	*Sargassum tenerrimum*
18 Jan 2019	Vainguinnim	0.4	14:30	*Sargassum tenerrimum*

Brown macroalgae are known to be exclusively marine. They present different forms ranging from simple, freely branched filaments to highly differentiated varieties. Many species have large massive thalli with special air bladders, vesicles or floats to make them buoyant. Some of the brown algae can form a marine forest (kelp-forest) or algae sea, attracting numerous marine organisms and drawing in abundant marine resources. Kelps usually have large thalli and can grow up to 70 m in length. *Laminaria*, a kind of kelp, tends to be distributed in colder waters. Brown algae vary in colouration from olive-yellow to deep brown (Fig. 2.2). Photosynthetic pigments of the brown algae are chlorophyll *a* & *c*, carotene, xanthophylls and fucoxanthin (pigment responsible for the brown colour). The cell wall is composed of an outer layer of algin and an inner layer of cellulose (Jung et al., 2013). The photosynthetic products of the brown algae are laminarin and mannitol (Adams et al., 2011; Dhargalkar and Kavlekar, 2004).

Padina tetrastromatica

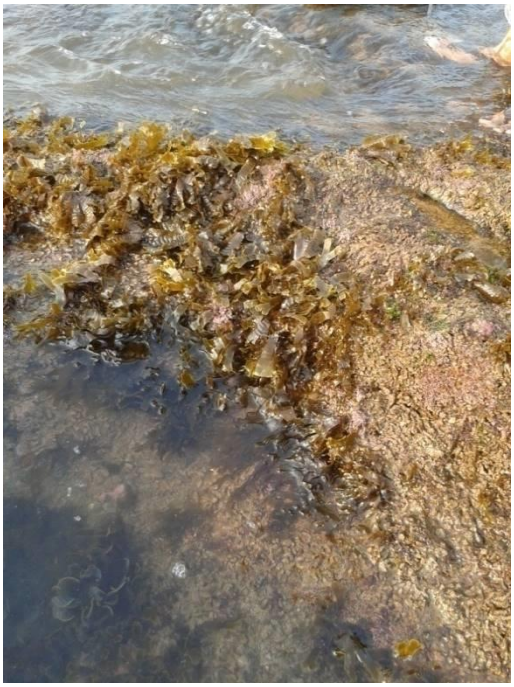

Stoechospermum marginatum

Sargassum tenerrimum

Fig. 2.2: Brown macroalgae

Green macroalgae are found in marine as well as freshwater habitats. From external morphology, they may appear to be filamentous, membranous, cylindrical, globular or coenocytic, depending on the way their cells divide (http://formosa.ntm.gov.tw/seaweeds/english/b/b3_01.asp). They generally appear green because they contain the same ratio of chlorophyll *a* and *b* as in higher plants (Fig. 2.3). Their photosynthetic products are starch and their cell walls are primarily composed of an outer layer of pectin and an inner layer of cellulose (Dhargalkar and Kavlekar, 2004).

Enteromorpha flexuosa

Chaetomorpha media

Ulva fasciata

Fig. 2.3: Green macroalgae

Red macroalgae are either epiphytes, growing as crust on rocks or shells or as large fleshy, cylindrical, long, slender, branched or blade-like thalli attached by a single holdfast (Fig. 2.4). The thallus is basically filamentous, simple or branched, free or compacted to form pseudoparenchyma with uni- or multi- axial construction. But for a few species, they are almost exclusively marine. Occurring in varying sizes and shapes, they inhabit intertidal to subtidal to deeper waters. Rhodophyta often tend to appear violet red, rose or dark red in colour due to water-soluble pigments, the red phycoerythrin and the blue phycocyanin. Other pigments present are chlorophyll *a* & *b*, lutein and β-carotene. Phycoerythrin can absorb blue light, hence red algae can grow in comparatively deeper ocean waters than other algae. It is at times possible to find red algae at 200 m depths. They can be found at all latitudes but are usually more abundant in temperate and tropical zones rather than in frigid zones. In general, the cell walls of red algae are rich in agar, carrageenan and mucopolysaccharides. The photosynthetic product of this group is Floridian starch (Dhargalkar and Kavlekar, 2004).

Gracilaria corticata

Fig. 2.4: Red macroalgae

Macroalgae representing each major seaweed type, namely, *Sargassum tenerrimum* (Phaeophyta), *Gracilaria corticata* (Rhodophyta) and *Ulva fasciata* (Chlorophyta) were used in this study. The shortlisting of these three macroalgal species for the present work was based

on their comparatively broad availability along the Goan coastline, seasonally as well as interannually.

More specifically, *Sargassum tenerrimum* (*ST*) plants are pyramidal in form, with a disc-shaped holdfast, yellowish-brown in colour, larger and broader in the lower portion and becoming smaller and narrower towards the apex marginal leaves. *Ulva fasciata* (*UF*) is a flat alga which grows without a stipe, and the membrane is soft, thin and translucent. The thallus consists of many long blades with undulated margins. The plants are attached to rocks with the help of a holdfast and thalli are lobed towards the basal part (Sahoo, 2010). *Gracilaria corticata* (*GC*) is cylindrical, branched, flattened and structurally composed of a central medulla surrounded by the cortex. The plants are strongly attached to the rocky substrate by a small disc.

Macroalgae are known to contain high amounts of water (70-90% fresh wt.). The moisture content of the fresh macroalgal samples *ST*, *GC* and *UF* was derived to be 88.56%, 88.26% and 90.83%, respectively.

This explains the need for repeated seasonal sampling so as to accumulate sufficient processed and dried biomass for the biofuel studies planned.

Chapter III

Methodology Development for Rapid Estimates of Macroalgal Lipid

In relation to biofuel production, the limited large-scale usage of macroalgae rather than microalgae has been attributed to a more complex structure, slower growth rate and lower lipid content (Ziolkowska et al., 2014). It should, however, be noted that unlike microalgae, macroalgae can be cultivated more easily in open sea rather than in a controlled environment system. They can be easily harvested and large amount of biomass could be obtained due to their bigger cell size (Sudhakar et al., 2018; Jung et al., 2013), while harvesting of quantities of microalgal biomass is more difficult due to their microscopic nature (Chen et al., 2015a; Ghosh et al., 2016). When compared to terrestrial plants, macroalgal biomass may be easily converted into biofuels by virtue of their low cellulose content coupled with the absence of lignin (Kraan, 2013). Marine macroalgae exhibit high potential to replace terrestrial biomass and generate sustainable bioenergy and biomaterials (Jung et al., 2013).

The most important criteria for any algal biofuel production would be screening and selection of algae. Numerous algal species exist on earth but all may not be ideal for biofuel production since crucial factors such as availability of algae, their abundance, growth rate, photosynthetic yield, biomass productivity as well as composition have to be taken into account.

Very little research has been carried out on production of biodiesel from macroalgae. One kind of biofuel production addressed in the present study being that of biodiesel, a significant starting point would be the identification of suitable algal species with sufficient triglyceride content. The fatty acid composition of macroalgae demonstrates some similarity with that of microalgae, with carbon chain lengths between C14 and C24 (Kumari et al., 2010; Gosch et al., 2012). Identification of desirable algal species/strains would require screening for the lipid content in the algae (Omirou et al., 2018). A need was therefore felt to develop a methodology for simple and rapid colorimetric quantification of lipid from seaweeds (macroalgae) and the work towards this end is described in this Chapter.

3.1. QUALITATIVE ANALYSIS

Nile Red (9-diethylamino-5H-benzo-[α-]phenoxa-phenoxazine-5-one), a photostable, lipid-soluble fluorescent dye, is commonly used to estimate neutral lipid yields in prokaryotic and eukaryotic cells (Greenspan and Fowler, 1985; Cooksey et al., 1987). Its fluorescence is produced in highly hydrophobic environments and quenched by hydrophilic ones (Greenspan

and Fowler, 1985). Nile Red has been used in evaluating the lipid content in mammalian cells (Genicot et al., 2005), bacteria (Izard and Limberger, 2003), fungi and yeasts (Evans et al., 1985; Kimura et al., 2004) as well as zooplankton (Kamisaka et al., 1999). Staining with Nile Red has also been developed as a high-throughput, rapid screening technique for the determination of neutral lipid content of many microalgae (Cooksey et al., 1987; Bertozzini et al., 2011). More recently, Chen et al. (2009) and Doan and Obbard (2011) have, in their respective studies, developed a modified Nile Red fluorescence technique and reported the improved estimation of lipids in green microalgae by using the solvent dimethyl sulfoxide (DMSO). To the best of our knowledge, no reports are available to date on Nile Red staining as a tool for macroalgal lipid studies, but for some preliminary studies from our own laboratory (Jabeen, 2011).

3.2. QUANTITATIVE ANALYSIS

While numerous methods have been developed to quantify lipids, the most frequently used continues to be the gravimetric method in which lipid is extracted from a sample using a suitable solvent, the solvent evaporated and the quantity of retained substance projected as an estimate of total lipid content (Bligh and Dyer, 1959). Nevertheless, reports also express that the results of the gravimetric method represent total content of all lipophilic materials contained in a sample. For instance, Griffiths and Harrison (2009) recognized that these methods could extract significant quantities of non-nutritive, non-saponifiable material such as chlorophyll pigments in addition to neutral lipids, leaning towards overestimation of total lipids in the biomass considered suitable for use as biofuel (Archanaa et al., 2012). In the present study attempts were hence made to derive an estimate of lipid content in the extracted oil, using the colorimetric Sulfo-phospho-vanillin (SPV) assay first described by Chabrol and Charronat (1937) for estimation of serum lipids, wherein lipids are heated in the presence of sulfuric acid at boiling temperature to form carbonium ions. Reaction of the carbonyl group of the phosphovanillin reagent with these ions would result in a pink product measurable at 530 nm (Knight et al., 1972).

The present study was hence initiated to rapidly gauge the algal lipid content and thereby the biodiesel potential of specific seaweed species available along the coast of North Goa, as a representative study for further generalization. The search was for: (a) a simple screening

procedure for macroalgal lipids using Nile Red staining as a tool and (b) a colorimetric assay to quantify the amount of neutral lipid in macroalgal species.

3.3. MATERIALS & METHODS

The sequence strategy adopted for the use of Nile Red staining and the SPV assay for selection of potential macroalgal species was as follows:

3.3.1. Nile Red staining

The Nile Red staining procedure was modified from that followed by Huang et al. (2009) and Doan and Obbard (2011) for microalgae. Fresh seaweed samples were blot dried, sectioned and soaked in 20% DMSO for 5-10 min followed by washing with distilled water. The sections were then stained with Nile Red solution (0.1 mg/ml) in acetone and observed under a fluorescence microscope (BX 53 Olympus fluorescence microscope, Japan) using 10x and 40x objective lenses. Cells would appear red while lipid droplets were golden yellow, as described by Greenspan et al. (1985) for mouse peritoneal macrophages.

3.3.2. Sulfo-Phospho-Vanillin (SPV) assay

Vanillin reagent was prepared according to Byreddy et al. (2016). Crude algal lipid extracted using an appropriate solvent system was used for the SPV assay, which was carried out as per Mishra et al. (2014). The standard curve was prepared using olive oil (1mg/ml) in chloroform. The lipid extract (100 µl) was boiled with 2ml conc. sulfuric acid for 10 min and then cooled in an ice bath. Vanillin reagent (5 ml) was added, incubated for 15 min at 37 °C and the absorbance immediately recorded at 530 nm.

3.3.3. Range of solvents used for lipid extraction

Dry macroalgal powder of *ST*, *GC* and *UF*, representative of the three macroalgal groups chosen for the present study, was subjected to extraction using five different solvent systems.

The following solvent systems, commonly reported in literature, were used:

- n-Hexane (H); (Miao and Wu, 2006)
- 1% diethyl ether and 10% methylene chloride in n-hexane (HD); (Kaluzny et al., 1985)

- Hexane: isopropanol :: 3:2 (HI); (Hara and Radin, 1978; Ryckebosch et al., 2012)
- Hexane: methanol: acetone :: 3:1:1 (HMA); (Dufreche et al., 2007)
- Chloroform: methanol ::1:2 (CM); (Bligh and Dyer, 1959)

3.3.4. Pretreatment of the dry algal powder

Pre-treatment of algae helps to disrupt the cell wall and improve the efficiency of the lipid extraction process by enhancing the solvent - lipid contact. The following methods were thus tested to maximize destruction of algal cells:

- autoclaving (121°C, 15 lb pressure, 15 min);
- sonication (5 min) using an ultrasonic probe at 24 kHz;
- autoclaving (15min) + sonication (5 min).

Extractions for these experiments were uniformly carried out using CM as solvent.

3.4. RESULTS & DISCUSSION

3.4.1. Nile Red staining

Although in Chapter II, the algae *ST*, *GC* and *UF* were narrowed down for detailed studies on biofuel production, the other macroalgal species collected were also used in the present analysis, to provide more statistically relevant information.

Nile Red is a lipid-soluble fluorescent dye. It is photostable and strongly fluorescent in organic solvents and hydrophobic environments. The dye enters into the cell wall, cytoplasmic membrane and eventually dissolves in the intracellular neutral and polar lipids to give the desired fluorescence to macroalgal samples, with the addition of DMSO as the stain carrier (Huang et al., 2009). The neutral lipids in seven selected macroalgal species were observed as yellow-gold fluorescence droplets (Fig. 3.1) while the rest of the cell stained red. This is the first report on the use of Nile Red staining as a preliminary screening technique for detecting lipids in macroalgae.

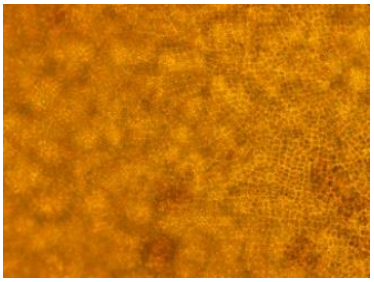

A1

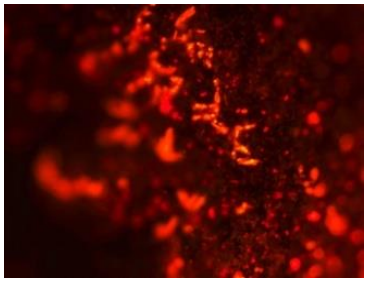

B1

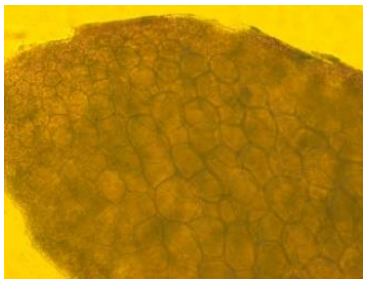

A2

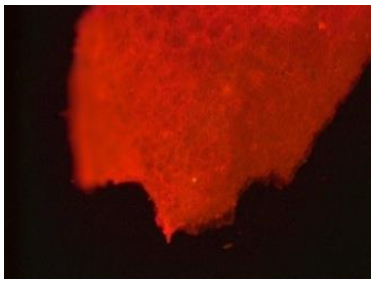

B2

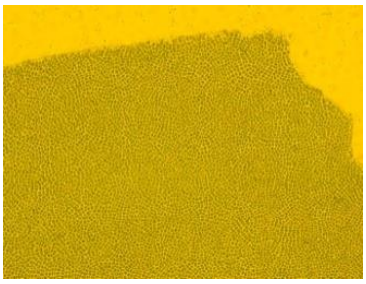

A3

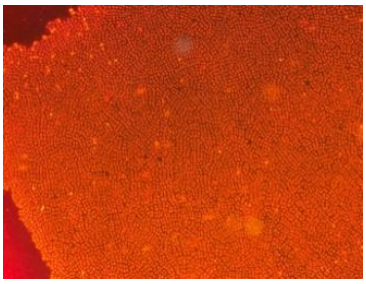

B3

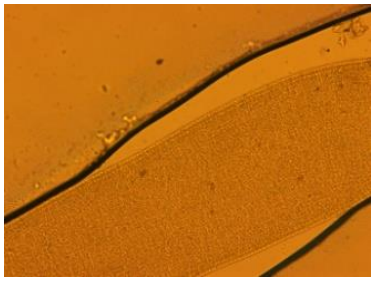

A4

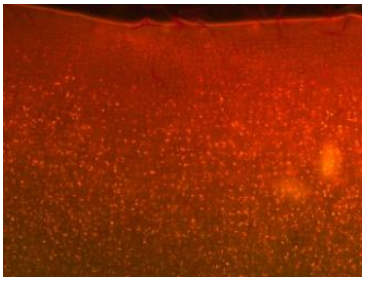

B4

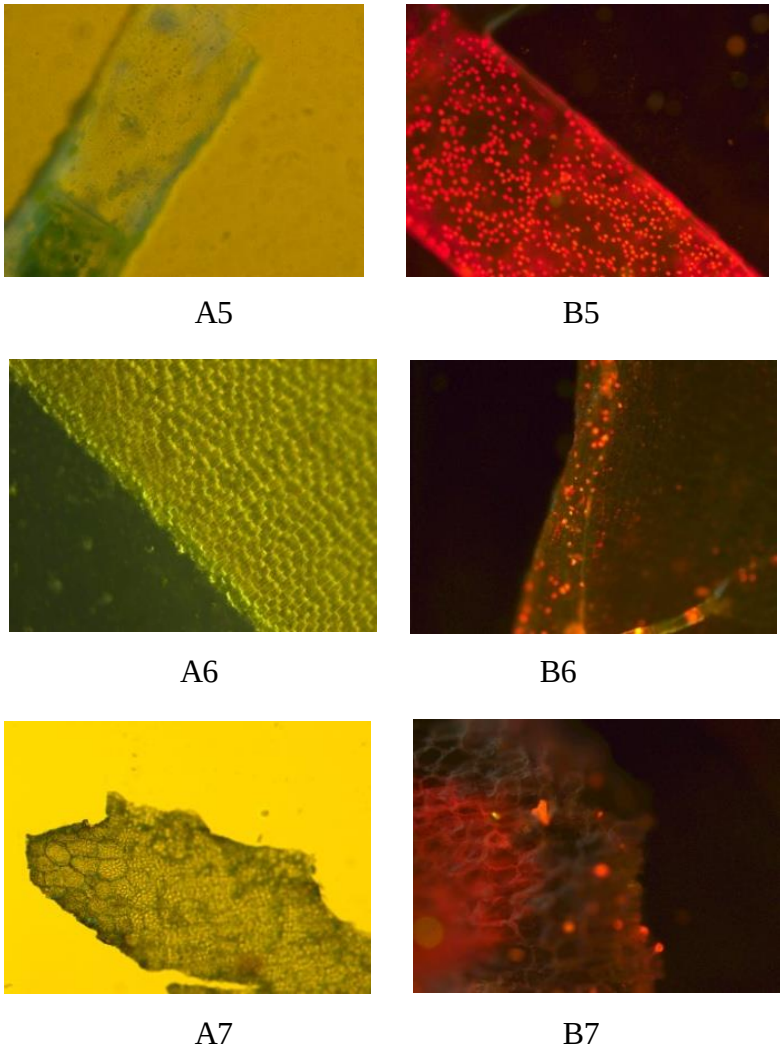

Fig. 3.1: Unstained algal samples (A1-A7). Algal samples stained by Nile Red, showing characteristic yellow fluorescence under the microscope (B1-B7). 1: *Sargassum tenerrimum*; 2: *Gracilaria corticata*; 3: *Ulva fasciata*, 4: *Enteromorpha flexuosa*; 5: *Chaetomorpha media*; 6: *Padina tetrastromatica*; 7: *Stoechospermum marginatum*.

3.4.2. The SPV assay

In this colorimetric method, lipids are heated in the presence of sulfuric acid at boiling temperature to form a carbonium ion. The carbonyl group of the phosphovanillin reagent forms a pink product on reaction with the carbonium ions, with a concentration dependent absorbance change at 530 nm (Fig. 3.2). Lipid standard curve was generated using olive oil

(1mg/ml) in chloroform. A good linear relationship (R^2 = 0.994) was observed at least up to the tested 1mg quantity (Fig. 3.3).

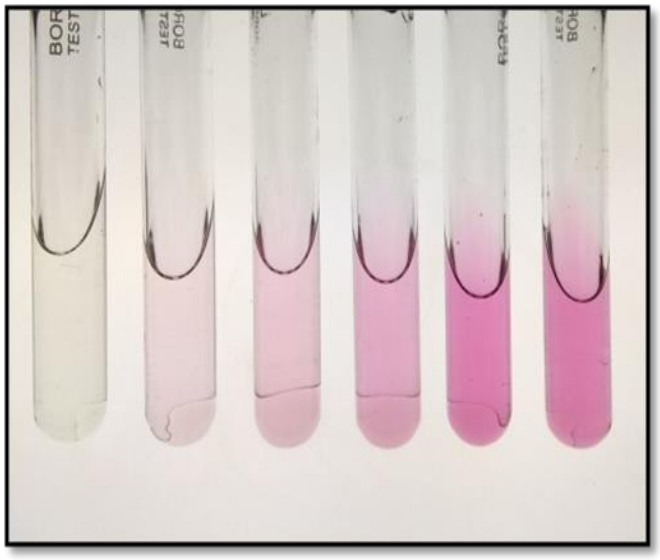

Fig. 3.2: Change of color resulting from reaction with SPV reagent

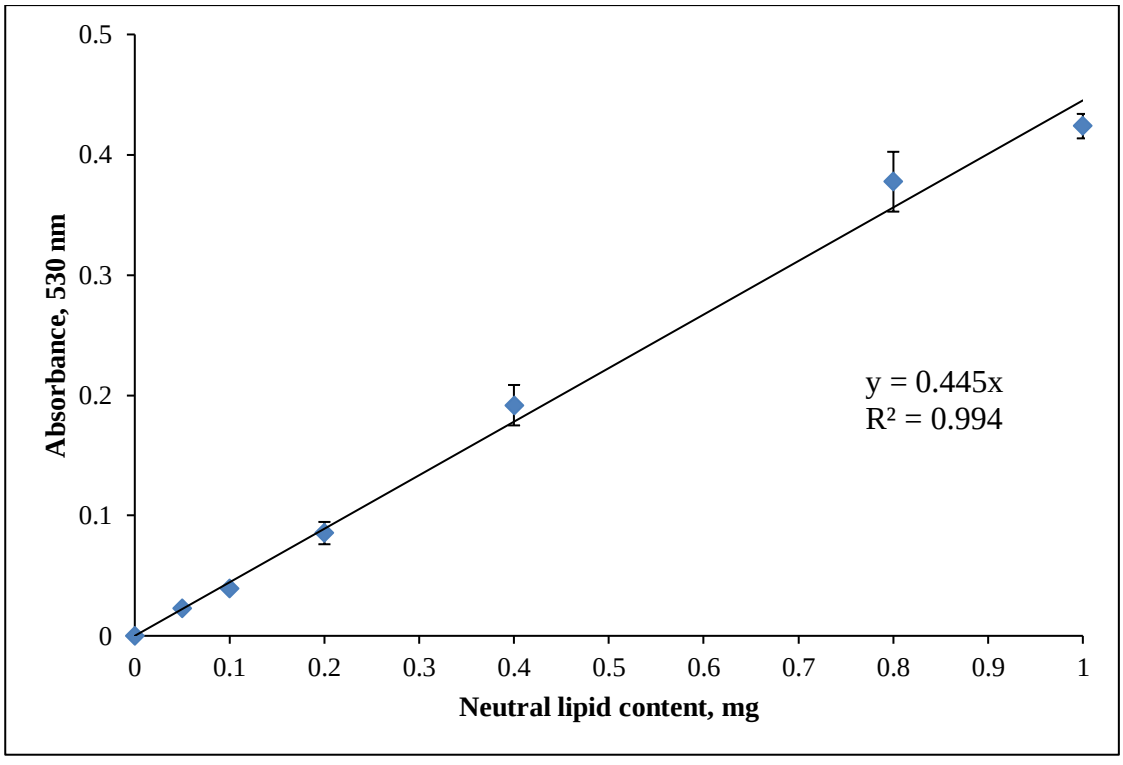

Fig. 3.3: SPV assay for estimating lipids

Out of the seven macroalgal extracts that were analyzed by the SPV assay, the brown alga *Stoechospermum marginatum* appeared to have the highest lipid content (2.6 wt.%), followed by *Sargassum tenerrimum* (0.89 wt.%), the red alga *Gracilaria corticata* (0.47 wt.%) and the green alga *Ulva fasciata* (0.43 wt.%) (Fig.3.4). On account of the restricted and sporadic availability of the *Stoechospermum* sp. (*StM*), *Sargassum tenerrimum* (*ST*) emerged the brown alga of choice for the work at hand.

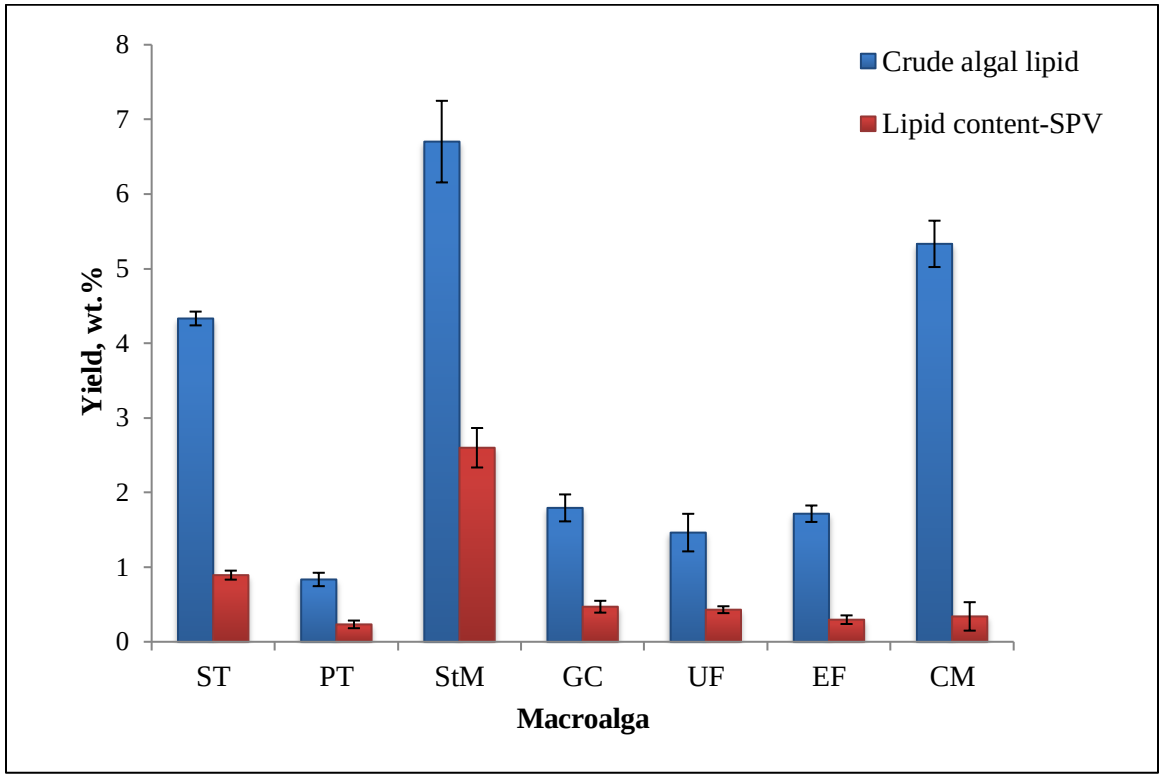

Fig. 3.4: Total crude lipid yield (gravimetric) in comparison with lipid content (SPV assay) as extracted in CM as solvent: *ST* (*Sargassum tenerrimum*); *PT* (*Padina tetrastromatica*); *StM* (*Stoechospermum marginatum*); *GC* (*Gracilaria corticata*); *UF* (*Ulva fasciata*); *EF* (*Enteromorpha flexuosa*); *CM* (*Chaetomorpha media*).

3.4.3. Effect of solvents on the lipid extraction

Dry algal powder of *ST*, *GC* and *UF*, representative of the three macroalgal groups chosen for the present study, was subjected to extraction using five different solvent systems to obtain maximal algal lipid. When algal lipid content was calculated from the SPV assay, *ST* appeared to have the highest amount of lipid (0.89 wt.%) followed by *UF* (0.45 wt.%) and *GC* (0.36 wt.%) (Fig 3.5). In all cases it was observed that the lipid content as estimated by the SPV assay was much lower than the amount of crude (total) lipid gravimetrically determined (Fig. 3.4). This is because non-saponifiable matter would also get included during solvent extraction and a gravimetric approach would thus also estimate all chloroform-soluble material such as pigments and other hydrophobic components (Higgins et al., 2014).

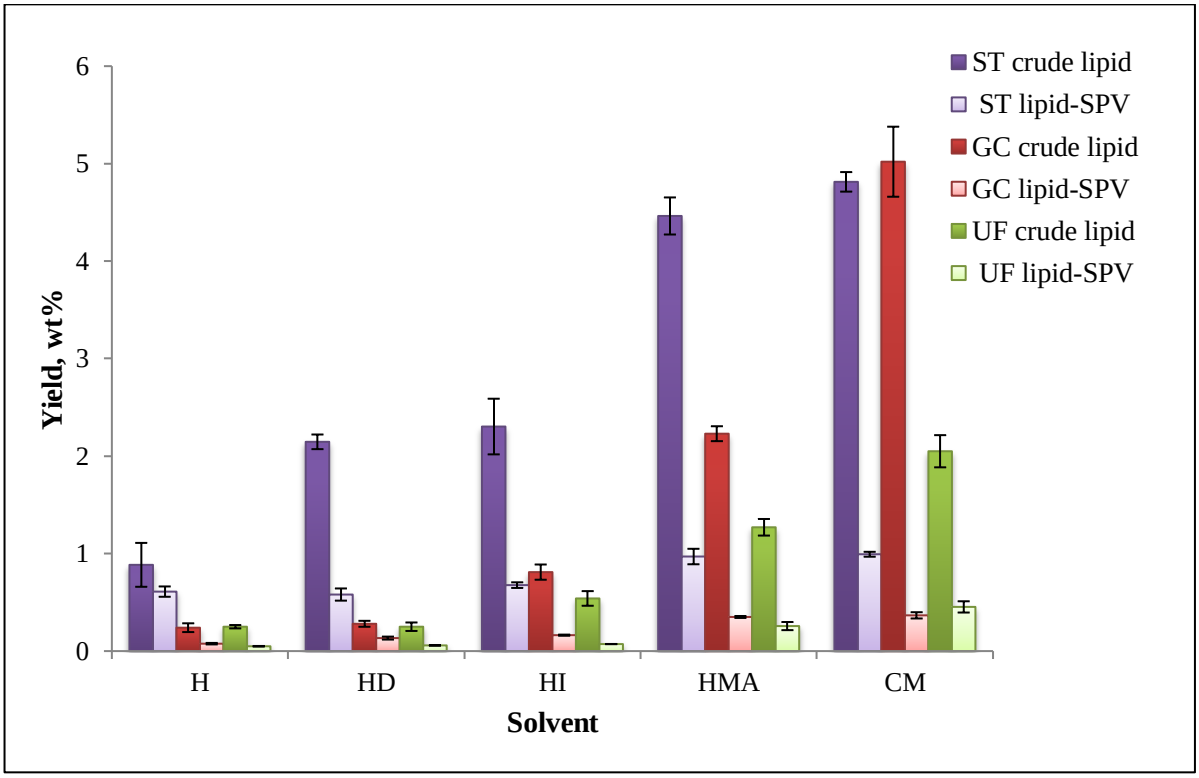

Fig. 3.5: Effect of solvents on crude macroalgal lipid and SPV assay-derived lipid content of the algae

3.4.4. Effect of pretreatment on the lipid content as determined by the SPV assay

Crude algal lipid extracts of *ST*, *GC* and *UF* obtained after subjecting the dry algal powder to various pre-treatments were analyzed by the SPV assay to evaluate which pretreatment method would better facilitate extraction of the lipid suitable for subsequent conversion to biodiesel. There was a considerable increase of lipid extracted in treated samples of *GC* and *UF*, the lipid yield having increased around 1.6-fold upon sonication and doubled in pre-autoclaved samples, although a combination of the two treatments was not effective (Fig. 3.6). Pre-treatments did not bring about a significant change in lipid output in samples of *ST*.

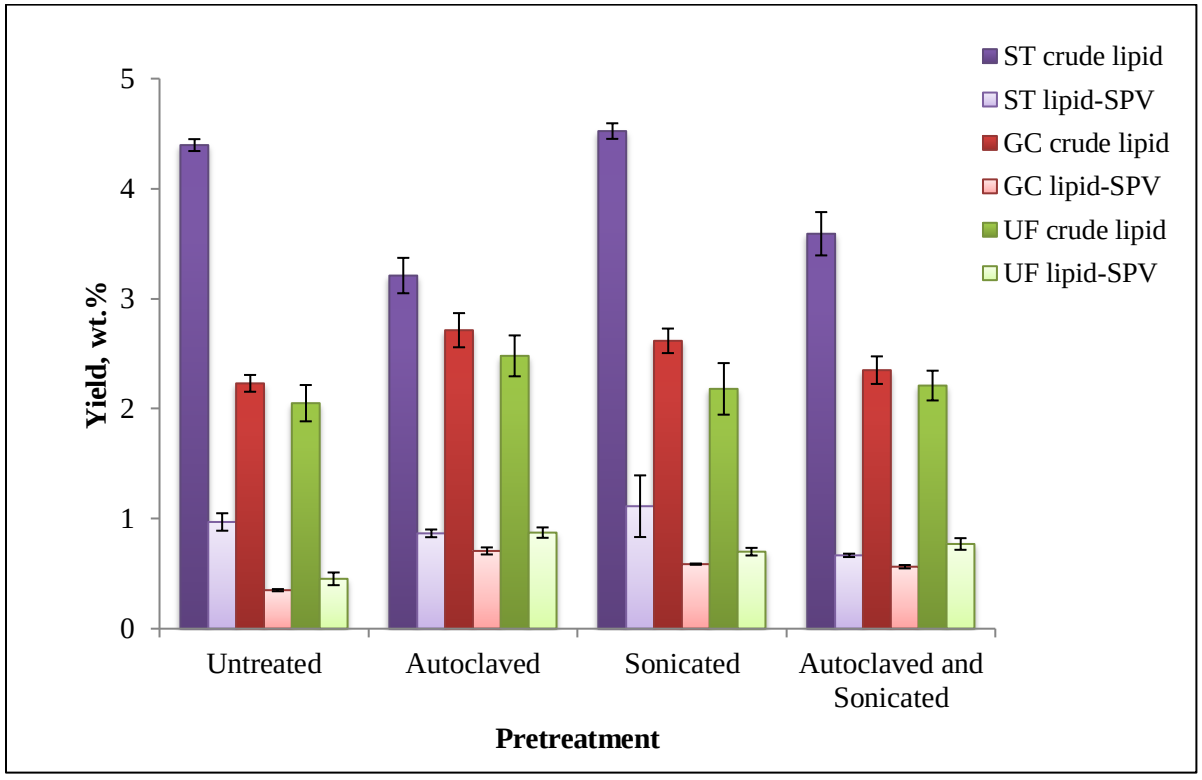

Fig. 3.6: Effect of pretreatment on crude macroalgal lipid and SPV assay-derived lipid content of algae

The SPV procedure brings down the possibility of overestimating lipids since non-specific products would be degraded by acid-thermal treatment (Mishra et al., 2014). It should be noted that the occurrence of various fatty acids in the extracted lipid would limit the precision

of this method (Byreddy et al., 2016), the color intensity varying from one lipid type to another due to differences in fatty acid structures. Molecules without double bonds do not measurably react with sulfo-phospho-vanillin reagent. This could be corrected for by selecting an appropriate reference oil with approximately the same fatty acid content. Olive oil was used for the present study, algal bio-oils with their higher unsaturated fatty acid ratio being relatively close in composition to vegetable oils (Cheng et al., 2011b).

Studies that have been carried out using the SPV assay to quantify lipids mostly aim at direct lipid analysis (specifically from microalgae) without any extraction step, thus saving on time during the screening for biodiesel potential (Mishra et al., 2014; Byreddy et al., 2016; Hao et al., 2013). In contrast, the present study focuses on quantifying lipids only from the crude algal lipid (oil) obtained from macroalgae after solvent extraction, which is what is actually used as the base for biodiesel production. Our SPV assay results showed that the amount of lipid extracted was proportional to the amount of crude algal lipid (by weight) obtained from *ST*, *GC* and *UF*.

The above results have demonstrated the utility of the Nile Red staining technique and the SPV reaction to gauge the lipid content of macroalgae. The qualitative analysis coupled with a quantitative approach has provided a simple and rapid strategy to detect even low amounts of lipid from environmental macroalgal samples. These methods involve minimum use of chemicals and would be useful as a primary step for the rapid and extensive screening of potential algal sources for biodiesel production.

Chapter IV

Optimization of Solvent Extraction Parameters for Biodiesel Production from Macroalgae

Extraction is one of the most important steps for obtaining lipid from macroalgal biomass for the production of biodiesel. Preferably, an extraction method to be used for lipid content analysis should be able to achieve complete lipid recovery with high selectivity. Organic solvent extraction is the most general and widely used method for lipid extraction. Traditionally, the Soxhlet apparatus (Fig. 4.1) has been used for lipid extraction, as evident from many studies (Cheung et al., 1998; Sheng et al., 2011; Halim et al., 2011; Sanchez et al., 2012; McNichol, 2012; Araujo et al., 2013; Balasubramaniam et al., 2013). It consists of three parts: (i) a round-bottom flask to contain the extracting organic solvent, (ii) the Soxhlet extractor to hold the macroalgal biomass (which is in the form of dried powder) and (iii) the condenser which is continuously cooled by running water. The round-bottom flask is kept heated using a heating mantle and the organic solvent from the flask starts vapourising to enter the condenser. As it enters the condenser, droplets of the solvent form and are gradually chanelled into the Soxhlet extractor. Here, the organic solvent comes in contact with the macroalgal biomass and enables lipid extraction. Macroalgal biomass is placed in a thimble in the extractor, which prevents the biomass from being carried away by the organic solvent flow and also serves as a filter to remove cell debris. Once the organic solvent in the extractor reaches the overflow level, a siphon unloads the organic solvent-lipids mixture from the extractor back into the round-bottom flask. The organic solvent gets heated and evaporates again while the extracted crude lipids remain in the round-bottom flask. This cycle is repeated until no more crude lipids are extracted in the Soxhlet extractor (Halim et al., 2012a). The Soxhlet apparatus constantly replenishes the biomass to be extracted with fresh organic solvent through its resourceful cycles of solvent evaporation and condensation, while at the same time minimizing the use of solvent.

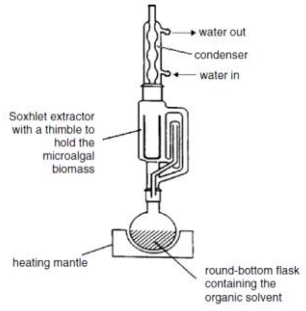

Fig 4.1: Soxhlet apparatus (from Halim et al., 2012a)

4.1. EFFECT OF SOLVENTS ON ALGAL LIPID EXTRACTION EFFICIENCY

Lipid extraction is in general based on the simple fact that lipids are insoluble in water but soluble in organic solvents (Halim et al., 2012a) and selection of an appropriate solvent thus becomes one of the most important tasks towards the development of an efficient lipid extraction method. A suitable extraction solvent should exhibit the properties of being not too soluble in water and have a density significantly different from that of water (Ryckebosch et al., 2013). The solvent should be easy to recover, have a lower boiling point and the viscosity should be low enough to ensure high mass transfer efficiency. Also, the solvent should be easily available, reasonably priced and the environmental impact of the whole extraction procedure should be minimal (Mercer and Armenta, 2011). A large variety of solvents have been proposed for extraction of lipids from various algal samples. One must particularly take into account the polarity of the solvent because lipid extraction yield highly depends on the solvent, lipids being bipolar in nature (Li et al., 2014c; D'Alessandro et al., 2016). For plant, animal or microbial cells, the lipids are enclosed in the cytoplasmic membrane, which is a bilayer membrane composed primarily of phospholipids bearing a polar head and two nonpolar tails (Fatty acid residues), with the former facing the hydrophilic environment and the latter facing each other to form a hydrophobic barrier. During extraction, the polar solvent first penetrates the cell wall to extract the polar lipid fraction. Polar solvents, however, have relatively low solubility of neutral lipids and low selectivity towards neutral lipids over polar ones. Non-polar solvents are thus necessary to increase both the selectivity and the efficiency of lipid extraction from cells, be they from microbial, plant, or animal cells (Soares et al., 2014). In most laboratory practices, both non-polar organic solvent and polar organic solvent are added to the macroalgal biomass to ensure the complete extraction of all neutral lipids, both in the form of freestanding globules and in the form of membrane-associated lipid complexes (Halim et al., 2012a).

Hexane is the most widely used nonpolar organic solvent to extract lipids from microalgae and macroalgae (Miao and Wu, 2006; Halim et al., 2011; Ryckebosch et al., 2012; Ambrozova et al., 2014; Schmid et al., 2016). Although hexane is reported to be one of the best solvents for lipid extraction, the overall efficiency is relatively low as a portion of the neutral lipids are held in the cytoplasm as a complex with polar lipids (Theegala et al., 2015).

Releasing lipids from this complex is not easy as the complex is strongly linked *via* hydrogen bonds to proteins in the cell membrane (Halim et al., 2012a). Due to this limitation, only a portion of the neutral lipids are extracted. The polar lipids in biomembranes, on the other hand, are in intimate contact with the aqueous phase of the electrolytes (Enssani, 1990) and the presence of membrane wetting media such as polar solvents is required for effective extraction. These limitations led to the development of co-solvent based extraction procedures. The co-solvent extraction method relies on the concept of "like dissolves like" and employs a combination of two solvents for effective extraction. Lipids that are largely hydrophobic (neutral lipids) will favorably interact with relatively non-polar solvents (such as chloroform, ethyl ether or benzene), while membrane-associated polar lipids will require polar solvents (such as ethanol, methanol or isopropanol) to disrupt the hydrogen bonding and electrostatic forces between the lipids and proteins (Kates 1986; Cooney et al., 2009).

Folch et al. (1957) were the first researchers to report a chloroform/methanol/water phase system for extraction of lipids from biological materials. This method, a popular choice for lipid extraction and which has been used for a long time, involves the solvent mixture chloroform-methanol. It was initially optimized for extraction of total lipids from animal tissues and uses chloroform-methanol (2:1) as the solvent. The method of Bligh and Dyer (1959) was basically used for measuring the lipid content in samples such as mammalian cells which do not contain chlorophyll. Subsequently, it has been adopted for various cell types, including those that contain chlorophyll (Archanaa et al., 2012). This method uses chloroform-methanol (1:2) for extraction of the lipids.

Various studies have proven the efficiency of chloroform:methanol as an effective choice of solvent system for lipid extraction. Ryckebosch et al. (2012) investigated the effect of seven solvent mixtures at different ratios on *Chlorella vulgaris*, and showed that extraction efficiency was highest using chloroform/methanol (1:1), followed by chloroform/methanol (2:1), dichloromethane/ethanol (1:1), hexane/isopropanol (3:2), acetone, diethyl ether, and methyl-tert-butyl ether/methanol (10:3). Sheng et al. (2011) reported that the Folch as well as the Bligh & Dyer methods elicited highest lipid recoveries from the cyanobacterium *Synechocystis*, when compared other solvents. Ambrozova et al. (2014) compared the Bligh & Dyer method and the use of hexane solvent on various microalgae (*Chlorella pyrenoidosa*,

Spirulina platensis and *Chlorella kessleri*) and macroalgae (*Porphyra tenera, Laminaria japonica, Undaria pinnatifida)* and inferred the Bligh & Dyer to be more effective. Araujo et al. (2013) carried out lipid extraction on *Chlorella vulgaris* and reported the Bligh and Dyer method to be better than those of Folch et al. (1957) and Hara and Radin (1978). Other solvents such as acetone (Jeong and Park, 2015; Ren et al., 2017), chloroform (Mercer and Armenta, 2011), methylene chloride (Anthony and Stuart, 2015), methanol, ethanol and butanol (Sheng et al., 2011) have also been investigated for lipid extraction. Ryckebosch et al. (2013) investigated various solvent systems for extractability of lipid components from the microalga *Nannochloropsis gaditana* and reported highest lipid yield in dichloromethane:ethanol (1:1), followed by chloroform:methanol (1:1), hexane:isopropanol (3:2), ethanol, ethyl acetate:hexane (2:3), hexane, ethyl acetate and acetone. While many lipid extraction methods have been investigated for microalgae, relatively few have been evaluated for use on macroalgae. Suganya et al. (2013) obtained lipid by microwave pretreatment and Soxhlet extraction using a solvent system of 1% diethyl ether and 10% methylene chloride in n-hexane. Shalaby et al. (2010) carried out studies on biodiesel production from different species encompassing the various macroalgal types, and observed that hexane/ether (1:1) and chloroform/methanol (2:1) yielded best results. Kumari et al. (2011) carried out a comparative evaluation and selection of a method for lipid extraction from the macroalgae, *Ulva fasciata*, *Gracilaria corticata* and *Sargassum tenerrimum*. Borghini et al. (2013) analyzed *Chaetomorpha linum*, *Gracilariopsis longissima* and *Ulva lactuca* lipids using the Bligh and Dyer method. Suganya and Renganathan (2012) analyzed various solvents for lipid extraction of *U. lactuca*, out of which 1% diethyl ether and 10% methylene chloride in n-hexane proved the most efficient. Renita et al. (2014) extracted lipids from *Sargassum myriocystum* using hexane and chloroform:methanol (2:1), optimized production of methyl esters using RSM and evaluated biodiesel storage characteristics. Martins et al. (2012), in their extensive study comparing three extraction methods with different solvents and using three different macroalgae *Hypnea musciformis*, *Sargassum cymosum* and *Ulva lactuca*, found that lipid extraction efficiency differed with biomass type as well as with the solvent system.

4.2. TRANSESTERIFICATION OF CRUDE ALGAL LIPID TO PRODUCE BIODIESEL

The production of biodiesel from algae essentially involves two main steps (i) lipid extraction from the biomass followed by (ii) conversion (transesterification) of lipids (FAs) to biodiesel (alkyl esters). To date, biodiesel production from algal biomass is usually achieved by one of the following three methods: (i) a two-step protocol in which algal oil is extracted with organic solvent and then transesterified to biodiesel using an acidic / alkaline / enzyme catalyst; (ii) direct production of biodiesel from algal biomass using an acid catalyst at atmospheric pressure and ambient temperature; and (iii) a one-step, single pot conversion to biodiesel at high pressure and high temperature in the absence of a catalyst (Chen et al., 2012a; Martinez-Guerra et al., 2014; Nelson and Viamajela, 2016).

Commonly, biodiesel is produced by the process of transesterification. Transesterification (also called alcoholysis) is basically the reaction of a fat or oil with an alcohol in the presence of a catalyst, to form esters and a byproduct, glycerol (Vyas et al., 2010). Transesterification consists of a sequence of three successive reversible reactions. Firstly, the conversion of triglycerides to diglycerides, followed by that of diglycerides to monoglycerides, and the final reaction of monoglycerides into glycerol, yielding one ester molecule from each glyceride at each step (Meher et al., 2006). The transesterification reaction is reversible, which implies that a greater amount of alcohol is generally needed to shift/force the reaction equilibrium to the product side (Aransiola et al., 2014). The stoichiometry for the transesterification reaction is theoretically 3:1 (alcohol to lipids), but in practice, the ratio usually needs to be higher (6:1 or more) to raise the product yield (Ma and Hannah, 1999; Sharma et al., 2008).

The alcohols generally used for transesterification are primary or secondary monohydric aliphatic alcohols having 1- 8 carbon atoms (Demirbas, 2005). Methanol and ethanol are the most frequently used alcohols in biodiesel production (Meneghetti et al., 2006; Anastopoulos et al., 2009; Suganya et al., 2013; Mandotra et al., 2014; Musa, 2016; Abomohra et al., 2018). Methanol is particularly preferred because of its physical and chemical (polar and shortest chain alcohol) advantages. Also, it is less costly and its reaction with triglycerides is quick. Various studies have reported the use of methanol (Antolin et al., 2002; Encinar et al., 2011; Chai et al., 2014) for transesterification with promising results. While triglycerides can react

with varieties of other alcohols such as ethanol, butanol, propanol, isopropanol or branched alcohols, these are costly and less effective, the short-chain alcohols providing better conversions under the same reaction time (Musa, 2016).

The nature of the catalyst used during transesterification is of prime importance in the reaction. Various catalysts have been investigated for converting triglycerides to biodiesel fuel, the frequently used being homogeneous catalysts and heterogeneous catalysts (Atadashi et al., 2013).

Direct use of solvent-extracted oil as biodiesel exhibits a limitation in terms of its higher viscosity than petroleum diesel. The high viscosity of oil affects the injection process and atomization of fuel. To overcome these problems, it is imperative to carry out the process of transesterification (Knothe, 2010; Maulidiyah et al., 2017).

4.2.1. Homogeneous Alkaline Catalysts

The most commonly used homogeneous alkaline catalysts are KOH (Thanh et al., 2013), NaOH (Kumar et al., 2013), CH_3ONa (Sharma et al., 2014), and CH_3OK (Griffiths et al., 2010; Ramos et al., 2009). These catalysts have the advantage of being able to perform under moderate temperatures in a short span of time (Lopez et al., 2015). Of these, CH_3ONa or CH_3OK are better and considered more suitable than NaOH and KOH (Demirbas, 2009) in terms of a better yield. However, the industrial biodiesel production process mostly employs NaOH and KOH because of lower costs (Fukuda et al., 2001). Leung and Guo (2006) compared various alkali catalysts and revealed that industrially, separation of esters is much easier when KOH catalyst is used compared to NaOH or CH_3ONa. Onukwuli et al. (2017) and Antolin et al. (2002) transesterified cottonseed oil and sunflower oil, respectively, with methanol, and using alkaline catalyst KOH to produce biodiesel. Vicente et al. (2004) compared different basic catalysts (CH_3ONa, CH_3OK, NaOH and KOH) for methanolysis of sunflower oil. The bio-diesel purity was close to 100 wt.% for all catalysts; high yields were obtained with sodium and potassium methoxide (99.33 wt.% and 98.46 wt.%, respectively). For alkali transesterification, however, the free fatty acid (FFA) content should not exceed a certain limit. In fact, the process was found unsuitable for producing esters if the FFAs were greater than 3% (Demirbas, 2009; Atadashi et al., 2013). Alkaline catalysts react with FFAs to

cause soap formation which leads to deactivation of catalyst and hindrance to the biodiesel purification process (Lotero et al., 2005). Presence of water in the feedstock leads to hydrolysis of oils to FFAs, which again encourages saponification. The feedstocks used in alkali-catalyzed transesterification therefore need to be anhydrous (Fukuda et al., 2001). Ideally, in order to prevent saponification during the reaction, FFA and water content of the feed must be below 0.5 wt.% and 0.05 wt.%, respectively, as per Vyas et al. (2010).

4.2.2. Homogeneous Acid Catalysts

Acid transesterification would be more suitable for feedstocks with high FFAs (Lotero et al., 2005). The most common acids used in the transesterification reaction include sulfuric acid and hydrochloric acid (Martins et al., 2012). Homogeneous acid-catalyzed reactions are about 4000 times slower than the homogeneous base-catalyzed reaction but the performance of the acid catalyst is not strongly affected by the presence of FFAs in the feedstock. In fact, acid catalysts can simultaneously catalyze both esterification and transesterification, providing a great advantage by being able to directly produce bio-diesel from low-cost lipid feedstocks generally associated with high FFA content; low-cost feedstocks such as used cooking oil and greases commonly have FFA levels over 6% (Canacki and Gerpen, 1999; Lotero et al., 2005). Chai et al. (2014) reported that sulfuric acid was suitable to carry out both direct esterification and transesterification reactions simultaneously, effectively converting used cooking oil containing high amount of FFAs. Supaporn and Yeom (2016) compared the transesterification of the blended sewage sludge lipid with methanol, wherein an acidic catalyst (H_2SO_4) showed improved performance over an alkaline catalyst (NaOH).

4.2.3. Two-step Acid-alkali Transesterification Process

This two-step process is useful for feedstocks containing high FFAs as alkaline catalysts cannot directly catalyze the transesterification of oil derived from them (Canacki, 2007). In this method, the first step is an acid-catalyzed process which involves esterification of the FFAs to fatty acid methyl esters (FAMEs) (Suganya et al., 2013), followed by a second alkali-catalyzed transesterification step. Various studies have first employed acid-catalyzed transesterification to decrease the content of FFAs before performing alkali-catalyzed transesterification on biodiesel sources such as animal fats (Encinar et al., 2011) and *Ceiba*

petandra oil (Sivakumar et al., 2013) which contain high FFAs. Chen et al. (2012a) produced biodiesel from the oil of microalga *Scenedesmus* using a two-step catalytic conversion. The conversion rate of triacylglycerols touched 100% under the methanol to oil molar ratio of 12:1 during catalysis with 2% KOH at 65 °C for 30 min. In another study, Chongkong et al. (2007) transesterified high FFA containing palm fatty acid distillate. The amount of FFAs was reduced from 93 wt.% to less than 2 wt.% at the end of the esterification process. Adopting a two-step transesterification technique could thus provide high biodiesel conversion of up to 98%. Thiruvengadaravi et al. (2012) also found the two-step process more effective for oils with high FFA content.

4.2.4. Heterogeneous Catalysts and Enzyme Catalysts

Heterogeneous catalysts and enzyme catalysts have been employed of late to catalyze the transesterification reaction for producing biodiesel. Deepalakshmi et al. (2015) used nano-size calcium-based heterogeneous catalyst derived from lime sludge to produce biodiesel from *Calophyllum inophyllum*. In a study by Thiruvengadaravi et al. (2012), 1% sulfated Zirconia was used as an acid catalyst to transesterify *Pongamia pinnata* oil. Dong et al. (2013) efficiently converted the FFAs of *Chlorella sorokiniana* into FAMEs using Amberlyst-15 as catalyst. Zhang et al. (2010) carried out ferric sulfate-catalyzed esterification followed by transesterification using calcium oxide (CaO) as an alkaline catalyst, from *Zanthoxylum bungeanum* seed oil with high FFAs. Heterogeneous catalysts offer many advantages over homogeneous catalysts, such as simpler catalyst recovery, reusability of catalyst, easier product purification, less consumption of water and energy and quicker glycerol recovery (Georgogianni et al., 2009).

Enzyme catalysts have also been researched in production of biodiesel from microalgae (Navarro et al., 2016) as well as vegetable oils (Hernandez-Martin & Otero, 2008). Biodiesel was synthesized using commercial immobilized enzymes (Novozym 435 and Lipozyme RM IM from Novozymes, as reported by Lee et al. (2011). Tran et al. (2013) developed a one-step extraction/transesterification process to directly convert wet oil-bearing microalgal biomass of *Chlorella vulgaris* ESP-31 into biodiesel using immobilized *Burkholderia* lipase as the catalyst. Iso et al. (2001) successfully used immobilized *Pseudomonas fluorescens* lipase for

transesterification of safflower oil and lipase from *Chromobacterium viscosum* was studied for the transesterification of *Jatropha curcas* oil by Shah et al. (2004). The cost factor, however, continues to be a retardant for the use of enzyme catalysts.

4.2.5. *In situ* Transesterification

Direct transesterification (DT) is a method of directly converting saponifiable lipids *in situ* to FAMEs which can be quantified by gas chromatography. This avoids the extraction step and results in a rapid, single-step procedure appropriate for small samples (Dong et al., 2013). Martinez-Guerra et al. (2014) described the use of microwaves for enhanced extractive-transesterification of algal lipids from dry algal biomass (*Chlorella* sp.). In a study by Sivaramakrishnan et al. (2016) the optimized two-step transesterification and direct transesterification showed similar yields for both the microalgae *Chlorella* sp. and *Scenedesmus* studied. Suganya et al. (2014a) carried out *in situ* transesterification on *Enteromorpha compressa*, a green macroalga**.**

4.3. FUEL PROPERTIES OF ALGAL BIODIESEL

Biodiesel produced after transesterifying the parent triacylglycerols (TAGs) can sometimes contain not only the desired alkyl ester product but also some unreacted starting material (TAG), residual alcohol and residual catalyst. Glycerol is formed as by-product and separated from biodiesel but traces thereof can be found in the final biodiesel product. Since transesterification is a stepwise process, mono- and di- acylglycerols formed as intermediates may also be found in biodiesel. Biodiesel standards such as those in the United States (ASTM D6751), Europe (EN 14214) and India (BIS IS 15607:2005) stipulate the permissible limit of contaminants in biodiesel fuel (Appendix B). As per these standards, restrictions are placed on the individual contaminants by inclusion of parameters such as free and total glycerol for limiting glycerol and acylglycerols, flash point for limiting residual alcohol, acid value for limiting FFA, ash value for limiting residual catalyst, *etc*. Sustainably high fuel quality with no operational problems is a prerequisite for market acceptance of biodiesel.

Very often, as is commonly the case for macroalgal biodiesel, it may be impossible to obtain a sufficiently large sample of biodiesel from an emerging feedstock oil for detailed analyses.

Notwithstanding this, the properties of a biodiesel may be predicted using information on the fatty acid (FA) profile of the parent oil, as all the relevant properties depend directly on the FA composition of the feedstock oil. A user-friendly public domain computer software, the Biodiesel Analyzer©, for estimating the properties of a biodiesel from the FA profile of the parent oil was used (Talebi et al., 2014). Biodiesel Analyzer Version 1.1 was released in the public domain on January 13, 2014, by the Biofuel Research Team (BRTeam). It is a useful tool for estimating the properties of a prospective biodiesel if the FA profile of the parent oil is known, or a small sample of the oil is available for analysis.

4.4. MATERIALS AND METHODS

4.4.1. Soxhlet Extraction of Crude Algal Lipid

Macroalgal powder (10 g) was fed in a thimble and inserted carefully into a Soxhlet extractor fitted with a round-bottom flask containing a specific organic solvent. The extraction was optimized for various parameters as discussed below. Upon completion of extraction, the organic phase was separated and evaporated at 50 °C using a rotary evaporator, collected in a pre-weighed flask and then heated to dryness in an oven at 60 °C to allow gravimetric quantification of the lipid extract. The crude algal lipid was re-dissolved in hexane/chloroform (approx. 15-20 ml) and transferred into a sealed glass vial for storage at -20 °C until further analysis. The gravimetric analysis was carried out in triplicate. The weight of the lipid was then calculated as wt.% of dry biomass.

4.4.2. Parameters Affecting Algal Lipid Extraction

4.4.2.1. *Use of different solvents*

Five different solvent mixtures were investigated as described in Chapter III (Section 3.3.3.)

Experiments were carried out in triplicate, using 10g of the algal sample each time. The process of Soxhlet extraction was carried out at 60 °C for (i) an initial 6h and (ii) a further 6h period. The solvent mixture was then evaporated at 50-60 °C using a rotary evaporator. The weight of the crude algal lipids obtained was then calculated as wt.% of dry biomass. Results were confirmed by repeating the experiments until values were consistently reproducible and

the data are presented as mean ± SD. The yields obtained were compared by analysis of variance (ANOVA), with values considered significant at $p < 0.05$.

4.4.2.2. *Solvent extraction period*

Extraction time is a significant parameter to be considered for optimal yield. The effect of time on algal crude lipid extraction was looked into in a two-stage process wherein the initial extraction of 6h was followed by a second round of extraction for a further 6h.

4.4.2.3. *Pretreatment of algal samples*

The pretreatments methods employed were as outlined in Chapter III (Section 3.3.4). The pretreated samples were subjected to crude lipid extraction using the selected solvent system. Average extracted crude lipid content of each method is reported as wt.% of dry biomass.

Reports from literature had indicated that sonication in distilled water would facilitate extraction of algal lipid content (Suganya and Renganthan, 2012). Algal samples were therefore also sonicated with water (water to biomass ratio of 4:1). Extraction was thereafter carried out in triplicate for 6h, using the specific solvent system.

4.4.2.4. *Solvent-to-solid ratio*

The solvent-to-solid ratio was determined for the crude lipid extraction from algal biomass. Different solvent-to-solid ratios ranging from 7:1 to 15:1 (solvent:solid) were tested. The experiments were carried out in triplicate using 10g of the algal sample each time. The solvent system and duration of extraction were kept unchanged. No pretreatment was carried out on the macroalgae before lipid extraction. Results were confirmed by repeating the experiments until values were consistently reproducible and the results are presented as mean ± SD.

4.4.3. Characterization of the Crude Algal Lipid

The crude lipid extract was dissolved in chloroform:methanol (1:1) and then washed with 10% NaCl solution in a separating funnel. After vigorous mixing and standing for several minutes, an upper and lower phase established (Fig. 4.2). The lower chloroform phase containing crude lipid was collected and used for further analysis.

Fig. 4.2: Crude lipid chloroform extract

4.4.3.1. *Removal of chlorophyll pigment*

Chlorophyll pigments in the lipid extract need to be removed as they could cause oxidation problems for the biodiesel at the industrial level (Soares et al., 2014). The chlorophyll pigments in the algal crude lipid were removed using activated fine charcoal powder (Fig. 4.3). The decolourized extract was used for further analysis.

Fig 4.3: Activated charcoal filtration

4.4.3.2 *Analysis of crude algal lipid*

a. ***Acid Value:***

The acid value is defined as milligram potassium hydroxide required to neutralize the FFAs present in one gram of fat. For alkali transesterification, the FFA content should be less than 1-3% (Vyas et al., 2010) to avoid soap formation leading to losses in biodiesel yield. A specific amount of lipid was dissolved in fat solvent and few drops of phenolphthalein were used as an indicator. The solution was titrated against 0.1 N KOH until pink color developed. The acid value was calculated using the formula:

Acid value (mg KOH/g) = Titre value x Normality of KOH x 56.1 / Weight of sample (g)

b. ***Iodine Value:***

The iodine value is a measure of the unsaturation of fats and oils and is defined as gram of iodine absorbed by 100g of the oil/fat, when determined by using Wij's solution (g I/ 100 g). Standards EN 14214 require the iodine value of biodiesel to not exceed 120 g iodine/100 g biodiesel (Chisti, 2007). A specific amount of lipid was dissolved in chloroform. Wij's iodine solution was added, mixed and allowed to stand in the dark for 30 min with occasional shaking. Then a 15% KI soloution was added to this mixture along with a certain amount of water to wash down any residual iodine on the stopper. The solution was titrated against 0.1 N sodium thiosulphate until the yellow solution turned almost colorless. Finally a few drops of starch indicator were added and titrated until the blue color disappeared. The iodine value was calculated using the formula:

Iodine number = (B-S) x N x 12.69 / Weight of sample (g)

where, B = ml thiosulphate for blank, S = ml thiosulphate for sample, N = normality of sodium thiosulphate

c. ***Saponification Value:***

The saponification value is defined as mg of KOH required to saponify 1 gram of oil/fat. Lower the saponification value, larger would be the molecular weight of FAs in the glycerides

and vice-versa. A specific amount of lipid was dissolved in alcoholic KOH and refluxed for 1h. A blank which contained only alcoholic KOH was maintained at the same time. After the solution cooled, phenolphthalein indicator was added and the solution titrated against 0.5 N HCl until the pink color disappeared. The saponification value was calculated using the formula:

Saponification value (mg KOH/g) = 28.05 x (titre value of blank - titre value of sample) / weight of sample (g).

4.4.4. Transeterification of the Crude Algal Lipid Extracted

A two-step process, *viz*., acid esterification using H_2SO_4 to reduce FFA, followed by alkali transesterification using KOH (Chen et al., 2012a) and NaOH (Suganya et al., 2013) was implemented for the production of biodiesel from algae. Acid esterification was performed at 65°C for 1.5 hrs at 8:1 ratio (methanol:lipid) and with 1 wt. % H_2SO_4 as catalyst. The esterified algal lipid thus obtained was further transesterified with an alkaline catalyst (1%). The alkaline catalyst was mixed with 65 °C heated esterified algal lipid. The methanol and lipid molar ratio were maintained at 10:1 throughout the transesterification process. Thereafter, FAMEs were extracted using hexane (3:1) and evaporated to dryness under nitrogen.

The transesterification process was further optimized using two protocols involving three different catalysts: (1) Two step acid-alkali transesterification using (i) NaOH and (ii) KOH and (2) Acid transesterification using HCl (Cavonius et al., 2014).

4.4.5. Characterization of FAMEs by Chromatographic Procedures

Fatty acid methyl esters (FAMEs) produced from crude algal lipid were analyzed by GC-HRMS. A SHIMADZU, (GCMS-QP2020) gas chromatograph equipped with a split injector was used. The capillary column used was BPX5. Initial temperature of the oven was 70ºC, which was then raised to 275 °C at a rate of 10 ºC min^{-1} and maintained at this temperature for 5 min. It was heated again to 280ºC at a rate of 5 °C min^{-1}. The injector temperature was maintained at 280 ºC in split mode with a split ratio of 10:1 for an injection volume of 1 µl. The oven temperature was maintained at 310 °C. For the identification and

quantification of FAMEs, their retention times were compared with those of standards. The values are expressed as percentage of the total FA content.

4.4.6. Analysis of the Biodiesel

The biodiesel obtained from the three macroalgae *ST*, *GC* and *UF* was analyzed for the tenable physicochemical properties using the Biodiesel Analyzer software© (http://www. brteam.ir/biodieselanalyzer). The FA values were taken as an input in predicting the biodiesel properties using the open access software. The properties such as acid value, pour point, flash point, viscosity, cetane number were analysed in relation to ASTM D6751 specifications and BIS IS 15607:2005 (Barabas & Todoruţ, 2010).

4.5. RESULTS AND DISCUSSION

4.5.1. Effect of Different Solvents on Crude Algal Lipid Extraction Ability

Crude algal lipid yield from the biomass of the three macroalgal species was estimated after extraction using five different solvent systems (Table 4.1). In the case of *ST*, the lowest yield of 1.12% (w/w of dry algal biomass) was obtained when hexane was used alone, significantly less ($p<0.05$) than those using other solvents. There was no significant difference in the yield obtained between solvents HD and HI. The highest yield of 5.90% was obtained with CM solvent (1:2), closely followed by 5.45% with HMA (3:1:1) which were significantly higher than from the other solvent systems. In the case of *GC*, no significant difference was observed ($p>0.05$) between solvents H and HD, the lowest yield being obtained with hexane, whereas CM gave a maximum yield of 5.61%, significantly higher ($p<0.05$) as compared to all the other solvents. Similarly, in the case of *UF*, no significant difference was observed ($p>0.05$) between solvents H and HD, the lowest yield being obtained with hexane and the highest with CM (significantly higher as compared to HMA and other solvents).

The macroalgal lipid yield obtained in our studies was higher than that obtained by Kumari et al. (2011) from *U. fasciata*, *G. corticata* and *S. tenerrimum* (2.2%, 1.8%, and 1.9% respectively). Thus in all cases, combination of polar and non-polar solvents could be more efficient better extracting the lipids (Ryckebosch et al., 2012). In the present study, since highest extraction yield was generally obtained in the chloroform/methanol (1: 2, v/v) solvent

system, this was chosen as the extraction solvent in subsequent evaluations; it would also work out more effective than HMA, which at times elicited comparable yields. As also reported in other studies, CM as solvent proved better for extraction of lipid from green macroalga *Enteromorpha intestinalis* (Jeong and Park, 2015), wherein among 13 options of organic solvents, the chloroform/methanol (2:1, v/v) system emerged the best. Similar results were obtained by Shalaby et al. (2010) who carried out studies on biodiesel production from different types of algae. In their studies on *U. lactuca*, Suganya and Renganathan (2012) analysed various solvents for their extraction efficiency, out of which 1% diethyl ether and 10% methylene chloride in n-hexane was considered superior to the other solvents used.

Table 4.1: Crude lipid yield after extraction using various solvents

Solvent	Crude lipid yield (wt.%)		
	ST	**GC**	**UF**
H	$1.12 \pm 0.16^{b,c}$	0.28 ± 0.06^{a}	0.27 ± 0.02^{a}
HD	2.26 ± 0.08^{d}	0.30 ± 0.05^{a}	0.28 ± 0.04^{a}
HI	$2.77 \pm 0.25^{d,e}$	1.34 ± 0.13^{c}	$0.59 \pm 0.07^{a,b}$
HMA	5.45 ± 0.32^{f}	2.87 ± 0.17^{e}	1.50 ± 0.03^{c}
CM	5.90 ± 0.35^{f}	5.61 ± 0.24^{f}	$2.50 \pm 0.13^{d,e}$

(Each value is the mean ± SD of three replicates. Within each column, different superscript letters are statistically significant (ANOVA, $p<0.05$ and subsequent post hoc multiple comparison with Tukey HSD test)

4.5.2. Effect of solvent extraction period on crude algal lipid yield

Extraction time is a significant parameter to be considered for optimal yield. The effect of time on algal lipid extraction was looked into in a two-stage process wherein the initial extraction of 6h was followed by a second round of extraction for a further 6h. In most

solvents, maximum lipid yield was obtained even in the first round of extraction, further increase in extraction time not showing any significant improvement on it (Fig. 4.4).

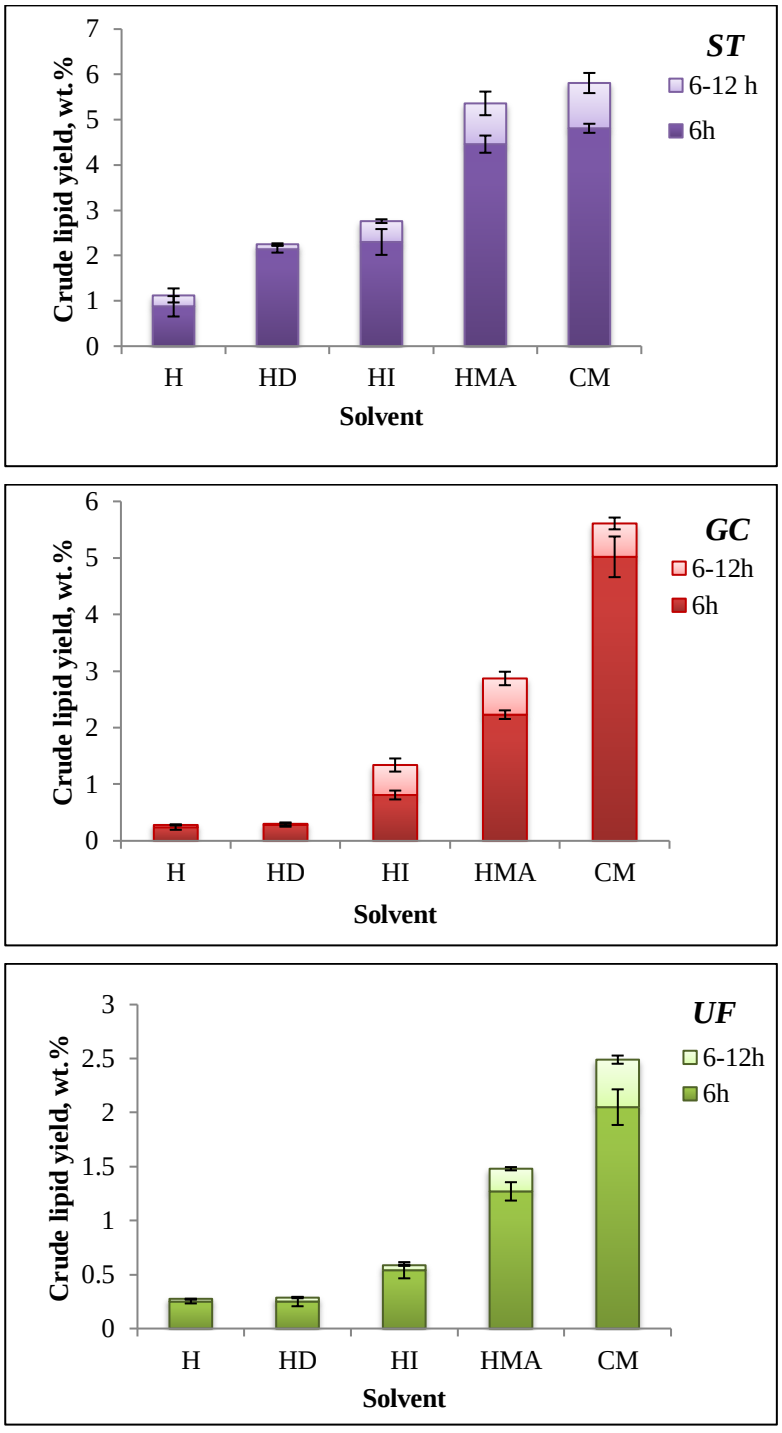

Fig 4.4: Variation of algal lipid yield with extraction time period

An extraction period of 6 h was hence opted for further studies. Optimization studies have been conducted for obtaining maximal lipid yield from macroalgal biomass, with respect to duration of extraction (Suganya and Renganathan, 2012; Jeong and Park; 2015).

4.5.3. Effect of Pretreatments on Crude Algal Lipid Yield

Different algae have different cell disruption tendencies and as a result, no single method can be universally applied to the various algal species (Halim et al., 2012b). Irrespective of the pre-treatment methods used, *ST* exhibited highest yield in comparison to *GC* and *UF* (Table 4.2). Significantly higher yield ($p<0.05$) was obtained when *ST* underwent no pretreatment (5.11%) or sonication (5.22%). No significant difference was observed between the autoclaved sample and autoclaved + sonicated sample. For *GC*, autoclaving was found to be the best method, showing significantly higher yield, followed by the sonication method. For *UF*, the autoclaved samples gave the highest yield of 2.76% but no significant difference was observed between the pretreatments ($p>0.05$). Likewise, no significant increase in lipid extraction was observed in *UF* after sonication.

Table 4.2: Algal lipid extraction using different pretreatments

Pretreatment	**Crude lipid yield (wt.%)**		
	ST	***GC***	***UF***
Untreated	5.11 ± 0.54^{e}	2.87 ± 0.17^{a}	$2.50 \pm 0.13^{a,b}$
Autoclaved	3.86 ± 0.09^{d}	$3.30 \pm 0.27^{c,d}$	$2.76 \pm 0.17^{a,b,c}$
Sonicated	5.22 ± 0.27^{e}	$3.10 \pm 0.14^{b,c}$	$2.65 \pm 0.24^{a,b,c}$
Autoclaved + Sonicated	4.02 ± 0.15^{d}	$2.66 \pm 0.07^{a,b,c}$	$2.59 \pm 0.14^{a,b}$

(Each value is the mean ± SD of three replicates. Within each column, different superscript letters are statistically significant (ANOVA, $p<0.05$ and subsequent post hoc multiple comparison with Tukey HSD test)

As mentioned above, there is no fixed pretreatment method that could be applied to all the samples uniformly. For example, ultrasonication gave highest yield than other pretreatments such as bead beating, osmotic shock, microwave treatment and lyophilisation for the oil extraction of *Gracilaria edulis*, *Enteromorpha compressa* and *Ulva lactuca* (Bharathiraja et al., 2015), whereas in a study by Balasubramaniam et al. (2013), ultrasonication was found to be the least effective method for the extraction of microalga *Nannochloropsis*. In another study, the use of the microwave oven was identified as the most simple, easy and effective for lipid extraction from microalgae compared to autoclaving, bead-beating and sonication (Lee et al., 2010).

Experiments were carried out to check for the efficiency of sonication in distilled water, as a means to disrupt the algal cells. On comparison of sonication with water, as seen in Fig. 4.5. Although a marginal increase was seen in the crude lipid extracted from *ST* and *GC*, the difference was not significant (p>0.05).

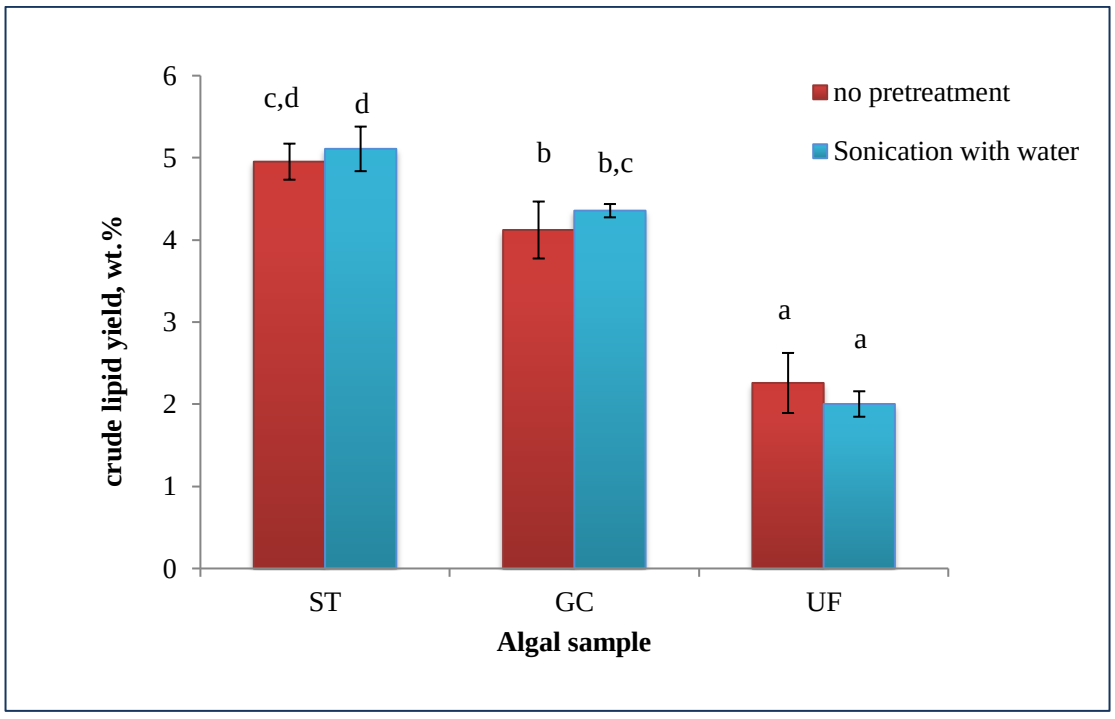

Fig. 4.5: Effect of sonication pretreatment on crude lipid extraction from macroalgae

(Each value is the mean ± SD of three replicates. Different superscript letters are statistically significant (ANOVA, p<0.05 and subsequent post hoc multiple comparison with Tukeys HSD test)

Taken together, the above results would indicate that the cell wall is sufficiently penetrated or dissolved by the solvents used, not further facilitated by mechanical cell disruption procedures (Ryckebosch et al., 2012).

4.5.4. Solvent-to-solid ratio

As the solvent-to-solid ratio increased from 7:1 to 15:1, the crude lipid yield was found to increase only marginally (Fig. 4.6). Increase in solvent-to-solid ratio above 10:1 did not show improvement in the crude lipid extractability. The solvent-to-solid ratio of 10:1 (v/w) was hence adopted as optimum for the further studies. In a study by Suganya and Renganathan (2012), highest lipid yield from *Ulva lactuca* was obtained at a solvent-to-solid ratio of 6:1. Ashokkumar et al. (2017) had shown that a 9:1 solvent to biomass ratio and an extraction time of 150 min increased the lipid extraction capacity in *Padina tetrastromatica* biomass.

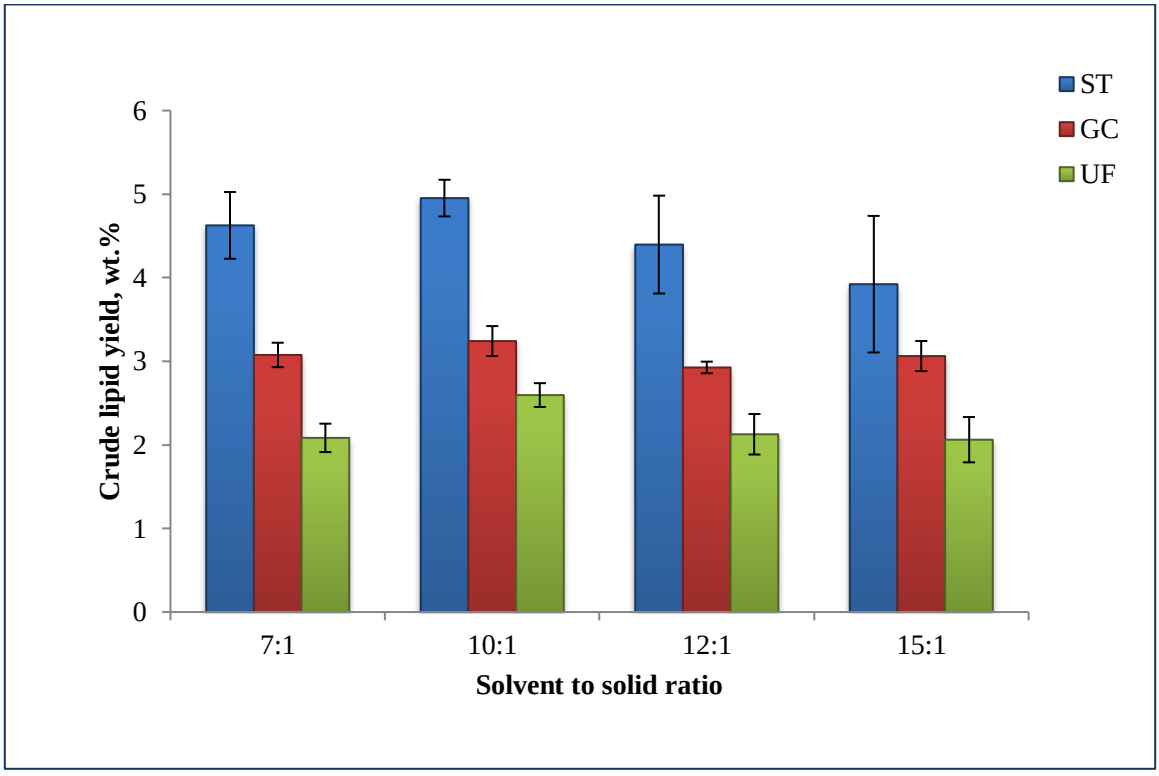

Fig. 4.6: Yield of crude lipid at varying solvent-to-solid ratios

4.5.5. Comparative Analysis of Algal Lipid from the Three Macroalgal Types

A comparative analysis was carried out for *ST*, *GC* and *UF* keeping the experimental parameters constant *i.e.*, solvent system, duration of extraction, temperature and solvent-to-solid ratio. Observations were confirmed by repeating the experiments until values were consistently reproducible. The crude lipid yields obtained for each macroalgal sample were compared by analysis of variance (ANOVA). The algal lipid extracted from the brown algae was significantly ($p<0.05$) higher than the other two algae. The results were in agreement with the optimization experiments in which maximum crude lipid was obtained from *ST*, followed by *GC* and *UF*. It should however be noted that seasonal changes in environmental conditions do have an effect on the biochemical composition of seaweed species (Polat and Ozagul, 2012), which could account for the small variations in the comparative data (unoptimized conditions) reported in Chapter III.

4.5.6. Removal of Chlorophyll Pigment

The chlorophyll pigments in the algal crude lipid were successfully removed using activated fine charcoal powder and the decolourized extract (Fig. 4.7) was used for further analysis. This was a significant achievement, in view of the likely deleterious effect of these pigments, especially should the extractions be scaled up to industrial levels (Soares et al., 2014).

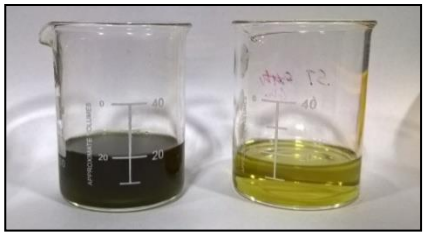

Fig. 4.7: Crude lipid extract, before and after after pigment reduction

4.5.7. Analysis of the Crude Algal Lipid Obtained

(a) *Acid Value*:

The acid value is defined as milligram potassium hydroxide required to neutralize the FFAs present in one gram of fat.

For alkali transesterification, FFA content should be less than 1-3% (Vyas et al., 2010) to avoid soap formation leading to losses in biodiesel yield. As seen in Table 4.3a. The high acid value of the algal lipid make them unsuitable for direct alkali transesterification thus suggesting the use of acid catalysis for biodiesel production. In a study carried out by Suganya and Renganathan (2012), the acid value of the macroalga *U. lactuca* was found to be 14.27 ± 1.12 mg of KOH/g whereas for *Caulerpa peltata* it was found to be 19.35 mg KOH/g with a FFA content of 9.675 wt% (2014). This indicated that macroalgal lipids tend to have higher amount of FFAs, which could hinder alkali catalysis.

Table 4.3a: Acid value of crude algal lipid

Algae	Acid value (mg KOH/g)
ST	39.06 ± 1.92
UF	71.29 ± 2.12
GC	44.93 ± 0.12

(b) *Iodine Value*:

The iodine value is a measure of the unsaturation of fats and oils and is defined as gram of iodine absorbed by 100g of the oil/fat, when determined by using Wij's solution (g I/ 100 g). Standards EN 14214 require the iodine value of biodiesel to not exceed 120 g iodine/100 g biodiesel (Chisti, 2007).

The iodine values of the algae (Table 4.3b) do not exceed the specifications. For reasons unknown, the data for *S. tenerrimum* showed substantial deviations. A study carried out by Bharathiraja et al. (2016) showed that the iodine value of the macroalgae *Gracilaria edulis*, *Enteromorpha compressa* and *Ulva lactuca* were below 100. Another study by Sanchez et al. (2012) reported the iodine value of sunflower oil (118.51 g/mol) to be higher than algal oil (61.22 g/mol). It could thus be interpreted that the algal oil contains a greater percentage of saturated or monounsaturated FAs such as palmitic and oleic acids, with smaller proportions

of linoleic and linolenic acids which could be beneficial for improving the storage properties of biodiesel obtained from algae.

Table 4.3b: Iodine value of crude algal lipid

Algae	Iodine value (mg KOH/g)
ST	62.82 ± 14.34
UF	60.77 ± 2.76
GC	78.47 ± 9.36

(c) *Saponification Value*:

The saponification value is defined by mg of KOH required to saponify 1 gram of oil/fat.

Saponification values of the algal lipids in the present investigation are depicted in Table 4.3c. Lower the saponification value, larger would be the molecular weight of FAs in the glycerides and vice-versa. Our *Ulva* samples are hence likely to be richer in larger molecular weight FAs. Suganya and Renganathan (2014b) reported a saponification value of 189.69 mg KOH/g for the green alga *Caulerpa peltata* and a study by Ashokkumar et al. (2017) showed that *Padina tetrastromatica* lipids had a saponification value of 194 mg KOH/g.

Table 4.3c: Saponification value of crude algal lipid

Algae	Saponification value (mg KOH/g)
ST	254.1 ± 17.27
UF	104.0 ± 3.44
GC	219.1 ± 5.15

4.5.8. Comparative study of catalysts used for transesterification

As seen in Fig. 4.8, among the three types of catalysts used for transesterification, a higher percentage of total FAMEs was obtained while adopting the two-step transesterification method with acid catalysis using H_2SO_4, followed by KOH catalyst. This was true for all the three macroalgae. The lowest yield of FAMEs was obtained during two-step transesterification method with NaOH as catalyst.

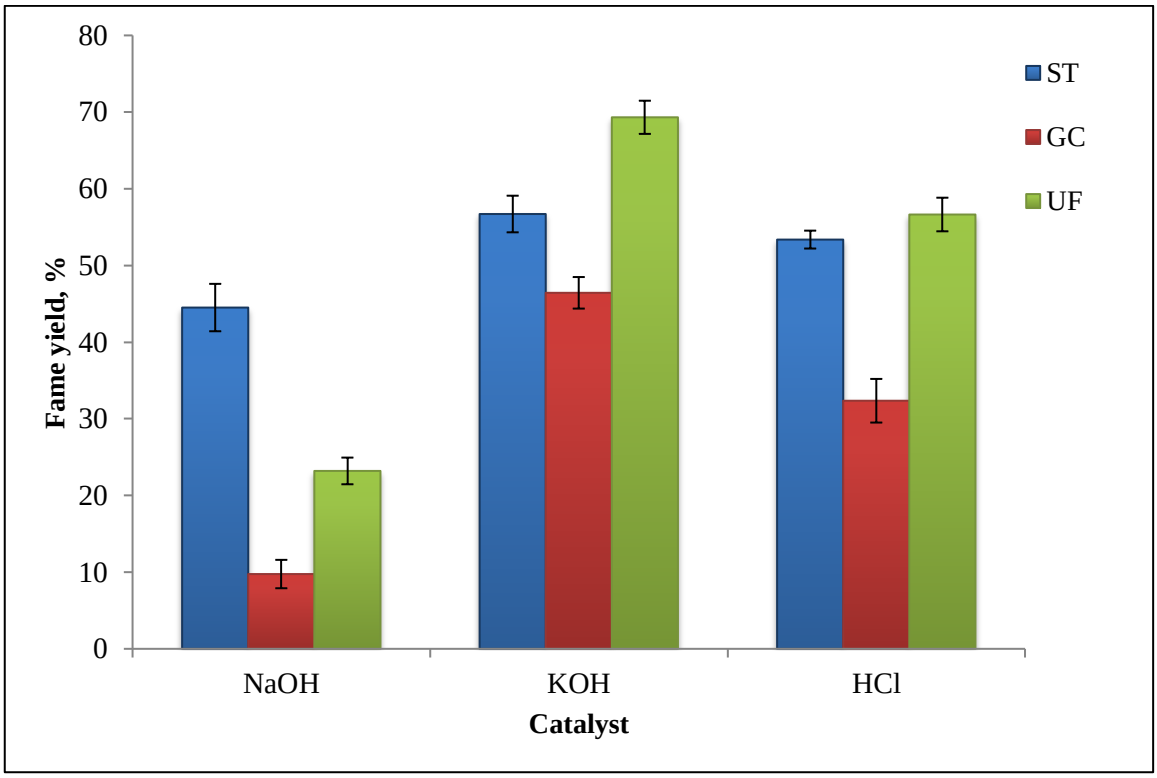

Fig. 4.8: FAME (%) obtained after transesterification of crude algal lipid with catalysts

4.5.9. Characterization of FAMEs by GC-MS

The FA composition of the crude algal biodiesel is presented in Tables 4.4a, 4.4b and 4.4c. The most common FA esters observed in biodiesel are those of palmitic (hexadecanoic) acid, stearic (octadecanoic) acid, oleic acid, linoleic acid and linolenic acid (Knothe, 2008). In this study, the FAME analysis confirmed the presence of myristic acid methyl ester, palmitoleic acid methyl ester, palmitic acid methyl ester, oleic acid methyl ester and stearic acid methyl ester in the three macroalgae *ST*, *UF* and *GC*. Palmitic acid methyl ester (a saturated FAME)

was found to be the most abundant one in all three algal species, followed by myristic acid methyl ester and stearic acid methyl ester. According to literature, palmitic acid (16:0) is predominant in macroalgae (Gressler et al., 2010) while polyunsaturated FAMEs *viz*., linoleic (C18:2) and linolenic (C18:3) acid esters are observed at a lower concentration. In all the three macroalgal species, especially in *ST*, monounsaturated FAMEs such as palmitoleic acid methyl ester and oleic acid methyl ester were found to be higher in quantity than polyunsaturated FAMEs. The presence of these FAMEs was also reported in studies carried out on other macroalgae such as *Enteromorpha compressa* (Suganya et al., 2013), *Jania rubens, Padina pavonica* (El Maghraby and Fakhry, 2015), *Hypnea musciformis, Sargassum cymosum* and *Ulva lactuca* (Martins et al., 2012) and *Ulva lactuca, Padina boryana and Ulva intestinalis* (Abomohra et al., 2018).

In conclusion, the FAME area percentage obtained depended upon the type of alga and the catalyst used for transesterification, *ST* appearing to have the highest amount of extractable FAMEs followed by *GC* and then *UF*. Two-step acid-alkali transesterification using KOH and acid transesterification with HCl appeared to be more effective than the two-step acid-alkali transesterification with NaOH. In all the three macroalgal species, saturated FAMEs figure as highest in content, followed by monounsaturated FAMEs and polyunsaturated FAMEs (Table 4.5).

Table 4.4a: Fatty acid composition of the crude biodiesel from *ST*

	Area %		
Common name of FAME (*ST*)	**NaOH**	**KOH**	**HCl**
Myristic acid methyl ester	5.11	6.155	6.925
Pentadecanoic acid, methyl ester	0.385	0.51	0.51
Palmitic acid methyl ester	32.6	37.43	38.215
Palmitoleic acid methyl ester	4.87	6.84	7.65

margaric acid methyl ester	0.285	-	0.285
Cis-10-heptadecenoic acid, methyl ester	0.19	-	-
stearic acid methyl ester	2.045	1.74	1.395
Oleic/ Elaidic acid, methyl ester	12.57	12.73	13.105
Linoleic acid, methyl ester	3.45	4.34	4.40
Linolenic acid, methyl ester	1.935	2.475	2.56
Stearidonic Acid methyl ester	1.145	1.65	1.7
arachidic acid methyl ester	0.585	0.7	0.67
Cis-13-eicosenoic acid, methyl ester	0.91	1.17	1.03
Methyl dihomo-gamma-linolenate	0.37	0.615	0.41
Arachidonic acid methyl eester	2.735	3.68	3.54
Eicosatetraenoic acid, methyl ester	5.28	-	0.21
Behenic acid methyl ester	0.575	0.875	0.68
Erucic acid methyl ester	0.81	1.075	0.98
Lignoceric acid methyl ester	0.435	0.645	0.57
Gamma.-linolenic acid, methyl ester	0.41	-	0.35

Table 4.4b: Fatty acid composition of the crude biodiesel from *GC*

	Area %		
Common name of FAME (*GC*)	**NaOH**	**KOH**	**HCl**
Lauric acid methyl ester	0.18	0.26	0.26
Myristic acid methyl ester	3.8	4.50	4.85

Pentadecanoic acid, methyl ester	1.81	1.95	1.19
Palmitic acid methyl ester	51.31	54.2	40.06
Palmitoleic acid methyl ester	2.61	3.08	2.20
margaric acid methyl ester	0.69	0.82	0.97
cis-10-Heptadecenoic acid, methyl ester	0.57	0.40	0.46
stearic acid methyl ester	3.95	4.65	4.16
Oleic/ Elaidic acid, methyl ester	4.24	5.15	5.1
Linoleic acid, methyl ester	0.59	0.65	0.88
Linolenic acid, methyl ester	0.39	0.40	0.34
Stearidonic Acid methyl ester	0.14	0.11	0.13
arachidic acid methyl ester	0.87	1.12	1.41
cis-13-Eicosenoic acid, methyl ester	-	-	-
Methyldihomo-gamma-linolenate	-	0.27	-
Arachidonic acid methyl eester	0.55	0.70	1.02
Eicosatetraenoic acid, methyl ester	-	-	-
Behenic acid methyl ester	0.48	0.54	3.14
Erucic acid methyl ester	-	-	-
Lignoceric acid methyl ester	0.36	0.58	0.58
gamma.-Linolenic acid, methyl ester	-	-	-

Table 4.4c: Fatty acid composition of the crude biodiesel from *UF*

Common name of FAME (*UF*)	Area %		
	NaOH	**KOH**	**HCl**
Myristic acid methyl ester	0.12	-	-
Pentadecanoic acid, methyl ester	0.69	0.97	1.12
Palmitic acid methyl ester	0.54	0.50	0.49
Palmitoleic acid methyl ester	27.34	32.87	31.5
margaric acid methyl ester	2.33	3.17	3.27
Cis-10-heptadecenoic acid, methyl ester	0.2	0.33	0.15
stearic acid methyl ester	1.05	0.62	0.64
Oleic/ Elaidic acid, methyl ester	1.22	2.14	2.27
Linoleic acid, methyl ester	4.95	4.88	8.64
Linolenic acid, methyl ester	4	4.6	3.29
Stearidonic Acid methyl ester	3.85	4.21	4
arachidic acid methyl ester	0.62	2.05	1.82
Cis-13-eicosenoic acid, methyl ester	0.3	0.67	-
Methyl dihomo-gamma-linolenate	-	-	-
Arachidonic acid methyl eester	0.16	-	-
Eicosatetraenoic acid, methyl ester	0.31	0.36	--
Behenic acid methyl ester	0.8	2.78	-
Erucic acid methyl ester	2.84	4.23	3.5
Lignoceric acid methyl ester	-	-	-

Gamma.-linolenic acid, methyl ester	-	0.3	-

Table 4.5. The FAME content (%) obtained upon transesterification of crude algal lipid

Alga	Catalyst	Saturated FAMEs (%)	Monounsaturated FAMEs (%)	Polyunsaturated FAMEs (%)
ST	HCl	48.35	21.74	12.79
	KOH	46.92	21.30	11.24
	NaOH	39.13	17.59	13.60
GC	HCl	50.12	7.30	1.61
	KOH	67.68	8.23	1.61
	NaOH	62.35	6.86	1.60
UF	HCl	38.88	11.91	9.55
	KOH	39.42	8.05	12.44
	NaOH	32.59	9.64	10.37

4.5.10. Comparative analysis of the fatty acid composition of macroalgal extracts prepared in different solvents

The objective of this experiment was to compare the efficiency of the five different solvent systems mentioned earlier in section 3.4.3 and 4.1.2.1., *viz.*, H, HD, HI, HMA and CM in carrying out lipid extraction from the three macroalgae species. The results were analysed with respect to quantity of lipid extracted, FAME content, and FA profile, evaluating the efficacy of each procedure for biodiesel production.

The lipid extraction and transesterification steps are of great significance in biodiesel production, in order to facilitate a feasible level of FAME production. This is because the quantity of soluble crude lipid differs based on the polarity of solvents used for extraction from the macroalgae. The FA content in macroalgae will also vary depending on the species and extraction methods used.

The lowest yields and least colored extracts were obtained with the use of hexane. The fact that hexane effected low extraction yields could indicate the probable presence of neutral lipids, consisting primarily of triglycerides, which was confirmed upon GC-MS analysis. Neutral lipids are a minority among the nonpolar and medium-polarity components extracted with different solvents. The addition of dichloromethane and isopropanol to the hexane used for extraction increased the yield of lipid extracted, indicating that increasing the polarity of the mixture should lead to a better yield of extract (Ryckebosch et al., 2013). As the polarity of the solvent mixture increased, so did the greenish color of the extract due to the extraction of pigments, especially chlorophyll, and some lipid classes, such as high-polarity phospholipids and glycolipids (Cheng et al., 2011a). This indicates that FA structures in macroalgae, like microalgae, must correspond to molecules that are more polar than triacylglycerides and may consist mainly of FFAs, monoacylglycerides, diacylglycerides, or steroid esters with FAs and a minority of higher polarity molecules such as phospholipids, or acylated glycoside steroids, which are also a source of FAs for biodiesel production (Soares et al., 2013). The solvent systems, *viz.*, HMA and CM (the latter traditionally used by many researchers) generated highest yield of extracted lipids compared with other solvents. This is probably because the solvent used in the extraction method contains methanol, a polar solvent that assists in the removal of lipids which are in contact with aqueous phases, and which, therefore, are more polar than neutral lipids. Thus, given the highly complex biochemistry of macroalgae, different extraction solvents may generate completely different FA profiles, making it difficult to assess the quality of a particular macroalga for use as a raw material for biodiesel production *via* conventional lipid extraction methods.

The FAMEs of the three macroalgae studied using different extraction solvents H, HD, HI, HMA and CM were analysed using GC-MS, since for biodiesel production, the FA content would provide more suitable inputs than mere crude lipid content. As reported before, CM as

solvent provided the highest crude lipid yield in all three macroalgae. However, for *ST*, the FA profile (Table 4.6a) shows that the conversion of lipids to FAMEs appeared to be better when HMA solvent system was used. For *GC*, (Table 4.6b), hexane solvent provided lowest crude lipid yield but the conversion of lipids to FAMEs appeared to be better than CM solvent. This indicates that although smaller amount of crude extract was obtained with hexane, it is a better solvent in terms of selectivity for targeted lipid such as mono-, di- and tri-glycerides (Prommuak et al., 2012). For *UF* (Table 4.6c), CM solvent provided the highest crude lipid yield as well as maximal conversion of lipids to FAMEs.

Table 4.6a: FAME profile of macroalga *ST*

FAME	Solvents, Area %				
	H	**HD**	**HI**	**HMA**	**CM**
Myristic acid methyl ester	9.2381	8.2507	9.5601	12.0622	8.0177
Pentadecanoic acid methyl ester	1.293	1.2303	1.3325	2.1757	1.3538
Palmitoleic acid methyl ester	2.0281	5.4301	5.3151	7.9118	2.6896
Palmitic acid methyl ester	49.3325	42.2283	47.5094	-	41.4257
Oleic acid methyl ester	6.4824	15.0309	14.9952	24.9761	12.516
Stearic acid methyl ester	4.5422	6.516	-	10.3645	-
Linoleic acid methyl ester	-	7.5435	-	-	-
Linolenic acid methyl ester	-	1.0904	1.1109	3.2543	0.9377
Arachidonic acid methyl ester	-	3.666	3.099	7.5583	2.3874
Arachidic acid methyl ester	1.5396	-	-	-	-
Erucic acid methyl ester	1.5623	1.1893	1.0289	2.276	1.1664

Behenic acid methyl ester	1.2308	1.8438	1.1665	1.7924	2.0186
Lignoceric acid methyl ester	-	-	-	0.8865	-

Table 4.6b: FAME profile of macroalga *GC*

FAME	Solvents, Area %				
	H	**HD**	**HI**	**HMA**	**CM**
Myristic acid methyl ester	6.5985	7.5904	7.2805	8.4595	6.758
Pentadecanoic acid, methyl ester	1.7941	2.3496	2.0175	3.1039	2.2832
Palmitoleic acid, methyl ester	3.745	1.687	-	-	1.2373
Palmitic acid methyl ester	-	62.277	74.2318	64.3905	61.6968
Elaidic acid, methyl ester	1.729	-	-	1.3756	1.448
Stearic acid methyl ester	9.4437	8.7544	8.6793	7.7631	7.7623
Behenic acid methyl ester.	1.431	2.1198	-	1.6165	1.7962
Lignoceric acid methyl ester	-	-	-	1.5571	-
Nonadecanoic acid, 18-methyl, methyl ester	2.5923	3.591	1.7654	2.5898	3.0915

Table 4.6c: FAME profile of macroalga *UF*

FAME	Solvents, Area %				
	H	**HD**	**HI**	**HMA**	**CM**
Myristic acid methyl ester	1.2644	0.9816	1.8742	1.6498	1.6153
Pentadecanoic acid, methyl ester	1.0175	-	-	1.4423	1.2425
Palmitoleic acid, methyl ester	1.554	-	-	3.3225	2.1656
Palmitic acid methyl ester	40.2771	28.4307	54.7316	49.9915	45.5635
Elaidic acid, methyl ester	3.3747	19.384	4.6213	1.7835	3.8751
Stearic acid methyl ester	-	9.9523	7.4218	-	-
Trans-Vaccenic acid, methyl ester	-	-	-	-	12.2136
Stearidonic acid methyl ester	-	-	-	-	1.3938
Eicosanoic acid, methyl ester	-	-	1.503	-	-
Behenic acid methyl ester.	4.7879	1.2735	5.45	3.5758	5.9661

4.5.11. Analysis of the biodiesel obtained

The results of physicochemical properties using the Biodiesel Analyzer software© are presented in Table 4.7 and compared with accepted biodiesel standards.

Table 4.7: Comparison of estimated biodiesel properties of the macroalgae against biodiesel standards

Characteristics	***ST***	***GC***	***UF***	**ASTM D6751**	**(BIS) IS 15607:2005**
Kinematic viscosity (mm^2/s)	2.27-3 .12	1.68-3.09	1.63- 2.44	1.9-6.0	2-6
Flash point °C	133	128	130	130°C	120
Cetane number	63-77	72-86	73-82	47 (minimum)	51 (minimum)
Acid value (mg KOH/g)	1.80	2.055	1.39	0.50 (minimum)	0.50 (minimum)
Cloud point °C	11.25-15.45	19.27-22.89	6.34-13.76	-	-
Pour point °C	5.64-9.95	14.1-20.02	3.37-8.81	-	-
CFPP °C	0.85-7.22	4.7-19.64	1.3-15.16	-	Summer 18 Winter 6

a) ***Kinematic viscosity***

Viscosity is the most important property of any fuel as it indicates the ability of a material to flow. Maximum allowable limit as per ASTM D445 ranges are 1.9-6.0 mm^2/s . The kinematic viscosity of *ST* was in the range 2.27-3 mm^2/s, *GC* was 1.68-3.09 mm^2/s and *UF* was 1.63 - 2.44 mm^2/s. The higher viscosity of the neat oil causes operational problems such as engine deposits. Kinematic viscosity, like the acid value, is useful in monitoring the fuel quality of biodiesel during storage since it continuously increases with decreasing fuel quality (Knothe and Steidley, 2005).

b) *Flash point*

The flash point of the algal biodiesel was evaluated. The main purpose of the flash point specification is to ensure that the manufactured biodiesel has been sufficiently purified in terms of removal of any excess methanol (Suganya et al., 2013). While the flash point does not affect the combustion directly, higher values make fuels safer with regard to storage, fuel handling and transportation (Knothe, 2005b).

c) *Acid value*

Acid value or neutralization number, is expressed in mg KOH required to neutralize 1 g of FAMEs and is set to a maximum value of 0.5 mg KOH/g. Higher amount of FFAs leads to higher acid values, which can cause severe corrosion in the fuel supply system of an engine. (Atabani et al., 2012; Atabani et al., 2013)

d) *Cold flow properties*

The cloud point (CP) is the temperature at which crystals first start to form in the fuel. The cloud point is reached when the temperature of the biodiesel is low enough to cause wax crystals to precipitate. The pour point is the temperature at which the fuel contains so many agglomerated crystals that it is essentially a gel and will no longer flow. The cold filter plugging point (CFPP) is the lowest temperature at which fuel passes through a filter within 60s by applying a vacuum (Ramos et al., 2009). The flow properties including cloud point and pour point (-5 ℃ to 17 ℃, and -15 ℃ to 16 ℃ respectively) were much higher for algal biodiesel than for conventional diesel (Van Gerpen et al., 2004). This may be due to nature of the feedstock used. Nevertheless, most standards require the determination of this parameter and its value is regulated depending on the climatic conditions (Table B-4, Appendix B) of each region or country (Barabas & Todoruţ, 2010).

In general, saturated FAs have significantly higher melting points than unsaturated fatty compounds, and in a mixture, tend to crystallize at temperatures where unsaturated FAs remain liquid. Methyl esters of palmitate and stearic acid are the first to precipitate and cause clogged biodiesel filters if the biodiesel is cooled, constituting a major share of material recovered from clogged biodiesel fuel filters (Mittelbach and Remschmidt, 2004).

e) *Cetane number* (CN)

The cetane number of the algal biodiesel was evaluated and found to be above the mininmum value established in the ASTM standard. CN is dimensionless measure of a fuel's autoignition quality characteristics. The CN of a diesel fuel is related to the ignition delay time, *i.e.*, the time that passes between injection of the fuel into the cylinder and onset of ignition (Pinzi et al., 2009). The shorter the ignition delay time, the higher the CN (and vice versa) and better would be its ignition properties (Meher et al., 2006). An adequate cetane number is thus required for good engine performance. High cetane numbers help ensure good cold start properties and minimize the formation of white smoke. The CN for biodiesel should be a minimum of 51 (UNE-EN 14214). Significantly, the CN of the biodiesel derived from crude algal lipids in our study are higher than this requirement. The CN of FA esters depends on chain length and degree of unsaturation, increasing with chain length as well as saturation (Knothe et al., 2003). Highly unsaturated compounds such as esters of linoleic (C18:2) and linolenic (C18:3) acids cause lowering of CN (Ramos et al., 2009; Knothe, 2010). Branched and aromatic compounds have low CNs. For example, compounds found in biodiesel, such as methyl palmitate and methyl stearate, have high CNs, while methyl linolenate has a very low CN (Knothe, 2008).

In summary, the quality of biodiesel is dependent on the composition of the FAMEs. As ideal biodiesel, the FAs should be oxidative and low-temperature stable. These FAs, based on their saturation quality, affect the biodiesel properties such as cetane number, oxidation stability, cold filter plugging point, *etc*. Generally, saturated FAs are oxidative stable while unsaturated FAs provide low-temperature stability (Knothe, 2008). A high iodine value has been linked with low oxidation stability, causing the formation of various degradation products which can negatively affect engine operability by forming deposits on engine nozzles, piston rings and piston ring grooves. Higher unsaturation leads to higher iodine value which is not suitable whereas saturated esters lower the iodine value (Mittelbach and Remschmidt, 2004). Saturated and long chain FAs give a high CN value, which increases with increasing saturation and the chain length of the FAs (Ramos et al, 2009). Saturated FAs have significantly higher melting points than unsaturated FAs and so in a mixture, saturated FAs crystallize at a higher temperature. Higher content of PUFA esters in the feedstock oil causes deterioration in the

quality of biodiesel upon storage, due to oxidation triggered by air, light, heat, peroxides, trace metal, or even the structural features of the FAs. Oxidation stability is thus another major issue affecting the use of biodiesel fuel. In the search of an ideal biodiesel composition, high presence of MUFAs (as oleic and palmitoleic acids), reduced presence of polyunsaturated acids and controlled saturated acid content are strongly recommended features. The enhanced proportion of oleic acid (C18:1) in the total FAs has been considered a feasible approach to balance the oxidative and low-temperature stability, with retaining the cetane number at an acceptable level (Knothe, 2008).

Chapter V

Hydrothermal Liquefaction of *Sargassum tenerrimum* for Biofuel Production

The previous Chapters have detailed ways and means to gauge the overall as well as saponifiable lipid content of macroalgal species and delved into the possibilities of maximizing parameters to optimise production of one kind of biofuel, namely, biodiesel. That the lipid content of macroalgae is not sufficiently high was a known fact, but with the information available at the commencement of the present research, these were the first systematic studies to prove, if only for academic interest, the economic non-feasibility of immediate commercialization of macroalgal biodiesel. This led us to move on to the next option of exploiting the potential of production of other biofuels such as bio-oil and biochar from seaweeds, through methodology that would involve not only their lipid but also their carbohydrate and protein resources.

While thermochemical methods such as gasification, pyrolysis and HTL have been employed for producing biofuel from biomass, HTL is most commonly used for wet biomass (Huang et al., 2016). Currently, HTL of algal biomass is gaining interest as a means for production of liquid fuels. The process in general is carried out by subjecting wet algal biomass to high temperatures and pressures in the range of 200-380 °C and 5-20 MPa in an inert environment (Vardon et al., 2011; Wang et al., 2016; Gollakota et al., 2018). The water in the reaction medium acts as a catalyst, solvent as well as hydrogen donor and the process thermochemically converts algal biomass into a bio-crude oil in addition to aqueous, gaseous, and solid phase by-products.

At conditions close to the critical point, water has several very interesting properties such as low viscosity and high solubility for organic substances, which make subcritical water an excellent medium for fast, homogeneous and efficient reactions (Kruse and Dinjus, 2007; Krammer and Vogel, 2000; De Caprariis et al., 2017). Subcritical water behaves very differently from supercritical water. The dielectric constant decreases from 78 Fm^{-1} at 25 ºC and 0.1 MPa to 14.07 Fm^{-1} at 350 ºC and 20 MPa (Uematsu and Franck, 1980). This gives rise to increased solubility of hydrophobic organic compounds such as FFAs (King et al., 1999). The high levels of H^+ and OH^- under subcritical conditions mean that many acid- or base-catalyzed reactions such as biomass hydrolysis are accelerated (Akiya and Savage, 2002). Furthermore, the density of subcritical water falls in the range between those of ambient and supercritical conditions. Despite the high temperature, the compressibility is still rather low.

The relatively high density combined with the high dissociation constant of subcritical water favors ionic reactions (De Caprariis et al., 2017). The HTL of organic components in algae involves three steps: (i) depolymerization, wherein temperature and pressure would change the molecular structure of long chain polymers to shorter chain polymers, (ii) decomposition of amino acids, fatty acids and sugars caused by dehydration, decarboxylation and deamination and (iii) recombination and decomposition of reaction intermediates to the final products (Elliot et al., 2015; Gollakota et al., 2018).

Many researchers have been focusing on bio-oil production from aquatic algal biomass *via* the HTL process (Biller and Ross, 2011; Jena and Das, 2011; Valdez et al., 2012; Barreiro et al., 2014; Huang et al., 2016; Hu et al., 2017). Liang et al. (2017) investigated the production of crude bio-oils from three laboratory cultivated and two commercial grade algal biomass sources *via* HTL process. The HTL reaction was carried out at temperatures ranging from 260 °C to 340 °C and residence time of 10 to 40 min. The bio-oil yields were in the range of 28-41 wt.%. The highest yield of 41.2 wt.% was obtained at 300 °C at a 20 min residence time. The crude bio-oils generated from laboratory cultivated algae had similar qualities as compared to those derived from commercially available algae. The bio-oils were composed mainly of aliphatic compounds (fatty acids, alkanes) which can be readily upgraded and refined into value added transportation fuels (e.g., renewable diesel). Barreiro et al. (2014) liquefied raw biomass (RA), after extracting lipids (LEA) and after extracting proteins (PEA) in micro-autoclave experiments at different temperatures. The results indicated that extracting the proteins from microalgae prior to HTL may serve to improve the economics of the process while at the same time reducing the nitrogen content of the bio-crude oil. A complete set of experiments was carried out at a reaction time of 15 min for RA, LEA and PEA, varying the reaction temperature from 300 to 375 °C. The product yields after HTL for each feedstock and temperature used, as well as the elemental composition and HHV of the bio-crude oil produced were evaluated. Most of the organic mass from the feedstock was converted into bio-crude oil, with yields varying from 51.2 ± 3.4 to 69.2 ± 1.9 wt.%. Shakya et al. (2017) performed HTL of nine algal species at two reaction temperatures (280 and 320 °C) to compare the effect of biomass composition on product yields and properties. The results obtained after HTL indicate large variations in terms of bio-oil yields and properties. The

maximum bio-oil yield (66 wt.%) was obtained at 320 °C with high lipid containing algae *Nannochloropsis*. The HHV of the bio-oils derived from the several algae ranged from 31 to 36 MJ/kg and around 50% of the bio-oil was in the vacuum gas oil range while *Nannochloropsis* contained a significant portion (33-42%) in the diesel range. A predictive relationship between bio-oil yields and biochemical composition was developed and there was a broad agreement between predictive and experimental yields. These studies brought out the fact that both the yields as well as the quality of bio-oil resulting from the HTL process were highly associated with operational parameters such as reaction temperature, retention time, ratio of feedstock and solvent type. The process of HTL is more suitable for feedstock which have a high moisture content (such as algae), on account of its inherent advantage of being a wet processing technique unimpeded by a requirement of drying the feedstock (Ross et al., 2010). Furthermore, oil products produced from HTL have much lower oxygen content and moisture as compared to those resulting from pyrolysis. Aquatic biomass HTL is one of the promising existing options to meet the escalating energy demand; saving arable lands as well as fighting against growing pollution loads on the environment are bonus points.

The HTL of a few brown macroalgae has been well studied. Anastasakis and Ross (2011) carried out HTL of *Laminaria saccharina* and obtained a maximum bio-oil yield of 19.3 wt.% with a 1:10 biomass:water ratio at 350 °C and 15 min, without use of a catalyst. Subsequently, HTL of four brown macroalgae *L. digitata, L. hyperborean, L. saccharina* and *Alaria esculenta* was used to produce bio-oil as well as biochar. Bio-oil yields between 9.8 wt% and 17.8 wt% with HHVs between 32 and 34 MJ/kg as well as biochar yields between 10.9 wt% and 18.6 wt% with HHVs between 15.7 and 26.2 MJ/kg were reported (Anastasakis and Ross, 2015). In another study, the effect on HTL of *L. saccharina* with respect to the heating rate was studied by Bach et al. (2014). Increase in the heating rate had a beneficial effect on the biocrude yield, achieving a maximal yield of 79 wt.% at 350 °C, 15 min and a heating rate of 585 °C min^{-1}. The algae *Fucus vesiculosus, L. saccharina* and *A. esculenta* were subjected to HTL for 15 min at temperatures from 330 to 370 °C. The maximum conversion to biocrude (29.4± 1.1 wt.%) at 360 °C was for *A. esculenta* (Barreiro et al., 2015). Li et al. (2012) carried out HTL on *Sargassum patens* C. Agardh, to obtain a maximum yield of 32.1 wt.% at 15 min and 340 °C. An attempt to liquefy macroalgae in a continuous set-up was reported by Elliott et

al. (2013), converting *Saccharina* spp. into biocrude oil and obtaining a maximum yield of 27.1 wt.%. They also reported that most of the organic matter stayed behind in the aqueous product. The HTL of *S. tenerrimum* was carried out by Biswas et al. (2017a) using different solvents (water, methanol and ethanol) and at different temperatures. A maximum bio-oil yield of 23.8 wt.% was obtained at 280°C with ethanol, the use of alcoholic solvents increasing the production of aliphatic ester compounds in general. More recently, catalytic studies on *S. tenerrimum* were conducted by Biswas et al. (2020), wherein highest bio-oil yield (33.0 wt.%) accompanied by higher conversion (70.5%) was obtained with CaO/ZrO_2 (10 wt.%) using a water-ethanol co-solvent system.

This Chapter explores the possibility of obtaining biofuels from the brown macroalgal biomass of *ST* under hydrothermal conditions. The HTL of this marine biomass has been looked into to understand the product profile at different temperatures for utilization of the whole biomass to produce biofuel. Other process parameters have also been optimized for maximizing yields.

5.1. MATERIALS & METHODS

5.1.1. Sample Collection

Samples of the brown macroalga *ST* were collected, washed, dried, powdered and stored for further analysis as described previously in Chapter II (Section 2.1).

5.1.2. Characterization of Feedstock and Products

Thermogravimetric analysis (TGA) was carried out on a Shimadzu DTG-60 instrument. These tests were conducted using 5-10 mg of *ST* algal biomass at a heating rate of 10 °C/min in a temperature range of 25-900 °C under N_2 atmosphere and the gross calorific value determined using Parr 6300 Bomb Calorimeter. Elemental analysis was carried out in an Elemental vario micro cube unit. Moisture content was obtained on a HR-83 Mettler Toledo Halogen Moisture Analyzer. Volatile matter content was calculated along the lines of ASTM D3175, by measuring the weight loss in the sample after placing it in a muffle furnace at 950 °C for 2 min. Volatile matter and ash analyses of the feed were carried out using oven-dried feedstock.

The ^{1}H NMR spectra were recorded on a BrukerAvance 500 Plus instrument using $CDCl_3$ as solvent. Powder X-ray diffraction (XRD) patterns were collected on Bruker D8 advance X-ray diffractometer fitted with a Lynx eye high-speed strip detector and a Cu Kα radiation source. Diffraction patterns in the 2°-80° region were recorded with a 0.04 step size (step time=4s). The FT-IR spectra were recorded on a Nicolet 8700 FT-IR spectrometer with the sample powder diluted in KBr.

The organic fraction of the bio-oil was analyzed using gas chromatography-mass spectrometry (GC/MS, Agilent 7890 B). The carrier gas was He and column flow rate was 1 ml min^{-1}. An HP-1 column (25 m × 0.32 mm × 0.17 µm) was used for the separation. An oven isothermal program was set at 50 °C for 2 min, followed by a heating rate of 5 °C min^{-1} up to 280 °C, where it was held for 5 min. The injected volume was 0.4 µL in a split less mode.

5.1.3. Hydrothermal liquefaction

The HTL experiments were conducted in a 100 ml high pressure autoclave (Parr reactor) made of Hastelloy under different reaction conditions of temperature. In a typical experiment, the reactor was loaded with *ST* with water as solvent (1:6 by weight). The reactor was purged five times with nitrogen to replace the air within. Reactants were agitated with a stirrer at ~200 rpm. The reaction temperature was then raised to the desired value and maintained for 15 min. The pressure build-up during the process was autogenous and maximum pressure was in the range of 40-83 bar under different reaction conditions. After the reaction, the reactor was left to cool down to room temperature to remove the reaction products. The gaseous products were vented and the liquid portion separated from solid residue using diethyl ether and vacuum filtration. The liquid portion was then extracted by adding an equal quantity of diethyl ether. The ether extract thus obtained was dried over anhydrous sodium sulfate, filtered and evaporated in a rotary evaporator at room temperature. Upon removal of diethyl ether, this fraction was dried in an oven at 80 °C for removing any residual solvent, weighed and designated 'Bio-oil 1'. The aqueous phase that remained after extraction contained the water-soluble hydrocarbons.

Solid products were extracted with acetone in a Soxhlet extraction apparatus until the solvent in the thimble became colourless. After removal of the acetone under reduced pressure in a

rotary evaporator, this fraction was dried, weighed and designated 'Bio-oil 2'. The ether soluble combined with the acetone soluble fraction were collectively designated 'Bio-oil'. The acetone insoluble fraction was dried at 80 °C, weighed and termed solid residue (or bio-residue / biochar).

The HTL experiments on *ST* were also conducted using co-solvent ethanol-water (1:1) at the optimal HTL temperature. The methodology was the same as described above.

The reactions were carried out in duplicate, and the average values are reported. Yield of various fractions and the percent conversion were calculated as below:

$$Conversion\ (\%) = \frac{W1 - W2}{W1} x\ 100$$

$$Bio - oil\ 1\ yield\ (wt.\%) = \frac{Wethersoluble}{W1} x\ 100$$

$$Bio - oil\ 2\ yield\ (wt.\%) = \frac{Wacetonesoluble}{W1} x\ 100$$

$$Total\ bio - oil\ yield\ (wt.\%) = Biooil\ 1 + Biooil\ 2$$

$$Biochar\ yield\ \ (wt.\%) = \frac{Wsolid}{W1} x\ 100$$

$$Gas\ yield\ (wt.\%)$$
$$= \frac{W(vessel + feed + water)before\ HTL - W(vessel + feed + water)after\ HTL}{Amount\ of\ feedtaken(g) + amount\ of\ water\ added\ (g)} x\ 100$$

$$Other\ yield\ (wt.\%) = \ 100 - (bio - oil\ 1 + bio - oil\ 2 + biochar + gas)$$

W1 is the weight of macroalgal feed; *W2* is the weight of biochar; $W_{ether\ soluble}$ is the weight of ether soluble bio-oil (bio-oil1); $W_{acetone\ soluble}$ is the weight of acetone soluble bio-oil (bio-oil2). All yields were calculated on a dry basis of material. 'Other yield' corresponded to the water soluble oxygenated hydrocarbons (aqueous yield) and some losses.

5.2. RESULTS & DISCUSSION

5.2.1. Characterization of *ST* Feed

The results of the proximate and ultimate analyses of the *ST* sample, including the total content of volatiles, moisture, fixed carbon and ash (*i.e.*, inorganic components of the samples) is summarized in Table 5.1. Total volatiles collected at 950°C represent 61.5% of total product. The moisture, ash and fixed carbon represent, respectively, 5.7%, 26.5% and 6.3% of the total product. Proximate analysis showed composition of the key elements as 32.1% C, 4.7% H, 0.9% N, 60.7% O and 1.5% S (calculated by difference). The calorific value of *ST* feed was 11.96 MJ kg^{-1}.

Table 5.1: Proximate and ultimate analyses of *ST* (%, dry basis)

Proximate (wt.%)		***Ultimate (wt.%)***	
Moisture	5.7	C	32.1
Ash content	26.5	H	4.7
Volatile matter	61.5	O	60.72
Fixed carbon	11.9	N	0.93
-	-	S	1.55

The moisture content was comparable to the data obtained for brown macroalgae *Laminaria digitata, L. hyperborea , L. saccharina* and *A. esculenta* which were in the range 5.6-6.8% (Anastasakis and Ross (2015). Moisture content (Table 5.1) was lower than in *Sargassum patens* - 14.38% (Li et al., 2012) and *ST* (13.18 %) sourced from Veraval in Gujarat, much further north along the west coast of India (Singh et al., 2015a). The ash content was slightly higher than that reported by Anastasakis and Ross (2015) which was between 16.6-25.2 % and

Li et al. (2012) for *S. patens* (17.7%). It was lower than the 32.0% reported by Singh et al. (2015a).

Thermogravimetric analysis helps to understand the temperature profile at which biomass degradation starts or to gauge the thermal degradation behaviour. Thermal behaviour of *ST* was determined by TGA and DTG, the results being as in Fig. 5.1. The profile of algal biomass normally presents three steps. The first one at 100 °C is attributed to moisture present in algal biomass (Kim et al., 2013; Bae et al., 2011). The mass loss between 200 and 370 °C would correspond to decomposition of carbohydrates while the one at higher temperature (320 - 450 °C) would indicate decomposition of the protein fraction (Ross et al., 2008). The major mass decomposition occurs between 200 and 350 °C, as was observed for other macroalgae also (Kim et al., 2013; Li et al., 2011). The mass loss at temperatures higher than 600 °C would be related to lipid degradation. The main components of feedstock, hemicelluloses and cellulose of *ST* start decomposing at 200 °C (Fig.5.1). The maximum decomposition temperature was determined as approximately 264 °C. From the thermal analysis (TGA/DTG) it has been shown that the temperature range between 200 and 327 °C may be considered as an active pyrolytic zone for *ST* biomass, where maximum decomposition (depolymerization) takes place.

A broad band in the FT-IR spectrum in frequency range 3500-3200 cm^{-1} (Fig. 5.2) corresponds to N-H and O-H stretching vibration of the feed, which indicates the presence of secondary amines that are attributed to proteins & lipids, and phenols & alcohols, respectively. The band at 2800-3000 cm^{-1} was related to =C–H and -C–H stretching vibrations. The peaks in the region 1650-1580 cm^{-1} may be attributed to N-H bending vibration arising from β-unsaturated ketones and amides. The C-H bending vibration was observed at 1435-1405 cm^{-1}, while C-O stretches and O-H bending vibrations were at 1350-1260 cm^{-1}. This vibration can also be attributed to asymmetric C-O-C stretching, which would indicate the presence of esters. Symmetric C-H stretching was observed in the range 1120-1030 cm^{-1}.

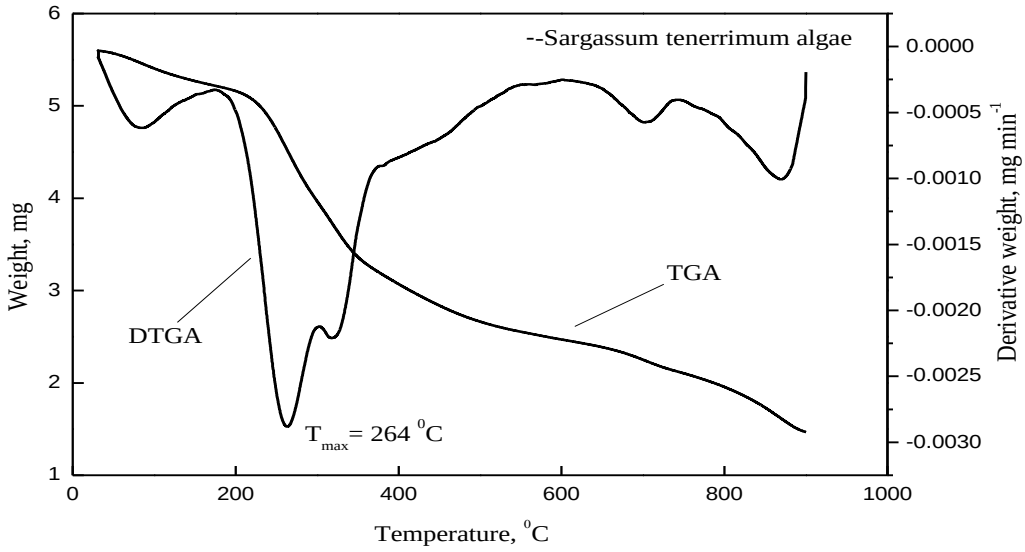

Fig. 5.1: Thermogravimetric and differential thermal analysis of *ST*

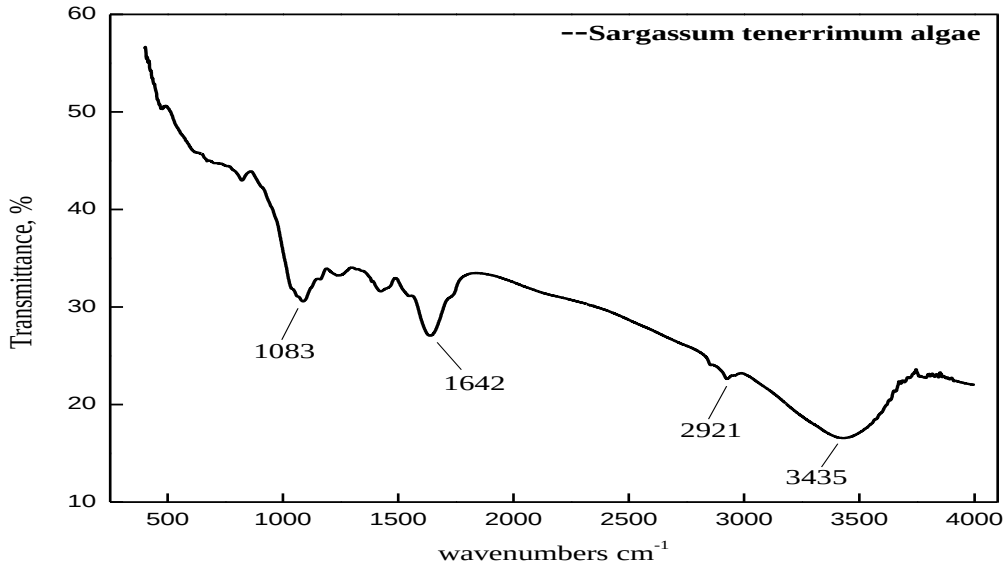

Fig. 5.2: The FT-IR spectrum of *ST* feed

5.2.2. Hydrothermal Liquefaction Product Yields

5.2.2.1. Effect of temperature

Processing temperature is understandably the most important factor affecting product yield during the hydrothermal conversion of biomass. Hydrothermal liquefaction of *ST* was performed at various temperatures (260, 280 and 300 °C) using distilled water as the solvent, with a residence time of 15 min. Reaction conditions have been selected based on earlier studies (Singh et al., 2015c) and as well as literature, to understand the effect of temperature on bio-oil product yield of *ST* under sub-critical water. The product distribution upon HTL of the sample is presented in Fig. 5.3.

With increase in temperature from 260 °C to 280 °C, the bio-oil yield improved from 11.5 wt.% to 16.3 wt.%. Further increase in temperature to 300 °C decreased the bio-oil yield to 14.7 wt.% (Fig. 5.3). The total bio-oil was composed of the ether fraction (bio-oil1) obtained from extraction of the liquid portion and the acetone fraction (bio-oil2) obtained from the solid-liquid (acetone) extraction. A reaction temperature of 280 °C was thus optimum for HTL of *ST*. A similar trend for effect of HTL temperature on bio-oil yield was observed for *Sargassum patens* by Li et al. (2012) where the yield of bio-oil increased with increasing temperature upto 340°C and then decreased at higher temperatures, with the yield ranging from 22.1 wt.% to 32.1 wt.%.

The biochar yields in our study decreased continuously from 61.2 wt.% to 24.2 wt.% as the temperature increased from 260 to 300°C. The results indicated that at lower temperature the decomposition of biomass was incomplete and left unreacted biomass which might suppress the bio-oil formation and increase the solid product. Increase in temperature should be able to accelerate the decomposition of the feedstock and benefit bio-oil formation; however, in our experiments an increase in temperature beyond 280 °C increased the breakdown of biomass as well as the bio-residue to water soluble products and thus led to a decrease in the bio-residue and bio-oil yields. The reducing yield of the solid residue suggested an increase in the overall biomass conversion upon increasing the temperature from 260 to 300 °C.

The yield of gaseous product initially showed an increase as the temperature was raised from 260 to 280 ºC but the yield dropped upon further rise in temperature to 300 ºC, whereas aqueous product yields increased as the temperature increased in the range of 260 to 300 °C. The conversion efficiencies at 260 °C, 280 °C and 300 °C, were calculated as 38.83%, 67.67% and 75.84%, respectively.

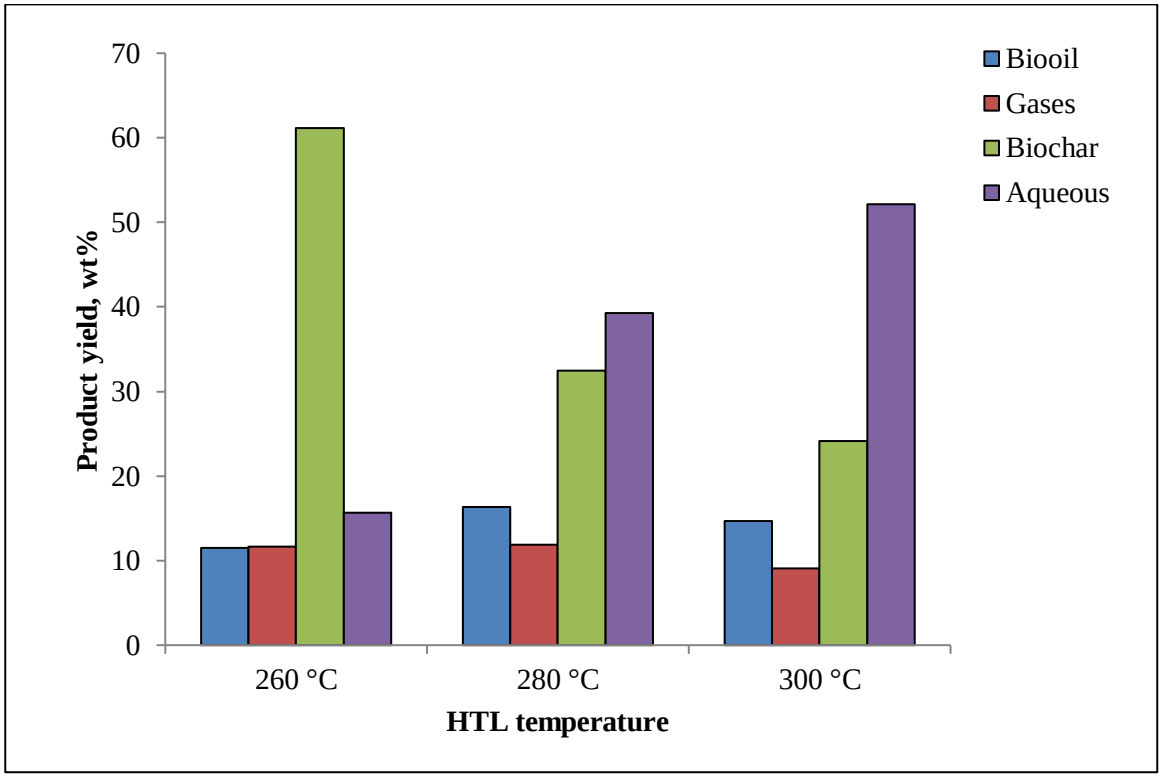

Fig. 5.3: Product distribution from HTL of *ST* in water

5.2.2.2. Effect of solvents

The use of co-solvents to improve the bio-oil yield was looked into. The product distribution from the HTL of *ST* using water and ethanol-water (co-solvent) is presented in Fig. 5.4. The product distribution from the HTL of *ST* using solvents ethanol and methanol has been reported by Biswas et al. (2017a). Liquefaction in alcoholic solvents gave a much higher bio-oil yield compared to that in water. A comparatively higher yield of bio-oil was obtained with

ethanol-water (32.06 wt.%) at 280°C in the present study (Fig. 5.4; Biswas et al., 2020). The solvents ethanol and methanol yielded bio-oil at 22.8 wt.% and 23.8 wt.%, respectively, at 280 °C (Biswas et al., 2017a). The synergistic effects of ethanol and water were mostly credited to the stronger hydrogen donor capability of ethanol to stabilize the free radicals and thus to inhibit residue formation (Liu et al., 2013) as well as stronger acidity of water to enhance solvolytic liquefaction (Cheng et al., 2010). The solid biochar yield was similar in the case of HTL with solvent compared to liquefaction with water. Aqueous yield dipped during liquefaction with alcohol solvents, the lowest being observed in ethanol (Biswas et al., 2017a) for *ST*.

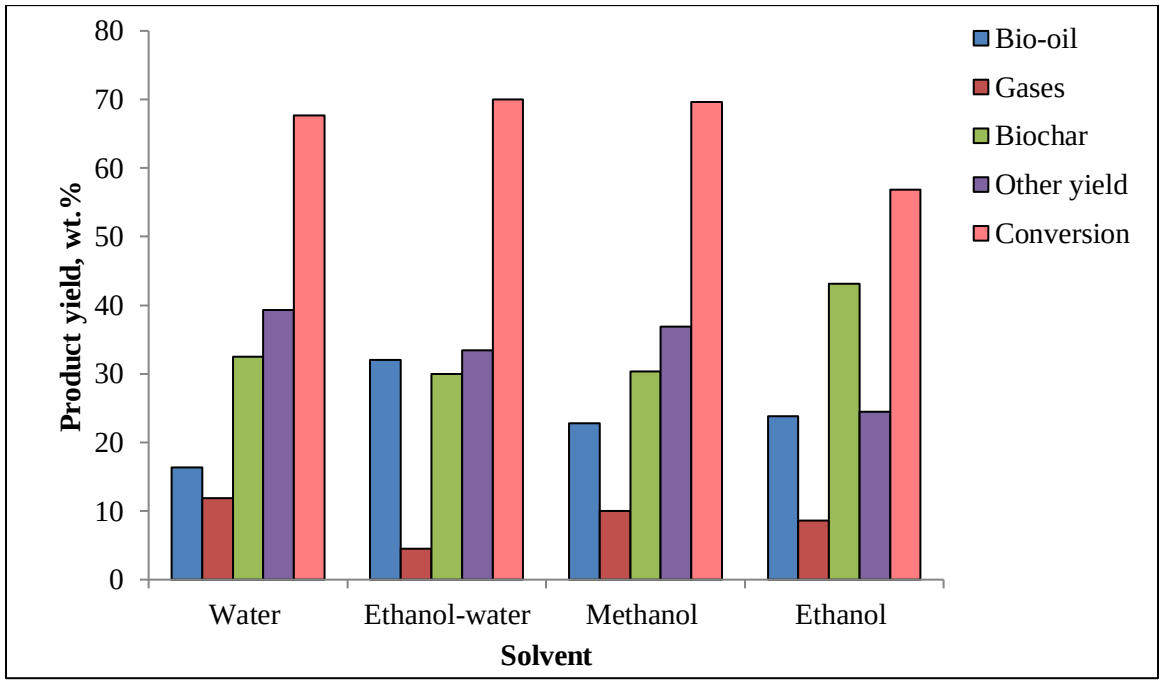

Fig. 5.4: Effect of solvent on product yield during HTL of *ST* at 280 °C.

*Product yield from Methanol and Ethanol: from Biswas et al. (2017a)

5.2.3. Bio-oil Characterization

5.2.3.1. Gas chromatography-Mass spectrometry (GC-MS) of bio-oil from *ST*

Identification of the main peaks of compounds was performed using NIST mass spectral database. From GC-MS analysis data (Table A1-Appendix A) it was obvious that liquefaction temperature affected the components of the bio-oils produced. As the HTL temperature varied from 260 to 300 °C, production of different compounds as well as different percentages of compounds had been observed. The components of the bio-oils were identified as phenols, ketones, aldehydes, acid, esters, alcohols, nitrogen-containing compounds (including amides and N-heterocyclic compounds) and hydrocarbons (Parsa et al., 2018). A semi-quantitative analysis was performed by calculating the relative percentage of area of the chromatographic peaks (Fig 5.5). The main compounds obtained by HTL of *ST* were methyl-3-pyridinol, 6-methyl-3-pyridinol, 2-methyl-1,4-benzenediol, *p*-hydroxybiphenyl, *n*-hexadecanoic acid, stigmastan-3,5-diene and bis(2-ethylhexyl) phthalate. Hexadecanoic acid is one of the components most frequently found in bio-oil obtained from algae (Chen et al., 2012b). Organic acid content in the bio-oils was observed to decrease with increasing temperature from 260 to 300 °C. Phenolic compounds such as phenol, *p*-cresol and 2-methyl-1, 4-benzenediol were observed in bio-oil obtained at the optimum temperature of 280 °C. The phenolics in *ST* bio-oil are likely to have been produced from the carbohydrate and crude fibre of the algal biomass (Brown et al., 2010; Huang et al., 2016; Shakya et al., 2017). Nitrogenated compounds are formed by decarboxylation, deamination, dehydration, depolymerization and decomposition reactions of proteins (Ross et al., 2010; Toor et al., 2011). Higher percentage area of 3-pyridinol (16.21%) was observed at the optimum temperature of 280 °C but further increase in temperature to 300 °C caused a significant decrease (9.61%). The increased percentage of branched amides may be due to the dehydration reactions of amines and carboxylic acids to form amides at higher temperatures. This can also be justified by the decrease in organic acid content with increase of temperature. Also, higher area percentage of other compounds such as bis (2-ethylhexyl) phthalate (15.05 area %) and stigmastan-3,5-diene (8.48 area %) at 260 °C were observed in the bio-oil. When water-ethanol co-solvent was used, the main components in the bio-oil were esters (75.2%),

hydroxyl (6.1%), and nitrogen (7.1%) (Biswas et al., 2020). As the composition of the liquid product is so complex, further upgrading such as denitrogenation and deoxygenation would be necessary to make the bio-oil suitable as engine fuel.

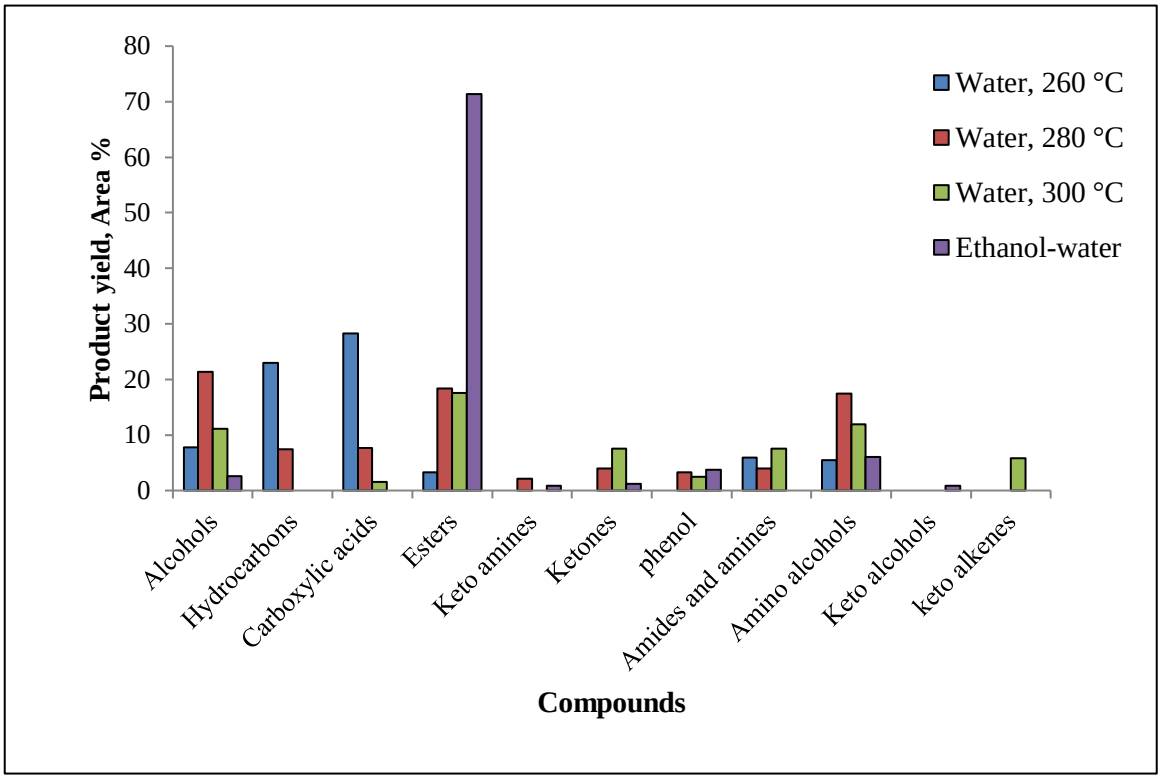

Fig. 5.5: Major chemical components of *ST* bio-oil obtained under best HTL conditions.

The pathways assumed for producing the compounds have been effectively described by Toor et al. (2011) and Parsa et al. (2018).

The first pathway considers carbohydrate as the source for producing compounds such as furans and cyclopenten derivatives. Carbohydrates such as alginate, mannitol, laminarin and fucoidan found in the macroalgae hydrolyze upon HTL (Ross et al., 2009) to monosaccharides such as glucose and fructose (Watanabe et al., 2006), which then undergo dehydration and decomposition to form furans or furfural-like compounds which could be unstable in alkaline conditions. These compounds in turn degrade by losing water and produce phenolic compounds (Barreiro et al., 2015; Toor et al., 2011).

The second reaction pathway is based on the reaction between carbohydrates and proteins under HTL conditions. As delineated by Toor et al. (2014), with increase in the HTL temperature, proteins degrade to peptides and amino acids which then go on to react with the monosaccharides as per the Maillard reaction, producing various types of N-containing heterocyclic compounds.

In the third suggested pathway, peptides convert to amines by a decarboxylation reaction (Toor et al., 2014).

The fourth reaction pathway is related to the lipid content in the feedstock. As the HTL process is initiated, lipid under high temperature reacts with water and produces fatty acids (Barreiro et al., 2015). The fatty acids released react with the amines produced by peptides to form amides. The amides thus obtained would then produce nitriles through dehydration reaction (Toor et al., 2011).

The fifth reaction pathway in producing compounds from lipids could be the decarboxylation of fatty acids which results in a chemical reaction that could produce alkanes and alkynes (Changi et al., 2012).

Triacylglycerols are readily hydrolyzed in hot compressed water and catalysts are normally not required. The dielectric constant of water is significantly lower at subcritical conditions, allowing greater miscibility (Peterson et al., 2008). The sixth pathway involves the production of methyl esters of fatty acids by chemical reaction of carbohydrates with the fatty acids resulting from lipid hydrolysis.

5.2.3.2. Fourier Transform-Infrared (FT-IR) spectroscopy of bio-oil

The FT-IR spectra of the *ST* feed and bio-oil obtained from liquefaction of the alga with water at 260, 280 and 300 °C are shown in Fig. 5.6. The broad band at around 3200-3405 cm^{-1} is attributed to the O-H or N-H stretching vibration caused by water, O-H groups or N-H groups present in bio-oil (Zhou et al., 2010; Shakya et al., 2017). A broad absorbance was displayed at around 3314 cm^{-1} for the raw material, which indicated a high content of carbohydrates and proteins (Wang et al., 2013; Arun et al., 2017). The bio-oils showed a weaker absorbance at

the wave number region of 3200-3405 cm^{-1}, suggesting that both carbohydrates and proteins were decomposed in the HTL process. The band at 2854-2950 cm^{-1}in the bio-oil obtained by liquefaction of *ST* and the absorbance of these peaks in all the bio-oils were stronger due to the C-H stretching vibrations, indicating the presence of alkyl C-H groups (Huang et al., 2016; Arun et al., 2017). The C=O stretching vibrations at around 1645-1720 cm^{-1} in the bio-oils indicate the presence of ketones, aldehydes, esters or acids (Zhou et al., 2010). Bio-oil obtained at 260 °C showed a slightly stronger absorbance in the C=O stretching region (1645–1720 cm^{-1}) than the 280 °C and 300 °C bio-oils, suggesting a greater abundance of unsaturated carboxylic acids (Cheng et al., 2017). The bands of bending vibrations at around 1580-1650 cm^{-1} indicate the presence of N-H groups of amines. The bands in the region 1430-1480 cm^{-1} were attributed to α-CH_2 bending vibrations present in the bio-oils. The presence of C-N stretching bands at around 1266-1342 cm^{-1}in the bio-oils was due to aromatic amines. The stretching band at 1266-1342 cm^{-1} showed higher intensity in the 280 °C bio-oil, suggesting a comparatively greater abundance of N-containing compounds in this bio-oil fraction (Table A1- Appendix A). In addition, some other absorbance peaks appearing in the range of 780-850 cm^{-1} are ascribed to the C-H out of plane bending vibrations which may be due to aromatics (Zhou et al., 2010). The band at 1083 cm^{-1} only appeared in the absorption profile of *ST* feed, which could be C-O connected with hydroxyl groups and were dehydrated after liquefaction. The FT-IR spectrum of different bio-oils from HTL of *ST* at different temperatures has majorly shown the same peaks, indicating the presence of the same functional groups in all the bio-oils. The bands that evidence the presence of alcohols, phenols, esters, ethers and alkanes were more prominent in the bio-oil than in the raw *ST* feed.

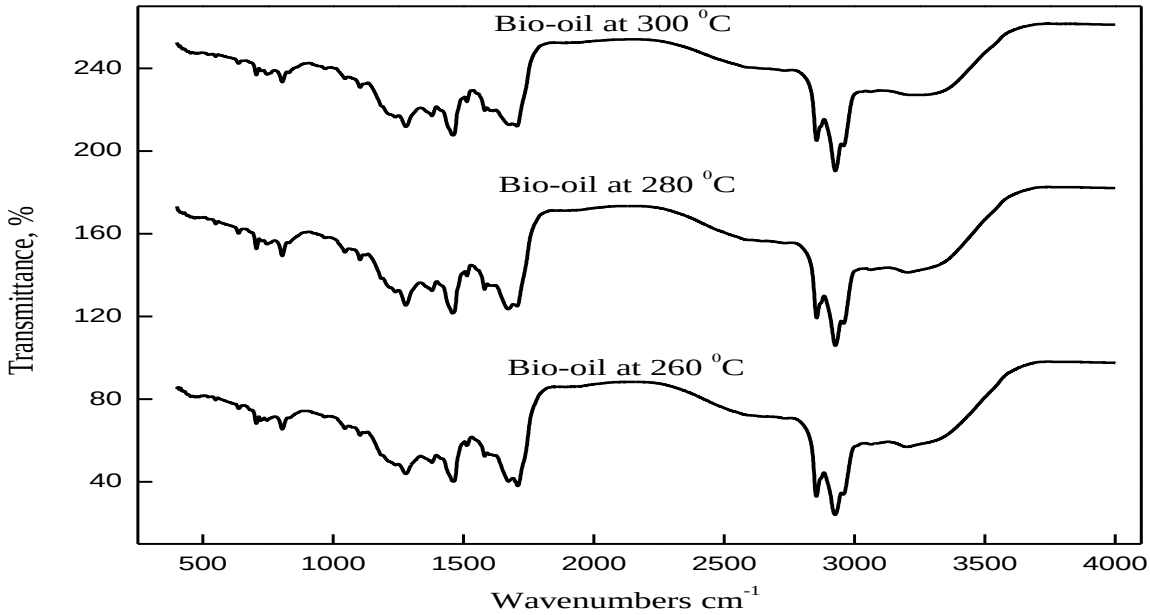

Fig. 5.6: The FT-IR spectra of *ST* bio-oil at different temperatures.

5.2.3.3. ^{1}H Nuclear magnetic resonance (NMR) spectral features of *ST* bio-oil

The ^{1}H NMR analysis of the bio-oil1 samples had been carried out to understand the ratios of chemical environments of the protons. The NMR spectra provided complementary functional group information to FT-IR spectra and the ability to quantify and compare integration areas between spectra. The FT-IR spectral data matched with the various peaks obtained in the NMR spectra of the bio-oils (Fig. 5.7). Similar to FT-IR, ^{1}H NMR spectra showed a high percentage of aliphatic functional groups for all bio-oils and a summary of integrated peak area regions assigned to different functional group classes is provided in Fig. 5.7. The most upfield region of the spectra, from 0.5 to 1.5 ppm, represents aliphatic protons that are attached to carbon atoms at least two bonds away from a C=C or heteroatom (O or N). The next integral region from 1.5 to 3.0 ppm represents protons on aliphatic carbon atoms that may be bonded to a C=C bond (Cheng et al., 2017). All the bio-oils have higher percentages of protons in the spectral region from 0.5 to 3.0 ppm. The bio-oil samples have higher percentage (56.73-64.26%) of protons in the region from 0.5 to 1.5 than in the region from 1.5 to 3.0 (24.06-27.84%). The difference of proton percentages is possibly due to a large number of nitrogenous and oxygenated compounds derived from the feedstock's high protein that has been shown to resonate in this area (Zhou et al., 2010; Mullen et al., 2009). The next portion

of the ^{1}H NMR spectrum at 3.0-4.5 ppm represents methoxyl protons (Kosa et al., 2011) or the methylene group that joins two aromatic rings. In this region very low proton percentages were observed, perhaps due to the methylene group that joins two aromatics rings not being evident. All bio-oils displayed a low percentage of methoxy/carbohydrate functionality (4.5-6.0 ppm). The maximum proton percentage (1.13%) was observed for the 280 °C liquefied bio-oil while the minimum (0.37 and 0.34 %) was observed for 260 and 300 °C liquefied bio-oils at 4.5-6.0 ppm. The section of the spectrum between 6.0 and 8.5 ppm corresponds to the aromatic region (Cheng et al., 2017). Maximum proton content of bio-oil was obtained at 280 °C at around 15.54% in this region. Aromatic/heteroaromatic functionality was also observed in all bio-oils (6.0-8.5 ppm), in agreement with the findings from FT-IR. The downfield spectral regions (8.5-10 ppm) of the bio-oils arise from the aldehydes. Aldehyde functionality (9.5-10.0 ppm) was absent from all bio-oils despite the observed C=O functional groups (1645-1720 cm^{-1}) in FT-IR. The appearance of such FT-IR bands could also be due to other carbonyl-bearing groups such as protonated carboxylic acids, carboxylic acid esters, amides or ketones.

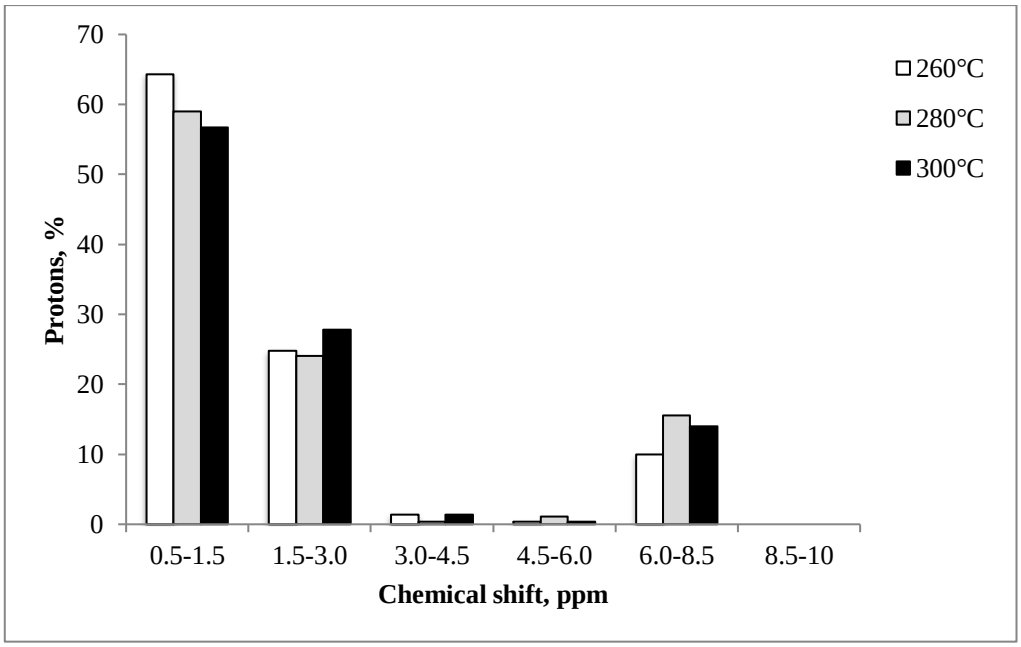

Fig. 5.7: ^{1}H NMR spectra of *ST* bio-oil obtained with water at different temperatures

5.2.3.4. FT-IR and XRD analyses of bio-residue

Figure 5.8 shows the FT-IR spectra of *ST* feed and the bio-residues. The broad bands at 3200-3500 cm^{-1} are assigned to the stretching vibrations of hydrogen-bonded O-H groups and N-H groups and these bands indicate the presence of polysaccharides, carbohydrates and proteins in the *ST* feed. This feed has strong stretching vibration peaks corresponding to the O-H and N-H groups but these transmittances decrease in the bio-residue. The peak at 1083 cm^{-1} disappeared in the bio-residue. The peak around 1600-1620 cm^{-1} corresponding to the N-H bending vibration was present in the *ST* feed as well as bio-residue. The peaks between 2800 and 2930 cm^{-1} in the spectra of residues were much weaker than those of the raw feed. The presence of a single peak at 1590-1630 cm^{-1} attributed to the C=C stretching indicates the formation of aromatic bio-residue (Uchimiya et al., 2013). The XRD spectra of *ST* feed and bio-residues (Fig. 5.9) at different temperatures showed no significant differences in the powder X-ray diffractogram. Peaks at the 2θ values around 20° and 22° are normally assigned to the crystalline region of cellulose in biomass (Yang et al., 2007). The biomass was decomposed partially at 260 °C, the crystalline structure of cellulose at 22.65° remaining due to the stability of cellulose at low temperatures. However, this peak was invisible in the XRD spectra for bio-residue at 280 °C and 300 °C, indicating that crystalline cellulose molecule was destroyed. However, upon liquefaction new XRD signals were detected at 2θ = 25.32° in all bio-residues (260, 280 and 300°C), which indicated presence of coke/char. The chemical crystal structure of the algae was destroyed and coke/char was formed during the liquefaction process due to decomposition of the *ST* macromolecular matrix (Xu et al., 2016). These are in good agreement with the results of FT-IR, suggesting the conversion of cellulose present in rice straw into products. The analysis of bio-residue obtained at various temperatures showed typical amorphous nature, indicating a rich carbon content.

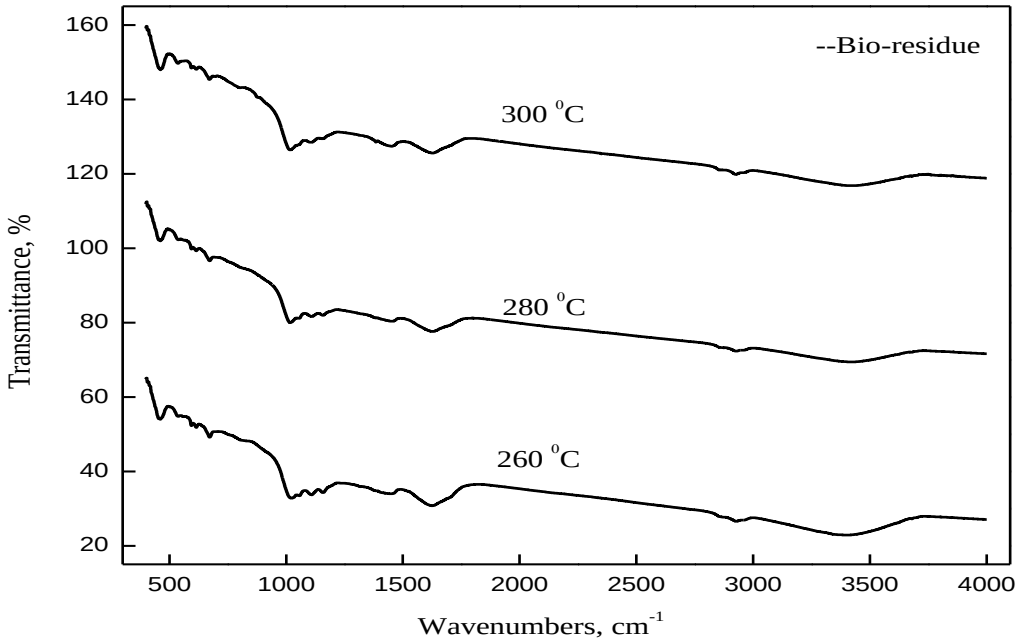

Fig.5.8: FT-IR spectra of *ST* bio-residue obtained at 260, 280 and 300 °C

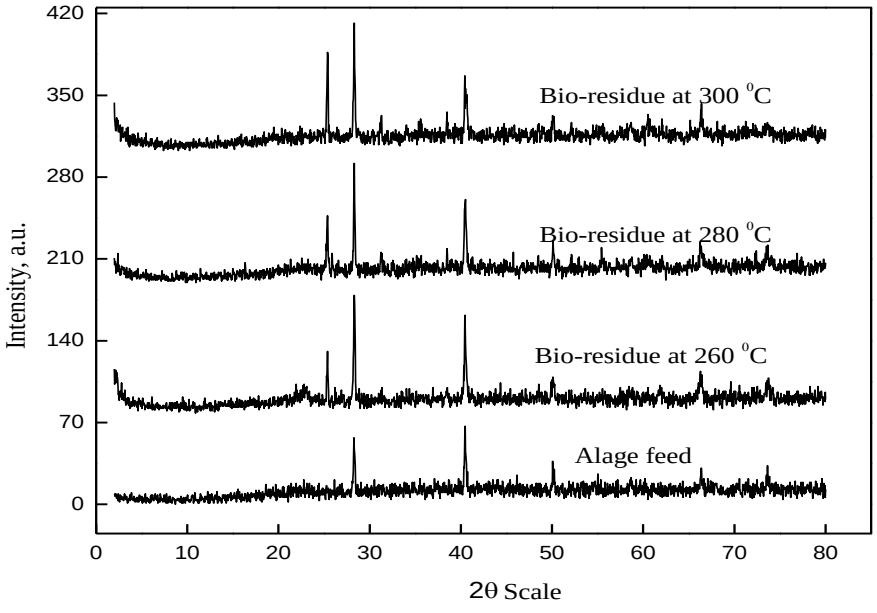

Fig. 5.9: XRD analysis of *ST* bio-residue obtained at 260, 280 and 300 °C

The results have demonstrated the effect of HTL temperature on the distribution of products obtained during the HTL of *ST*. The use of co-solvent increased the bio-oil yield two-fold. Bio-oil analysis by GC-MS, FT-IR and ^{1}H NMR spectra indicated the presence of alcohols, amides, ketones, phenols, ethers and alkanes, besides the esters. This suggests that HTL could be an effective way to convert *ST* biomass (owing to its wide availability and yield obtained) into renewable bio-oil that can be processed and upgraded into transportation fuels. The biochar analysis encourages the application as potential fertilizer / in soil amendment.

Chapter VI

Value addition of *Gracilaria corticata* through Hydrothermal Liquefaction

Bio-oil production from aquatic algal biomass *via* the HTL process has been examined by several researchers (Biller and Ross, 2011; Jin et al., 2013; Raikova et al., 2017; Han et al., 2019). Their studies have revealed that the quality as well as the yield of bio-oil obtained by the HTL process was strongly linked to operating parameters such as reaction temperature, solvent, ratio of feedstock and retention time. Water is often the preferred medium for an HTL process and is responsible for a share of the oxygen content in the biocrude obtained. Processes such as decarboxylation, dehydration, and condensation render the overall oxygen content of biocrude typically lower than that of the feedstock. Since solvents have a remarkable effect on the reaction, liquefaction of biomass with appropriate solvents can be integrated with optimized conditions to simultaneously produce fuel additives and valuable chemicals (Liu and Zhang, 2008). Alcoholic solvents would have several advantages such as a lower critical temperature and pressure compared to water, which could help in achieving much milder reaction conditions. Also, a low dielectric constant of the solvent would be expected, thus leading to an increase in the dissolution of the biomass fragmented products and thereby the liquefaction process. Alcohols being hydrogen donor species are considered potential co-solvents in HTL of biomass since they can promote the deoxygenation processes (Huang et al., 2011). Water-alcohol binary solvents are bestowed with unique thermodynamic properties that speed up reactions such as hydrolysis, decarboxylation, and condensation to a rate higher than what would be possible with the use of a single solvent such as water (Jena et al, 2015).

Very few studies have reported the liquefaction of macroalgae using alcohols. Zhang and Zhang (2014) obtained biocrude through liquefaction of *Chlorella pyrenoidosa* and examined the effects of ethanol:water ratio on its yield and properties. The use of co-solvent was found to improve the yield, which peaked to 57.3 wt.% at an ethanol:water ratio of 5:2 at 280 °C. Zhou et al. (2012) carried out HTL of another green macroalga *Enteromorpha prolifera* using methanol and ethanol. Under conditions of a reaction time of 15 min and algae:solvent ratio set at 1:10, the liquefaction in methanol at 280 °C gave a bio-oil yield of 31.1 wt.% while ethanol at 300 °C yielded bio-oil at 35.3 wt%. The HTL of the brown macroalga *ST* was carried out by Biswas et al. (2017a) wherein using different alcoholic solvents increased the production of aliphatic ester compounds in general. A study by He et al. (2016) examined the use of organic co-solvent (n-heptane, toluene and anisole) in the HTL of macroalgal biomass

of a green alga *Oedogonium,* as a means of achieving *in situ* polarity-based fractionation of the biocrude product. The potential of a red macroalga *Gracilaria gracilis* from the Caspian Sea has been investigated for biocrude oil production under HTL at 350 °C and 15 min by Parsa et al. (2018), yielding 15.7 wt% biocrude, with a HHV of 36.01 MJ/kg. The corresponding values for the green alga *Cladophora glomerata* were 16.9 wt% and 33.06 MJ/kg, respectively.

In this Chapter, *Gracilaria corticata,* a commonly found red macroalgal species in the seas of peninsular India, has been subjected to liquefaction under hydrothermal conditions. The effects of reaction temperature (260 to 300 ºC) and solvents (water, ethanol, methanol, ethanol-water and acetone) at a reaction holding time of 15 min and feedstock:water mass ratio 1:6 were evaluated and the resulting liquid products characterized by ^{1}H NMR, GC-MS and FT-IR techniques. To the best of our knowledge, this is the first HTL study conducted on red macroalgae from this region, the process being employed on the whole algal biomass for its complete valorization. In fact, the only such other systematic study on red algae appears to be that by Parsa et al. (2018), on another species *G. gracilis* obtained from the Caspian Sea and a very recent study by Li et al. (2020) in China on catalytic HTL of *G. corticata*.

6.1. MATERIALS & METHODS

6.1.1. Sample Collection

Samples of the red macroalga *GC* were collected, washed, dried, powdered and stored for further analysis as described in Chapter II (Section 2.1).

6.1.2. Characterization of Feedstock and Products

Procedures for TGA of algal biomass, determination of Gross calorific value and volatile matter content have been described in Chapter V (Section 5.1.2). Moisture content and ash content were obtained at 105 °C and 550°C, respectively (AOAC, 1990) by measuring the sample weight loss after 3 h in a muffle furnace. Elemental analysis was carried out using a CHNS/O Thermofinnigan Flash EA 1112 series Elemental Analyzer. Oven-dried feedstock was used for volatile matter and ash analyses of the feed.

The ^{1}H NMR spectra were recorded on a Bruker Avance 500 Plus instrument as described in Section 5.1.2 of this thesis. The FT-IR spectra of the sample powder diluted in KBr were recorded on a Perkin Elmer FT-IR spectrometer.

Gas chromatography-mass spectrometry (GC/MS, Agilent 7890 B) was used to analyze the organic fraction of the bio-oil. Separation was effected in a DB column (25 m × 0.32 mm × 0.17 μm) at a flow rate of 1 ml min^{-1} and with He as the carrier gas. The parameters used have been detailed in Chapter V.

The total organic carbon (TOC) and total nitrogen (TN) analyses of the aqueous products obtained were carried out on a Shimadzu TOC analyser. For aqueous products, the sample was diluted 200 times for analysis. Detection of organic carbon was done by subjecting the aqueous samples to oxidization by incineration in the presence of platinum catalyst at 900 °C using CO_2-free air.

6.1.3. Hydrothermal Liquefaction Procedures

The HTL experiments using water as solvent were carried out in a 100 ml high pressure autoclave (Parr reactor) made of Hastelloy, as per the procedures elaborated in Chapter V, section 5.1.3.

For HTL with solvents (ethanol, methanol and acetone) and ethanol-water (1:1), the above protocol was as followed at the respective optimal temperature. Pressure build-up during the process was autogenous, with a maximum in the range of 40-155 bar, depending on the reaction conditions. At the end of the reaction the gaseous products were vented and the solid residue separated out from the liquid portion using the same solvent used for the particular reaction. The organic solution thus obtained was dried over anhydrous sodium sulfate, filtered and evaporated in a rotary evaporator at 45-50°C. Upon removal of the respective solvents, this organic fraction was dried in an oven at 80 °C for removing any residual solvent, weighed and designated 'bio-oil'. The solid residue / biochar was dried at 80 °C and weighed. The reactions were carried out in duplicate, and the average values have been reported.

The yield of bio-oil from solvents ethanol, methanol and acetone was calculated as follows.

$$Bio-oil\ yield\ (\ wt.\%) = \frac{Wsolvent\ soluble}{W1} x\ 100$$

$W_{solvent\ soluble}$ is the weight of bio-oil obtained after extracting it from the respective solvent.

Yield of the various fractions *i.e.*, biochar, gas, aqueous yield and the percent conversion were calculated as explained in Chapter V.

6.2. RESULTS & DISCUSSION

6.2.1. Characterization of *GC* Feed

The results of proximate and ultimate analyses of the *GC* sample as summarized in Table 6.1 include the total content of moisture, fixed carbon, volatiles and ash (representing inorganic components of the samples). The contribution of total volatiles produced at 950°C was 69.70% of the total product. The content of carbon (38.63%), hydrogen (5.96%), nitrogen (2.87%), sulphur (0.56%) and oxygen (51.98%, calculated by difference) was obtained from elemental analysis. The calorific value of *GC* feed was 15.28 MJ kg^{-1}.

Table 6.1: Proximate and ultimate analyses of *GC* alga (%, dry basis)

Proximate (wt.%)		***Ultimate (wt.%)***	
Moisture	11.59	C	38.63
Ash content	9.77	H	5.96
Volatile matter	69.70	O	51.98
Fixed carbon	8.94	N	2.87
-	-	S	0.56

It is more desirable for the HTL-derived oil to have a high carbon but low oxygen and nitrogen content. In comparison with the results from the brown alga *ST* reported earlier by us (Biswas et al., 2018a; Chapter V, section 5.2.1), this red alga *GC* did have a higher carbon and lower oxygen content, while the nitrogen content was about three-fold higher (Table 6.1).

Nitrogen in fuel directly forms NO_x compounds which would be undesirable for environmental and legislative reasons, besides negating the advantages of higher carbon and lower oxygen contents (Biller and Ross, 2011). While large marine algal cells have a higher ash content (sea salt) than microalgae, resulting in lower yields of biocrude oil (Li et al., 2012; Anastasakis and Ross, 2011), during the HTL process much of this content as released into the aqueous phase could be recycled (Guo et al., 2015; Zhou et al, 2010). As mentioned by Biller and Ross (2011), it may not be appropriate at this point to invoke a quantitative relation between ash content and biocrude oil, the latter being affected by many factors and highly dependent on algal species and organic components. Notably, however, the ash content in *GC* was only about 36 % of that in the brown alga *ST* as evidenced from our previous studies (Biswas, et al., 2018a; Chapter V, Section 5.2.1).

Anastasakis and Ross (2015), while reporting that the biocrude oil from macroalgae *L. digitata, L. hyperborean, L. saccharina* and *Alaria esculenta* had 10-20% of oxygen, 3-4 % nitrogen and an energy density that was generally in the range of 32-34 MJ/kg, stressed that quality as well as HHV of the biocrude oil were directly influenced by algal composition. The challenge of algal HTL would thus understandably be to increase the yield and improve the quality of biocrude oil in parallel (Chakraborty et al., 2012).

Thermal behavior of *GC* was determined by TGA and DTG (Fig. 6.1). The typical profile of algal biomass portrays three steps. Moisture present in algal biomass could be responsible for the first dip at 100 °C, as discussed by Bae et al. (2011). Carbohydrate decomposition would account for the mass loss between 250 and 370 °C, followed by the decomposition of proteins which occurs at 320 - 450 °C (Ross et al., 2008). The mass loss at temperatures beyond 600 °C could be linked to degradation of lipids. The red alga *GC* exhibited decomposition profiles with largest decrease in sample weight (T_{max}) at 276 °C (Fig. 6.1). Occurrence of major mass decomposition between 200 and 350 °C is a common trend, as reported for some brown and red seaweeds such as *Gracilaria gracilis* (Parsa et al., 2018), *Sargassum* sp. (Kim et al., 2013) and *Laminaria digitata* (Adams et al., 2011). Our TGA/DTG data analysis thus suggests that the temperature range from 200 to 374 °C wherein maximal depolymerization was evidenced, would be an active pyrolytic zone for the *GC* macroalgal biomass. Maximum mass loss occurred at a comparatively higher temperature and a broader range of degradation

temperature in relation to *ST* from our earlier study (Biswas et al., 2018a; Chapter V, section 5.2.1).

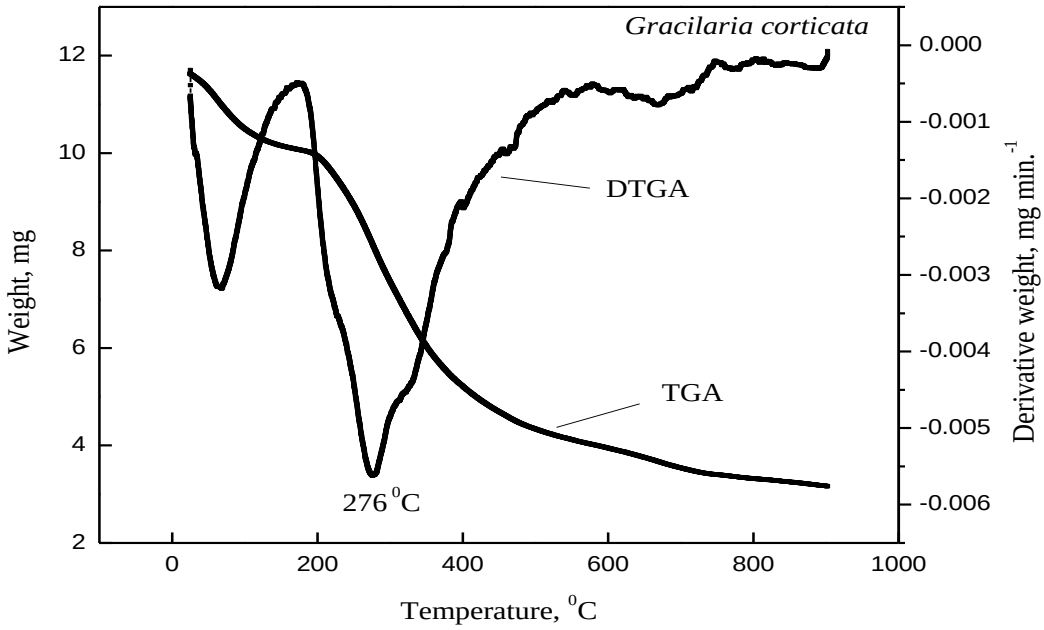

Fig. 6.1: TGA and DTG of *GC*

6.2.2. Hydrothermal Liquefaction Product Yields

6.2.2.1. Effect of temperature

The HTL of *GC* was carried out at various temperatures (260, 280 and 300 °C) with distilled water as solvent, the residence time being 15 min. In general, the yield of biocrude would increase with the process temperature (Valdez and Savage, 2013). The total bio-oil yields from *GC* were 3.88, 2.83 and 5.25 wt.% at 260, 280 and 300°C, respectively (Fig 6.2). A reaction temperature of 300 °C was thus optimum for HTL of *GC*. However, it was observed that these yields were lower than the ones obtained for the brown seaweed *ST* reported earlier in our study (Chapter V, Section 5.2.2.1; Biswas et al., 2018a). As the reactor temperature increases to near supercritical point (300-375 °C), biocrude yield would increase due to protein and cellulose degradation (Torri et al., 2012).

Biochar yield increased from 21.67 to 26 wt.% with increasing temperature (Fig. 6.2), while the conversion of macroalgal liquefaction decreased from 78.33 to 74 wt.%. A similar observation was projected in a study by Jin et al. (2013) which indicated that lower the solid residue yield, higher the conversion of the algal biomass. The gas yield decreased when the temperature was raised to 280 °C but increased again at 300°C. An increase in the aqueous yield was observed at 280 °C but it then decreased at 300°C. The conversion efficiency was 74% at 300 °C.

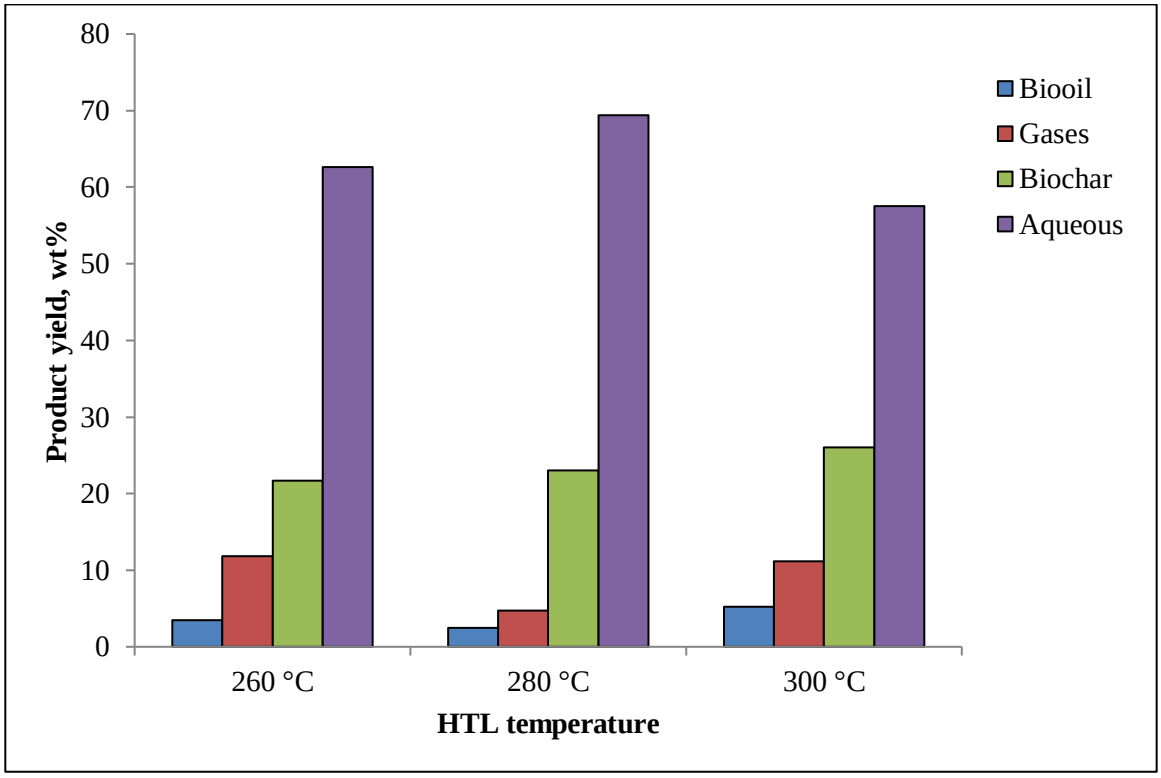

Fig. 6.2: Product distribution from HTL of *GC* in water

6.2.2.2. Effect of solvents

After optimization, solvents such as methanol, ethanol and acetone as well as a combination of ethanol-water (1:1) were used for HTL of *GC*. The mass balance from the HTL using

different solvents, *viz.*, water, methanol, ethanol, acetone and ethanol-water is presented in Fig. 6.3. Liquefaction in alcoholic solvents gave a much higher bio-oil yield compared to that in water. Comparatively higher yields of 8.18, 14, 16.16 and 13.33 wt.% were obtained for methanol, ethanol, acetone and ethanol-water, respectively, at 300 °C. On the basis of oil yield, the solvent efficiency in the biomass liquefaction can be graded as follows: acetone>ethanol>ethanol-water>methanol>water. The higher yield obtained through solvent liquefaction has been suggested to be due to the lower dielectric constants of organic solvents which help to better dissolve and stabilize the reaction intermediates and also aid in the alkylation and esterification reactions between solvents and the intermediate products (Chen et al., 2015b, Yuan et al., 2011).

The solid biochar yield was higher in the case of HTL with alcoholic solvents compared to liquefaction with water at the optimal HTL temperature (280 ^{o}C). Similar results were obtained upon HTL of *ST* (Chapter V, Section 5.2.2.1; Biswas et al., 2017a). The highest biochar yield was obtained upon liquefaction with acetone (44 wt.%) and lowest in water (26 wt.%). Maximum bio-oil and biochar formation was thus observed during liquefaction with acetone as solvent, whereas gas yield, aqueous yield and conversion rates were lowest compared to liquefaction in other solvents. Aqueous yield dipped during liquefaction with alcohol solvents, the lowest (40.6 wt.%) being observed in methanol while the highest (58.48 wt.%) was in water.

Maximum conversion was observed during liquefaction with water (most polar) whereas lowest was observed in acetone (least polar). The solvent type had an obvious influence on the conversion, which was in agreement with the results of Yuan et al. (2011) on *Spirulina* sp. Mazaheri et al. (2010) also observed that the polarity of solvents might play an important role in the conversion process of biomass liquefaction, higher conversion being achieved in more polar solvents.

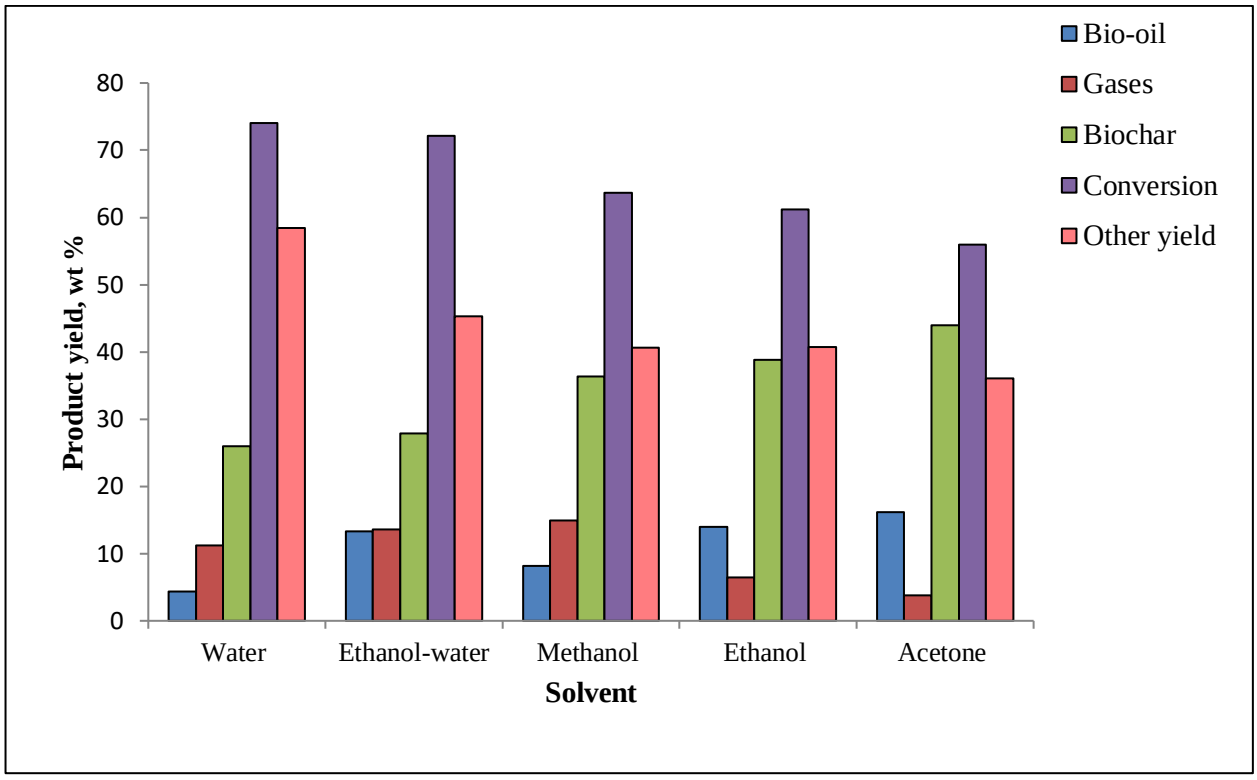

Fig. 6.3: Effect of solvent on product yield during HTL of *GC* at 300 °C.

6.2.3. Bio-oil Characterization

6.2.3.1. Gas chromatography-Mass spectrometry (GC-MS) of bio-oil from *GC*

The main components of the bio-oils were analyzed using a NIST library (The major compounds detected have been detailed in Table A2-Appendix A). Liquefaction temperature affected the components of the bio-oils produced. Different types as well as different percentages of compounds were observed with change in HTL temperature from 260 to 300 °C. The bio-oil components were identified as phenols, ketones, keto alcohols, amines, amino alcohols, amides, N-heterocyclic compounds, aldehydes, acids, esters, alcohols, nitrogen-containing compounds and hydrocarbons. Relative percentage areas of the chromatographic peaks were calculated to facilitate a semi-quantitative analysis (Fig. 6.4). In the HTL process,

carbohydrate and crude fibre first hydrolyze into monosaccharides. Then different cyclic ketones or phenols are formed through dehydration, isomerization and cyclization. The pyrazine derivatives might be due to the Maillard reactions which are reactions between amines and sugars (Muppaneni et al., 2017). The proteins present in the algae are rapidly hydrolyzed to amino acids which in turn get converted into amines and amides by various decarboxylation and deamination dehydration, depolymerization and decomposition reactions (Ross et al., 2010). Most of the ketones were extracted in water and acetone. A ketone compound, 2-butanone, 4-(5-methyl-2-furanyl)- was extracted in acetone but not observed in other solvents. Highest yield (5.348 %) of 3-benzyl-6-isopropyl-2,5-piperazinedione - a ketoamine - was obtained at 260° C, which reduced as liquefaction temperature increased. Ketoamines were mostly extracted in acetone and water, but none were extracted in ethanol. All keto-enes were extracted only in acetone. Keto alcohols were also extracted in acetone. The compound 4-hydroxy-4-methyl-2-pentanone was extracted in all solvents except in ethanol. 3-Pyridinol was extracted in highest amount (10.6%) in water at 300 °C while 3-Pyridinol, 6-methyl- amino alcohols were extracted maximally at 280 °C. Alcohols were primarily extracted in water while phenols were mostly extracted in water at 300 °C and ethanol-water at 300 °C. Butylated hydroxytoluene was observed in highest amount (6.99%) in water at 300°C. Most of the esters were extracted in solvents. Hexadecanoic acid is one of the components most commonly observed in algal bio-oil (Chen et al., 2012b). Amides were extracted in water at 300°C while amines were extracted in acetone. Heterocyclic amines, alkanes, aromatic amines, hydrocarbons, lactans and alkenes were extracted in water at 300°C. The high level of complexity in the composition of the liquid product would necessitate further upgrading such as through denitrogenation and deoxygenation, in order to render the bio-oil suitable as engine fuel.

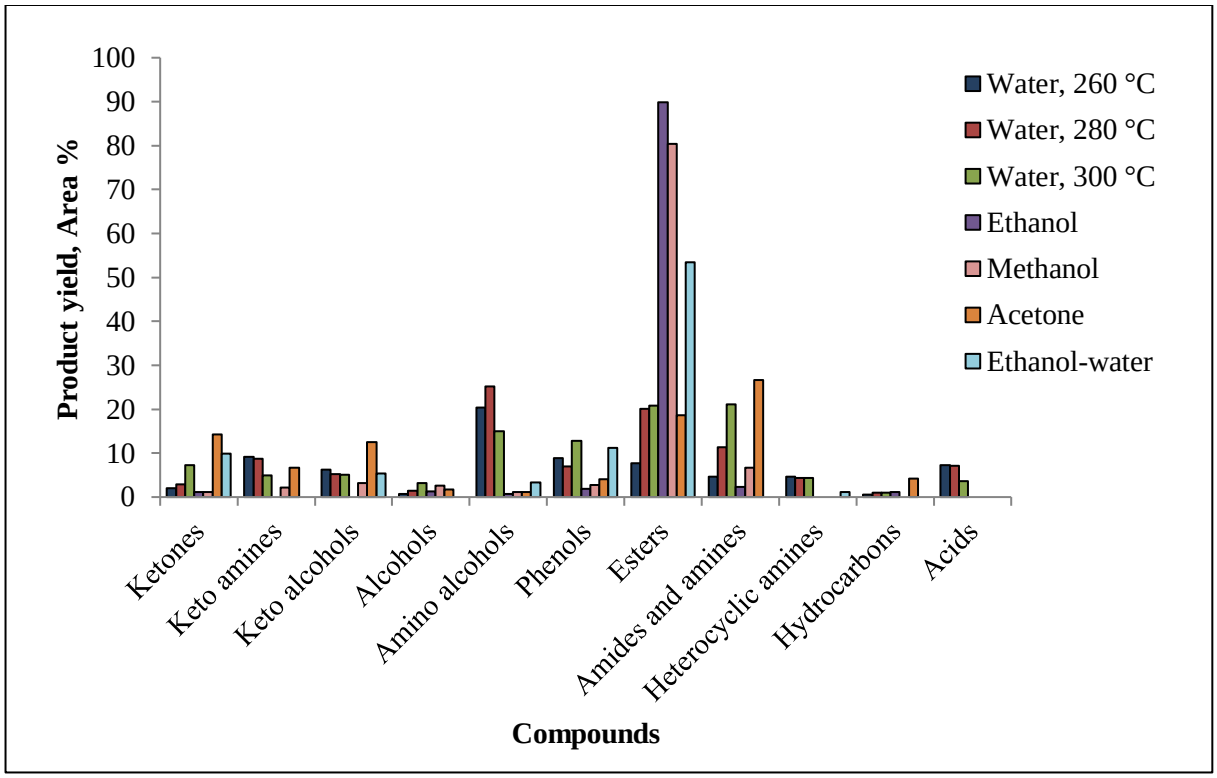

Fig. 6.4: Major chemical components of *GC* bio-oil obtained under best HTL conditions.

6.2.3.2. Fourier Transform-Infrared (FT-IR) spectroscopy of bio-oil

The various functional groups present in the raw biomass and bio-oil obtained from HTL of *GC* were unfolded through FT-IR analysis (Fig. 6.5). Functionality of the bio-oil resulting from HTL differed from that of the raw sample. This implies that the algal macromolecules degrade with significant differences under water, ethanol, methanol and ethanol-water solvent systems. The band at 3437 cm^{-1} confirmed the existence of hydroxyl group in the bio-oil. The presence of C-H symmetric and asymmetric vibrations was indicated by the bands at 2939 cm^{-1} and 2843 cm^{-1} (Yan et al., 2019). Least intensity band was found in bio-oil extract from ethanol-water solvent mixture, which suggested the presence of less aliphatic functional compounds therein. Occurrence of such compounds in the bio-oil was also confirmed by GC-MS analysis data. The absorption band at 1719 cm^{-1} corresponds to the C=O functional group of ketones, aldehydes, and esters and that at 1599 cm^{-1} corresponds to the aryl group (Yan et al., 2019). Absorption in the 1599-1470 cm^{-1} region indicates the symmetric and asymmetric vibrations of aromatic C=C bonds. The occurrence of C-O ether linkages in the bio-oil was

confirmed by the absorption peak at 1269-1024 cm^{-1} (Ma et al., 2020). High intensity absorbance peaks were found in ethanol solvent liquefied bio-oil compared to others solvents. This was also confirmed from the GC-MS results wherein higher amounts of ester compounds were obtained during HTL in ethanol solvents. The bands at 830 and 854 cm^{-1} signify the out of plane C-H vibrations of aromatic compounds, their lower intensity being indicative of a decreased presence of such compounds in the bio-oils.

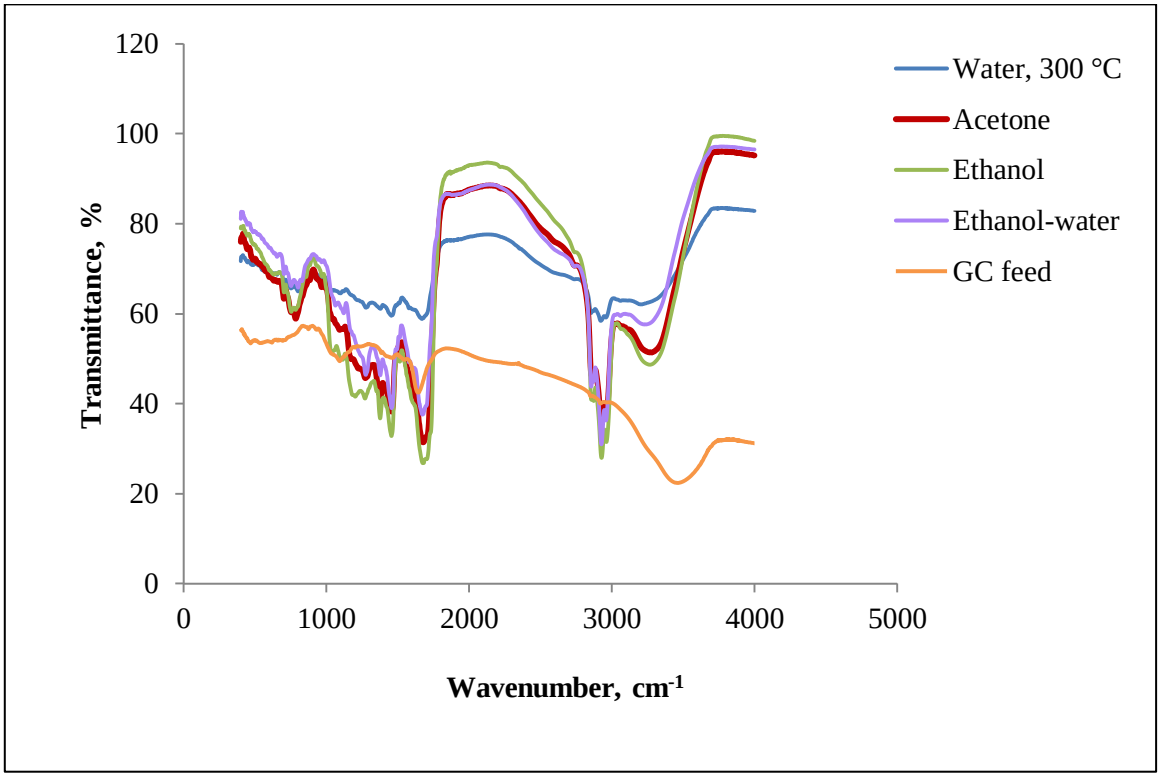

Fig. 6.5: FT-IR spectra of *GC* feed and of bio-oil obtained by HTL in different solvents

6.2.3.3. ^{1}H Nuclear magnetic resonance spectral features of *GC* bio-oil

Analysis of ^{1}H NMR spectral data would provide complementary functional group information to FT-IR spectral data and help to quantify and compare integration areas between the spectra. The presence of various protons in the bio-oil was confirmed by NMR spectral analysis (Fig 6.6). The integrated peak area corresponding to different types of protons was divided into numerous classes. The region from 0.5-1.5 ppm (the highly up-field region) indicates the presence of protons in small chain aliphatic compounds, they being linked to

carbon atoms which are at least two bonds farther from the hetero atom or C=C (Ma et al., 2020). The bio-oil in ethanol solvent showed maximum area percentage protons (55%) in this region. The region from 1.5-3.0 ppm pertains to protons which are bonded to sp^3 hybridized carbon, which is directly linked to the sp^2 carbon of aromatics or olefins. A higher percentage (46%) was found with acetone as solvent, compatible with the GC-MS data of higher methyl-cyclohexanone compounds. The presence of methoxy carbon proton or methylene group proton was confirmed by the peak in the 3.0-4.5 ppm region (Yan et al., 2019). A higher methoxy or methylene functional proton was obtained during ethanol-water mixture liquefaction (Fig. 6.6). The spectral features in the 6.0-8.5 ppm region were confirmatory of aromatic protons (Biswas et al., 2017a). Ethanol solvent liquefied bio-oil showed higher oxygenated compounds, consistent with the GC-MS results.

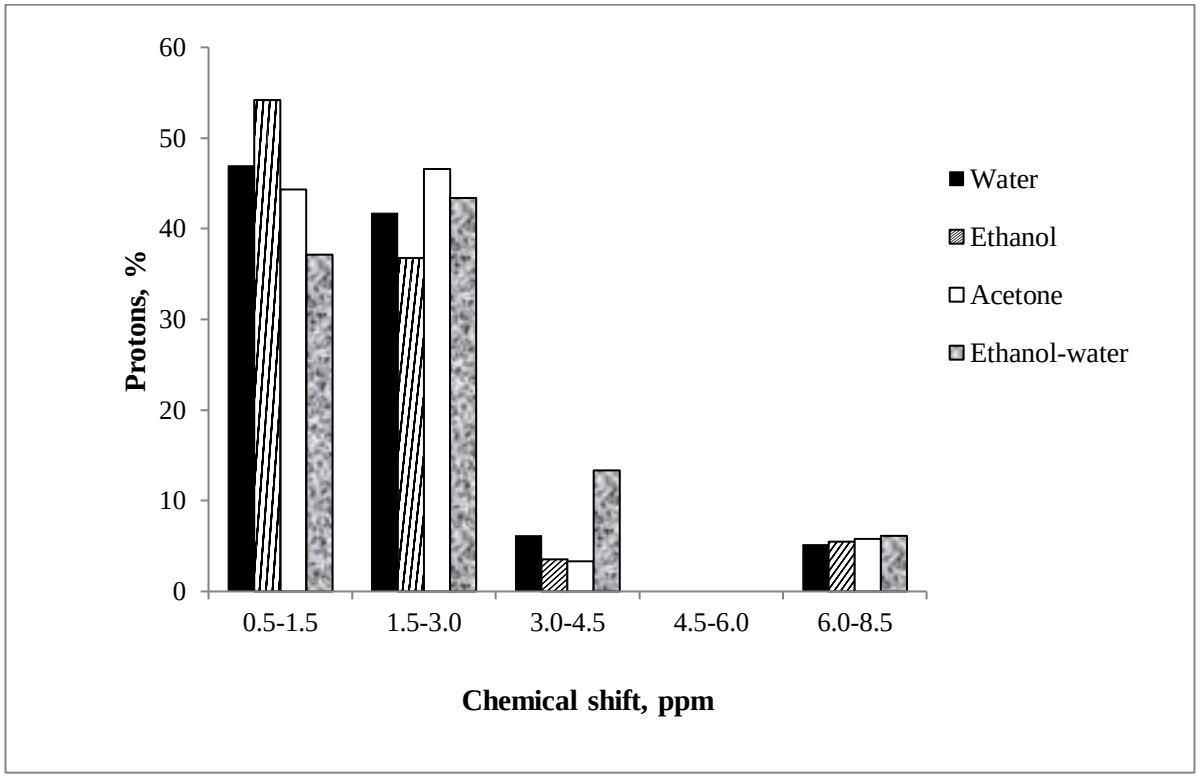

Fig. 6.6: ^{1}H NMR spectral summary of *GC* bio-oil obtained using different solvents at 300 °C.

6.2.4. Aqueous Fraction Analysis

The aqueous fractions obtained at 260, 280 and 300 ºC during water-based HTL have been analyzed (Table 6.2). As the reaction temperature was increased from 260 to 300 ºC, TOC in the aqueous fraction decreased. This implies that increasing the reaction temperature caused the organic carbon fraction to be drawn into the bio-oil fraction by dehydration of carbohydrates, which also accounts for the decreased TOC content in the aqueous fraction. Total nitrogen (TN) in the aqueous fraction decreased marginally from 1.36 g/L to 1.33 g/L as the liquefaction temperature increased from 260 to 280 ºC, while on further increasing the reaction temperature to 300 ºC the TN increased to 1.88 g/L. This is attributed to the fact that at higher temperature, protein degradation compounds majorly remained in the aqueous fraction with the formation of ammonium, which is highly soluble in water (Madsen et al., 2016). Higher temperature thus brought carbohydrate components into the bio-oil rather than the aqueous fraction, while increasing the soluble nitrogen compound content in the aqueous fraction (Muppaneni et al., 2017).

Table 6.2: TOC and TN analyses of aqueous products from HTL of *GC* in water

Liquefaction temp. in water (°C)	**TOC (g/L)**	**TN (g/L)**
260	36.74	1.36
280	34.08	1.33
300	21.26	1.88

In summary, HTL of the red macroalga *GC* was carried out in five different solvents and at different temperatures. Best bio-oil yield (16.16%) was obtained at 300°C with acetone. Maximum amount of ester compounds was obtained with the use of alcoholic solvents (ethanol > methanol > ethanol-water). Bio-oil analysis by GC-MS, FT-IR and ^{1}H NMR spectra indicated the presence of alcohols, amides, ketones, phenols, ethers and alkanes, besides the esters. As the reaction temperature increased, TOC of the aqueous fraction decreased while nitrogen (TN) content increased, which implied that higher temperature pushed the carbon products with lower nitrogen content into the bio-oil. These results encourage the application of macroalgae for potential production of bio-oil and other value-added products such as biochar (fertilizer). Improvement of the yield and quality of bio-oil would entail further studies such as optimization using different catalysts and testing other solvents/solvent combinations for the liquefaction.

Chapter VII

Valorization of *Ulva fasciata* through Hydrothermal Liquefaction

The major components of algae are basically proteins, lipids, carbohydrates and ash. The process of HTL provides a route to produce a higher yield of a bio-crude (bio-oil) product based on the conversion of not just the lipids but of all the biomass components, including carbohydrates and proteins. Bio-oil yield obtained from algae through HTL is thus significantly higher than the lipid content in algae (Biller and Ross, 2011).

Fuel additives and valuable chemicals may be simultaneously produced by integrating biomass liquefaction with appropriate solvents with optimized conditions (Liu and Zhang, 2008). The several advantages of alcoholic solvents have been brought out in Chapter VI.

Many efforts have been made toward producing bio-oil by HTL of green macroalgae such as *Enteromorpha flexuosa* and *Ulva fasciata* (Singh et al., 2015a), *Enteromorpha prolifera* (Zhou et al., 2010; Yang et al., 2014), *Cladophora glomerata* (Parsa et al., 2018) and *Oedogonium* (He et al., 2016). Liquefaction using solvents was studied by Zhou et al. (2012) who conducted HTL of *E. prolifera* using methanol and ethanol at 280 °C, which elicited a bio-oil yield of 31.1 wt.% and 35.3 wt.%, respectively. Similar experiments have been conducted on *U. fasciata* (Singh et al., 2015b). The biocrude yield was 44 wt.% upon liquefaction with methanol, 40 wt.% with ethanol and only 11 wt.% with water.

Catalytic HTL studies were carried out by Yan et al. (2019) on *Ulva prolifera* where a bio-oil yield of 12.0 wt.% was recorded for non-catalytic HTL at 290°C, which shot up to 26.7 wt.% with KOH as catalyst. Another catalytic HTL study by Xu et al. (2015) on *E. prolifera* maximally yielded bio-oil at 34.7 wt.%, with a catalyst loading of 20 wt.%. Jin et al. (2013) conducted co-liquefaction studies of *Spirulina platensis* and *E. prolifera* in subcritical water at different temperature (250 to 370 °C), for 5 to 120 min, SP/EP mass ratio from 0 to 100 %, and water/algae ratio in the range 1:1 to 6:1. They reported an increase in bio-oil yield from 16.7 to 21.6 wt.% with rise in temperature (250 to 340°C). The results suggested that co-liquefaction of algae would be an effective approach to improve the energy utilization efficiency of biomass feedstocks. Neveux et al. (2014a) converted four species of marine macroalgae *Derbesia tenuissima, Ulva ohnoi, Chaetomorpha linum* and *Cladophora coelothrix* and two species of freshwater macroalgae *Cladophora vagabunda* and *Oedogonium* sp. to bio-crude via HTL. The species yielding highest conversion to bio-crude

oil was *Oedogonium* sp (35.9 wt.%) and the influence of biochemical composition of the biomass on biocrude yield and composition was assessed.

Raikova et al. (2017) bridged the gaps among the previous accounts on macroalgal HTL by carrying out a more comprehensive screening of a number of species from all three major macroalgae classes, and examining the correlations between biomass biochemical composition and HTL reactivity. Thirteen macroalgal species were processed by HTL to produce bio-crude oil, biochar, gas and aqueous phase products. The reaction was carried out at a temperature 345 °C. Highest overall bio-crude yields of 28.8 wt.% and 29.9 wt.% were obtained for *U. intestinalis* and *U. lactuca*, respectively. Brown macroalgae *Laminaria digitata* and *L. hyperborean* yielded 16.4 wt.% and 9.8 wt.% bio-crude, respectively..

In this Chapter, green macroalgal biomass *UF* commonly found in the region was examined under hydrothermal conditions. The hydrothermal process was employed on whole *UF* algal biomass for its complete valorization. Effects of the reaction temperature (varied from 260 ºC to 300 ºC), solvents (water, ethanol, methanol, ethanol-water and acetone) with reaction holding time 15 min and water/feedstock mass ratio 1:6 were studied. The liquid products obtained upon HTL were characterized using GC-MS, ^{1}H NMR and FT-IR techniques.

A comparative evaluation of all the three macroalgal types in relation to the product distribution has also been attempted.

7.1. MATERIALS & METHODS

7.1.1. Sample Collection

Samples of the green macroalgal type *UF* were collected and processed as described previously.

7.1.2. Characterization of Feedstock and Products

The details on TGA of algal biomass, determination of Gross calorific value and volatile matter content have been provided in Chapter V, Section 5.1.2. Elemental analysis, moisture and ash content of the algal sample, GC-MS, ^{1}H NMR and FTIR analyses of the organic

fraction of the bio-oil, as well as TOC and TN analyses of the aqueous products were carried out as detailed previously (Chapter VI, Section 6.1.2).

7.1.3. Procedure for HTL

The HTL experiment protocols using water as solvent are described in Chapter V (Section 5.1.3). For HTL with solvents (ethanol, methanol and acetone) the procedures followed were as in Chapter VI, (Section 6.1.3). The maximum autogenous pressure generated during the process was in the range of 40-130 bar under different reaction conditions. The reactions were carried out in duplicate, and the average values have been reported. Yield of various fractions and the percent conversion were calculated as elaborated in Chapter V, while the bio-oil yield after extraction in organic solvents was computed as mentioned in Chapter VI.

7.2. RESULTS & DISCUSSION

7.2.1. Characterization of *UF* Feed

Results of proximate and ultimate analyses of the *UF* sample are summarized in Table 7.1, which include the total content of volatiles, moisture, fixed carbon and ash (*i.e.*, inorganic components of the samples). The calorific value of *UF* was determined as 11.58 MJ kg^{-1}.

Table 7.1: Proximate and ultimate analyses of *UF* alga (%, dry basis)

Proximate (wt.%)		***Ultimate (wt.%)***	
Moisture	14.68	C	36.6
Ash content	16.01	H	6.65
Volatile matter	77.55	O	51.19
Fixed carbon	6.44	N	2.87
-	-	S	2.69

Higher the volatile matter, higher the conversion of feed to products (Yan et al., 2019). Comparison with our earlier studies on the brown macroalga *ST* (Biswas et al., 2018a) in Chapter V, section 5.2.1 and the red macroalga *GC* (Chapter VI, section 6.2.1) indicated that the amount of volatile matter followed the trend *UF* > *GC*> *ST*, which would imply that the conversion rate should also follow the same pattern. This was confirmed in the present study. Moisture content (Table 7.1) was higher than in other *Ulva* species reported, *viz*., *U. prolifera*- 11% (Yan et al., 2019); *U. ohnoi* - 7.2% (Neveux et al., 2014a); *U. lactuca* - 3.7% and *U. intestinalis* - 7.7% (Raikova et al., 2017) but lower than in an earlier reported *UF* sample (16.05%) sourced from Veraval in Gujarat, much further north along the west coast of India (Singh et al., 2015a). The ash content was also much lower than the 25.4% reported by Singh et al. (2015a). Calorific value of our *UF* sample was comparable to those from all the above species of *Ulva*, which had ranged from 11 to 15.4 MJ kg^{-1}.

Thermal behaviour of *UF* was determined by TGA and DTG (Fig. 7.1). The first curve at around 100 °C is due to loss of the moisture present in the algal biomass (Yan et al., 2019). This is followed by mass loss between 200 and 326 °C which would correspond to decomposition of carbohydrates such as cellulose and hemicelluloses (Yan et al., 2019), while the one at higher temperature of 320 - 450 °C would indicate decomposition of the protein fraction (Ross et al., 2008). The mass loss at temperatures higher than 600 °C would be related to lipid degradation. Our *UF* sample exhibited decomposition profiles wherein the largest decrease in sample weight (T_{max}) occurred at 226 °C. The major mass decomposition occurring between 200 and 350 °C was reported for other macroalgae as well (Adams et al., 2011; Kim et al., 2013; Parsa et al., 2018). Thermal analysis through TGA/DTG has thus indicated that the temperature range between 200 and 300 °C may be considered an active pyrolytic zone for the *UF* biomass, where maximum decomposition (depolymerization) takes place.

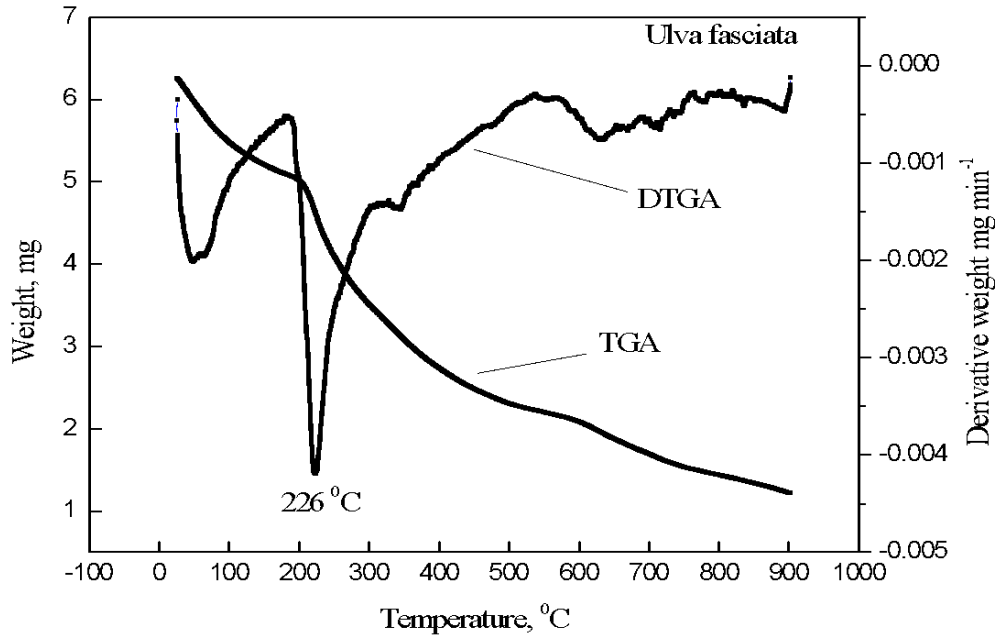

Fig. 7.1: Thermogravimetric and differential thermal analysis of *UF*

7.2.2. Effect of Temperature on HTL Product Yields

7.2.2.1. Bio-oil yield

The HTL of *UF* was performed at various temperatures (260, 280 and 300 °C) in distilled water, with a residence time of 15 min. Reaction conditions were selected based on our earlier studies (Biswas et al., 2018a) and on literature reports (Singh et al., 2015a). With increase in temperature from 260 °C to 280 °C, the bio-oil yield improved from 5.75 wt.%. to 6.67 wt.% . Further increase in temperature to 300 °C decreased the bio-oil yield to 6.50 wt.% (Fig.7.2). A reaction temperature of 280 °C was thus optimum for HTL of *UF*.

A similar trend in the effect of liquefaction temperature on bio-oil yield had been observed for the brown alga *ST*, wherein a decrease in yield was observed at above 280 °C (Chapter V; Biswas et al., 2018a). Yan et al. (2019) recorded highest bio-oil yield (12 wt.%) from HTL of *U. prolifera* at 290 °C, beyond which the yield decreased, dropping to 10.7 wt.% at 310 °C. Zhou et al. (2010) observed that bio-oil production from *E. prolifera* increased with temperature in the range of 220-300 °C but then decreased at 320 °C, sustaining a maximum yield of 20.4 wt.%. In another study on the same algal species, bio-oil yield improved from

10.95 wt.% at 230 °C to 28.43 wt.% at 290 °C, but then decreased to 18.59 wt.% at 310 °C (Yang et al., 2014). The highest overall bio-crude yields at 345°C for *U. intestinalis* and *U. lactuca* were 28.8 wt.% and 29.9 wt.%, respectively (Raikova et al., 2017). Xu et al. (2015) observed an increase in *Enteromorpha prolifera* bio-oil yield from 16.9 wt.% at 250 °C to 31.7 wt.% at 370 °C, a further increase in temperature marginally decreasing the yield. They suggested that this could be due to the subsequent reactions such as polymerization and cracking of the bio-oil. An initial increase in *E. prolifera* bio-oil yield followed by a decline at higher temperatures was also observed by Jin et al. (2013), which was attributed to the further condensation and decomposition of bio-oil into char and light ends, respectively, these remaining uncaptured in the oil fraction. The total bio-oil yield (12 wt.%, obtained at 280 °C) from *UF* sourced from a quite distant coastal region along the west coast of India (Singh et al., 2015a), was twice that obtained from the same species used for the present study. Regional and seasonal differences in composition of the same macroalgal species could be largely responsible for such variations, as noted by Khairy and El-Shafay (2013) and Adams et al. (2011).

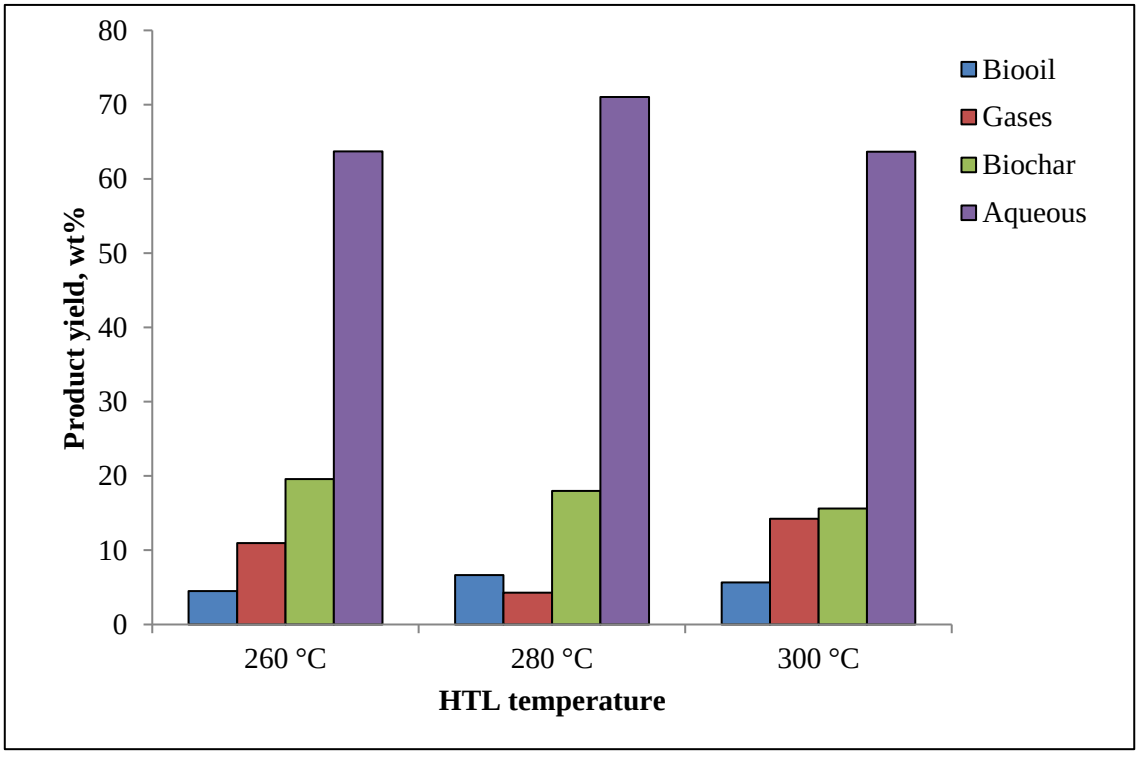

Fig. 7.2: Product distribution from HTL of *UF* in water

7.2.2.2. Biochar yield

The biochar yield was quantified after separation of the other products. As the reaction temperature increased from 260 to 300 °C the yield dropped from 19.67 to 15.67 wt.% (Fig.7.2). This trend was similar to that observed for *Enteromorpha prolifera* by Zhou et al. (2010) who recorded a decreasing biochar yield from 20.2 to 16.9 wt.%, and the results on *Ulva prolifera* (Yan et al., 2019) wherein the yield decreased from 43 to 39.8 wt.% with increase in reaction temperature from 270 to 310 °C. Singh et al. (2015a) had reported a biochar yield of 19 wt.% for *UF*, comparable with the 18 wt.% yield obtained at 280 ºC. Decreased yields could possibly arise from the gradual conversion of organic matter in the feedstock with increasing temperature (Jin et al., 2013). More specifically, lower biochar yield with increasing temperature has been attributed to the conversion of constituent components to biocrude oil, water soluble compounds and gaseous products at higher temperatures, which do not occur at lower temperatures (Muppaneni et al., 2017). Biochar yield was thus negatively correlated to the conversion of feedstock, *i.e.*, lower the biochar yield, higher the conversion of the algal biomass to the products (Jin et al., 2013). Biochar generally contains feedstock ash which is rich in inorganics (Tian et al., 2014) and as per Jena and Das (2011), biochar yield would highly depend on ash content in the feedstock.

7.2.2.3. Gas yield

The gas yield decreased (from 10.95 to 4.28 wt.%) with increase in temperature from 260 to 280°C, and increased again to 14.25 wt.% as the temperature was raised to 300°C (Fig. 7.2). A gas yield of 8 wt.% was observed by Singh et al. (2015a) during *UF* liquefaction at 280°C. Increased gas production at higher HTL temperature was also reported in other studies on green macroalgae (Zhou et al., 2010; Jin et al., 2013; Yan et al., 2019). As the reaction temperature approaches the critical point of water, gasification dominates the hydrothermal reaction medium and forms increased amounts of gaseous products, a probable reason for the lower bio-oil yield (Jin et al., 2013). Reporting temperature effects on microalgal liquefaction, Reddy et al. (2016) opined that repolymerization of water-soluble compounds at comparatively higher temperatures might have led to their conversion to either biocrude oil or

gaseous products. Inorganic salts in the feedstock are also responsible for the higher gas yield at more severe temperatures (Patwardhan et al., 2010).

7.2.2.4. Aqueous products

Aqueous phase products made up the largest fraction of components obtained upon HTL (Parsa et al., 2018; Raikova et al., 2017) on account of a large ash component (water-soluble inorganic sea salts) in the algal biomass (Zhou et al., 2010). Most of these inorganic salts being water soluble, remain in the aqueous phase after reaction. The highest aqueous yield of 71.05 wt.% was at 280°C, which decreased to 63 wt.% with increase of the HTL temperature (Fig. 7.2). A similar trend was reported by Zhou et al. (2010) and Xu et al. (2015) for *E. prolifera*. Anastasakis and Ross (2015) have also shown that the aqueous yield from HTL of macroalgae decreased with increasing temperature. Higher aqueous yield at lower temperatures might be attributed to the accumulation of a large amount of hydrolysis products from protein and carbohydrate molecules in the biomass (Xu et al., 2015). With rise in temperature, aqueous products would undergo complex reactions such as dehydration, deoxygenation, decarboxylation, and polymerization reactions to form oil and gas products. Singh et al. (2015a) had reported an aqueous yield of 61 wt% and maximum conversion of 81 wt.% from *UF* biomass, akin to the 82 wt.% conversion obtained in the present study. The conversion efficiencies observed at 260, 280 and 300°C were, respectively, 80.3%, 82% and 84.18%.

7.2.3. Effect of solvent on HTL product yields from *UF*

7.2.3.1. Bio-oil yield

Alcoholic solvents gave a much higher bio-oil yield compared to HTL with water, the highest yield being obtained from a co-solvent system of ethanol:water (24.66 wt.%), followed by methanol (15.5 wt.%), ethanol (14.66 wt.%) and acetone (11.33 wt.%) (Fig. 7.3). In a study by Zhou et al. (2012) on the green macroalga *E. prolifera*, highest bio-oil yields were obtained in methanol at 280 °C (31.1 wt.%) and ethanol at 300 °C (35.3 wt %). Increase in bio-oil yield was also reported in the microalga *Nannochloropsis oceanica* (Caporgno et al., 2016), wherein ethanol:water in a ratio of 1:1 increased biomass conversion and the bio-oil yield rose

to 60 wt.%, in comparison to HTL using only water as solvent (54 wt.%). Zhang et al. (2014) obtained a maximum bio-oil yield of 57.3 wt.% from the microalga *C. pyrenoidosa* using ethanol-water (1:1). In our earlier studies wherein the brown macroalga *ST* was subjected to HTL using water, methanol, ethanol, and ethanol-water co-solvent, the bio-oil yields at 280 °C were 16.33 wt.% (Biswas et al., 2018a), 22.8 wt.%, 23.3 wt.%, (Biswas et al., 2017a), and 32.0 wt.%, (Biswas et al., 2020; Chapter V, Section 5.2.2), respectively.

7.2.3.2. Biochar yield

The solid biochar yield was higher in the case of HTL with alcoholic solvents compared to liquefaction with water, the highest being in acetone (41.16 wt.%) compared to the other solvents. (Fig.7.3). In a study by Zhou et al. (2012) on the green macroalga *E. prolifera*, the biochar yield was found to be in the range 50.5 wt.% to 41.1 wt % for methanol and 52.4 wt.% to 39.0 wt % for ethanol. Biochar yield was observed to be quite low in the ethanol: water system (27.33 wt.%). This could be due to the ability of co-solvents to act as radical scavenging agents to reduce char formation (Pedersen et al., 2016).

7.2.3.3. Aqueous yields

The aqueous yields (42.54 wt.% - 45.85 wt.%) were comparable in all the solvents used, except water, which gave a much higher yield of 71.05 wt.% (Fig. 7.3). According to Kim et al. (2017), while using co-solvents, solvent penetration helps to extract lipids from algal cells, and the biphasic mixture enables hydrophilic ions to remain in the aqueous phase, reducing post-treatment steps. The conversion was observed to be highest in water (82 wt.%) followed by the ethanol:water solvent combination (72.6 wt.%).

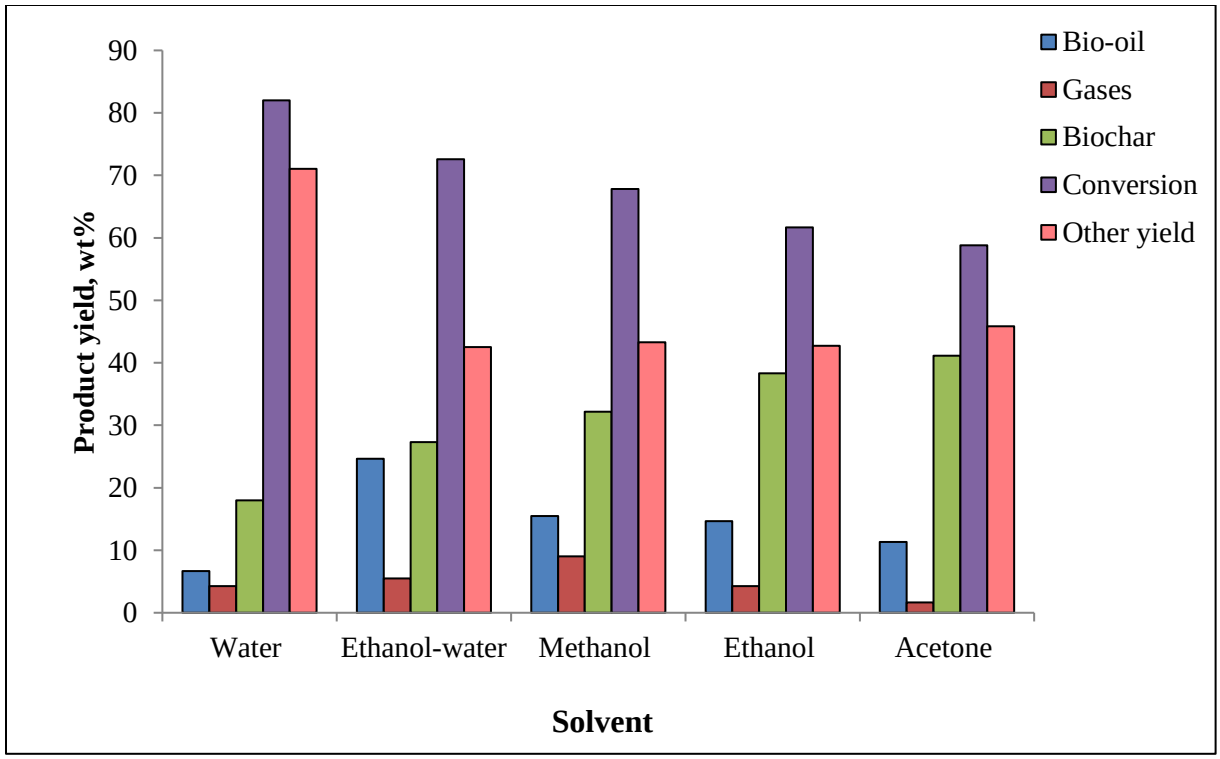

Fig. 7.3: Effect of solvent on product yield during HTL of *UF* at 280 °C.

7.2.4. Bio-oil Characterization

7.2.4.1. Gas chromatography-Mass spectrometry (GC-MS) of bio-oil from *UF*

The main components of the bio-oils were analyzed using a NIST library (The analysis results are presented in Table A3-Appendix A). Liquefaction temperature affected the composition of the bio-oils produced. As the HTL temperature varied from 260 to 300 °C, different types of compounds as well as different percentages of compounds were observed. The components of the bio-oils were identified as phenols, ketones, keto alcohols, amines, amino alcohols, amides, N-heterocyclic compounds, aldehydes, acids, esters, alcohols, nitrogen-containing compounds and hydrocarbons. In the HTL process, carbohydrates and crude fibers first hydrolyze into monosaccharides. Then different cyclic ketones or phenols are formed through dehydration, isomerization and cyclization of polysaccharides and celluloses (Yang et al., 2014). The pyrazine derivatives might have resulted from the Maillard reactions between amines and sugars (Muppaneni et al., 2017). Algal protein would be rapidly hydrolyzed to

amino acids which in turn get converted into amines and amides by various decarboxylation and deamination dehydration, depolymerization and decomposition reactions (Ross et al., 2010). The N-containing compounds (such as hexadecanamide and dodecanamide) were formed by reaction between FAs and ammonia (Chen et al., 2015d; Yu et al., 2014).

A semi-quantitative analysis was performed by calculating the relative percentage area of the chromatographic peaks (Fig 7.4). Amines were extracted mostly in water and acetone. High percentage areas of 3-pyridinol (16.57 % and 17.09 %) were observed during aqueous extraction at 280 and 300°C, respectively. This compound was also obtained in acetone (15.16 %) and maximally in ethanol-water (20.72 %). Ketoalcohols were best extracted in water at 260°C while ketones were extracted in water as well as other solvents but not in ethanol:water. Highest content (12.9%) of ketoalcohol (2-pentanone, 4-hydroxy-4-methyl-) was observed at 260 ºC and was significantly lower at higher temperature. Butylated hydroxytoluene was obtained in water at 260°C (7.83%), 280°C (7.63 %) and 300°C (7.05 %) but was not extracted in the alcoholic solvents. Phenolic compounds, alcohols, carboxylic acids, alkenes and keto amines were mostly extracted during HTL with water. Amines were seen in higher amount in acetone extracts but to a lesser extent in other solvents. Esters were obtained in very low quantities during liquefaction with water - *e.g.*, hexadecanoic acid methyl ester (0.73 %), and hexadecanoic acid ethyl ester (5.77 %) - compared to the much better yields during extraction with organic solvents, *viz.*, 55 % hexadecanoic acid methyl ester (in methanol) and 57 % hexadecanoic acid ethyl ester (in ethanol). However, even though ethanol-water solvent gave the best bio-oil yield, the ester yield obtained was less. Hexadecanoic acid methyl ester yield, for instance, decreased to 17.8 %, suggesting that the bio-oil quality could be compromised, hexadecanoic acid being one of the components most frequently found in algal bio-oil (Chen et al., 2012b). Alkanes were observed upon HTL with water at 300°C (Fig.7.4). Amides were extracted mostly in water as well as acetone. The complex composition of the liquid product would call for further upgrading such as denitrogenation and deoxygenation, if the bio-oil is to be made suitable for use as engine fuel.

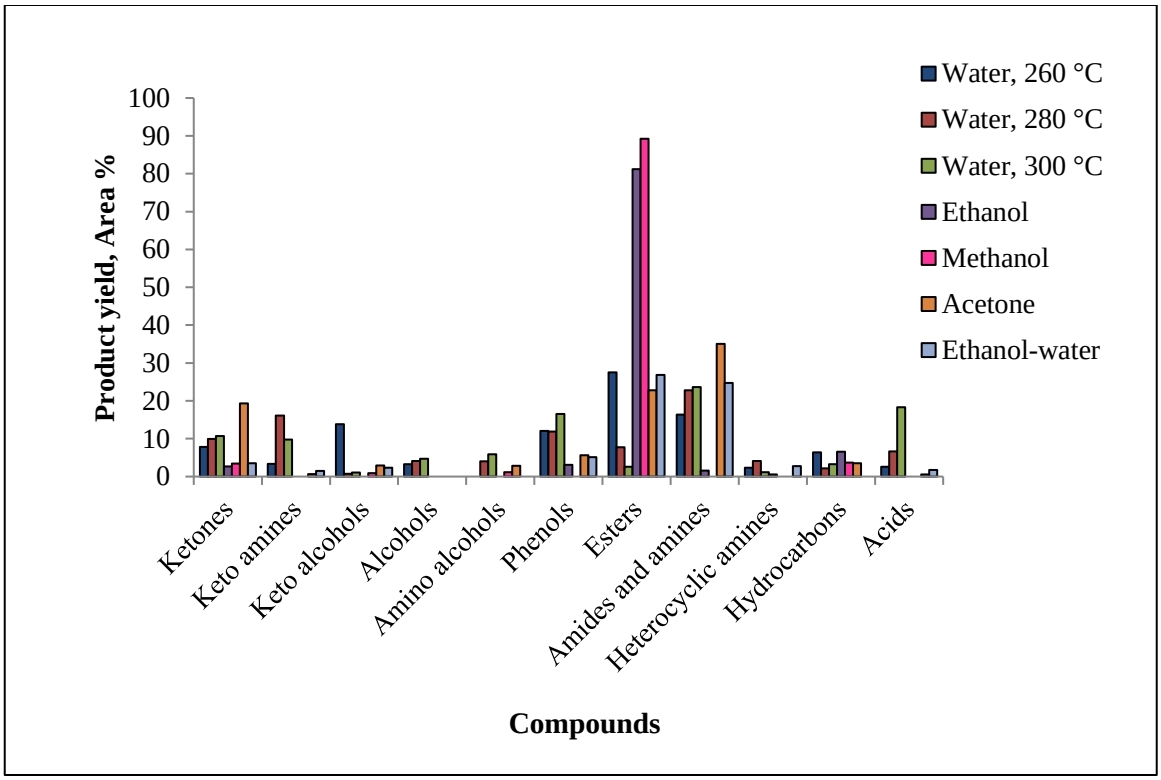

Fig. 7.4: Major chemical components of *UF* bio-oil obtained under best HTL conditions.

7.2.4.2. Fourier Transform-Infrared (FT-IR) spectroscopy of bio-oil

Functional groups of compounds present in bio-oils and raw material from *UF* were analyzed by FT-IR spectroscopy. There was clear indication of the breaking of algal biomass into various functional compounds corresponding to different fundamental vibration bands (Fig. 7.5). The band at 3378 cm^{-1} indicating the presence of –OH groups in the bio-oil samples was noticed at 3415 cm^{-1} in the algal feedstock. The bands at 2925 cm^{-1} and 2850 cm^{-1} showed the asymmetric and symmetric stretching of –CH of bio-oils and although less intense, the 2915 cm^{-1} and 2835 cm^{-1} bands for the algal sample indicated similar stretching. In case of bio-oils, the fundamental stretching vibration of unconjugated carbonyl was found at 1815 cm^{-1}, while it was observed at 1790 cm^{-1} in the feedstock. That at 1645 cm^{-1} indicated the vibration band of conjugated carbonyl *e.g.*, amines, which was found with high intensity in the bio-oil from acetone and ethanol-water extraction (Biswas et al., 2018b). The vibration band of methyl and methylene were found at 1452 cm^{-1} in all bio-oils, while it was noticed at 1398 cm^{-1} in raw

algae (Kim et al., 2020). In addition, the bands observed at 1245-1000 cm^{-1} represent the vibration of C-O linkages (Biswas et al., 2020). Taken together, the change in intensity of vibrational band of different functional groups clearly indicated breakdown of the algal biomass during the HTL process.

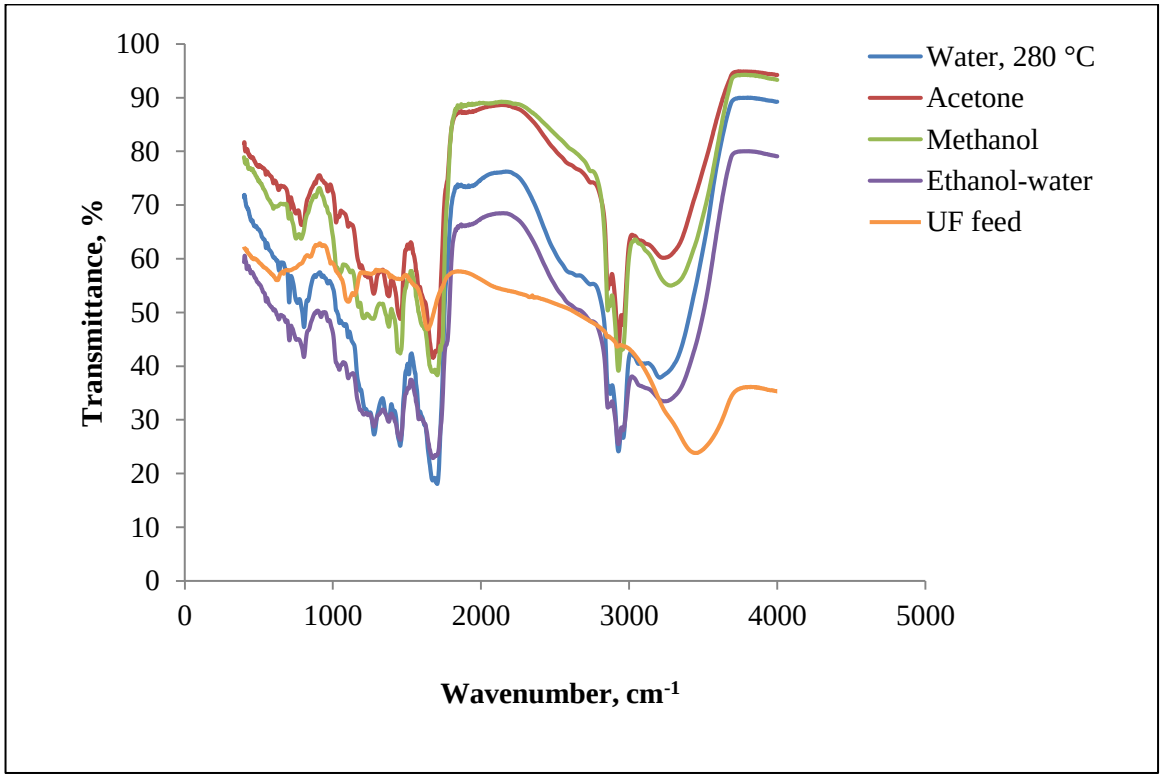

Fig. 7.5: FT-IR spectra of *UF* feed and of bio-oil obtained by HTL in different solvents

7.2.4.3. ^{1}H Nuclear magnetic resonance (NMR) spectral features of bio-oil

Different types of protons present in the bio-oils were analyzed by their characteristic ^{1}H-NMR spectral features in specific chemical shift regions in the range of 0.5 to 8.5 ppm (Fig. 7.6). The upfield region (0.5-1.5 ppm) showed aliphatic protons attached to sp^3 hybridized carbon atom or away from any hetero atom and double bonded carbon. In this region, maximum proton percentage (34.6%) was found in the bio-oil obtained with acetone, and 34% in the bio-oil with ethanol-water as solvent. It indicated the presence of high percentage area of GC-MS derived compounds having aliphatic (sp^3) protons. The bio-oil obtained upon HTL with water and methanol showed 28.0 and 26.2 % of this type of aliphatic protons. The ^{1}H-

NMR region of 1.5-3.0 ppm indicated the aliphatic protons attached to carbon of olefins or aromatics (Biswas et al., 2017b). The bio-oil from HTL in acetone showed maximum proton percentage (37.2%) of this type of protons, while those derived through HTL in water, methanol and ethanol-water showed proton percentages of 36.4, 33.1 and 34.8, respectively. While all bio-oils thus showed high proton percentage in this region, a relatively higher percentage of such protons was observed with acetone. Moreover, the region at 4.5 to 6.5 ppm represented protons of aromatic ethers such as methoxyphenol (Singh et al., 2014). A significant proton percentage was noticed in this region, the maximum (8.4 %) being with water. The next significant ^{1}H-NMR zone (6.5-8.5 ppm) corresponded to the aromatic region of the spectrum, where a relatively high percentage (13.1%) of aromatic protons was observed in the bio-oil. Thus FT-IR as well as ^{1}H-NMR analyses of bio-oil indicated the presence of aliphatic, aromatic and ether constituents in the bio-oil obtained from the HTL of *UF*. This validated the GC-MS results and the formation of different types of functional compounds as a result of breaking of various types of linkages.

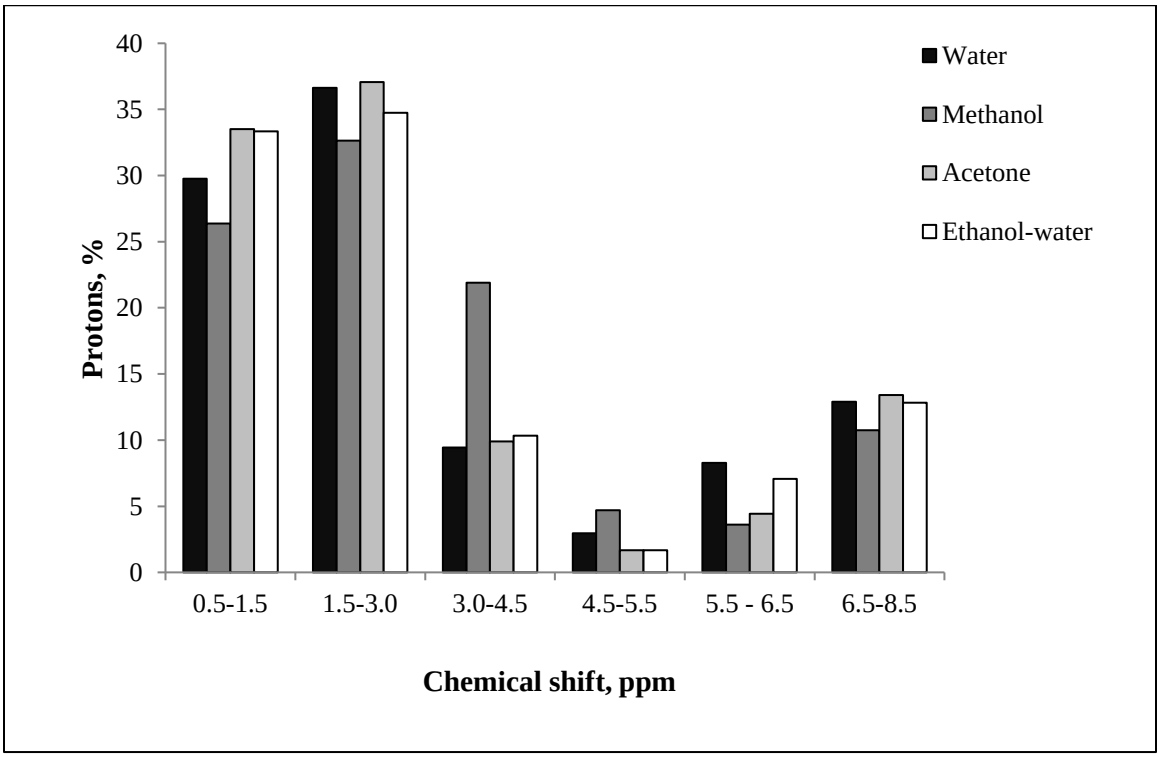

Fig. 7.6: ^{1}H NMR spectra of *UF* bio-oil obtained using different solvents at 280°C

7.2.5. Aqueous fraction analysis

Analyses of TOC and TN were carried out for the aqueous fraction obtained from HTL of the algae at different temperatures (Table 7.2). The results were in good agreement with those on liquefaction of *UF* algae at different reaction temperatures. A maximum TOC value of 38.56 g/L was observed at 280 °C, the identified optimum temperature. The TN in the aqueous fraction, on the other hand, decreased at 280 ºC and then increased upon raising the reaction temperature to 300 ºC.

Table 7.2: TOC and TN Analyses of aqueous products from HTL of *UF* in water

Liquefaction temp. in water (°C)	TOC (g/L)	TN (g/L)
260	34.28	1.60
280	38.56	1.43
300	32.44	1.59

7.2.6. Comparison of product distribution for the three different classes of macroalgae upon HTL in water

During HTL in water, bio-oil yield of the brown alga *ST*, which increased from 11.5 wt.% to a maximum of 16.33 wt.% with increase in temperature from 260°C to 280 °C, subsequently decreased to 14.67 wt.% as the temperature was raised to 300 °C (Fig. 7.7). A similar trend was followed by the green alga *UF*, which yielded a maximum of 6.67 wt.% at 280ºC. Bio-oil yields from the red alga *GC* increased from 3.88 wt.% to 5.25 wt.% as the optimum temperature of 300 °C was attained. In summary, the maximum yields from these three representative samples *ST*, *UF* and *GC* were 16.33, 6.67 and 5.25 wt.% at the respective optimum temperatures of 280, 280 and 300°C.

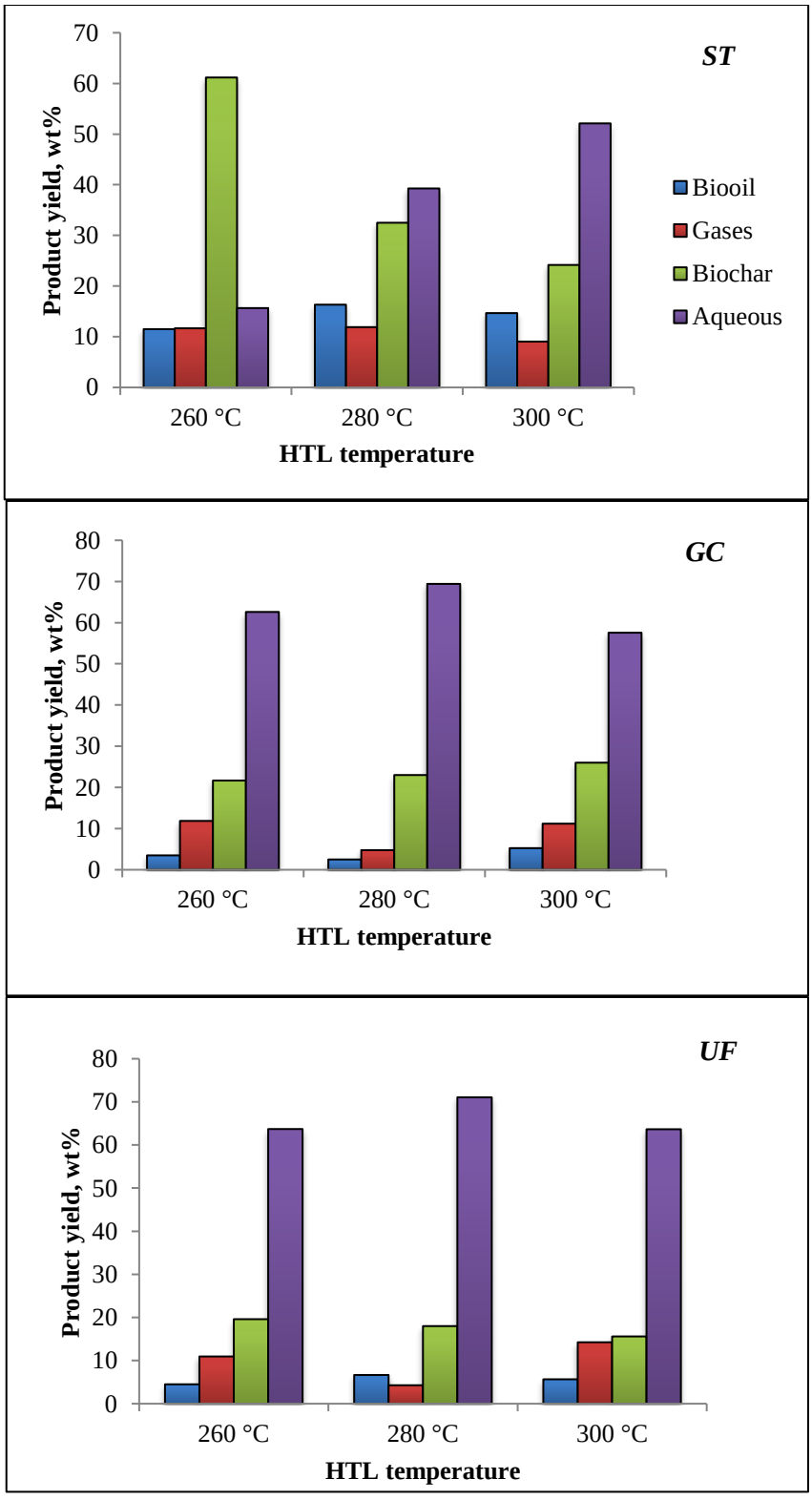

Fig.7.7: Product distribution of macroalgae from hydrothermal treatment at varying temperatures, using water as solvent

Biochar yield was quantified after the separation of products. As the reaction temperature increased from 260 to 300 °C the biochar yield for *UF* decreased from 19.67 to 15.67 wt.% (Fig. 7.7). The solid residue yields for *ST* also decreased continuously from 61.2 wt.% to 24.2 wt.% as the temperature increased from 260 to 300°C (Biswas et al., 2018a). Such decrease in biochar yield has been attributed to improved conversion of the constituent components to biocrude oil, water soluble compounds and gaseous products, which occurs only at higher temperatures (Muppaneni et al., 2017). In *GC*, however, biochar yield increased from 21.67 to 26 wt.% with increasing temperature, and the conversion through macroalgal liquefaction dropped from 78.33 to 74 wt.%.

The yield of gaseous product from *ST* initially showed an increase as the temperature was raised from 260 to 280 ºC (11.67 - 11.9 wt. %) but dropped to 9.05 wt.% with further increase in temperature to 300 ºC (Table 7.3). The gas yield from *UF* decreased with increase in temperature from 260 to 280°C (10.95 to 4.28 wt. %) and then increased again as the temperature was raised to 300°C (4.28 to 14.25 wt.%). Likewise, in the case of *GC*, the gas yield decreased (from 11.86 to 4.76 wt. %) when the temperature was raised to 280 °C but increased again to 11.19 wt.% at 300°C. A similar trend was observed for the gas yield from *Sargassum patens* (Li et al., 2012), wherein there was an initial increase followed by a decrease between 320 and 340 ºC, which then improved upon further rise in temperature, indicative of decomposition of the bio-oil.

The aqueous phase made up the largest fraction of the products obtained after HTL. The aqueous yield obtained from *UF* (71.05 wt.%) was highest at 280°C, the yield decreasing to 63 wt.% with increase in the liquefaction temperature (Fig. 7.7). An increase in the aqueous yield from *GC* (from 62.6 to 69.41 wt.%) was observed at 280 °C but it then decreased to 57.56 wt.% at 300°C. This decrease in the aqueous yield might be due to the repolymerization of water-soluble compounds into biocrude or gaseous phase (Muppaneni et al., 2017). In contrast, in the case of *ST* the aqueous yield increased from 15.66 to 52.11 wt.% with increase in temperature from 260 to 300°C.

The product yields from HTL of *ST*, *GC* and *UF* at different optimal temperatures (selected on the basis of best bio-oil yield) are shown in Fig. 7.8.

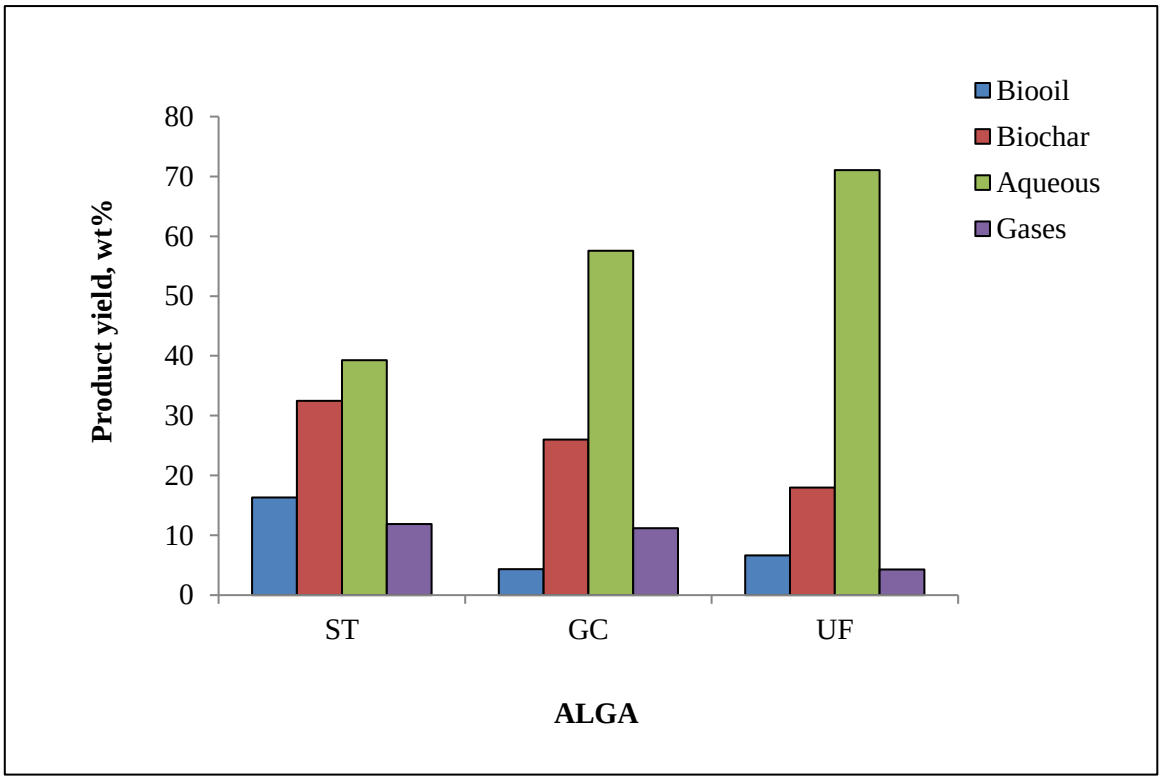

Fig. 7.8: Product yields from HTL of *ST*, *GC* and *UF* at their respective optimal temperatures

The best bio-oil yield from *ST* was 16.33 wt.% at 280°C, which was higher than those from *UF* (6.67 wt.% at 280°C) and *GC* (5.25 wt.% at 300°C). The respective biochar yields were 32.5, 18 and 26 wt.%. These may be related to the higher ash content (26 wt.%) in S*T* feedstock which led to greater char formation under our experimental conditions, inorganic elements in the ash being known to catalyze char forming reactions during liquefaction (Maddi et al., 2011). This reasoning, however, could not be applied while comparing between the other two algal types, since *UF* had a higher ash content but yielded less biochar than *GC*. The gas yield was comparable for *ST* (11.9 wt.%) and *GC* (11.19 wt.%) but was much lower for *UF* (4.28 wt.%). This may be attributed to the algal polysaccharides and proteins which were degraded to small molecules by dehydration, deoxygenation and decarboxylation reactions occurring simultaneously during liquefaction (Li et al., 2012). Additionally, the

product oil partially decomposed, also leading to gas production. The aqueous yield was highest in *UF* (71 wt.%), followed by *GC* (57 wt.%) and *ST* (39 wt.%).

7.2.7. Comparison of Mass Balance for the Three Different Classes of Macroalgae upon HTL in Solvents.

The total bio-oil yield from *ST* was 16.33 wt.% at 280 °C (Table 7.3). Comparatively higher yields were obtained with ethanol-water (Biswas et al., 2020), ethanol and methanol, respectively, at 280 °C (Biswas et al., 2017a). Similarly, for *UF* the highest bio-oil yield of 24.66 wt.% was obtained with ethanol-water. Contrasting results were obtained with *GC*, wherein maximum bio-oil yield (16.16 wt.%) was obtained with acetone and the lowest with water. The use of alcoholic solvents increased the total bio-oil yield in all the three algal types studied by us.

Biochar yield was also the least during liquefaction in water, in the case of *GC* (26 wt. %) and *UF* (18 wt.%), better yields resulting from HTL in alcoholic solvents. In the case of *S. tenerrimum*, however, it was lowest with ethanol-water (30 wt.%). While biochar yield was maximum for liquefaction with acetone in the case of *GC* (44 wt.%) and *UF* (41.16 wt.%), for *ST* (Biswas et al., 2017a) it was highest with the use of ethanol (43.16 wt.%).

The yield of gaseous products was in the range of 4.52-11.9 wt.% in *ST*, while a slightly lower range of 1.66-9.04 wt.% was observed in *UF*. Gas yield was highest for *GC* (up to 14.92 wt.%).

Maximum conversion of 82 wt.% was observed during liquefaction of *UF* with water at 280 ^{o}C, followed by 74 wt.% for *GC* with water at 300 ^{o}C. The maximum conversion of 70 wt.% was obtained for *ST* during liquefaction in ethanol-water.

Highest aqueous yield resulted from HTL with water for *UF* (71 wt.%), *GC* (58.47wt. %) and *ST* (39.27wt. %), whereas with other solvents, it was in the range of 42.54-45.85, 36.04-45.27 and 24.47-36.87 wt.%, respectively. Variation in solvent types hence strongly affected the distribution of products in the HTL of all the three algal varieties.

Table 7.3: Product distribution of macroalgae from hydrothermal treatment in various solvents

Sample and solvent used	Total Bio-oil (wt. %)	Gases (wt.%)	Biochar (wt.%)	Conversion (wt.%)	Other yield (wt.%)
ST-W	16.33	11.9	32.5	67.67	39.27
ST-M*	22.8	10.0	30.33	69.66	36.87
ST-E*	23.8	8.57	43.16	56.83	24.47
ST-EW	32.06	4.52	30	70	33.42
GC-W	5.25	11.19	26	74	58.48
GC-M	8.18	14.92	36.33	63.66	40.6
GC-E	14	6.43	38.83	61.16	40.74
GC-EW	13.33	13.57	27.83	72.16	45.27
GC-A	16.16	3.8	44	56	36.04
UF-W	6.67	4.28	18	82	71.05
UF-M	15.5	9.04	32.16	67.83	43.3
UF-E	14.66	4.28	38.33	61.66	42.73
UF-EW	24.66	5.47	27.33	72.6	42.54
UF-A	11.33	1.66	41.16	58.83	45.85

* From Biswas et al. (2017a)

W= water as solvent, E = ethanol as solvent and M = methanol as solvent, EW= Ethanol-water as solvent , A= acetone as solvent.

7.2.8. GC-MS Analysis of Bio-oil from the Three Macroalgae

Analysis of components of the bio-oil derived from *ST* at 280°C, *GC* at 300°C and *UF* at 280°C was carried out by GC-MS. Biochemical composition of macroalgae is known to significantly influence the composition of their bio-oil (Parsa et al., 2018, Barreiro et al., 2015). Different compounds at differing concentrations were obtained under varied reaction

conditions and liquefaction solvents. The same compounds were at times detected but with different percentage yields (Tables A 1-3: Appendix A; Biwas et al., 2017a; Biswas et al., 2018a).

Most of the esters were observed in all the three macroalgal types, albeit at varying concentrations. Ethanol and methanol appear to be comparatively more effective in extraction of these esters. Also, while liquefaction with co-solvents gives an overall improved bio-oil yield (Biwas et al., 2017a; Biswas et al., 2018a), the quality of the oil is likely to be compromised on account of the lower content of valuable esters.

The above results suggest the potential use of *ST*, *GC* and *UF* as sources for biofuel production through hydrothermal processes. The bio-oil needs to be processed further and upgraded / refined for use as transportation fuels. The biochar could be researched upon to analyze its benefits for soil amendment in agriculture.

Summary, Conclusions and Beyond…

The prolonged and intensive use of fossil fuels has been increasingly leading to decline in their reserves and also causing emission of harmful air pollutants such as oxides of sulphur and nitrogen, carbon monoxide and suspended particulate matter. Renewable energy is widely accepted as a promising replacement to fossil fuels because it is clean and environmentally secure. The use of biomass as an energy source is generally considered completely carbon neutral because the CO_2 released during the combustion or conversion of biomass into chemicals basically replaces the CO_2 that is removed from the environment by photosynthesis during the production of biomass. Biofuels are carbon neutral, renewable, can be used as a replacement for petroleum fuels with slight engine modifications, as they are sustainable, biodegradable, environmentally friendly and promote green industries. Algal biofuels have their own merits of having no competition with food supply and land. They have a much higher photosynthetic productivity over terrestrial biomass. Algal biofuels would promote an eco-friendly environment and their effective contribution in the transport sector will lead to an increase in the share of biofuel in the automobile market and provide a rapid growth in the near future. The present research focused on screening for suitable macroalgal sources for production of biofuels, as information on these sources was very limited compared to the related research on microalgae.

Three macroalgal species representing each of the major groups of seaweed, namely, *Sargassum tenerrimum* (Phaeophyta), *Gracilaria corticata* (Rhodophyta) and *Ulva fasciata* (Chlorophyta) were selected for this study. This choice was primarily based on the broad and sustained annual availability of these species along the Goan coastline. Regular collection was necessitated throughout the five year period, in view of the seasonal variations of the algal biodiversity and also to amass reasonable quantity of specific processed samples for the entire study.

A need was felt to develop a methodology for simple and rapid colorimetric quantification of lipid from seaweeds. A qualitative analysis was adopted using Nile Red staining technique to determine the lipid content of seaweeds coupled with a quantitative approach involving the Sulfo-phospho-vanillin (SPV) assay. This is the first reported instance of the use of the

technique of Nile Red staining in relation to macroalgal samples. The methodology provided two simple and rapid methods which could detect even low amounts of lipid, involve minimum use of chemicals and which could serve as a primary step for extensive screening of potential macroalgal sources for biodiesel production.

The first potential biofuel type that was looked into was biodiesel. That the lipid content of macroalgae is not sufficiently high was a known fact, but with the minimal information available on macroalgal biodiesel production, our study planned to systematically address, if primarily for academic interest, the economic feasibility/non-feasibility of its commercialization. The possibilities of maximizing parameters to optimise its production were looked into. To begin with, optimization of extraction parameters such as solvents systems, pretreatments, duration of extraction and solvent:solid ratios for the selected macroalgal species was undertaken to obtain maximum crude lipid yield.

Subsequently, transesterification was carried using three different catalysts. A higher percentage of total FAMEs was obtained from all the three macroalgae by using a two-step transesterification method with KOH as catalyst, followed by acid catalysis using HCl. A methodical analysis of the FAME composition and its relative fuel properties is essential for selection of species for biodiesel production. In this study, the FAME analysis confirmed the presence of myristic acid methyl ester, palmitoleic acid methyl ester, palmitic acid methyl ester, oleic acid methyl ester and stearic acid methyl ester in all the three algal species, *ST, GC* and *UF*. Palmitic acid methyl ester (a saturated FAME) was found to be the most abundant, followed by myristic acid methyl ester and stearic acid methyl ester. Comparisons were made in relation to Biodiesel standards such as those in Europe (EN 14214), the United States (ASTM D6751) and India (BIS: IS 15607) which set out desirable properties and permissible limits on ‘contaminants’ in biodiesel fuel. In addition, the parameters that could be derived with regard to biodiesel properties were also analyzed using the Biodiesel Analysis software and found to be in the range set by the ASTM.

Given the low lipid content of macroalgae in general, alternative methods for effectively converting the entire biomass into potential biofuel were also looked into. Thermochemical methods such as gasification, pyrolysis and HTL are commonly employed, of which HTL is

the most preferred for wet biomass. The hydrothermal process was employed on whole algal biomass for its complete valorization. The maximum yields were 16.33 wt. %, 6.67 wt. % and 5.25 wt. % at the optimum temperature of 280, 280 and 300°C for *S. tenerrimum*, *U. fasciata* and *G. corticata* respectively.

Characterization of the liquid products was carried out. The use of alcoholic solvents significantly increased the total bio-oil yield in all the three algae. Aqueous products were also analyzed for total carbon and nitrogen content. Characterization of the components in three liquid oils from *S. tenerrimum* at 280°C, *G. corticata* at 300°C and *U. fasciata* at 280°C were carried out by GC-MS. Biochemical composition of the macroalgae would significantly affect the composition of the bio-oil. The components of the biooils were identified as phenols, ketones, and aldehydes, acid, esters, alcohols, nitrogen-containing compounds (including amides and N heterocyclic compounds), hydrocarbons, *etc*.

Taken together, our results encourage the application of macroalgae for potential production of bio-oil and other value-added products such as biochar (fertilizer). Improvement of the yield and quality of bio-oil would, of course, entail further studies such as optimization using different catalysts and testing other solvents/solvent combinations for the liquefaction. Nevertheless, upgrading and refining of macroalgal biocrude oil for use as a transport fuel no longer appears to be a very distant prospect.

Bibliography

- Abomohra, A. E., El-Naggar, A. H., & Baeshen, A. A. (2018). Potential of macroalgae for biodiesel production: Screening and evaluation studies. J. Biosci. Bioeng., 125: 231-237.
- Achten, W., Verchot, L., Franken, Y., Mathijs, E., Singh, V., Aerts, R., & Muys, B. (2008). *Jatropha* biodiesel production and use. Biomass Bioenergy, 32: 1063-1084.
- Adams, J.M.M., Ross, A.B., Anastasakis, K., Hodgson, E.M., Gallagher, J.A., Jones, J.M., & Donnison, I.S. (2011). Seasonal variation in the chemical composition of the bioenergy feedstock *Laminaria digitata* for thermochemical conversion. Bioresour. Technol., 102: 226-234.
- Adams, T.N., & Appell, B.S. (2004). Power-gen converting turkey offal into bio-derived hydrocarbon oil with the CWT thermal process. In: Renewable Energy Conference, Las Vegas, Nevada.
- Ahmed, A.S., Khan, S., Hamdanm S., Rahman, R., Kalam, A., Masjuki, H.H., & Mahlia, T.M.I. (2010). Biodiesel production from macroalgae as a green fuel for diesel engine. J. Energ. Environ., 2: 1-5.
- Akiya, N., & Savage, P.E. (2002). Roles of water for chemical reactions in high-temperature water. Chem. Rev.,102: 2725-2750.
- Ambrozova, J., Misurcova, L., Vicha, R., Machu, L., Samek, D., Baron, M., Mlcek, J., Sochor, J., & Jurikova, T. (2014). Influence of extractive solvents on lipid and fatty acids content of edible freshwater algal and seaweed products, the green microalga *Chlorella kessleri* and the cyanobacterium *Spirulina platensis*. Molecules, 19: 2344-2360.
- Anastasakis, K., & Ross, A. (2011). Hydrothermal liquefaction of the brown macroalga *Laminaria saccharina*: Effect of reaction conditions on product distribution and composition. Bioresour. Technol., 102: 4876-4883.
- Anastasakis, K., & Ross, A. (2015). Hydrothermal liquefaction of four brown macro-algae commonly found on the UK coasts: An energetic analysis of the process and comparison with biochemical conversion methods. Fuel, 139: 546-553.
- Anastopoulos, G., Zannikou, Y., Stournas, S., & Kalligeros, S. (2009). Transesterification of vegetable oils with ethanol and characterization of the key fuel properties of ethyl esters. Energies, 2: 362-376.

- Andrade, P. B., Barbosa, M., Matos, R. P., Lopes, G., Vinholes, J., Mouga, T., & Valentao, P. (2013). Valuable compounds in macroalgae extracts. Food Chem., 138: 1819-1828.
- Anthony, R., & Stuart, B. (2015). Solvent extraction and characterization of neutral lipids in *Oocystis* sp. Front. Energy Res., 2: 1-5.
- Antolin, G., Tinaut F.V., Briceno Y., Castano, V., Perez, C., & Ramirez, A.I. (2002). Optimisation of biodiesel production by sunflower oil transesterification. Bioresour. Technol., 83: 111-114.
- AOAC (Association of Official Analytical Chemists), Official Methods of Analysis, 15th ed., Arlington, Virginia: USA; 1990.
- Aransiola, E., Ojumu, T., Oyekola, O., Madzimbamuto, T., & Ikhu-Omoregbe, D. (2014). A review of current technology for biodiesel production: State of the art. Biomass Bioenergy, 61: 276-297.
- Araujo, G. S., Matos, L. J., Fernandes, J. O., Cartaxo, S. J., Gonçalves, L. R., Fernandes, F. A., & Farias, W. R. (2013). Extraction of lipids from microalgae by ultrasound application: Prospection of the optimal extraction method. Ultrason. Sonochem., 20: 95-98.
- Archanaa, S., Moise, S., & Suraishkumar, G.K. (2012). Chlorophyll interference in microalgal lipid quantification through the Bligh and Dyer method. Biomass Bioenergy, 46: 805-808.
- Aresta, M., Dibenedetto, A., Carone, M., Colonna, T., & Fragale, C. (2005a). Production of biodiesel from macroalgae by supercritical CO_2 extraction and thermochemical liquefaction. Environ. Chem. Lett., 3: 136-139.
- Aresta, M., Dibenedetto, A., & Barberio, G. (2005b). Utilization of macroalgae for enhanced CO_2 fixation and biofuels production: Development of a computing software for an LCA study. Fuel Process. Technol., 86: 1679-1693.
- Arun, J., Shreekanth, S.J., Sahana, R., Raghavi, M.S., Gopinath, K.P., & Gnanaprakash, D. (2017). Studies on influence of process parameters on hydrothermal catalytic liquefaction of microalgae (*Chlorella vulgaris*) biomass grown in wastewater. Bioresour. Technol., 244: 963-968.

- Ashokkumar, V., Salim, M. R., Salam, Z., Sivakumar, P., Chong, C. T., Elumalai, S., Suresh, V., & Ani, F. N. (2017). Production of liquid biofuels (biodiesel and bioethanol) from brown marine macroalgae *Padina tetrastromatica*. Energy Convers. Manag., 135: 351-361.
- Asif, M. & Muneer, T. (2007). Energy supply, its demand and security issues for developed and emerging economies. Renew. Sust. Energ. Rev., 11: 1388-1413.
- Atabani, A.E., Silitonga, A.S., Badruddin, I.A., Mahliaa, T.M.I., Masjukia, H.H., & Mekhilefd, S. (2012). A comprehensive review on biodiesel as an alternative energy resource and its characteristics. Renew. Sust. Energ. Rev., 16: 2070-93.
- Atabani, A., Silitonga, A., Ong, H., Mahlia, T., Masjuki, H., Badruddin, I. A., & Fayaz, H. (2013). Non-edible vegetable oils: A critical evaluation of oil extraction, fatty acid compositions, biodiesel production, characteristics, engine performance and emissions production. Renew. Sust. Energ. Rev., 18: 211-245.
- Atadashi, I., Aroua, M., Abdul Aziz, A., & Sulaiman, N. (2013). The effects of catalysts in biodiesel production: A review. J. Ind. Eng. Chem., 19: 14-26.
- Babu, V., Rao, A., & Kumar, R. (2009). Transesterification for the preparation of biodiesel from crude-oil of *Pongamia pinnata*. Therm. Sci., 13: 201-206.
- Bach, Q. A., Sillero, M. V., Tran, K., & Skjermo, J. (2014). Fast hydrothermal liquefaction of a Norwegian macroalga: Screening tests. Algal Res., 6: 271-276.
- Backhaus, R. (2017). 125 Years of Diesel. MTZ ind., **7:** 3. Retrieved from: https://link.springer.com/article/10.1007%2Fs40353-017-0023-0.
- Bae, Y. J., Ryu, C., Jeon, J., Park, J., Suh, D. J., Suh, Y., & Park, Y. (2011). The characteristics of bio-oil produced from the pyrolysis of three marine macroalgae. Bioresour. Technol., 102: 3512-3520.
- Bala, B.K. (2005). Studies on biodiesel from transformation of vegetable oils for diesel engines. Edu. Sci. Technol., 15:1-43.
- Balasubramanian, R. K., Yen Doan, T. T., & Obbard, J. P. (2013). Factors affecting cellular lipid extraction from marine microalgae. Chem. Eng. J., 215-216: 929-936.
- Barabas, I., & Todorut, I.A. (2011). Biodiesel quality, standards and properties. In G. Montero & M. Stoytcheva (Eds.), Biodiesel-quality, emissions and by-products (pp. 3-28). In Tech: Rijeka, Croacia.

- Barreiro, D.L., Prins, W., Ronsse, F., & Brilman, W. (2013). Hydrothermal liquefaction (HTL) of microalgae for biofuel production: State of the art review and future prospects. Biomass Bioenergy, 53: 113-127.
- Barreiro, D.L., Samori, C., Terranella, G., Hornung, U., Kruse, A., & Prins, W. (2014). Assessing microalgae biorefinery routes for the production of biofuels via hydrothermal liquefaction. Bioresour. Technol., 174:256-265.
- Barreiro, D.L., Beck, M., Hornung, U., Ronsse, F., Kruse, A., & Prins, W. (2015). Suitability of hydrothermal liquefaction as a conversion route to produce biofuels from macroalgae. Algal Res., 11: 234-241.
- Bast, F. (2014). Seaweeds: ancestors of land plants with rich diversity, Resonance, 19: 149-159.
- Bastianoni, S., Coppola, F., Tiezzi, E., Colacevich, A., Borghini, F., & Focardi, S. (2008). Biofuel potential production from the Orbetello lagoon macroalgae: A comparison with sunflower feedstock. Biomass Bioenergy, 32: 619-628.
- Beetul, K., Sadally, S. B., Taleb-Hossenkhan, N., Bhagooli, R., & Puchooa, D. (2014). An investigation of biodiesel production from microalgae found in Mauritian waters. Biofuel Res. J., 2: 58-64.
- Behrendt, F., Neubauer, Y., Oevermann, M., Wilmes, B., & Zobel, N. (2008). Direct liquefaction of biomass. Chem. Eng. Technol., 31: 667-77.
- Berardi, U. (2017). A cross-country comparison of the building energy consumption and their trends. Resour. Conserv. Recy., 123: 230-241.
- Bertozzini, E., Galluzzi, L., Penna, A., & Magnani, M. (2011). Application of the standard addition method for the absolute quantification of neutral lipids in microalgae using Nile red. J. Microbiol. Meth., 87: 17-23.
- Bharathiraja, B., Chakravarthy, M., Kumar, R.R., Yogendran, D., Yuvaraj, D., Jayamuthunagai, J., Kumar, P.P., & Palani, S. (2015). Aquatic biomass (algae) as a future feed stock for bio-refineries: a review on cultivation, processing and products. Renew. Sust. Energy Rev., 47: 634-53.
- Bharathiraja, B., Kumar, R.R., Kumar, R.P., Chakravarthy, M., Yogendran, D., & Jayamuthunagai, J. (2016). Biodiesel production from different algal oil using

immobilized pure lipase and tailor made r *Pichia pastoris* with Cal A and Cal B genes. Bioresour. Technol., 213: 69-78.

- Biller, P., & Ross, A. (2011). Potential yields and properties of oil from the hydrothermal liquefaction of microalgae with different biochemical content. Bioresour. Technol., 102: 215-225.
- Biswas, B., Arun Kumar, A., Bisht, Y., Singh, R., Kumar, J., & Bhaskar, T. (2017a). Effects of temperature and solvent on hydrothermal liquefaction of *Sargassum tenerrimum* algae. Bioresour. Technol., 242: 344-350.
- Biswas, B., Pandey, N., Bisht, Y., Singh, R., Kumar, J., & Bhaskar, T. (2017b). Pyrolysis of agricultural biomass residues: Comparative study of corn cob, wheat straw, rice straw and rice husk. Bioresour. Technol., 237: 57- 63.
- Biswas, B., Fernandes, A. C., Kumar, J., Muraleedharan, U. D., & Bhaskar, T. (2018a). Valorization of *Sargassum tenerrimum*: Value addition using hydrothermal liquefaction. Fuel, 222: 394-401.
- Biswas, B., Singh, R., Kumar, J., Singh, R., Gupta, P., Krishna, B.B., & Bhaskar, T. (2018b). Pyrolysis behavior of rice straw under carbon dioxide for production of bio-oil. Renew. Energy, 129: 686-694.
- Biswas, B., Kumar, A., Fernandes, A. C., Saini, K., Negi, S., Muraleedharan, U. D., & Bhaskar, T. (2020). Solid base catalytic hydrothermal liquefaction of macroalgae: Effects of process parameter on product yield and characterization. Bioresour. Technol., 307: 123232.
- Bligh, E. G., & Dyer, W. J. (1959). A rapid method of total lipid extraction and purification. Can. J. Biochem. Biophysiol., 37: 911-917.
- Borghini, F., Lucattini, L., Focardi, S., Focardi, S., & Bastianoni, S. (2013). Production of biodiesel from macroalgae of the Orbetello lagoon by various extraction methods. Int. J. Sustain. Energy, 33: 695-703.
- Bouvier, J.M., Gelus, M., & Maugendre, S. (1988). Wood liquefaction - an overview. Appl. Energy., 30: 85-98.
- Bozbas, K. (2008). Biodiesel as an alternative motor fuel: Production and policies in the European Union. Renew. Sust. Energ. Rev., 12: 542-552.

- BP (2014). Retrieved from https://www.bp.com/content/dam/bp/business-sites/en/global/corporate/pdfs/energy-economics/energy-outlook/bp-energy-outlook-2014.pdf
- BP (2019a). Retrieved from: https://www.bp.com/content/dam/bp/business-sites/en/global/corporate/pdfs/energy-economics/statistical-review/bp-stats-review-2019-india-insights.pdf
- BP (2019b). Retrieved from : https://www.bp.com/content/dam/bp/business-sites/en/global/corporate/pdfs/energy-economics/energy-outlook/bp-energy-outlook-2019-country-insight-india.pdf
- Brennan, L., & Owende, P. (2010). Biofuels from microalgae - A review of technologies for production, processing, and extractions of biofuels and co-products. Renew. Sust. Energ. Rev., 14: 557-577.
- Brown, T.M., Duan, P., & Savage, P.E. (2010). Hydrothermal liquefaction and gasification of *Nannochloropsis* sp. Energy Fuels, 24: 3639-3646.
- Byreddy, A.R., Gupta, A., Barrow, C.J., & Puri, M. (2016). A quick colorimetric method for total lipid quantification in microalgae. J. Microbiol. Meth., 125:28-32.
- Canakci, M. (2007). The potential of restaurant waste lipids as biodiesel feedstocks. Bioresour. Technol., 98: 183-190.
- Canakci, M., & Van Gerpen, J. (1999). Biodiesel production via acid catalysis. Trans. ASAE, 42: 1203-1210.
- Cancela, A., Maceiras, R., Urrejola, S., & Sanchez, A. (2012). Microwave - assisted transesterification of macroalgae. Energies, 5: 862-871.
- Caporgno, M., Pruvost, J., Legrand, J., Lepine, O., Tazerout, M., & Bengoa, C. (2016). Hydrothermal liquefaction of *Nannochloropsis Oceanica* in different solvents. Bioresour. Technol., 214: 404-410.
- Carriquiry, M.A., Du, X., & Timilsina, G.R. (2011). Second generation biofuels: economics and policies. Energy Policy, 39: 4222-34.
- Castello, D., Pedersen, T., & Rosendahl, L. (2018). Continuous hydrothermal liquefaction of biomass: A critical review. Energies, 11: 3165.

- Cavonius, L. R., Carlsson, N.G., & Undeland, I. (2014). Quantification of total fatty acids in microalgae: comparison of extraction and transesterification methods. Anal. Bioanal. Chem., 406: 7313-7322.
- Chabrol, E., & Charonnet, R. (1937). Une novelle reaction pour letude des lipides. Presse Med., 45: 13-17.
- Chai, M., Tu, Q., Lu, M., & Yang, Y. J. (2014). Esterification pretreatment of free fatty acid in biodiesel production, from laboratory to industry. Fuel Process. Technol., 125: 106-113.
- Chakraborty, M., Miao, C., McDonald, A., & Chen, S. (2012). Concomitant extraction of bio-oil and value added polysaccharides from *Chlorella sorokiniana* using a unique sequential hydrothermal extraction technology. Fuel, 95: 63-70.
- Changi, S., Brown, T.M., & Savage, P.E. (2012). Reaction kinetics and pathways for phytol in high-temperature water. Chem. Eng. J., 189: 336-345.
- Chen, H., Zhou, D., Luo, G., Zhang, S., & Chen, J. (2015a). Macroalgae for biofuels production: progress and perspectives. Renew. Sust. Energ. Rev., 47: 427-37.
- Chen, Y., Wu, Y., Hua, D., Li, C., Harold, M., Wang, J., & Yang, M. (2015b). Thermochemical conversion of low-lipid microalgae for the production of liquid fuels: challenges and opportunities. RSC Adv., 5: 18673-18701.
- Chen, W.H., Lin, B.J., Huang, M.Y., & Chang, J.S. (2015c). Thermochemical conversion of microalgal biomass into biofuels: a review. Bioresour. Technol., 184: 314-27.
- Chen, Y., Wu, Y., Ding, R., Zhang, P., Liu, J., Yang, M., & Zhang, P. (2015d). Catalytic hydrothermal liquefaction of *D. tertiolecta* for the production of bio-oil over different acid/base catalysts. AIChE J., 61: 1118-1128.
- Chen, L., Liu, T., Zhang, W., Chen, X., & Wang, J. (2012a). Biodiesel production from algae oil high in free fatty acids by two-step catalytic conversion. Bioresour. Technol., 111: 208-214.
- Chen, Y., Wu, Y., Zhang, P., Hua, D., Yang, M.D., Li, C., Chen, Z., & Liu, J. (2012b). Direct liquefaction of *Dunaliella tertiolecta* for bio-oil in sub/supercritical ethanol-water. Bioresour. Technol., 124:190-198.

- Chen, W., Zhang, C.W., Song, L.R., Sommerfeld, M., & Hu, Q. (2009). A high throughput Nile red method for quantitative measurement of neutral lipids in microalgae. J. Microbiol. Meth., 77: 41-47.
- Cheng, F., Cui, Z., Chen, L., Jarvis, J., Paz, N., Schau, T., Nirmalakhandan, N., & Brewer, E.C. (2017). Hydrothermal liquefaction of high- and low-lipid algae: Bio-crude oil Chemistry. Applied Energy, 206: 278-292.
- Cheng, S., D'cruz, I., Wang, M., Leitch, M., & Xu, C.(C). (2010). Highly efficient liquefaction of woody biomass in hot-compressed alcohol-water co-solvents. Energy Fuels, 24: 4659-67.
- Cheng, H.C., Du, T.B., Pi, H.C., Jang, S.M., Lin, H.Y., & Lee, H.T. (2011a). Comparative study of lipid extraction from microalgae by organic solvent and supercritical CO_2. Bioresour. Technol., 102: 10151-10153.
- Cheng, Y.S., Zheng, Y., & Vander Gheynst, J.S. (2011b). Rapid quantitative analysis of lipids using a colorimetric method in a microplate format. Lipids, 46: 95-103.
- Cheung, P. C., Leung, A. Y., & Ang, P. O. (1998). Comparison of supercritical carbon dioxide and soxhlet extraction of lipids from a brown seaweed, *Sargassum hemiphyllum* (Turn.) C. Ag.†. J. Agr. Food Chem., 46: 4228-4232.
- Chhetri, A., Tango, M., Budge, S., Watts, K., & Islam, M. (2008). Non-edible plant oils as new sources for biodiesel production. Int. J. Mol. Sci., 9: 169-180.
- Chisti, Y. (2007). Biodiesel from microalgae. Biotechnol. Adv., 25: 294-306.
- Chisti, Y. (2008). Biodiesel from microalgae beats bioethanol. Trends Biotechnol., 26: 126-131.
- Chiu, Y.W., Walseth, B., & Suh, S. (2009). Water embodied in bioethanol in the United States. Environ. Sci. Technol., 43: 2688-2692.
- Chongkhong, S., Tongurai, C., Chetpattananondh, P., & Bunyakan, C. (2007). Biodiesel production by esterification of palm fatty acid distillate. Biomass Bioenergy, 31: 563-568.
- Chopin, T., & Neish, I. (2014). The 21st International Seaweed Symposium: seaweed science for sustainable prosperity. J. Appl. Phycol., 26: 695-8.
- Chung, I., Beardall, J., Mehta, S., Sahoo, D., & Stojkovic, S. (2011). Using marine macroalgae for carbon sequestration: a critical appraisal. J. Appl. Phycol., 23: 877-886.

- Cooksey, K.E., Guckert, J.B., Williams, S.A., & Callis, P.R. (1987). Fluorometric determination of the neutral lipid content of microalgal cell using Nile red. J. Microbiol. Meth., 6: 333-345.
- Cooney, M., Young, G., & Nagle, N. (2009). Extraction of bio-oils from microalgae. Sep. Purif. Rev., 38: 291-325.
- D'Alessandro, E. B., & Antoniosi Filho, N. R. (2016). Concepts and studies on lipid and pigments of microalgae: A review. Renew. Sust. Energ. Rev., 58: 832-841.
- Dawczynski, C., Schubert, R., & Jahreis, G. (2007). Amino acids, fatty acids, and dietary fibre in edible seaweed products. Food Chem., 103: 891-899.
- De Caprariis, B., De Filippis, P., Petrullo, A., & Scarsella, M. (2017). Hydrothermal liquefaction of biomass: Influence of temperature and biomass composition on the bio-oil production. Fuel, 208:618-625.
- Deepalakshmi, S., Sivalingam, A., Thirumarimurugan, M., Sivakumar, P., Ashokkumar, V. (2015). Optimization of biodiesel synthesis from *Calophyllum inophyllum*. Energy Sour. A Recovery Util. Environ. Effects, 37: 2601-2608.
- Demirbas, A. (2005). Biodiesel production from vegetable oils via catalytic and non-catalytic supercritical methanol transesterification methods. Prog. Energy Combust. Sci., 31: 466-87.
- Demirbas, A. (2007). Importance of biodiesel as transportation fuel. Energ. Policy, 35: 4661-4670.
- Demirbas, A. (2008a). Biodiesel: A realistic fuel alternative for diesel engines (pp. 1-3, 5-16, 112). Springer-Verlag London Limited.
- Demirbas, A. (2008b). Biofuels sources, biofuel policy, biofuel economy and global biofuel projections. Energ. Convers. Manag., 49: 2106-16.
- Demirbas, A. (2009). Combustion efficiency impacts of biofuels. Energy Sources, A, 31: 602-609.
- Demirbas, A. (2010). Use of algae as biofuel sources. Energ. Convers. Manag., 51: 2738-2749.
- Demirbas, A., & Arin, G. (2002). An overview of biomass pyrolysis. Energy Sources, Part A, 24: 471- 482.

- Dhargalkar, V.K., & Kavlekar, D. (2004). Seaweeds-a field manual, National Institute of Oceanography, Dona Paula, Goa. 403004.
- Diaz-Vazquez LM, Rojas-Perez, A., Fuentes-Caraballo, M., Robles, I. V., Jena, U., & Das, K. C. (2015). Demineralization of *Sargassum* spp. macroalgae biomass: Selective hydrothermal liquefaction process for bio-oil production. Front. Energy Res., 3: 1-11.
- Dimitriadis, A., & Bezergianni, S. (2017). Hydrothermal liquefaction of various biomass and waste feedstocks for biocrude production: a state of the art review. Renew. Sust. Energ. Rev., 68: 113-25.
- Doan, T.T.Y., & Obbard, J.P. (2011). Improved Nile Red staining of *Nannochloropsis* sp. Appl. Phycol., 23: 895-901.
- Dong, T., Wang, J., Miao, C., Zheng, Y., & Chen, S. (2013). Two-step in situ biodiesel production from microalgae with high free fatty acid content. Bioresour. Technol., 136: 8-15.
- Duan, P., & Savage, P.E. (2011). Upgrading of crude algal bio-oil in supercritical water. Bioresour. Technol., 102: 1899-906.
- Dufreche, S., Hernandez, R., French, T., Sparks, D., Zappi, E., & Alley, E. (2007). Extraction of lipids from municipal wastewater plant microorganisms for production of biodiesel. J. Am. Oil Chem. Soc., 84: 181-187.
- Dutta, K., Daverey, A., & Lin, J. (2014). Evolution retrospective for alternative fuels: First to fourth generation. Renew. Energy, 69: 114-122.
- El Maghraby, D. M., & Fakhry, E.M. (2015). Lipid content and fatty acid composition of Mediterranean macroalgae as dynamic factors for biodiesel production. Oceanologia, 57: 86-92.
- Elliott, D. C., Biller, P., Ross, A. B., Schmidt, A. J., & Jones, S. B. (2015). Hydrothermal liquefaction of biomass: Developments from batch to continuous process. Bioresour. Technol., 178: 147-156.
- Elliott, D. C.,Hart, T. R., Neuenschwander, G. G., Rotness, L. J., Roesijadi, G., Zacher, A. H., & Magnuson, J. K. (2013). Hydrothermal processing of macroalgal feedstock in continuous-flow reactors. ACS Sustain. Chem. Eng., 2: 207-215.

- Encinar, J., Sánchez, N., Martínez, G., & García, L. (2011). Study of biodiesel production from animal fats with high free fatty acid content. Bioresour. Technol., 102: 10907-10914.
- Enssani, E. (1990). A Method for the extraction of liquid hydrocarbons from microalgal biomass. Energy conversion engineering conference, IECEC-90, Proceedings of the 25th Intersociety, Piscataway, NJ, 6:250-255.
- Evans, C.T., Ratledge, C., & Gilbert, S.C. (1985). Rapid screening method for lipid accumulating yeast using a replica-printing technique. J. Microbiol. Meth., 4: 203-210.
- FAO. (2011). Algae based biofuels: A review of challenges and opportunities for developing countries. In S.K. Bhatnagar, A. Saxena, & S. Kraan (Eds.), Algae biofuel (pp. 1-40). Stadium Press (India) Pvt. Ltd.
- Feng, W., van der Kooi, H.J., & de Swaan Arons, J. (2004). Phase equilibria for biomass conversion processes in subcritical and supercritical water. Chem. Eng. J., 98: 105-13.
- Folch, J., Lees, M., & Sloane Stanley, G. H. (1957). A simple method for the isolation and purification of total lipides from animal tissues. J. Biol. Chem., 226: 497-509.
- Fukuda, H., Koda, A., & Noda, H. (2001). Biodiesel fuel production by transesterification of oils. J. Biosci. Bioeng., 92: 405-416.
- Gallagher, J. A., Turner, L. B., Adams, J. M., Barrento, S., Dyer, P. W., & Theodorou, M. K. (2018). Species variation in the effects of dewatering treatment on macroalgae. J. Appl. Phycol., 30: 2305-2316.
- Ganesan, M., Trivedi, N., Gupta, V., Madhav, S. V., Radhakrishna Reddy, C., & Levine, I. A. (2019). Seaweed resources in India - current status of diversity and cultivation: Prospects and challenges. Bot. Mar., 62: 463-482
- Gaurav, N., Sivasankari, S., Kiran, G., Ninawe, A., & Selvin, J. (2017). Utilization of bioresources for sustainable biofuels: A review. Renew. Sust. Energ. Rev., 73: 205-214.
- Genicot, G., Leroy, J.L.M.R., Van Soom, A., & Donnay, I. (2005). The use of a fluorescent dye, Nile red, to evaluate the lipid content of single mammalian oocytes. Theriogenology, 63:1181-1194.

- Georgogianni, K., Katsoulidis, A., Pomonis, P., Manos, G., & Kontominas, M. (2009). Transesterification of rapeseed oil for the production of biodiesel using homogeneous and heterogeneous catalysis. Fuel Process. Technol., 90: 1016-1022.
- Ghosh, A., Khanra, S., Mondal, M., Halder, G., Tiwari, O.N., Saini, S., Bhowmick, T. K., & Gayen, K. (2016). Progress toward isolation of strains and genetically engineered strains of microalgae for production of biofuel and other value added chemicals: a review. Energ. Convers. Manag., 113: 104-18.
- Goldemberg, J. (2000). World Energy Assessment. United Nations Development Programme (pp: 10-11, 224-225). New York. USA.
- Gollakota, A., Kawale, H. D., Kishore, N., & Gu, S. (2018). A Review on hydrothermal liquefaction of biomass. Renew. Sust. Energ. Rev., 81: 1378-1392.
- Gosch, B.J., Magnusson, M., Paul, N.A., & Nys, R. (2012). Total lipid and fatty acid composition of seaweeds for the selection of species for oil-based biofuel and bioproducts. GCB Bioenergy, 4: 919-930.
- Greenspan, P., & Fowler, S.D. (1985). Spectrofluorometric studies of the lipid probe, Nile Red. J. Lipid Res., 26: 781-789
- Greenspan, P., Mayer, E.P., & Fowler, S.D. (1985). Nile red - a selective fluorescent stain for intracellular lipid droplets. J. Cell Biol., 100: 965-973.
- Gressler, V., Yokoya, N., Fujii, M., Colepicolo, P., Filho, J., Torres R., & Pinto, E. (2010). Lipid, fatty acid, protein, amino acid and ash contents in four Brazilian red algae species. Food Chem., 120: 585-590.
- Griffiths, M.J., & Harrison, S.T.L. (2009). Lipid productivity as a key characteristic for choosing algal species for biodiesel production. J. Appl. Phycol., 21: 493-507.
- Griffiths, M.J., Van Hille, R.P., & Harrison, S.T.L. (2010). Selection of direct transesterification as the preferred method for assay of fatty acid content of microalgae. Lipids, 45: 1053-1060.
- Guo, Y., Yeh, T., Song, W., Xu, D., & Wang, S. (2015). A review of bio-oil production from hydrothermal liquefaction of algae. Renew. Sust. Energ. Rev., 48: 776-790.
- Halim, R., Gladman, B., Danquah, M.K., & Webley, P.A. (2011). Oil extraction from microalgae for biodiesel production. Bioresour. Technol., 102: 178-185.

- Halim, R., Danquah, M. K., & Webley, P. A. (2012a). Extraction of oil from microalgae for biodiesel production: A review. Biotechnol. Adv., 30: 709-732.
- Halim, R., Harun, R., Danquah, M.K., & Webley, P.A. (2012b). Microalgal cell disruption for biofuel development. Appl. Energ., 91:116-121.
- Hall, D.O., Rosillo-Calle, F., & de Groot, P. (1992). Biomass energy lessons from case studies in developing countries. Energy Policy, 20: 62-73.
- Han, Y., Hoekman, S. K., Cui, Z., Jena, U., & Das, P. (2019). Hydrothermal liquefaction of marine microalgae biomass using co-solvents. Algal Res., 38: 101421.
- Hao, Z., Liu, P., Yang, X., Shi, J., Zhang, S. (2013). Screening method for lipid-content microalgae based on sulfo-phospho-vanillin reaction. Adv. Mat. Res., 610-613: 3532-3535.
- Hara, A., & Radin, N.S. (1978). Lipid extraction of tissues with a low toxicity solvent. Anal. Biochem., 90: 420-426.
- He, Y., Liang, X., Jazrawi, C., Montoya, A., Yuen, A., Cole, A. J., Neveux, N., Paul, N.A., de Nys, R., Maschmeyer, T., & Haynes, B. S. (2016). Continuous hydrothermal liquefaction of macroalgae in the presence of organic co-solvents. Algal Res., 17: 185-195.
- Hernandez-Martin, E., & Otero, C. (2008). Different enzyme requirements for the synthesis of biodiesel: Novozym® 435 and Lipozyme® TL IM. Bioresour. Technol., 99: 277-286.
- Hidalgo, P., Ciudad, G., & Navia, R. (2016). Evaluation of different solvent mixtures in esterifiable lipids extraction from microalgae *Botryococcus braunii* for biodiesel production. Bioresour. Technol., 201: 360-364.
- Higgins, B.T., Thornton-Dunwoody, A., Labavitch, J. M., Vander Gheynst, J.S. (2014). Microplate assay for quantitation of neutral lipids in extracts from microalgae. Anal. Biochem., 465: 81-89.
- Ho, D. P., Ngo, H. H., & Guo, W. (2014). A mini review on renewable sources for biofuel. Bioresour. Technol., 169: 742-749.
- Hong, I.K., Jeon, H., & Lee, S.B. (2014). Comparison of red, brown and green seaweeds on enzymatic saccharification process. J. Ind. Eng. Chem., 20: 2687-91.

- Hossain, A.B.M.S., Salleh, A., Boyce, A.N., Chowdhury, P., & Naqiuddin, M. (2008). Biodiesel fuel production from algae as renewable energy. Am. J. Biochem. Biotechnol., 4: 250-254.
- http:// formosa. ntm.gov.tw/seaweeds/english/b/b3_01.asp
- http:// petroleum.nic.in/sites/default/files/biofuelpolicy2018_1.pdf
- http://www.brteam.ir/analysis/
- http://www.eia.gov/countries/analysisbriefs/India/india.pdf
- http://www.seaweed.ie/algae/phaeophyta.php
- https://www.ag.ndsu.edu/agmachinery/documents/pdf/biodiesel%20specifications%203-2007.pdf
- https://www.americanscientist.org/article/the-science-of-seaweeds
- https://www.investopedia.com/investing/worlds-top-oil-producers/
- https://www.opec.org/opecweb/en/datagraphs/330.htm
- https://www.windfinder.com/tide/panaji_goa
- Hu,Y., Gong, M., Xu, C. (C)., & Bassi, A. (2017). Investigation of an alternative cell disruption approach for improving hydrothermal liquefaction of microalgae. Fuel, 197: 138-144.
- Huang, G.H., Chen, G., & Chen, F. (2009). Rapid screening method for lipid production in alga based on Nile red fluorescence. Biomass Bioenergy, 33: 1386-1392.
- Huang, H., Yuan, X., Zeng, G., Wang, J., Li, H., Zhou, C., Pei, X., You, Q., & Chen, L. (2011). Thermochemical liquefaction characteristics of microalgae in sub- and supercritical ethanol. Fuel Process Technol., 92: 147-153.
- Huang, Y., Chen, Y., Xie, J., Liu, H., Yin, X., & Wu, C. (2016). Bio-oil production from hydrothermal liquefaction of high-protein high-ash microalgae including wild Cyanobacteria sp. and cultivated Bacillariophyta sp. Fuel, 183: 9-19.
- Immanuel, S., & Sathiadas, R. (2004). Employment potential of fisherwomen in the collection and post harvest operations of seaweeds in India. Seaweed Res. Utiln., 26: 209-215.
- Iso, M., Chen, B., Eguchi, M., Kudo, T., & Shrestha, S. (2001). Production of biodiesel fuel from triglycerides and alcohol using immobilized lipase. J. Mol. Catal. B

Enzym., 16: 53-58.

- Izard, J., & Limberger, R.J. (2003). Rapid screening method for quantitation of bacterial cell lipids from whole cells. J. Microbiol. Meth., 55: 411-418.
- Jabeen, S. (2011). Studies on biodiesel production from macroalgae. M.Sc. dissertation, Goa University, 66 pp.
- Jena, U., McCurdy, A. T., Warren, A., Summers, H., Ledbetter, R. N., Hoekman, S. K., Seefeldt, L.C., & Quinn, J. C. (2015). Oleaginous yeast platform for producing biofuels via co-solvent hydrothermal liquefaction. Biotechnol. Biofuels, 8: 167-186.
- Jena, U., & Das, K. C. (2011). Comparative evaluation of thermochemical liquefaction and pyrolysis for bio-oil production from microalgae. Energy Fuels, 25: 5472-5482.
- Jensen, A. (1993). Present and future needs for algae and algal products. Hydrobiologia, 260/261: 15-23.
- Jeong, G., & Park, D. (2015). Optimization of lipid extraction from marine green macroalgae as biofuel resources. Korean J. Chem. Eng., 32: 2463-2467.
- Jin, B., Duan, P., Xu, Y., Wang, F., & Fan, Y. (2013). Co-liquefaction of micro- and macro- algae in subcritical water. Bioresour. Technol., 149: 103-110.
- Johari, A., Nyakuma, B. B., Mohd Nor, S. H., Mat, R., Hashim, H., Ahmad, A., Zakaria, Y.Z. & Tuan Abdullah, T. A. (2015). The challenges and prospects of palm oil based biodiesel in Malaysia. Energy, 81: 255-261.
- John, R.P., Anisha, G.S., Nampoothiri, K. M. & Pandey, A. (2011). Micro and macroalgal biomass: A renewable source for bioethanol. Bioresour. Technol., 102: 186-193.
- Jung, K.A., Lim, S.R., Kim, Y., & Park, J.M. (2013) Potentials of macroalgae as feedstocks for biorefinery. Bioresour. Technol., 135:182-190.
- Kadam, S. U., Alvarez, C., Tiwari, B. K., & O'Donnell, C. P. (2017). Extraction and characterization of protein from Irish brown seaweed *Ascophyllum nodosum*. Food Res. Int., 99: 1021-1027.
- Kaladharan, P., & Kaliaperumal, N. (1999). Seaweed industry in India. Naga, the ICLARM Quarterly, 22: 11-4.

- Kaluzny, M. A., Duncan, L. A., Merritt, M. V., & Eppse, D. E. (1985). Rapid separation of lipid classes in high yield and purity using bonded phase columns. J. Lipid Res., 26: 135-140.
- Kamenarska, Z., Gasic, M. J., Zlatovic, M., Rasovic, A., Sladic, D., Kljajic, Stefanov, K. Seizova, K., Najdenski, H., Kujumgiev, A., Z., Tsvetkova , I., & Popov, S. (2002). Chemical composition of the brown alga *Padina pavonia* (L.) Gaill. from the Adriatic sea. Bot. Mar., 45: 339-345.
- Kamisaka, Y., Noda, N., Sakai, T. & Kawasaki, K. (1999). Lipid bodies and lipid body formation in an oleaginous fungus *Mortierella ramanniana* var. angulispora. Biochim. Biophys. Acta, 1438: 185-198.
- Karmakar, A., Karmakar, S., & Mukherjee, S. (2010). Properties of various plants and animals feedstocks for biodiesel production. Bioresour. Technol., 101: 7201-7210.
- Karmakar, R., Kundu, K., & Rajor, A. (2017). Fuel properties and emission characteristics of biodiesel produced from unused algae grown in India. Pet. Sci., 15: 385-395.
- Kartika, A.I., Yani, M., Ariono, D., Evon, P., & Rigal, L. (2013). Biodiesel production from *Jatropha* seeds: Solvent extraction and in situ transesterification in a single step. Fuel, 106: 111-117.
- Kates, M. (1986). Techniques of lipidology: isolation, analysis, and identification of lipids. In R.H. Bruden & P.H. Van Knippenberg (Eds.), Laboratory techniques in biochemistry and molecular biology, 2nd edn.,Vol 3(2), (pp 100-111). Elsevier, New York.
- Khairy, H.M. & El-Shafay, S. M. (2013). Seasonal variations in the biochemical composition of some common seaweed species from the coast of Abu Qir Bay, Alexandria, Egypt. Oceanologia, 55: 435-452.
- Khan, A. M., Obaid, M., & Sultana, R. (2015). Production of biodiesel from marine algae to mitigate environmental pollution. J. Chem. Soc. Pak., 37: 612-620.
- Khan, A.M., Ameen, M., & Fatima, N. (2017). Production of green and renewable diesel from marine brown algae *Sargassum tenerrimum*. Indian J. Geo-Mar. Sci., 46: 815-822.

- Khan, S.I., & Satam, S.B. (2003). Seaweed mariculture: scope and potential in India. Aquac. Asia., 8: 26-29.
- Khan, A. M., Fatima, N., Hussain, M. S., & Yasmeen, K. (2016). Biodiesel production from green seaweed *Ulva fasciata* catalyzed by novel waste catalysts from Pakistan steel industry. Chinese J. Chem. Eng., 24: 1080-1086.
- Khola, G., & Ghazala, B. (2012). Biodiesel production from algae. Pak. J. Bot., 44: 379-381**.**
- Khotimchenko, S.V., Vaskovsky, E.V., & Titlyanova, V.T. (2002). Fatty acids of marine algae from Pacific coast of North California. Bot. Mar., 45: 17-22.
- Kim, B., Park, J., Son, J., & Lee, J.W. (2017). Catalyst-free production of alkyl esters from microalgae via combined wet in situ transesterification and hydrothermal liquefaction (iTHL). Bioresour. Technol., 244: 423-432.
- Kim, J.Y., Moon, J., Lee, J., Jind, X., & Choi, J.W. (2020). Conversion of phenol intermediates into aromatic hydrocarbons over various zeolites during lignin pyrolysis. Fuel, 279: 118484.
- Kim, S.S., Ly, H.V., Kim, J., Choi, J.H., & Woo, H.C. (2013). Thermogravimetric characteristics and pyrolysis kinetics of alga *Sargassum* sp. biomass. Bioresour. Technol., 139: 242-248.
- Kimura, K., Yamaoka, M., & Kamisaka, Y. (2004). Rapid estimation of lipids in oleaginous fungi and yeasts using Nile red fluorescence. J. Microbiol. Meth., 56: 331-338.
- King, J.W., Holliday, R.L., & List, G.R. (1999). Hydrolysis of soybean oil in a subcritical waterflow reactor. Green Chem., 1: 261-264.
- Knight, J.A., Rawle, J. M., & Anderson, S. (1972). Chemical basis of sulfo-phospho-vanillin reaction for estimating total serum lipids. Clin. Chem., 18: 199-202.
- Knothe, G. & Steidley, K.R. (2005). Kinematic viscosity of biodiesel fuel components and related compounds.Influence of compound structure and comparison to petrodiesel fuel components. Fuel, 84:1059-1065.
- Knothe, G. (2005a).The history of vegetable oil-based diesel fuels. In G**.** Knothe, J. Van Gerpen, & J. Krahl (Eds.), The biodiesel handbook (pp 12-18). AOCS Press, Champaign, Illinois.

- Knothe, G. (2005b). Fuel properties. In G**.** Knothe, J. Van Gerpen, & J. Krahl (Eds.), The Biodiesel Handbook (pp 84-90). AOCS Press, Champaign, Illinois.
- Knothe, G. (2008). **"**Designer" biodiesel: Optimizing fatty ester composition to improve fuel properties. Energ. Fuel, 22: 1358-1364.
- Knothe, G. (2010). Biodiesel and renewable diesel: A comparison. Prog. Energ. Combust., 36: 364-373.
- Knothe, G., De Castro, M. E., & Razon, L. F. (2015). Methyl esters (biodiesel) from and fatty acid profile of *Gliricidia sepium* seed oil. J. Am. Oil Chem. Soc., 92: 769-775.
- Knothe, G., Matheaus, A.C., & Ryan, T.W. (2003). Cetane numbers of branched and straight-chain fatty esters determined in an ignition quality tester. Fuel, 82: 971-975.
- Kosa, M., Ben, H., Theliander, H., & Ragauskas, A.J. (2011). Pyrolysis oils from CO_2 precipitated kraft lignin. Green Chem., 13: 3196-3202.
- Kraan, S. (2013). Mass cultivation of carbohydrate rich macroalgae, a possible solution for sustainable biofuel production. Mitig. Adapt. Strateg. Glob. Change., 18: 27-46.
- Krammer, P., & Vogel, H. (2000). Hydrolysis of esters in subcritical and super critical water. J. Supercrit. Fluids, 16: 189-206.
- Kruse, A., & Dinjus, E. (2007). Hot compressed water as reaction medium and reactant properties and synthesis reactions. J. Supercrit. Fluids, 39: 362-380.
- Kulkarni, M.G., & Dalai, A.K. (2006). Waste cooking oil - An economical source for biodiesel: A review. Ind. Eng. Chem. Res., 45: 2901-2913.
- Kumar, K., Ghosh, S., Angelidaki, I., Holdt, S. L., Karakashev, D. B., Morales, M. A., & Das, D. (2016). Recent developments on biofuels production from microalgae and macroalgae. Renew. Sust. Energ. Rev., 65: 235-249.
- Kumar, R., Tiwari, P., & Garg, S. (2013). Alkali transesterification of linseed oil for biodiesel production. Fuel, 104: 553-560.
- Kumari, P., Kumar, M., Gupta, V., Reddy, C.R.K., & Jha, B. (2010). Tropical marine macroalgae as potential sources of nutritionally important PUFAs. Food Chem., 120: 749-757.

- Kumari, P., Reddy, C.R.K., & Jha, B. (2011). Comparative evaluation and selection of a method for lipid and fatty acid extraction from macroalgae. Anal. Biochem ., 415: 134-144.
- Ladanai, S., & Vinterback, J. (2009). Global Potential of Sustainable Biomass for Energy, Report 013, SLU, Swedish University of Agricultural Sciences, Department of Energy and Technology (pp. 1- 14). Uppsala, Sweden.
- Lang, X., Dalai, A.K., Bakhshi, N.N., Reaney, M.J., & Hertz, P.B. (2001). Preparation and characterization of biodiesel from various oils. Bioresour. Technol., 80: 53-62.
- Langlois, J., Sassi, J.F., Jard, G., Stever, J.P., Delgenes, J.P., & Helias, A. (2012). Life cycle assessment of biomethane from offshore-cultivated seaweed. Biofuels Bioprod. Bioref., 6: 387-404.
- Lardon, L., Helias, A., Sialve, B., Stayer, J.P., & Bernard, O. (2009). Life-cycle assessment of biodiesel production from microalgae. Environ. Sci. Technol., 43: 6475-6481.
- Leduc, S., Natarajan, K., Dotzauer, E., McCallum, I., & Obersteiner, M. (2009). Optimizing biodiesel production in India. Appl. Energy, 86: 125-131.
- Lee, J., Yoo, C., Jun, S., Ahn, C., & Oh, H. (2010). Comparison of several methods for effective lipid extraction from microalgae. Bioresour. Technol., 101: 75-77.
- Lee, M., Lee, J., Lee, D., Cho, J., Kim, S., & Park, C. (2011). Improvement of enzymatic biodiesel production by controlled substrate feeding using silica gel in a solvent free system. Enzyme Microb. Technol., 49: 402-406.
- Leung, D.Y.C., & Guo, Y. (2006). Transesterification of neat and used frying oil: optimization for biodiesel production. Fuel Process. Technol., 87: 883-90.
- Li, D., Chen, L., Zhang, X., Ye, N., & Xing, F. (2011). Pyrolytic characteristics and kinetics studies of three kinds of red algae. Biomass Bioenerg., 35: 1765-1772.
- Li, Y., Zhu, C., Jiang, J., Yang, Z., Feng, W., Li, L., Guo, Y., & Hu, J. (2020). Catalytic hydrothermal liquefaction of *Gracilaria corticata* macroalgae: Effects of process parameter on bio-oil up-gradation. Bioresour. Technol., 124163.
- Li, D., Chen, L., Xu, D., Zhang, X., Ye, N., Chen, F., & Chen, S. (2012). Preparation and characteristics of bio-oil from the marine brown alga *Sargassum patens* C. Agardh. Bioresour. Technol., 104: 737-742.

- Li, H., Liu, Z., Zhang, Y., Li, B., Lu, H., Duan, N., Liu, M., Zhu, Z., & Si, B. (2014a). Conversion efficiency and oil quality of high-lipid low-protein microalgae via hydrothermal liquefaction. Bioresour. Technol., 154: 322-329.
- Li, J., Wang, G., Chen, M., Li, J., Yang, Y., Zhu, Q., Jiang, X., Wang, Z., & Liu, H. (2014b). Deoxy - liquefaction of three different species of macroalgae to high - quality liquid oil. Bioresour. Technol., 169: 110-118.
- Li, Y., Naghdi, F.G., Garg, S., Adarme -Vega, T.C., Thurecht, K.J., Ghafor, A., Tannock, S., & Schen, P.M. (2014c). A comparative study: the impact of different lipid extraction methods on current microalgal lipid research. Microb.Cell Fact., 13:14.
- Liu, J., Huang, J., Fan, K.W., Jiang, Y., Zhong, Y., Sun, Z., & Chen, F. (2010). Production potential of *Chlorella zofingienesis* as a feedstock for biodiesel. Bioresour. Technol., 101: 8658-8663.
- Liu, Z., & Zhang, F. (2008). Effects of various solvents on the liquefaction of biomass to produce fuels and chemical feedstocks. Energ. Convers. Manag., 49: 3498-3504.
- Liu,Y., Yuan, X., Huang, H., Wang, X., Wang, H., & Zeng, G. (2013). Thermochemical liquefaction of rice husk for bio-oil production in mixed solvent (ethanol-water). Fuel Process. Technol., 112:93-9.
- Lopez, B.C., Cerdan, E.L., Medina, A.R., Lopez, N.E., Valverde, M. L., Pena, H. E., Moreno, P.A.G., & Grima, M. E. (2015). Production of biodiesel from vegetable oil and microalgae by fatty acid extraction and enzymatic esterification. J. Biosci. Bioeng., 119:706-711.
- Lotero, E., Yijun, L., Dora, E. L., Kaewta, S., David, A. B., & James, G.G. (2005). Synthesis of biodiesel via acid catalysis. Ind. Eng. Chem. Res., 44: 5353-63.
- Lu, J., Sheahan, C., & Fu, P. (2011). Metabolic engineering of algae for fourth generation biofuels production. Energy Environ. Sci., 4: 2451-2466.
- Lu, J., Liu, Z., Zhang, Y., Li, B., Lu, Q., Ma, Y., Xen, R., & Zhu, Z. (2017). Improved production and quality of biocrude oil from low-lipid high-ash macroalgae *Enteromorpha prolifera* via addition of crude glycerol. J. Clean. Prod., 142: 749-757.
- Ma, C., Geng, J., Zhang, D., & Ning, X. (2020). Hydrothermal liquefaction of macroalgae: Influence of zeolites based catalyst on products. J. Energy Inst., 93: 581-590.

- Ma, F., & Hannah, M. A. (1999). Biodiesel Production: A review. Bioresour. Technol., 70: 1-15.
- Mac Monagail, M., Cornish, L., Morrison, L., Araújo, R., & Critchley, A. T. (2017). Sustainable harvesting of wild seaweed resources. Eur. J. Phycol., 52: 371-390.
- Maceiras, R., Cancela, A., Sanchez, A., Perez, L., & Alfonsin, V. (2016). Biofuel and biomass from marine macroalgae waste. Energy Sources, A, 38: 1169-1175.
- Maddi, B., Viamajala, S., & Varanasi, S. (2011). Comparative study of pyrolysis of algal biomass from natural lake blooms with lignocellulosic biomass Bioresour. Technol., 102: 11018-11026.
- Madsen, R. B., Biller, P., Jensen, M. M., Becker, J., Iversen, B. B., & Glasius, M. (2016). Predicting the chemical composition of aqueous phase from hydrothermal liquefaction of model compounds and biomasses. Energy Fuels, 30: 10470-10483.
- Mahmudul, H., Hagos, F., Mamat, R., Adam, A. A., Ishak, W., & Alenezi, R. (2017). Production, characterization and performance of biodiesel as an alternative fuel in diesel engines - A review. Renew. Sust. Energ. Rev., 72: 497-509.
- Mandotra, S.K., Kumar, P., Suseela, M.R., & Ramteke, P.W. (2014). Fresh water green microalga *Scenedesmus abundans*: A potential feedstock for high quality biodiesel production. Bioresour. Technol., 156: 42-47.
- Marchetti, J., Miguel, V., & Errazu, A. (2007). Possible methods for biodiesel production. Renew. Sust. Energ. Rev., 11: 1300-1311.
- Martinez-Guerra, E., Gude, V. G., Mondala, A., Holmes, W., & Hernandez, R. (2014). Extractive - transesterification of algal lipids under microwave irradiation with hexane as solvent. Bioresour. Technol., 156: 240-247.
- Martins, A.P., Yokoya, N.S., & Colepicolo, P. (2012). Comparison of extraction and transesterification methods on the determination of the fatty acid contents of three brazilian seaweed species. Braz. J. Pharmacog., 22: 854-860.
- Maulidiyah, N. M., Fatma, F., Natsir, M., & Wibowo, D. (2017). Characterization of methyl ester compound of biodiesel from industrial liquid waste of crude palm oil processing. Anal. Chem. Res., 12: 1-9.

- Mazaheri, H., Lee, K.T., Bhatia, S., & Mohamed, A.R. (2010). Sub/supercritical liquefaction of oil palm fruit press fiber for the production of bio-oil: effect of solvents. Bioresour. Technol., 101: 7641-7.
- Mazanov, S. V., Gabitova, A. R., Usmanov, R. A., Gumerov, F. M., Labidi, S., Amar, M. B., Passarello, J.P., Kanaev, A, Volle, F., & Neindre, B. L. (2016). Continuous production of biodiesel from rapeseed oil by ultrasonic assist transesterification in supercritical ethanol. J.Supercrit. Fluids, 118: 107-118.
- McNichol, J., MacDougall, K. M., Melanson, J. E., & McGinn, P. J. (2012). Suitability of soxhlet extraction to quantify microalgal fatty acids as determined by comparison with *in situ* transesterification. Lipids, 47: 195-207.
- Meher, L.C., Vidya Sagar, D., & Naik, S.N. (2006**).** Technical aspects of biodiesel production by transesterification - a review. Renew. Sust. Energ. Rev., 10: 248-268.
- Meinita, M., Hong, Y.K., & Jeong, G.T., (2012). Detoxification of acidic catalyzed hydrolysate of *Kappaphycus alvarezii* (*cottonii*). Bioprocess Biosyst. Eng., 35: 93-98.
- Meneghetti, S. M., Meneghetti, M. R., Wolf, C. R., Silva, E. C., Lima, G. E., De Lira Silva, L., Serra, T.M., Cauduro, F., & De Oliveira, L. G. (2006). Biodiesel from castor oil: A comparison of ethanolysis versus methanolysis. Energy Fuels, 20: 2262-2265.
- Mercer, P., & Armenta, R.E. (2011). Developments in oil extraction from microalgae. Eur. J. Lipid Sci. Technol., 113: 539-547.
- Miao, X., & Wu, Q. (2006). Biodiesel production from heterotrophic microalgal oil. Bioresour. Technol., 97: 841-846.
- Milledge, J.J., & Harvey, P.J. (2016) Potential process 'hurdles' in the use of macroalgae as feedstock for biofuel production in the British Isles. J. Chem. Technol. Biot., 91:2221–2234.
- Mishra, S. K., Suh, W. I., Farooq, W., Moon, M., Shrivastav, A., Park, M. S., & Yang, J.W. (2014). Rapid quantification of microalgal lipids in aqueous medium by a simple colorimetric method. Bioresour. Technol., 155: 330-333.
- Mittelbach, M., & Remschmidt, C. (2004). Biodiesel - The comprehensive handbook, Karl-Franzens- Universität Graz, Graz, Austria.
- Miyashita, K., Mikami, N., & Hosokawa, M. (2013). Chemical and nutritional characteristics of brown seaweed lipids: A review. J. Funct. Foods, 5: 1507-1517.

- Mofijur, M., Masjuki, H., Kalam, M., Hazrat, M., Liaquat, A., Shahabuddin, M., & Varman, M. (2012). Prospects of biodiesel from *Jatropha* in Malaysia. Renew. Sust.Energ. Rev., 16: 5007-5020.
- Moreira, A.L., Dias, J.M., Almeida, M. F., & Alvim-Ferraz, M.C.M. (2010). Biodiesel production through transesterification of poultry fat at 30°C. Energ. Fuel., 24: 5717-5721.
- Morshed, M., Ferdous, K., Khan, M. R., Mazumder, M., Islam, M., & Uddin, M. (2011). Rubber seed oil as a potential source for biodiesel production in Bangladesh. Fuel, 90: 2981-2986.
- Moser, B.R. (2009). Biodiesel production, properties, and feedstocks. In vitro Cell. Dev. Biol - Plant, 45: 229-66.
- Mullen, C.A., Strahan, G.D., & Boateng, A.A. (2009). Characterization of various fast pyrolysis bio-oils by NMR spectroscopy. Energy Fuels, 23: 2707-2718.
- Muppaneni, T., Reddy, H. K., Selvaratnam, T., Dandamudi, K. P., Dungan, B., Nirmalakhandan, N., Schaub, T., Holguin, O., Voorhies, W., Lammers, P. & Deng, S. (2017). Hydrothermal liquefaction of *Cyanidioschyzon merolae* and the influence of catalysts on products. Bioresour. Technol., 223: 91-97.
- Musa, I. A. (2016). The effects of alcohol to oil molar ratios and the type of alcohol on biodiesel production using transesterification process. Egypt. J. Petrol., 25: 21-31.
- Navarro, L. E., Medina, A. R., Moreno, P.A.G., Cerdán, L.E., & Grima, E. M. (2016). Extraction of microalgal lipids and the influence of polar lipids on biodiesel production by lipase-catalyzed transesterification. Bioresour. Technol., 216: 904-913.
- Nejat, P., Jomehzadeh, F., Taheri, M. M., Gohari, M., & Abd. Majid, M. Z. (2015). A global review of energy consumption, CO_2 emissions and policy in the residential sector (with an overview of the top ten CO_2 emitting countries). Renew. Sust. Energ. Rev., 43: 843-862.
- Nelson, D. R., & Viamajala, S. (2016). One-pot synthesis and recovery of fatty acid methyl esters (FAMEs) from microalgae biomass. Catal., 269: 29-39.
- Neveux, N., Yuen, A.K.L., Jazrawi, C., Magnusson, M., Haynes, B.S., Masters, A.F., Montoya, A., Paul, N.A., Maschmeyer, T., & De Nys, R. (2014a). Biocrude yield and

productivity from the hydrothermal liquefaction of marine and freshwater green macroalgae. Bioresour. Technol. 155: 334-341.

- Neveux, N., Yuen, A., Jazrawi, C., He, Y., Magnusson, M., Haynes, B., Masters, A.F., Montoya, A., Paul, N.A., Maschmeyer, T., & De Nys, R. (2014b). Pre- and post-harvest treatment of macroalgae to improve the quality of feedstock for hydrothermal liquefaction. Algal Res., 6: 22-31.
- Noraini, M.Y., Ong, H.C., Badrul, M.J., & Chong, W.T. (2014). A review on potential enzymatic reaction for biofuel production from algae. Renew. Sustain. Energy. Rev., 39: 24-34.
- Norziah, M. H., & Ching, C. Y. (2000). Nutritional composition of edible seaweed *Gracilaria changgi*. Food Chem., 68: 69-76.
- Nwosu, F., Morris, J., Lund, V. A., Stewart, D., Ross, H. A., & McDougall, G. J. (2011). Anti-proliferative and potential anti-diabetic effects of phenolic-rich extracts from edible marine algae. Food Chem., 126: 1006-1012.
- Omirou, M., Tzovenis, I., Charalampous, P., Tsaousis, P., Polycarpou, P., Chantzistrountsiou, X., Economou-Amillib, A., & Ioannides, I. M. (2018). Development of marine multi-algae cultures for biodiesel production. Algal Res., 33: 462-469.
- Onukwuli, D. O., Emembolu, L. N., Ude, C. N., Aliozo, S. O., & Menkiti, M. C. (2017). Optimization of biodiesel production from refined cotton seed oil and its characterization. Egypt. J. Pet., 26: 103-110.
- Osada, M., Sato, T., Watanabe, M., Shirai, M., & Arai, K. (2006). Catalytic gasification of wood biomass in subcritical and supercritical water. Combust. Sci. Technol., 178: 537-52.
- Pangestuti, R., & Kim, S.K. (2011). Neuroprotective effects of marine algae. Mar. Drugs, 9: 803-818.
- Parsa, M., Jalilzadeh, H., Pazoki, M., Ghasemzadeh, R., & Abduli, M. (2018). Hydrothermal liquefaction of *Gracilaria gracilis* and *Cladophora glomerata* macroalgae for biocrude production. Bioresour. Technol., 250: 26-34.

- Patwardhan, P.R., Satrio, J.A., Brown, R.C., & Shanks, B.H. (2010). Influence of inorganic salts on the primary pyrolysis products of cellulose. Bioresour. Technol., 101: 4646-4655.
- Pedersen, T.H., Grigoras, I.F., Hoffmann, J., Toor, S.S., Daraban, I.M., Jensen, C.U., Iversen, S.B., Madsen, R.B., Glasius, M., & Arturi, K.R. (2016). Continuous hydrothermal co-liquefaction of aspen wood and glycerol with water phase recirculation. Appl. Energy, 162: 1034-1041.
- Peralta-Garcia, E., Caamal-Fuentes, E., Robledo, D., Hernandez-Nunez, E., & Freile-Pelegrin, Y. (2016). Lipid characterization of red alga *Rhodymenia pseudopalmata* (Rhodymeniales, Rhodophyta). Phycol. Res., 65: 58-68.
- Peterson, A.A., Vogel, F., Lachance, R.P., Froling, M., Antal Jr, M.J., & Tester, J.W. (2008). Thermochemical biofuel production in hydrothermal media: A review of sub- and supercritical water technologies. Energy Environ. Sci., 1: 32-65.
- Pienkos, P. T., & Darzins, A. (2009). The promise and challenges of microalgal-derived biofuels. Biofuel. Bioprod. Biorefin., 3: 431-440.
- Pinzi, S., Garcia, I. L., Lopez-Gimenez, F. J., Luque de Castro, M. D., Dorado, G., & Dorado, M.P. (2009). The ideal vegetable oil-based biodiesel composition: A review of social, economical and technical implications, Energy Fuels, 23: 2325-2341.
- Pittman, C.U., Mohan, D., Eseyin, A., Li, Q., & Ingram, L. (2012). Characterization of bio-oils from fast pyrolysis of corn stalks in an auger reactor. Energy Fuels, 26: 3816-3825.
- Polat, S., & Ozogul, Y. (2013). Seasonal proximate and fatty acid variations of some seaweeds from the northeastern Mediterranean coast. Oceanologia, 55: 375-391.
- Prommuak, C., Pavasant, P., Quitain, A. T., Goto, M., & Shotipruk, A. (2012). Microalgal lipid extraction and evaluation of single-step biodiesel production. Eng. J., 16: 157-166.
- Raheem, A., Wan Azlina, W.A.K.G., Taufiq Yap Y.H., Danquah, M.K., & Harun, R. (2015). Thermochemical conversion of microalgal biomass for biofuel production. Renew. Sust. Energ. Rev., 49: 990-999.

- Raikova, S., Le, C., Beacham, T., Jenkins, R., Allen, M., & Chuck, C. (2017). Towards a marine biorefinery through the hydrothermal liquefaction of macroalgae native to the United Kingdom. Biomass Bioenergy, 107: 244-253
- Ramos, M.J., Fernandez, C. M., Casas, A., Rodriguez, L., & Perez, A. (2009). Influence of fatty acid composition of raw materials on biodiesel properties. Bioresour. Technol., 100: 261-268.
- Ravindranath, N., Sita Lakshmi, C., Manuvie, R., & Balachandra, P. (2011). Biofuel production and implications for land use, food production and environment in India. Energy Policy, 39: 5737-5745.
- Reddy, C.R.K. & Subba Rao, P.V, Ganesan, M., Eswaran, K., Zaidi, S. H., & Mantri, V.A. (2014).The seaweed resources of India. In A. T. Critchely, M. Ohno & D. Largo (Eds.), World seaweed resources (pp 5-6). ETI Information Services Ltd., Wokingham, Berkshire, U. K.
- Reddy, H.K., Muppaneni, T., Ponnusamy, S., Sudasinghe, N., Pegallapati, A., Selvaratnam, T., Seger, M., Dungan, B., Nirmalakhandan, N., Schaubb, T., Holguin, O. F., Lammers, P., Voorhiese, W., & Deng, S. (2016). Temperature effect on hydrothermal liquefaction of *Nannochloropsis gaditana* and *Chlorella* sp. Appl. Energy, 165: 943-951.
- Ren, X., Zhao, X., Turcotte, F., Deschenes, J., Tremblay, R., & Jolicoeur, M. (2017). Current lipid extraction methods are significantly enhanced adding a water treatment step in *Chlorella prototheco*ides. Microb. Cell Fact., 16:1-13.
- Renita, A.A., Sreedhar, N., & Peter, D. M. (2014). Optimization of algal methyl esters using RSM and evaluation of biodiesel storage characteristics. Bioresour. Bioprocess, 1: 1-9.
- Ross, A.B., Anastasakis, K., Kubacki, M., & Jones, J. (2009). Investigation of the pyrolysis behavior of brown algae before and after pre-treatment using PY-GC/MS and TGA. J. Anal. Appl. Pyrolysis, 85: 3-10.
- Ross, A.B., Biller, P., Kubacki, M.L., Li, H., Lea-Langton, A., & Jones, J.M. (2010). Hydrothermal processing of microalgae using alkali and organic acids. Fuel, 89: 2234-2243.

- Ross, A.B., Jones, J.M., Kubacki, M.L., & Bridgeman. T. (2008). Classification of macroalgae as fuel and its thermochemical behavior. Bioresour. Technol., 99: 6494-6504.
- Ryckebosch, E., Bermudez, S. P., Termote-Verhalle, R., Bruneel, C., Muylaert, K., Parra-Saldivar, R., & Foubert, I. (2013). Influence of extraction solvent system on the extractability of lipid components from the biomass of *Nannochloropsis gaditana*. J. Appl. Phycol., 26: 1501-1510.
- Ryckebosch, E., Muylaert, K., & Foubert, I. (2012). Optimization of an analytical procedure for extraction of lipids from microalgae. J. Am. Oil Chem. Soc., 89: 189-198.
- Sahoo, D. (2010). Common seaweeds of India. I. K. International Pvt. pp26, 98, 126.
- Sanchez, A., Maceiras, R., Cancela, A., & Rodriguez, M. (2012). Influence of n-hexane on *in situ* transesterification of marine macroalgae. Energies, 5: 243-257.
- Sanchez-Machado, D.I., Lopez-Cervantes, J., Lopez-Hernandez, J., & Paseiro - Losada, P. (2004). Fatty acids, total lipid, protein and ash contents of processed edible seaweeds. Food Chem., 85: 439-444.
- Santos, E.M., Piovesan, N.D., Gonçalves de Barros, E., & Moreira, M.A. (2013). Low linolenic soybeans for biodiesel: Characteristics, performance and advantages. Fuel, 104: 861-864.
- Sapkale, G.N., Patil, S.M., Surwase, U.S., & Bhatbhage, P.K. (2010). Supercritical fluid extraction. Int. J. Chem. Sci., 8: 729-43.
- Savage, P.E., (2009). A perspective on catalysis in sub- and supercritical water. J.Supercrit. Fluids, 47: 407-414.
- Schaleger, L., Figueroa, C., & Davis, H.G. (1982). Direct liquefaction of biomass: results from operation of continuous bench scale unit in liquefaction of water slurries of douglas fir wood. Biotechnol. Bioeng. Symp.,12: 3-14.
- Schmid, M., Guiheneuf, F., & Stengel, D. B. (2016). Evaluation of food grade solvents for lipid extraction and impact of storage temperature on fatty acid composition of edible seaweeds *Laminaria digitata* (Phaeophyceae) and *Palmaria palmata* (Rhodophyta). Food Chem., 208: 161-168.

- Shah, S., Sharma, S., & Gupta, M. N. (2004). Biodiesel preparation by lipase-catalyzed transesterification of *Jatropha* oil. Energy Fuels, 18: 154-159.
- Shakya, R., Adhikari, S., Mahadevan, R., Shanmugam, S.R., Nam, H., Hassan, B.E., & Dempster, T.A. (2017). Influence of biochemical composition during hydrothermal liquefaction of algae on product yields and fuel properties. Bioresour. Technol., 243: 1112-1120.
- Shalaby, E. A., El-Moneim M. R. Afify, A., & Shanab, S. M. (2010). Enhancement of biodiesel production from different species of algae. Grasas Aceites, 61: 416-422.
- Liang, S., Wei, L., Passero, M.L., Feris, K., & McDonald A.G. (2017). Hydrothermal liquefaction of laboratory cultivated and commercial algal biomass into crude bio-oil. Environ. Prog. Sust., 36: 781-787.
- Sharma, Y.C. & Singh, V. (2017). Microalgal biodiesel: A possible solution for India's energy security. Renew. Sust. Energ. Rev., 67: 72-88.
- Sharma, Y.C., Singh, B., & Upadhyay, S.N. (2008). Advancements in development and characterization of biodiesel: A review. Fuel, 87: 2355-2373.
- Sharma, Y. C., Singh, B., Madhu, D., Liu, Y., & Yaakob, Z. (2014). Fast synthesis of high quality biodiesel from 'waste fish oil' by single step transesterification. Biofuel Res. J., 3: 78-80.
- Sheehan, J., Dunahay, T., Benemann, J., & Roessler, P. (1998). A look back at the U.S. Department of Energy's Aquatic Species Program: Biodiesel from Algae, Report No. NREL/TP-580 - 24190. The National Renewable Energy Laboratory, U.S. Department of Energy, Washington.
- Sheng, J., Vannela, R., & Rittmann, B. E. (2011). Evaluation of methods to extract and quantify lipids from *Synechocystis* PCC 6803. Bioresour. Technol., 102: 1697-1703.
- Siddiqua, S., Mamun, A.A., & Enayetul Babar, S.M. (2015). Production of biodiesel from coastal macroalgae (*Chara vulgaris*) and optimization of process parameters using Box-Behnken design. Springerplus, 4: 1-11.
- Singh, R., Balagurumurthy, B., & Bhaskar, T. (2015a). Hydrothermal liquefaction of macro algae: Effect of feedstock composition. Fuel, 146: 69-74.

- Singh, R., Bhaskar, T., & Balagurumurthy, B. (2015b). Effect of solvent on the hydrothermal liquefaction of macro algae *Ulva fasciata*. Process. Saf. Environ., 93: 154-160.
- Singh, R., Balagurumurthy, B., Prakash, A., & Bhaskar, T. (2015c). Catalytic hydrothermal liquefaction of water hyacinth. Bioresour. Technol., 178: 157-165.
- Singh, R., Prakash, A., Dhiman, S.K., Balagurumurthy, B., Arora, A.K., Puri, S.K., Bhaskar, T. (2014). Hydrothermal conversion of lignin to substituted phenols and aromaticethers. Bioresour. Technol., 165: 319-322.
- Sirajunnisa, A. R., & Surendhiran, D. (2016). Algae - A quintessential and positive resource of bioethanol production: A comprehensive review. Renew. Sust. Energ. Rev., 66: 248-267.
- Sivakumar, P., Sindhanaiselvan, S., Gandhi, N. N., Devi, S. S., & Renganathan, S. (2013). Optimization and kinetic studies on biodiesel production from underutilized *Ceiba pentandra* oil. Fuel, 103: 693-698.
- Sivaramakrishnan, R., & Incharoensakdi, A. (2016). Production of methyl ester from two microalgae by two-step transesterification and direct transesterification. Environ. Sci. Pollut. Res., 24: 4950-4963.
- Soares, A.T., Silva, B.F., Fialho, L.L., Pequeno, M.A.G., Vieira, A.A.H., Souza, A.G., & Antoniosi Filho, N.R. (2013). Chromatographic characterization of triacylglycerides and fatty acid methyl esters in microalgae oils for biodiesel production. J. Renew. Sustain. Energ., 5:1-8.
- Soares, A.T., Costa, A.D., Silva, B.F., Lopes, R.G., Derner, R.B., & Antoniosi Filho, N.R. (2014). Comparative analysis of the fatty acid composition of microalgae obtained by different oil extraction methods and direct biomass transesterification. Bioenerg. Res. 7: 1035-1044.
- Soler-Vila, A., Coughlan, S., & Guiry, M.D. (2009). The red alga, *Porphyra dioica*, as a fish-feed ingredient for rainbow trout *Oncorhynchus mykiss* effects on growth, feed efficiency, and carcass composition. J. Appl. Phycol., 21: 617- 624.
- Stevens, D.J. (1994). Review and analysis of the 1980-1989 biomass thermochemical conversion program. NREL/TP-421-7501. U.S. Department of Energy;

- Subba Rao, P.V., & Mantri, V.A. (2006). Indian seaweed resources and sustainable utilization: Scenario at the dawn of a new century. Curr. Sci., 91:164-74.
- Subba Rao, P.V., Periyasamy, C., Suresh Kumar, K., Srinivasa Rao, A., & Anantharaman, P. (2018). Seaweeds: Distribution, production and uses. In M.N. Noor, S.K. Bhatnagar & S. K. Sinha (Eds.), Bioprospecting of algae (pp: 60-61). Society for plant research: Shri Gyansagar Publications, Meerut, India.
- Sudhakar, K., Mamat, R., Samykano, M., Azmi, W., Ishak, W., & Yusaf, T. (2018). An overview of marine macroalgae as bioresource. Renew. Sust. Energ. Rev., 9: 165-179.
- Suganya, T., & Renganathan, S. (2012). Optimization and kinetic studies on algal oil extraction from marine macroalgae *Ulva lactuca*. Bioresour. Technol., 107: 319-326.
- Suganya, T., Gandhi, N.N. & Renganathan, S. (2013). Production of algal biodiesel from marine macroalga *Enteromorpha compressa* by two step process: Optimization and kinetic study. Bioresour. Technol., 128: 392-400.
- Suganya, T., Kasirajan, R., & Renganathan, S. (2014a). Ultrasound - enhanced rapid *in situ* transesterification of marine macroalgae *Enteromorpha compressa* for biodiesel production. Bioresour. Technol., 156: 283-290.
- Suganya, T., & Renganathan, S. (2014b). Ultrasonic assisted acid base transesterification of algal oil from marine macroalgae *Caulerpa peltata*: Optimization and characterization studies. Fuel, 128: 347-355.
- Supaporn, P., & Yeom, S. H. (2016). Optimization of a two-step biodiesel production process comprised of lipid extraction from blended sewage sludge and subsequent lipid transesterification. Biotechnol. Bioproces. Eng., 21: 551-560.
- Talebi, A.F., Mohtashami, S.K., Tabatabaei, M., Tohidfar, M., Bagheri, A., Zeinalabedini, M., Mirzaei, H.H., Mirzajanzadeh, M., Shafaroudi, S.M., & Bakhtiari, S. (2013). Fatty acids profiling: A selective criterion for screening microalgae strains for biodiesel production Algal Res., 2: 258-267.
- Taravus, S., Temur, H., & Yartasi, A. (2009). Alkali-catalyzed biodiesel production from mixtures of sunflower oil and beef tallow. Energy Fuels, 23: 4112-4115.
- Tekin, K., Karagoz, S., & Bektaş, S. (2012). Hydrothermal liquefaction of beech wood using a natural calcium borate mineral. J. Supercrit. Fluid, 72: 134-139.

- Thanh, L. T., Okitsu, K., Sadanaga, Y., Takenaka, N., Maeda, Y., & Bandow, H. (2013). A new co-solvent method for the green production of biodiesel fuel - Optimization and practical application. Fuel, 103: 742-748.
- Theegala, C.S. (2015). Algal cell disruption and lipid extraction: A review on current technologies and limitations. In A. Prokop, R.K. Bajpai, & M.E. Zappi (Eds.), Algal biorefineries, Vol. 2: products and refinery design (pp. 426). Springer, Cham.
- Thigpen, P.L. (1982). Final Report: An Investigation of Liquefaction of Wood at the Biomass Liquefaction Facility, Albany, Oregon, Battelle Pacific Northwest Laboratories, Department of Energy, Wheelabrator Cleanfuel Corporation. Technical Information Center, Office of Scientific and Technical Information, U.S. Department of Energy, contract.
- Thiruvengadaravi, K., Nandagopal, J., Baskaralingam, P., Sathya Selva Bala, V., & Sivanesan, S. (2012). Acid-catalyzed esterification of karanja (*Pongamia pinnata*) oil with high free fatty acids for biodiesel production. Fuel, 98: 1- 4.
- Tian, C., Li, B., Liu, Z., Zhang, Y., & Lu, H. (2014). Hydrothermal liquefaction for algal biorefinery: A critical review. Renew. Sust. Energ. Rev., 38: 933 - 950.
- Toor, S.S., Rosendahl, L., & Rudolf, A. (2011). Hydrothermal liquefaction of biomass: a review of subcritical water technologies. Energy, 36: 2328-2342.
- Toor, S.S., Rosendahl, L.A., Hoffmann, J., Pedersen, T.H., Nielsen, R.P., & Sogaard, E.G. (2014). Hydrothermal liquefaction of biomass. In F. Jin (Eds.), Application of hydrothermal reactions to biomass conversion (pp. 189-217). Springer, Berlin, Germany.
- Toor, S. S., Reddy, H., Deng, S., Hoffmann, J., Spangsmark, D., Madsen, L. B., Holm-Nielsen, J.B., & Rosendahl, L. A. (2013). Hydrothermal liquefaction of *Spirulina* and *Nannochloropsis salina* under subcritical and supercritical water conditions. Bioresour. Technol., 131: 413-419.
- Torri, C., Garcia Alba, L., Samori, C., Fabbri, D., & Brilman, D.W.F. (2012). Hydrothermal treatment (HTT) of microalgae: Detailed molecular characterization of HTT oil in view of HTT mechanism elucidation. Energy Fuels, 26: 658-671.
- Tran, D., Chen, C., & Chang, J. (2013). Effect of solvents and oil content on direct transesterification of wet oil-bearing microalgal biomass of *Chlorella vulgaris* ESP-31

for biodiesel synthesis using immobilized lipase as the biocatalyst. Bioresour. Technol., 135: 213-221.

- Tripathi, L., Mishra, A., Dubey, A. K., Tripathi, C., & Baredar, P. (2016). Renewable energy: An overview on its contribution in current energy scenario of India. Renew. Sust. Energ. Rev., 60: 226-233.
- Trivedi, N., Gupta, V., Reddy, C., & Jha, B. (2013). Enzymatic hydrolysis and production of bioethanol from common macrophytic green alga *Ulva fasciata* Delile. Bioresour. Technol., 150: 106-112.
- U.S. Energy Information Administration (April 2020). Retrieved from: https://www.eia.gov/tools/faqs/faq.php?id=709&t=6
- U.S. Energy Information Administration (June, 2020). Retrieved from: https://www.eia.gov/energyexplained/what-is-energy/sources-of-energy.php
- U.S. Energy Information Administration (September 2020). Retrieved from: https://www.eia.gov/international/content/analysis/countries_long/India/india.pdf
- Uchimiya, M., Orlov, A., Ramakrishnan, G., & Sistani, K. (2013). *In situ* and *ex situ* spectroscopic monitoring of biochar's surface functional groups. J. Anal. Appl. Pyrolysis, 102: 53-59.
- Uematsu, M., & Franck, E.U. (1980). Static dielectric constant of water and steam. J. Phys. Chem. Ref. Data, 9: 1291-1306.
- Ullah, K., Ahmad, M., Sofia, Sharma, V.K., Lu, P., Harvey, A., Zafar, M., & Sultana, S. (2015). Assessing the potential of algal biomass opportunities for bioenergy industry: a review. Fuel, 143: 414-23.
- Umdu, E. S., Tuncer, M., & Seker, E. (2009). Transesterification of *Nannochloropsis oculata* microalga's lipid to biodiesel on Al_2O_3 supported CaO and MgO catalysts. Bioresour.Technol., 100: 2828-2831.
- Urrejola, S., Maceiras, R., Perez, L., Cancela, A., & Sanchez, A. (2012). Analysis of macroalgae oil transesterification for biodiesel production. Chem. Eng. Transact., 29:1153-1158.
- Valdez, P.J., & Savage, P.E. (2013). A reaction network for the hydrothermal liquefaction of *Nannochloropsis* sp. Algal Res., 2: 416-425.

- Valdez, P.J., Nelson, M.C., Wang, H.Y., Lin, X.X., & Savage, P.E. (2012). Hydrothermal liquefaction of *Nannochloropsis* sp: Systematic study of process variables and analysis of the product fractions. Biomass Bioenerg., 46:317-331.
- Van Den Hoek, C. (1981). Phaeophyta: morphology and classification. In C. S. Lobban & M. J. Wynne (Eds.), The biology of seaweeds (pp 52-54). Blackwell Scientific Publications: London, England.
- Van Gerpen, J., Shanks, B., Pruszko, R., Clements, D., & Knothe, G. (2004). Biodiesel analytical methods: NREL/SR-510-36240. Colorado, USA: National Renewable Energy Laboratory.
- Vardon, D. R., Sharma, B. K., Blazina, G. V., Rajagopalan, K., & Strathmann, T. J. (2012). Thermochemical conversion of raw and defatted algal biomass via hydrothermal liquefaction and slow pyrolysis. Bioresour. Technol., 109: 178-187.
- Vardon, D. R., Sharma, B., Scott, J., Yu, G., Wang, Z., Schideman, L., Zhang, Y., & Strathmann, T. J. (2011). Chemical properties of biocrude oil from the hydrothermal liquefaction of *Spirulina* algae, swine manure and digested anaerobic sludge. Bioresour. Technol., 102: 8295-8303.
- Vassilev, S. V., & Vassileva, C. G. (2016). Composition, properties and challenges of algae biomass for biofuel application: An overview. Fuel, 181: 1-33.
- Vicente, G., Martínez, M., & Aracil, J. (2004). Integrated biodiesel production: a comparison of different homogeneous catalysts systems. Bioresour. Technol., 92: 297-305.
- Viera, M.P., Gomez Pinchetti, J.L., Courtois De Vicose, G., Bilbao, A., Suarez, S., Haroun, R.J., & Izquierdo, M.S. (2005). Suitability of three red macroalgae as a feed for the abalone *Haliotis tuberculata coccinea* Reeve. Aquaculture, 248: 75-82.
- Vyas, A.P., Verma, J. L., & Subrahmanyam, N. (2010). A review on FAME production processes. Fuel, 89: 1-9.
- Wang, F., Chang, Z., Duan, P., Yan, W., Xu, Y., Zhang, L., Miao, J., & Fan, Y. (2013). Hydrothermal liquefaction of *Litsea cubeba* seed to produce bio-oils. Bioresour. Technol., 149: 509-515.
- Wang, H. D., Chen, C., Huynh, P., & Chang, J. (2015). Exploring the potential of using algae in cosmetics. Bioresour. Technol., 184: 355-362.

- Wang, Z., Adhikari, S., Valdez, P., Shakya, R., & Laird, C. (2016). Upgrading of hydrothermal liquefaction biocrude from algae grown in municipal wastewater. Fuel Process. Technol., 142: 147-156.
- Wardle, D.A. (2003). Global sale of green air travel supported using biodiesel. Renew. Sust. Energy Rev., 7: 1- 64.
- Watanabe, M., Bayer, F., & Kruse, A. (2006). Oil formation from glucose with formic acid and cobalt catalyst in hot-compressed water. Carbohydr. Res. 341: 2891-2900.
- Wegeberg, S., & Felby, C. (2010). Algae Biomass for Bioenergy in Denmark: Biological/ Technical Challenges and Opportunities. Pp 4. (Retrieved from: http://www. bio4 bio. dk/~/media /Bio 4bio/publications /Review _of_ algae _biomass _for_ energy_ SW_ CF_ April2010.ashx.)
- Wei, N., Quarterman, J., & Jin, Y.S. (2013). Marine macroalgae: an untapped resource for producing fuels and chemicals. Trends Biotechnol., 31: 70-77.
- Williams, P.T., & Slaney, E. (2007). Analysis of products from the pyrolysis and liquefaction of single plastics and waste plastic mixtures. Resour. Conserv. Recycl., 51: 754-69.
- www.nio.org
- Wynne, M.J. (1981). Chlorophyta: morphology and classification. In C. S. Lobban & M. J. Wynne (Eds.), The biology of seaweeds (pp 86-87). Blackwell Scientific Publications: London, England.
- Xu, H., Miao, X., & Wu, Q. (2006). High quality biodiesel production from microalga *Chlorella protothecoides* by heterotrophic growth fermenters. J. Biotechnol., 126: 499-507.
- Xu, X., Kim, J.Y., Oh, Y.R., & Park, J.M. (2014a). Production of biodiesel from carbon sources of macroalgae, *Laminaria japonica*. Bioresour. Technol., 169: 455-61.
- Xu, Y., Zheng, X., Yu, H., & Hu, X. (2014b). Hydrothermal liquefaction of *Chlorella pyrenoidosa* for bio-oil production over Ce/HZSM-5. Bioresour. Technol., 156: 1-5.
- Xu, Y., Hu, X., Yu, H., Wang, K., & Cui, Z. (2016). Hydrothermal catalytic liquefaction mechanisms of algal biomass to bio-oil. Energ. Source Part A, 38: 1478-1484.

- Xu, Y., Duan, P., & Wang, F. (2015). Hydrothermal processing of macroalgae for producing crude bio-oil. Fuel Process. Technol., 130: 268-274.
- Yaich, H., Garna, H., Besbes, S., Paquot, M., Blecker, C., & Attia, H. (2011). Chemical composition and functional properties of *Ulva lactuca* seaweed collected in Tunisia. Food Chem., 128: 895-901.
- Yan, L., Wang, Y., Li, J., Zhang, Y., Ma, L., Fu, F., Chen, B., & Liu, H. (2019). Hydrothermal liquefaction of *Ulva prolifera* macroalgae and the influence of base catalysts on products. Bioresour. Technol., 292: 121286.
- Yang, H., Yan, R., Chen, H., Lee, D.H., & Zheng, C.G. (2007). Characteristics of hemicellulose, cellulose, and lignin pyrolysis. Fuel, 86:1781-1788.
- Yang, W., Li, X., Liu, S., & Feng, L. (2014). Direct hydrothermal liquefaction of undried macroalgae *Enteromorpha prolifera* using acid catalysts. Energy Convers. Manag., 87: 938-945.
- Yin, S., Dolan, R., Harris, M., & Tan, Z. (2010). Subcritical hydrothermal liquefaction of cattle manure to bio-oil: Effects of conversion parameters on bio-oil yield and characterization of bio-oil. Bioresour. Technol., 101: 3657-3664.
- Yu, G., Zhang, Y., Guo, B., Funk, T., & Schideman, L. (2014). Nutrient flows and quality of bio-crude oil produced via catalytic hydrothermal liquefaction of low-lipid microalgae. BioEnergy Res., 7: 1317-1328.
- Yuan, X., Wang, J., Zeng, G., Huang, H., Pei, X., Li, H., Liu, Z., & Cong, M. (2011). Comparative studies of thermochemical liquefaction characteristics of microalgae using different organic solvents, Energy, 36: 6406-6412.
- Zhai, Y., Chen, H., Xu, B., Xiang, B., Chen, Z., Li, C., & Zeng, G. (2014). Influence of sewage sludge based activated carbon and temperature on the liquefaction of sewage sludge: yield and composition of bio-oil, immobilization and risk assessment of heavy metals. Bioresour. Technol., 159: 72-79.
- Zhang, J., Chen, S., Yang, R., & Yan, Y. (2010). Biodiesel production from vegetable oil using heterogenous acid and alkali catalyst. Fuel, 89: 2939-2944.
- Zhang, J., & Zhang, Y. (2014). Hydrothermal liquefaction of microalgae in an ethanol-water co-solvent to produce biocrude oil. Energy Fuels, 28: 5178-5183.

- Zhang, J., Zhang, Y., & Luo, Z. (2014). Hydrothermal liquefaction of *Chlorella pyrenoidosa* in ethanol-water for bio-crude production. Energy Procedia, 61: 1961-1964.
- Zhou, D., Zhang, L., Zhang, S., Fu, H., & Chen, J. (2010). Hydrothermal liquefaction of macroalgae *Enteromorpha prolifera* to bio-oil. Energy Fuels, 24: 4054-61.
- Zhou, D., Zhang, S., Fu, H., & Chen, J. (2012). Liquefaction of macroalgae *Enteromorpha prolifera* in sub-/supercritical alcohols: Direct production of ester compounds. Energy Fuels, 26: 2342-2351.
- Ziolkowska, J.R., & Simon, L. (2014). Recent developments and prospects for algae-based fuels in the US. Renew. Sustain. Energy Rev., 29: 847-53.
- Ziolkowska, J. R. (2020). Biofuels technologies: An overview of feedstocks, processes, and technologies. In J. Ren, A. Scipioni, A. Manzardo, & H. Liang (Eds.), Biofuels for a more sustainable future (pp. 1-19). Elsevier, New York.

Appendices

Appendix A

This appendix consists of GC-MS tables that were referenced in the previous chapters.

Table A-1: Chemical composition of *S. tenerrimum* bio-oil as obtained from GC-MS analysis.

Sr No.	Compounds identified in Bio-oil	Area %			
		Water 260°C	Water 280°C	Water 300 °C	Ethanol-water
1.	3-Pyridinol	5.5	16.21	9.61	4.0628
2.	(1-methylethyl)-, (4a.alpha.,7.beta.,8a.beta.)-	1.51	-	-	-
3.	(S)-6,6-Dimethyl-2-azaspiro[4.4]non-1-ene	-	-	-	1.1434
4.	(Z)-14-Tricosenyl formate	2.22	-	-	-
5.	1,3-Benzenediol, 4-ethyl-	-	-	1.03	-
6.	1,4-Benzenediol, 2-methyl-	-	2.66	2.85	-
7.	1,9-Tetradecadiene	1.08	-	-	-
8.	13-Tetradecen-1-ol acetate	1.27	-	-	-
9.	1-Heptadecene	1.12	-	-	-
10.	1-Nonadecene	0.01	-	-	-
11.	2(1H)-Naphthalenone, octahydro-4a-methyl-7-	-	-	-	-
12.	2,3-Dimethylhydroquinone	-	-	1.07	-
13.	2,5-Piperazinedione, 3-benzyl-6-isopropyl-	-	2.13	-	-
14.	26,27-Dinorergosta-5,23-dien-3-ol, (3.beta.)-	-	-	2.86	-
15.	2-Cyclohexen-1-one, 4-ethyl-3,4-dimethyl-	-	-	1.53	-
16.	2-Cyclopenten-1-one, 2,3-dimethyl-	-	1.54	-	-
17.	2-Cyclopenten-1-one, 2-methyl-	-	1.48	-	-

18.	2-Hydrazino-4-methyl-6-methylthiopyrimidine	3.14	-	-	-
19.	2-Myristynoyl-glycinamide	-	-	2.3	-
20.	2-Pentadecanone, 6,10,14-trimethyl-	-	-	-	1.2267
21.	2-Pentanone, 4-hydroxy-4-methyl-	-	-	-	0.8569
22.	2-Propenoic acid, 2-methyl-, 1-methylethyl ester	-	3.28	-	-
23.	3-Pyridinol, 6-methyl-	-	1.24	2.29	1.0324
24.	4-Octanone, 2-(dimethylamino)-1-phenyl-	-	-	-	0.8557
25.	5,8,11,14-Eicosatetraenoic acid, ethyl ester, (all-Z)-	-	-	-	2.8461
26.	7-Ethyl-4,6-heptadecandione	-	-	3.02	
27.	9,12,15-Octadecatrienoic acid, ethyl ester, (Z,Z,Z)-	-	-	-	1.7607
28.	9,12-Octadecadienoic acid (Z,Z)-	4.8	2.72	-	
29.	9,12-Octadecadienoic acid, ethyl ester	-	-	-	5.7952
30.	9-Octadecenamide, (Z)-	1.21	-	-	-
31.	9-Tricosene, (Z)-	6.38	-	-	-
32.	Adipic acid, isohexyl trans-2-methylcyclohexyl ester	1	-	-	-
33.	Benzene, 1,2-bis(1-buten-3-yl)-	3.25	-	-	-
34.	Bis(2-ethylhexyl) phthalate	-	15.05	13.4	-
35.	cis-13-Octadecenoic acid	2.16	-	-	-
36.	Creosol	-	-		0.8579
37.	Cyclo-(l-leucyl-l-phenylalanyl)	1.57	-	-	-
38.	Diethyldithiophosphinic acid				1.4821
39.	Dodecanamide	-	-	3.1	-
40.	d-Proline, N-isobutoxycarbonyl-, isohexyl ester	-	-	4.18	-

41.	Ethanol, 2,2'-oxybis-	-	-	-	2.535
42.	Ethyl 13-docosenoate(ethyl erucate)	-	-	-	0.8565
43.	Ethyl 9-hexadecenoate	-	-	-	4.176
44.	Ethyl Oleate	-	-	-	11.5415
45.	Ethyl tetracosanoate	-	-	-	0.7393
46.	Heptadecanoic acid, ethyl ester	-	-	-	0.8784
47.	Hexadecanamide	-	4	-	
48.	Hexadecanoic acid, ethyl ester	-	-	-	36.2259
49.	Hydroquinone	-	0.98	1.97	
50.	l-Valine, N-allyloxycarbonyl-, isobutyl ester	-	-	-	3.0647
51.	Methyl 19-methyl-eicosanoate	-	-	-	1.5853
52.	Naphthalene, 1,6-dimethyl-	-	3.05	-	-
53.	n-Decanoic acid	1.6	-	-	-
54.	n-Hexadecanoic acid	13.85	4.97	1.53	-
55.	o-Butyl O,O-diethyl phosphorothioate	-	-	-	1.2245
56.	Octadecanoic acid, ethyl ester	-	-	-	1.0598
57.	Octanamide, N,N-dimethyl-	-	-	2.17	-
58.	Palmitoleic acid	2.9	-	-	-
59.	p-Cresol	-	1.58	-	-
60.	Pentadecanal-	1.18	-	-	-
61.	Pentadecanoic acid, ethyl ester	-	-	-	0.8462
62.	Phenol	-	1.26	-	
63.	Phenol, 2,5-bis(1,1-dimethylethyl)-	-	-	-	1.7397
64.	Phenol, 3,5-bis(1-methylethyl)-, acetate	-	1.68	2.49	
65.	Phenol, 3,5-dimethoxy-	-	-	-	1.1835

66.	Phenol, 4-amino-	-	-	-	0.8914
67.	Phthalic acid, di(2-propylpentyl) ester	6.46	-	-	-
68.	p-Hydroxybiphenyl	-	5.11	-	-
69.	Pyrrolo[1,2-a]pyrazine-1,4-dione, hexahydro-3-(2-methylpropyl)-	-	-	-	1.2732
70.	Stigmast-4-en-3-one	-	-	5.8	-
71.	Stigmasta-5,24(28)-dien-3-ol, (3.beta.,24Z)-	6.48	12.31	4.37	-
72.	Stigmastan-3,5-diene	8.48	4.41	-	-
73.	Tetradecanoic acid, ethyl ester	-	-	-	6.6067
74.	trans-13-Octadecenoic acid	2.92	-	-	-
75.	Vitamin E	-	3.64	2.22	-

Table A-2: Chemical composition of *G. corticata* bio-oils as obtained from GC-MS analysis

Sr. no.	Compounds identified in Bio-oil	Area %						
		Water 260°C	Water 280°C	Water 300 °C	Ethanol	Methanol	Acetone	Ethanol -water
1.	1-(2-Pyrazinyl)-1-ethanol	-	-	-	-	-	1.7113	-
2.	1,1'-Biphenyl, 3-nitro-	-	-	-	1.3143	-	-	-
3.	1,2-Cyclopentanedione, 3-methyl-	0.8194	-	-	-	-	-	-
4.	1,4-Benzenediol, 2,5-dimethyl-	-		1.0335	-	-	-	-
5.	1,4-Benzenediol, 2-methyl-	-	1.3868	1.5171	-	-	-	-
6.	18-Nor-estra-1,3,5(10),9(11)-tetraen-12-one	-	1.4277	-	-	-	-	-
7.	1H-Imidazole, 1-methyl-4-nitro-	-	-	-	-	3.0561	-	-

8.	1H-Indole, 2,3-dimethyl-	-	-	0.8939	-	-	-	1.1523
9.	1H-Pyrrole, 2,3,4,5-tetramethyl-	-	-	1.5674	-	-	-	-
10.	1H-Pyrrole, 2,3,5-trimethyl-	-	-	-	-	-	1.2299	-
11.	1H-Pyrrole, 2-ethyl-3,4,5-trimethyl-	-	-	-	-	-	1.9138	-
12.	1H-Pyrrole-2,5-dione, 1-(4-methylphenyl)-	-	-		-	-	1.9021	-
13.	1-Phenethyl-pyrrolidin-2,4-dione	-	1.112	1.4897	-	-	-	-
14.	2(1H)-Pyridinone, 3-methyl-	-	1.0122	1.123	-	-	-	-
15.	2(1H)-Pyrimidinone, 4,6-diamino-	-	-	-	-	-	9.0266	-
16.	2,4-Difluorobenzoic acid, 3,5-difluophenyl ester	0.7472	-	-	-	-	-	-
17.	2,4-Difluorobenzoyl chloride	-	0.8822		-	-	-	-
18.	2,5-Difluorobenzoic acid, 3,5-dimethylphenyl ester	-	0.6879	-	-	-	-	-
19.	2,5-Piperazinedione, 3-(phenylmethyl)-	0.9525	2.1779	-	-	-	-	-
20.	2,5-Piperazinedione, 3,6-bis(2-methylpropyl)-	2.8754	-	-	-	-	-	-
21.	2,5-Piperazinedione, 3-benzyl-6-isopropyl-	5.3488	4.7945	3.0839	-	-	-	-
22.	2,6-Difluorobenzoic acid, 2-phenylethyl ester	-	1.2197	-	-	-	-	-
23.	2,7-Octadien-4-ol, 2-methyl-6-methylene-, (S)-	-	-	-	-	1.2916	-	-
24.	2-Amino-4,6-dihydroxypyrimidine			1.5248	-	-	-	-
25.	2-Butanone, 4-(5-methyl-2-furanyl)-	-	-	-	-	-	6.3534	-
26.	2-Buten-1-one, 3-amino-1-phenyl-	-	-	-	-	-	1.403	-
27.	2-Cyclohexen-1-	-	-	-	-	-	3.4372	-

	one, 3,5-dimethyl-							
28.	2-Cyclohexen-1-one, 4,4,5-trimethoxy-	-	-	-	-	1.0943	-	-
29.	2-Cyclopenten-1-one, 2-hydroxy-3-methyl-	-	-	-	-	1.5486	-	-
30.	2H-Indol-2-one, 3-ethyl-1,3-dihydro-1-methyl-	-	-	-	-	-	1.2538	-
31.	2-Pentadecanone, 6,10,14-trimethyl-	-	-	0.9752	-	-	1.651	2.5862
32.	2-Pentanol, 2,4-dimethyl-	-	-	-	1.3444	-	-	-
33.	2-Pentanone, 4-hydroxy-4-methyl-	6.2377	5.1638	5.0783	-	1.6162	6.2731	5.2982
34.	2-Pyrrolidinone, 1-methyl-	-	-	-	-	2.1542	-	-
35.	2-Tridecanone	-	-	-	1.2036	-	-	-
36.	3,4-Dihydropyridin-2-one-5-carboxylic acid	2.8064	-	-	-	-	-	-
37.	3,5-Difluoropropiophenone	-	-	1.3888	-	-	-	-
38.	3,6-Diisopropylpiperazin-2,5-dione	1.1534	1.293	0.6093	-	-	-	-
39.	3-Acetyl-1-methylpyrrole	-	-	-	-	-	2.9679	
40.	3-Buten-2-one, 4-(2-furanyl)-	-	-	-	-	-	6.6025	
41.	3-Ethyl-2,4-nonandione	1.141	1.5363	-	-	-	-	-
42.	3-Hydroxy-4-methoxybenzaldehyde, acetate	-	1.0159	-	-	-	-	-
43.	3-Iodopentanedioic acid, diethyl ester	3.3435	-	-	-	-	-	-
44.	3-Methoxybenzylamine	-	-	2.1936	-	-	-	-
45.	3-Penten-2-one, 4-	-	-	-	-	-	1.5832	7.3024
46.	3-Pyridinol	5.9794	8.516	10.5993	-	-		1.1637
47.	3-Pyridinol, 6-methyl-	13.5476	14.8477	1.1232	-	-	1.1853	2.1413

48.	4-Amino-2,3-xylenol	-	-	1.3189	-	-	-	-
49.	4-Hydroxy-6-methylhexahydropyrimidin-2-thione	-	-	1.5866	-	-	-	-
50.	4-Nitro-1H-pyrazole-3-carboxylic acid (2,4-difluoro-	-	-	2.0595	-	-	-	-
51.	4-Piperidinone, 1-(phenylmethyl)-, oxime	1.7783	1.4035	-	-	-	-	-
52.	4-Piperidinone, 2,2,6,6-tetramethyl-	-	-	-	-	-	2.1365	-
53.	4-Pyridinol, 2,6-dimethyl-	-	-	1.1177	-	-	-	-
54.	5-Ethylcyclopent-1-ene-1-carboxylic acid	1.7903	1.9968		-	-	-	-
55.	Adipic acid, 4-heptyl tetradecyl ester	-	-	1.5641	-	-	-	-
56.	Benzamide, N-4-piperidinyl-	-	-	2.8495	-	-	-	-
57.	Benzenamine, 4-methoxy-	-	-	0.7017	-	-	-	-
58.	Benzene, 1-(1,1-dimethylpropoxy)-4-methyl-	-	-	-	-	-	1.4612	-
59.	Benzene, 2-fluoro-1,3,5-trimethyl-	-	-	1.0007	-	-	-	-
60.	Benzeneacetic acid, methyl ester	-	-	-	-	1.3723	-	-
61.	Benzeneethanol, 3-hydroxy-	-	-	-	-	-	2.1552	-
62.	Benzenepropanoic acid, ethyl ester	-	-	-	1.548	-	-	1.7809
63.	Benzenepropanoic acid, methyl ester	-	-	-	-	2.1717	-	-
64.	Butanedioic acid, diethyl ester	-	-	-	2.9562	-	-	-
65.	Butanedioic acid, dimethyl ester	-	-	-	-	1.963	-	-
66.	Butanedioic acid, methyl-, dimethyl ester	-	-	-	-	1.1557	-	-
67.	Butylated Hydroxytoluene	5.7618	3.8588	6.9941	-	-	-	-
68.	Cholesta-3,5-diene	-	-	1.0259	-	-	-	-

69.	Cyclohexanone, 2-isopropyl-2,5-dimethyl-	-	-		-	-	1.3882	-
70.	Cyclohexanone, 3-(4-hydroxybutyl)-2-methyl-	-	-	1.5063	-	-	-	-
71.	Cyclopenta[c]pyrazol-3-amine, 2,4,5,6-tetrahydro-2-methyl-	0.6517	1.87	-	-	-	-	-
72.	Cyclopentane, 1,1,3-trimethyl-3-(2-methyl-2-propenyl)-	-	-	-	-	-	1.9252	-
73.	Diethyl 1,1-cyclopropanedicarboxylate	-	3.0943	-	-	-	-	-
74.	Diethyl isopropylphosphonate	-	0.9709	-	-	-	-	-
75.	Diethyldithiophosphinic acid	-	1.5253	-	-	-	-	-
76.	Diethyldithiophosphinic acid	2.7018	2.7195	1.5434	-	-	-	-
77.	Ethanone, 1-(1-methyl-1H-pyrrol-2-yl)-	-	-	-	-	1.9624	-	-
78.	Ethanone, 1-(2-hydroxy-5-methylphenyl)-	-	-	-	-	-	5.0323	-
79.	Ethanone, 1-(3,4-dimethoxyphenyl)-	-	-	1.2154		-	-	-
80.	Ethyl 13-methyl-tetradecanoate	-	-	-	2.0975	-	-	1.1807
81.	Ethyl Oleate	-	-	-	1.1112	-	-	-
82.	Glutaric acid, 4-chlorophenyl octyl ester	-	-	1.6672		-	-	-
83.	Heptadecane	-	-	-	1.2167	-	-	-
84.	Hex-5-enamide, N-(2-phenylethyl)-	-	-	1.5357	-	-	-	-
85.	Hexadecanoic acid, ethyl ester	-	-	1.2247	60.9352	2.031	10.587	38.3426
86.	Hexadecanoic acid, methyl ester	-	-	3.6159	2.9053	53.8233	-	5.4191
87.	Hydantoin, 1-butyl-	14.5041	-	-	-	-	-	-
88.	Hydroquinone	-	-	1.0534	-	-	-	-

89.	Imiprothrin	-	-	0.6136	-	-	-	-
90.	Isophorone	-	-	-	-	-	1.8237	-
91.	L-Alanine, N-methyl-N-(trifluoroacetyl)-, butyl ester	-	-	1.1645	-	-	-	-
92.	l-Isoleucine, N-allyloxycarbonyl-, heptyl ester	1.4859	-	-	-	-	-	-
93.	l-Leucine, N-allyloxycarbonyl-, undec-10-enyl ester	-	-	1.0298	-	-	-	-
94.	l-Norvaline, N-allyloxycarbonyl-, nonyl ester	-	-	9.1466	-	-	-	-
95.	l-Norvaline, n-propargyloxycarbonyl-, tetradecyl	-	1.7067	-	-	-	-	-
96.	l-Valine, N-allyloxycarbonyl-, dodecyl ester	-	14.7617	-	-	-	-	-
97.	Methanone, cyclobutyl-1H-imidazol-4-yl-	-	-	-	-	-	1.2822	-
98.	Methyl 19-methyl-eicosanoate	-	-	-	1.2261	-	-	-
99.	Methyl stearate	-	-	-	-	3.4255	-	-
100.	Methyl tetradecanoate	-	-	-	-	4.3405	-	-
101.	N,3-Diethyl-3-octanamine	2.8267	-	-	-	-	-	-
102.	N,N-Dimethyldodecanamide	-	-	0.7974	-	-	-	-
103.	N-[2-Hydroxyethyl]succinimide	-	-	1.0772	-	-	-	-
104.	N-Methoxy phenacetin	-	-	-	-	-	1.2609	-
105.	N-Methyl-1H-benzimidazol-2-amine	-	-	1.7648	-	-	-	-
106.	o-Butyl O,O-diethyl phosphorothioate	8.0987	2.0632	-	-	-	-	-
107.	o-Butyl O,O-diethyl phosphorothioate	2.2508	2.2115	-	-	-	-	-

108.	Octadecanoic acid, ethyl ester	-	-	-	4.8747	-	-	3.0182
109.	p-Cresol	-	-	1.6845	-	-	-	3.9534
110.	Pentadecane	-	-	-	-	-	2.2788	-
111.	Pentadecanoic acid, 14-methyl-, methyl ester	-	-	-	-	-	8.0184	-
112.	Pentadecanoic acid, methyl ester	-	-	-	-	2.1004	-	-
113.	Pentanedioic acid, diethyl ester	-	-	-	1.5738	-	-	-
114.	Pentanedioic acid, dimethyl ester	-	-	-	-	2.3844	-	-
115.	Pentanoic acid, 2-propenyl ester	-	-	-	-	2.1619	-	-
116.	Pentanoic acid, 4-oxo-, ethyl ester	-	-	-	1.297	-	-	-
117.	Pentanoic acid, 4-oxo-, methyl ester	-	-	-	-	3.5022	-	-
118.	Phenol	-	-	1.3204	-	-	-	1.7059
119.	Phenol, 2,4-bis(1,1-dimethylethyl)-	-	1.2777	-	-	-	-	2.9654
120.	Phenol, 2,4-bis(1,1-dimethylethyl)-	-	-	-	1.0879	-	-	-
121.	Phenol, 2,4-dimethyl-	-	-	-	-	1.3056	-	-
122.	Phenol, 2-ethyl-6-methyl-	-	-	-	-	1.4646	-	-
123.	Phenol, 2-methyl-	-	-	-	0.8353	-	-	1.187
124.	Phenol, 3,5-dimethoxy	0.8776	1.0439	-	-	-	-	-
125.	Phenol, 3,5-dimethoxy-, acetate	1.5403	-	-	-	-	-	-
126.	Phenol, 3,5-dimethyl	-	-	-	-	-	1.9468	-
127.	Phenol, 4-(ethylamino)-	-	-	0.8921	-	-	-	-
128.	Phenol, 4-amino-	0.725	0.841	-	-	-	-	-
129.	Phenol, 4-ethyl-	-	-	0.7986	-	-	-	1.3224
130.	Piperazine-1-carboxamide, 4-(4-	-	3.4173	-	-	-	-	-
131.	Pipradrol	-	-	-	-	1.1771	-	-
132.	Pyridine, 2,4,6-trimethyl-	-	-	-	-	-	5.9298	-

133.	Pyridine, 2,4-dimethyl-	-	-	-	-	-	2.2997	-
134.	Pyridine, 3-methoxy-	-	-	-	-	1.613	-	-
135.	Pyrido[3,4-d]pyrimidin-4(3H)-one, 2,6,8-trimethyl-	-	-	-	-	-	1.979	-
136.	Pyrrolo[1,2-a]pyrazine-1,4-dione, hexahydro-3-(2-	-	2.5092	1.8742	-	-	-	-
137.	Pyrrolo[1,2-a]pyrazine-1,4-dione, hexahydro-3-(2-methylpropyl)-	2.4891	-	-	-	-	-	-
138.	Pyrrolo[1,2-a]pyrazine-1,4-dione, hexahydro-3-(phenylmethyl)-	1.355	-	-	-	-	-	-
139.	Ribitol, 1,3:4,5-di-O-(ethylboranediyl)-2-	-	-	-	-	1.2846	-	-
140.	Safrole	-	-	0.9722	-	-	-	-
141.	Tetradecanamide	-	-	4.2665	-	-	-	-
142.	Tetradecanoic acid, ethyl ester	-	-	-	6.5616	-	-	3.6557

Table A-3: Chemical composition of *U. fasciata* bio-oils as obtained from GC-MS analysis.

Sr. no.	Compounds identified in Bio-oil	Area %						
		Water 260°C	Water 260°C	Water 260°C	Ethanol	Methanol	Acetone	Ethanol-water
1.	(2-Cyclohexyl-ethyl)-(1-methyl-pentyl)-amine	0.9914	-	-	-	-	-	-
2.	(4-Methyl-6-phenyl-pyrimidin-2-yl)-(4,6,7-trimethyl-quinazolin-2-yl)-amine	-	-	-	-	-	1.0094	-
3.	(S)-6,6-Dimethyl-2-azaspiro[4.4]non-1-ene	-	-	-	-	-	1.1705	-
4.	(S)-6,6-Dimethyl-2-azaspiro[4.4]non-1-ene	-	-	-	1.2591	-	-	-

5.	1,2-Benzenediamine, 4-methyl-	-	-	-	-	-	0.9899	-
6.	1,3-Bis(trimethylsiloxy)benzene		1.016	0.9822	-	-	-	-
7.	1,3-Dimethyl-3,4,5,6-tetrahydro-2(1H)-pyrimidinone	2.1297	-	-	-	-	1.6438	1.2784
8.	1,3-Dimethyl-6-phenylpiperidin-4-one	-		0.9744	-	-	-	-
9.	1,4-Benzenediol, 2-methyl-	-	1.0953	1.3877	-	-	-	-
10.	10-Methyldodecan-4-olide	-				1.6879		
11.	1H-Pyrazole, 1,3,5-trimethyl-	-	1.7849	1.1184	-	-	-	-
12.	1-Methoxy-1,4-cyclohexadiene	2.0299			-	-	-	-
13.	1-Octanamine, N-methyl-N-octyl-	0.9732			-	-	-	-
14.	1-Phenethyl-pyrrolidin-2,4-dione	0.7935	1.1378		-	-	-	-
15.	1-Propanone, 1-(2,4-dimethylphenyl)-2-(1-	-	-	-	-	1.1651	-	-
16.	2(1H)-Quinolinone, 3,4-dimethyl-	-	-	-	-	-	1.528	
17.	2,3-Dimethylhydroquinone	0.8773	-	-	-	-	-	-
18.	2,5-Piperazinedione, 3,6-bis(2-methylpropyl)-	2.6012		1.3369	-	-	-	-
19.	2,5-Piperazinedione, 3,6-bis(2-methylpropyl)-	-	1.5145	1.0886	-	-	-	-
20.	2,5-Piperazinedione, 3-benzyl-6-isopropyl-	-	2.9578	1.0376	-	-	-	0.6408
21.	2,5-Pyrrolidinedione, 1-methyl-	-	-	-	-	1.3806		
22.	2-Benzimidazolinethione, hexahydro-	-	-	-	-	-	3.3077	4.0193
23.	2-Butanone, 4-(5-methyl-2-furanyl)-	-	-	-	-	-	2.859	
24.	2-Cyclopenten-1-one, 2-hydroxy-3-methyl-	-	1.0445	1.1248		0.8514		1.34
25.	2-Hexadecene, 3,7,11,15-tetramethyl-, [R-[R*,R*-(E)]]-	-	-	-	0.9148	-	-	-
26.	2-Hexadecene, 3,7,11,15-tetramethyl-, [R-[R*,R*-(E)]]-	-	-	-	1.1802	-	-	-
27.	2-Hexadecenoic acid, methyl ester, (E)-	-	-	-	-	1.1789	-	

28.	2H-Naphtho[1,8-bc]furan-2-one	-	-	6.939	-	-	-	-
29.	2H-Naphtho[1,8-bc]furan-2-one	1.195	-		-	-	-	-
30.	2-Pentanone, 4-hydroxy-4-methyl-	12.9998	0.7706	1.0584	-	0.8613	2.903	2.3251
31.	3,3-Diethoxy-2,3-dihydro-1H-pyrrole-4-carboxylic acid	-	4.2839		-	-	-	-
32.	3,4-Difluoropropiophenone		1.175		-	-	-	-
33.	3,6-Diisopropylpiperazin-2,5-dione	2.5045	1.0347	0.9687	-	-	-	-
34.	3,6-Diisopropylpiperazin-2,5-dione	-	12.0492	7.3994	-			0.8471
35.	3-Buten-2-one, 4-(2-furanyl)-	-			-	-	3.2913	
36.	3-Ethyl-2,4-nonandione	-	1.1245	0.9487	-	-	-	-
37.	3H-1,4-Benzodiazepin-2,5(1H,4H)-dione	-	0.9823	-	-	-	-	-
38.	3-Methoxybenzyl alcohol	1.0079	-	-	-	-	-	-
39.	3-Pyridinol	-	16.571	17.0942	0.8207		15.1669	20.7286
40.	3-Pyridinol, 2,6-dimethyl-	-			-	1.1324		-
41.	3-Pyridinol, 6-methyl-	-	4.031	5.1304	-	-	2.8673	-
42.	4-Hydroxy-3-methylacetophenone	-	-	-	-	-	10.9471	-
43.	5'-Iod-uridine	-	-	0.9598	-	-	-	-
44.	5-Isopropylidene-3,3-dimethyl-dihydrofuran-2-one	-	-	1.5927	-	-	-	-
45.	5-Methyl-2-pyrazinylmethanol	-	-	-	-		1.266	-
46.	7-Octadecenoic acid, methyl ester	-	-	-	-	3.1357	-	-
47.	9-Octadecene, 1,1-dimethoxy-, (Z)-	1.0302	-	-	-		-	-
48.	9-Octadecenoic acid, methyl ester, (E)-	-	-	-	-	12.4399	-	-
49.	Acetamide, N-(5,8-dihydro-1-naphthalenyl)-	-	-	-	-	-	3.1889	-
50.	Benzenamine, 4-methoxy-	-	-	-	-	-	2.0822	-
51.	Benzene, (1,1-dimethylethoxy)-	-	-	-	-	-	1.3705	-

52.	Benzene, (4-methyl-4-pentenyl)-	-		1.5036	-	-	-	-
53.	Benzenemethanol, 4-methoxy-	-	1.3801		-	-	-	-
54.	Butylated Hydroxytoluene	7.835	7.6296	7.0507	-	-	-	-
55.	Cycloheptasiloxane, tetradecamethyl-	1.0708	-	-	-	-	-	-
56.	Cyclohex-2-enone, 3-(N',N'-dimethylhydrazino)-	1.7556	-	-	-	-	-	-
57.	Cyclohexanone, 2,5-dimethyl-2-(1-methylethenyl)-	-	-	-	-	-	-	-
58.	Cyclohexasiloxane, dodecamethyl-	1.0248	-	-	-	-	-	-
59.	Cyclopentanone, 2-(1-methylpropyl)-		-	-	1.8677		-	-
60.	Cyclopentasiloxane, decamethyl-	1.5699	-	-			-	-
61.	Diethyl 1,1-cyclopropanedicarboxylate		1.8949	-	-	-	-	-
62.	Diethyldithiophosphinic acid	2.1835		-	-	-	-	-
63.	Diethyldithiophosphinic acid	-	2.3484	-	-	-	0.5816	1.7292
64.	Docosane	-	-	1.0669	-	-	-	-
65.	Docosanoic acid, methyl ester	-	-	-	-	5.6222	-	-
66.	Ethanol, 2,2'-oxybis-	-	1.6511	0.8156	-	-	-	-
67.	Ethanone, 1-(1-methyl-1H-pyrrol-2-yl)-	-	1.0233	-	-	-	-	-
68.	Ethoxycyclohexyldimethyl silane	-	-	-	-	-	1.2202	
69.	Ethyl Oleate	-	-	-	11.1813	-	1.7956	4.3647
70.	Heneicosane	-	-	2.6212		-	-	-
71.	Heptadecanoic acid, ethyl ester	-	-	-	1.4801	-	-	-
72.	Heptadecene	-	-	-	2.0089	0.9524	0.9716	-
73.	Hexacosane	-	-	4.3022	-	-	-	-
74.	Hexadecane, 2,6,10,14-tetramethyl-	-	-	2.5389	-	-	-	-
75.	Hexadecanoic acid, ethyl ester	5.7687	2.0861		57.2586	3.6344	16.1452	17.8786
76.	Hexadecanoic acid, methyl	0.7287			1.0604	55.1609	2.8281	-

	ester							
77.	Hydroquinone	-	1.857	2.4762	-	-	-	-
78.	l-Proline, N-allyloxycarbonyl-, heptyl ester	-	1.1819		-	-	-	1.157
79.	l-Proline, N-propoxycarbonyl-, butyl ester	-	1.9059		-	-	-	-
80.	l-Proline, N-propoxycarbonyl-, heptyl ester	-	-	0.9713	-	-	-	-
81.	l-Proline, N-propoxycarbonyl-, pentyl ester	4.0186	-	-	-	-	-	-
82.	l-Valine, N-allyloxycarbonyl-, propyl ester	16.3728	-	-	-	-	-	-
83.	Metaraminol	0.8547	-	-	-	-	-	-
84.	m-Menth-1(7)-ene, (R)-(-)-	-	-	-	-	1.592		
85.	N,3-Diethyl-3-nonanamine	7.6442	-	-	-	-	-	-
86.	N-[2-Hydroxyethyl]succinimide	-	-	1.1648	-	-	-	-
87.	N-Aminopyrrolidine	-	-	-	-	-	0.9093	
88.	Naphthalene, 1,6-dimethyl-	2.0701		-	-	-	-	-
89.	N-Ethyl-5-propyl-5-nonanamine	-	-	2.689	-		-	-
90.	Nonanedioic acid, dimethyl ester	-	-	-	-	1.72112	-	-
91.	o-Butyl O,O-diethyl phosphorothioate	-	7.0069	-	-	-	-	1.3323
92.	Octacosane	-	-	1.4589	-	-	-	-
93.	Octadecanamide	-	-	-	-	-	1.3212	-
94.	Octadecanoic acid, ethyl ester	-	-	-	4.3142	-	1.2107	1.8091
95.	Octanedioic acid, dimethyl ester	-	-	-	-	0.9144	-	-
96.	p-Cresol	-	0.8064	1.09	1.1642	-	2.4643	-
97.	Pentacosane	-		4.6802		-	-	-
98.	Pentadecanenitrile	-	-	-	1.5212	-	1.4224	-
99.	Pentadecanoic acid, ethyl ester	-	-	-	1.3812	-	-	-

100.	Pentadecanoic acid, methyl ester	-	-	-	-	2.3751	-	-
101.	Pentane, 3-(bromomethyl)-	-	-	-	-	1.1058	-	-
102.	Phenol	-	-	0.9103	-	-	0.9103	
103.	Phenol, 2,4-bis(1,1-dimethylethyl)-	3.1986	0.5425		1.3761	-	-	2.1931
104.	Phenol, 3,5-dimethoxy-	-	-	0.8315	-	-	-	-
105.	Phenol, 4-(methylamino)-	-	-	1.2021	-	-	-	-
106.	Phenol, 4-amino-	-	1.0369	0.6021	-	-	-	2.9667
107.	Phenol, 4-ethyl-	-	-		-	-	0.9814	-
108.	p-Hydroxybiphenyl	-	-	0.8981	-	-	-	-
109.	Pyridine, 2-methyl-5-phenyl-	-	0.9522	-	-	-	-	-
110.	Pyrrolidine, 2-butyl-1-methyl-	-		-	-	-	1.5489	-
111.	Pyrrolo[1,2-a]pyrazine-1,4-dione, hexahydro-3-(2-methylpropyl)-	2.3485	2.3577	-	-	-	-	1.3627
112.	Quinoline, 4-methyl-	-	1.1508	-	-	-	-	-
113.	Succinic acid, ethyl 2-hexyl ester	-	-	-	0.712	-	-	-
114.	t-Butylhydroquinone	1.0505	-	-	-	-	-	-
115.	Tetracosane	-	-	4.1479	-	-	-	-
116.	Tetradecanoic acid, ethyl ester	-	-	-	2.5201	-	-	-
117.	Tetradecanoic acid, methyl ester	-	-	-	-	1.3879	-	1.6482
118.	Undecyl (E)-2-methylbut-2-enoate	-	-	-	-	-	0.8346	-
119.	Urea, 1-(butoxycarbonyl)-3-(5-methylpyrid-2-yl)-	-	-	-	-	-	2.3581	-

Appendix B

This appendix consists of Biodiesel Standards that were referenced in the previous chapters.

Table B-1: ASTM D6751 (United States): Standard Specification for Biodiesel (B100) Blend Stock for Distillate Fuels.

SPECIFICATION FOR BIODIESEL (B100) -ASTM D6751-11a

[#]Biodiesel (B100) and the petroleum diesel must meet their respective ASTM specifications before blending.

Property	**ASTM Method**	**Limits**	**Units**
Calcium & Magnesium, combined	EN 14538	5 maximum	ppm (µg/g)
Flash Point (closed cup)	**D 93**	**93 minimum**	°C
Alcohol Control (one to be met)			
1. Methanol Content	EN 14110	0.2 maximum	mass %
2. Flash Point	D93	130 minimum	°C
Water & Sediment	**D 2709**	**0.05 maximum**	**% vol.**
Kinematic Viscosity, 40 C	D 445	1.9 – 6.0	$mm^2/sec.$
Sulfated Ash	D 874	0.02 maximum	% mass
Sulfur **S 15 Grade** **S 500 Grade**	 **D 5453** **D 5453**	 **0.0015 max. (15)** **0.05 max. (500)**	 **% mass (ppm)** **% mass (ppm)**
Copper Strip Corrosion	D 130	No. 3 maximum	
Cetane	D 613	47 minimum	
Cloud Point	**D 2500**	**report**	°C

Carbon Residue 100% sample	D 4530*	0.05 maximum	% mass
Acid Number	**D 664**	**0.5 maximum**	**mg KOH/g**
Free Glycerin	**D 6584**	**0.020 maximum**	**% mass**
Total Glycerin	**D 6584**	**0.240 maximum**	**% mass**
Phosphorus Content	D 4951	0.001 maximum	% mass
Distillation	D 1160	360 maximum	°C
Sodium/Potassium, combined	EN 14538	5 maximum	ppm (µg/g)
Oxidation Stability	**EN 15751**	3 minimum	**hours**
Cold Soak Filtration **For use in temperatures below -12 °C**	**D7501** **D7501**	**360 maximum** **200 maximum**	**seconds** **seconds**

(Source:https://www.ag.ndsu.edu/agmachinery/documents/pdf/biodiesel%20specifications%203-2007.pdf).

BOLD = BQ-9000 <u>Critical Specification Testing</u> Once <u>Production Process Under Control</u>

* The carbon residue shall be run on the 100% sample.

\# A considerable amount of experience exists in the US with a 20% blend of biodiesel with 80% diesel fuel (B20). Although biodiesel (B100) can be used, blends of over 20% biodiesel with diesel fuel should be evaluated on a case-by-case basis until further experience is available.

Table B-2: EN 14214 (Europe): Automotive Fuels: FAME for Diesel Engines. Requirements and Test Methods (Van Gerpen et al., 2004)**.**

Property	Test method	Limits		Unit
		min	max	
Ester content	EN 14103	96.5	–	% (m/m)
Density at 15°C	EN ISO 3675, EN ISO 12185	860	900	kg/m3
Viscosity at 40°C	EN ISO 3104, ISO 3105	3.5	5.0	mm2/s
Flash point	EN ISO 3679	120	–	°C
Sulfur content	EN ISO 20846, EN ISO 20884	–	10.0	mg/kg
Carbon residue (in 10% dist. residue)	EN ISO 10370	–	0.30	% (m/m)
Cetane number	EN ISO 5165	5 1	–	–
Sulfated ash	ISO 3987	–	0.02	% (m/m)
Water content	EN ISO 12937	–	500	mg/kg
Total contamination	EN 12662	–	24	mg/kg
Copper strip corrosion (3 hours, 50°C)	EN ISO 2160	–	1	class
Oxidative stability, 110°C	EN 14112	6.0	–	hours
Acid value	EN 14104	–	0.50	mg KOH/g
Iodine value	EN 14111	–	120	g I/100 g
Linolenic acid content	EN 14103	–	12	% (m/m)
Content of FAME with ≥4 double bonds		–	1	% (m/m)
Methanol content	EN 14110	–	0.20	% (m/m)
Monoglyceride content	EN 14105	–	0.80	% (m/m)
Diglyceride content	EN 14105	–	0.20	% (m/m)
Triglyceride content	EN 14105	–	0.20	% (m/m)
Free glycerine	EN 14105; EN 14106	–	0.02	% (m/m)
Total glycerine	EN 14105	–	0.25	% (m/m)
Alkali metals (Na + K)	EN 14108; EN 14109	–	5.0	mg/kg
Earth alkali metals (Ca + Mg)	EN 14538	–	5.0	mg/kg
Phosphorus content	EN 14107	–	10.0	mg/kg

Table B-3: BIS IS 15607:2005: Biodiesel standard India, Requirements and Test Methods (Barabas & Todoruţ, 2010).

Property	Test method	Limits min	Limits max	Units
Density at 15ºC	ISO 3675 /P 32	860	900	kg/m3
Kinematic viscosity at 40ºC	ISO 3104 / P25	2.5	6.0	mm2/s
Flash point (closed cup)	P21	120	–	ºC
Sulphur	D5443/P83	–	50	mg/kg
Carbon resiue (Ramsbottom)	D4530	–	0.05	% (m/m)
Sulfated ash	ISO 6245/P4	–	0.02	% (m/m)
Water content	D2709 / P40	–	500	mg/kg
Total contamination	EN 12662	–	24	mg/kg
Copper corrosion 3 hr at 50ºC	ISO 2160 / P15	–	1	–
Cetane number	ISO 5156/ P9	51	–	–
Acid value	P1	–	0.50	mg KOH/g
Methanol	EN 14110	–	0.20	% (m/m)
Ethanol		–	0.20	% (m/m)
Ester content	EN 14103	–	96.5	% (m/m)
Free glycerol, max	D6584	–	0.02	% (m/m)
Total glycerol, max	D6584	–	0.25	% (m/m)m
Phosphorous, max	D 4951	–	10.0	mg/kg
Sodium and potassium	EN 14108	To report		mg/kg
Calcium and magnesium	–	To report		mg/kg
Iodine value	EN 14104	To report		–
Oxidation stability at 110ºC	EN 14112	6	–	hours

Table B-4: ASTM D975-97: Requirements for Diesel Fuel (Van Gerpen et al., 2004).

Grade Property	Grade LS #1	Grade LS #2	Grade No. 1-D	Grade No. 2-D	Grade No. 4-D
Flash point °C, min	38	52	38	52	55
Water and sediment, % vol, max.	0.05	0.05	0.05	0.05	0.50
Distillation temp., °C, 90%					
Min.	--	282	--	282	--
Max.	288	338	288	338	--
Kinematic Viscosity, mm^2/s at 40°C					
Min.	1.3	1.9	1.3	1.9	5.5
Max.	2.4	4.1	2.4	4.1	24.0
Ramsbottom carbon residue, on 10%, %mass, max.	0.15	0.35	0.15	0.35	--
Ash, % mass, max.	0.01	0.01	0.01	0.01	0.10
Sulfur, % mass, max	0.05	0.05	0.50	0.50	2.00
Copper strip corrosion, Max 3 hours at 50°C	No. 3	No. 3	No. 3	No. 3	--
Cetane Number, min.	40	40	40	40	30
One of the following Properties must be met:					
(1) cetane index	40	40	--	--	--
(2) Aromaticity, % vol, max	35	35	--	--	--
Cloud point, °C, max.	Determined by local climate Should be 6°C higher than the tenth percentile minimum ambient temperature for the region. For Iowa:				

Month	10th % minimum temp
Oct	-2°C
Nov	-13
Dec	-23
Jan	-26
Feb	-22
Mar	-16

Frequently used Abbreviations

ANOVA	Analysis of Variance
ASTM	American Standard Test Method
BHT	Butylated hydroxytoluene
BIS	Bureau of Indian Standard (BIS)
CFPP	Cold filter plugging point
CM	*Chaetomorpha media*
CM	Chloroform: methanol (1:2)
CN	Cetane number
CNG	Compressed natural gas
CP	Cloud point
DMSO	Dimethyl sulfoxide
DTG	Differential thermogravimetry
EF	*Enteromorpha flexuosa*
EN14214	European Standard 14214
EPA	Environmental Protection Agency
FAME	Fatty Acid Methyl Ester
FA	Fatty acid
FFA	Free Fatty Acid
Fm^{-1}	Farads per meter
FTIR	Fourier Transform-Infrared (FT-IR) spectroscopy
GC	*Gracilaria corticata*
GC-MS	Gas Chromatography-Mass Spectrometry
GHG	Greenhouse gases
H	n-Hexane

HD	1% diethyl ether and 10% methylene chloride in n-hexane
HHV	Higher heating value
HI	Hexane: isopropanol (3:2)
HMA	Hexane: methanol: acetone (3:1:1)
HTL	Hydrothermal liquefaction
KV	Kinematic Viscosity
MC	Moisture Content
MPa	Mega pascal
MUFA	Monounsaturated fatty acids
NMR	^{1}H Nuclear Magnetic Resonance Spectroscopy
PT	*Padina tetrastromatica*
PUFAs	Polyunsaturated fatty acids
SD	Standard deviation
SFAs	Saturated fatty acids
SFE	Supercritical fluid extraction
SPV	Sulfo-phospho-vanillin
ST	*Sargassum tenerrimum*
StM	*Stoechospermum marginatum*
SV	Saponification value
TAGs	Triacylglycerols
TCC	Thermochemical conversion
TGA	Thermogravimetric analysis
TN	Total Nitrogen
TOC	Total organic carbon
UF	*Ulva fasciata*
XRD	X-ray diffraction

PUBLICATIONS

Manuscripts published in peer-reviewed journals:

1. Biswas, B., **Fernandes, A.C.**, Kumar, J., Muraleedharan, U.D. & Bhaskar, T. (2018). Valorization of *Sargassum tenerrimum:* Value addition using hydrothermal liquefaction. Fuel, 222: 394 - 401.

2. Biswas, B., Kumar, A., **Fernandes, A. C.,** Saini, K., Negi, S., Muraleedharan, U. D. & Bhaskar, T. (2020). Solid base catalytic hydrothermal liquefaction of macroalgae: Effects of process parameter on product yield and characterization. Bioresour. Technol., 307: 123232.

Manuscript communicated:

1. **Fernandes, A. C.,** Biswas, B., Kumar, J, Bhaskar, T. & Muraleedharan, U.D. Hydrothermal liquefaction of *Gracilaria corticata*: Effect of reaction parameters on product yields. (submitted to: Bioresource Technology Reports).

Manuscripts under preparation:

1. Simple fluorescence and colorimetric procedures enable rapid screening for macroalgal bio-oil sources. (**Fernandes, A. C.** & Muraleedharan, U.D.)
2. Studies on crude lipid extraction methods from marine macroalgae for biodiesel production. (**Fernandes, A. C.** & Muraleedharan, U.D.)
3. Hydrothermal liquefaction of a marine macroalga *Ulva fasciata* for biofuel production. (**Fernandes, A. C.,** Biswas, B., Kumar, J, Bhaskar, T. & Muraleedharan, U. D.)

Posters presented/accepted at conferences:

1. **Fernandes, A.C**. & Muraleedharan, U.D., *"Macroalgae for Biodiesel?"*. Poster presented at the ***International Conference on New Horizons in Biotechnology (NHBT - 2015)***,Trivandrum, Kerala. 22nd - 25th November 2015.

2. **Fernandes, A.C.** & Muraleedharan, U.D., "*A Rapid and Effective Screening Strategy Assisting the Selection of Macroalgae with Potential for Biodiesel Production".* Poster presented at the ***International Conference on Algal Technologies***, Jalandhar, Punjab. 14th - 16th July 2016. (Awarded 2nd place).

3. **Fernandes, A.C.** & Muraleedharan, U.D., "*Macroalgal Lipids that Favour Biodiesel Production: Extraction Protocols for Maximization of Yield".* Poster accepted for presentation at ***The 8th International Conference on Algal Biomass, Biofuels and Bioproducts*** (https://www.elsevier.com/)**,** Seattle, USA, 11th - 13th June 2018.

Fuel 222 (2018) 394–401

Contents lists available at ScienceDirect

Fuel

journal homepage: www.elsevier.com/locate/fuel

Full Length Article

Valorization of *Sargassum tenerrimum*: Value addition using hydrothermal liquefaction

Bijoy Biswas[a,b], Alisha C. Fernandes[c], Jitendra Kumar[a], Usha D. Muraleedharan[c], Thallada Bhaskar[a,b,*]

[a] Thermo-catalytic Processes Area(TPA), Bio-Fuels Division (BFD), CSIR-Indian Institute of Petroleum (IIP), Dehradun 248005, India
[b] Academy of Scientific and Innovative Research (AcSIR), New Delhi, India
[c] Department of Biotechnology, Goa University, Goa – 403206, India

ARTICLE INFO

Keywords:
Sargassum tenerrimum algae
Hydrothermal liquefaction
Bio-oil
Bio-residue

ABSTRACT

Sargassum tenerrimum has been used for the production of bio-oil by hydrothermal liquefaction in water sub-critical conditions at a temperature range of 260–300 °C for reaction time 15 min. Maximum bio-oil (16.3 wt%) was obtained at 280 °C and maximum conversion was observed (75.8 wt%) at 300 °C. The solid residue yields decreased continuously from 61.2 wt% to 24.2 wt% as the temperature increased from 260 to 300 °C. The liquid products obtained upon hydrothermal liquefaction were characterized with the help of ^{1}H NMR, GC–MS and FT-IR techniques and bio-residue using FT-IR and XRD. Analysis of bio-oil showed that their components and functional structure of bio-oils were greatly distinguished and consisted of many compounds including phenols, ketones, aldehydes, acid, esters, alcohols, nitrogen-containing compounds, and hydrocarbons. From the GC–MS analysis it has been seen that, organic acid content in the bio-oils were decreased with the increasing temperature from 260 to 300 °C. The band at 1083 cm^{-1} only appeared in the absorption profile of *S. tenerrimum* feed, which could be C-O connected with hydroxyl groups and were dehydrated after liquefaction. All the bio-oils showed higher percentages of aliphatic protons in the spectral region from 0.5 to 3.0 ppm. The analysis of bio-residue obtained at various temperatures showed typical amorphous nature that indicated richness of carbon content in the residue.

1. Introduction

Energy plays a crucial role in the economic growth and development of modern industrial society. Nevertheless, energy crisis and environmental concerns have become increasingly serious due to utilization of the limited fossil fuel [1]. To ensure energy safety and to reduce environmental problems, accelerating the development and utilization of clean and renewable energy sources has gained increasing attention over the past decades [2]. Biomass has been recognized as a renewable energy source that can be used to replace fossil fuels and absorb CO_2 from the atmosphere, reducing the greenhouse effect [3].

Biomass is currently regarded as the fourth largest primary energy source in the world, followed by coal, petroleum and natural gas [4]. As an energy source, it has been considered a potential substitute for fossil fuels because of its abundant capital, large distribution and being carbon neutral. Biomass can be classified basically into first, second and third generation categories according to the difference in raw materials obtained from the different sources [5]. Generally, first and second generation biomass is produced from food crops such as corn, cassava and soybean and non-food crops such as rape straw, pine sawdust, etc. [6]. While these have a competition with food crops and land resources, the third generation aquatic biomass shows attractive promise by saving arable lands and stabilizing effective food supplies. Aquatic biomass is one of the most abundant sources of renewable energy and will be an important part of a more sustainable future energy system [7].

For producing biofuels from biomass, thermochemical methods such as gasification, pyrolysis and hydrothermal liquefaction (HTL) have been employed, of which hydrothermal liquefaction most commonly is used for wet biomass [8]. Hydrothermal liquefaction is a potential conversion route for biomass with high water content into bio-oil and produces liquid bio-crude through treatment of biomass at high pressures of 50–200 atm and temperatures of 250–400 °C [9]. This method exploits the properties of superheated fluids to reduce mass transfer resistances [10]. The high pressure also enables higher penetration of solvent into the biomass structure to facilitate fragmentation

* Corresponding author at: Thermo-catalytic Processes Area(TPA), Bio-Fuels Division (BFD), CSIR-Indian Institute of Petroleum (IIP), Dehradun – 248005, India.
E-mail address: tbhaskar@iip.res.in (T. Bhaskar).

https://doi.org/10.1016/j.fuel.2018.02.153
Received 11 October 2017; Received in revised form 8 January 2018; Accepted 22 February 2018

of biomass molecules [11]. The nature of the process allows for feedstock with high moisture content and therefore a wide range of material can be subjected to HTL to produce bio-crude. It is therefore the most promising technique for producing biofuels from wet biomass, having a lower reaction temperature and higher energy efficiency than the pyrolysis process since energy-intensive drying and dewatering steps are not imperative.

In the HTL procedure, water simultaneously acts as reactant and catalyst, making the process significantly different from pyrolysis. At conditions close to the critical point, water has several very interesting properties such as low viscosity and high solubility of organic substances, which make subcritical water an excellent medium for fast, homogeneous and efficient reactions [12,13,5]. Subcritical water behaves very differently from supercritical water. The dielectric constant decreases from 78 Fm^{-1} at 25 °C and 0.1 MPa to 14.07 Fm^{-1} at 350 °C and 20 MPa [14]. This gives rise to increased solubility of hydrophobic organic compounds such as free fatty acids [15]. The ionic product of water (K_W) is relatively high in the subcritical range (10^{-12}, compared to 10^{-14} at ambient conditions). The high levels of H^+ and OH^- under subcritical conditions mean that many acid or base catalyzed reactions such as biomass hydrolysis are accelerated [16]. Furthermore, the density of subcritical water falls in the range between those of ambient and supercritical conditions. Despite the high-temperature, the compressibility is still rather low. The relatively high density combined with the high dissociation constant of subcritical water favors ionic reactions [5].

Many researchers have been focusing on bio-oil production from aquatic biomass algae *via* the HTL process [8,17–25]. Shaobo et al., were investigated the production of crude bio-oils from three laboratory cultivated and two commercial grade algal biomass sources via hydrothermal liquefaction (HTL) process [21]. The HTL reaction was carried out at temperature ranging from 260 °C to 340 °C and residence time 10–40 min. The bio-oil yields were between 28 and 41%. The highest yield of 41.2% was obtained at 300 °C with 20 min. residence time. The generated crude bio-oils have similar qualities as compared to those derived from commercial algae. The bio-oils were composed mainly of aliphatic compounds (fatty acids, alkanes) which can be readily upgraded and refined into value added transportation fuels (e.g., renewable diesel). Barreiro et al., were liquefied as raw biomass (RA), after extracting lipids (LEA) and after extracting proteins (PEA) in micro-autoclave experiments at different temperatures (300–375 °C) for 5 and 15 min [22]. The results indicate that extracting the proteins from the microalgae prior to HTL may be interesting to improve the economics of the process while at the same time reducing the nitrogen content of the bio-crude oil. A complete set of experiments was carried out at a reaction time of 15 min for RA, LEA and PEA, varying the reaction temperature from 300 to 375 °C. They showed the product yields after HTL for each feedstock and temperature used, as well as the elemental composition and high heating value of the bio-crude oil produced. Most of the organic mass from the feedstock was converted into bio-crude oil, with yields varying from 51.2 ± 3.4 to 69.2 ± 1.9 wt%. Raikova et al. [23] were study to bridge the gaps between previous accounts of macroalgal HTL by carrying out a more comprehensive screen of a number of species from all three major macroalgae classes, and examining the correlations between biomass biochemical composition and HTL reactivity. HTL was used to process thirteen South West UK macroalgae species from all three major classes (Chlorophyceae, Heterokontophyceae and Rhodophyceae) to produce bio-crude oil, a bio-char, gas and aqueous phase products. The reaction was carried out at temperature 345 °C. The highest overall bio-crude yields were obtained for the two macroalgae of the genus Ulva (28.8% and 29.9% for U. intestinalis and U. lactuca, respectively), although the third Chlorophyta R. riparium performed significantly worse, yielding a modest 15.0% bio-crude product. L. digitata and L. hyperborean yielded 16.4% and 9.8% bio-crude. Parsa et al., were carried out hydrothermal liquefaction of Gracilaria gracilis (G. gracilis) and Cladophora glomerata (C. glomerata) macro-algae species harvested from Caspian Sea for bio-crude oil production at temperature 350 °C and 15 min [24]. The bio-crude yield for G. gracilis and C. glomerata was 15.7 and 16.9 wt%, respectively with higher heating value (HHV) of 36.01 and 33.06 MJ/kg. Shakya et al., were performed a Hydrothermal liquefaction (HTL) of nine algae species at two reaction temperatures (280 and 320 °C) to compare the effect of their biomass composition on product yields and properties [25]. Results obtained after HTL indicate large variations in terms of bio-oil yields and its properties. The maximum bio-oil yield (66 wt%) was obtained at 320 °C with a high lipid containing algae Nannochloropsis. The higher heating value of bio-oils ranged from 31 to 36 MJ/kg and around 50% of the bio-oils was in the vacuum gas oil range while high lipid containing algae Nannochloropsis contained a significant portion (33–42%) in the diesel range. A predictive relationship between bio-oil yields and biochemical compositions was developed and showed a broad agreement between predictive and experimental yields. Through these studies, it was found that both the yield and the quality of bio-oil resulting from the HTL process were highly associated with the operating parameters such as reaction temperature, retention time, ratio of feedstock and solvent. HTL is more suitable for feedstock with high moisture content (e.g., algae), due to its inherent advantage of being a wet processing technique without the requirement drying the feedstock [3]. Furthermore, oil products produced from HTL have much lower oxygen content and moisture as compared to that after pyrolysis.

Aquatic biomass hydrothermal liquefaction is one of the options existing to meet the escalating energy demand and saving arable lands as well as to fight against the growing pollution loads on environment. In the present investigation, brown macroalgal biomass (*Sargassum tenerrimum)* commonly found in the seas of peninsular India is being examined under hydrothermal conditions. The hydrothermal liquefaction of waste aquatic biomass has been explored to understand the products profile at different temperature for utilization of whole biomass to produce fuel/chemicals. Effects of the reaction temperature (varied from 260 °C to 300 °C) with reaction holding time 15 min and water/feedstock mass ratio 1:6 were studied. The liquid products obtained upon hydrothermal liquefaction were characterized with the help of ^{1}H NMR, GC–MS and FT-IR techniques and bio-residue using FT-IR and XRD.

2. Material and methods

Sargassum tenerrimum (ST) (brown alga, phaeophyta family, Macroalgae) was sampled during the post-monsoon season from the intertidal region at Anjuna in north Goa. The collected samples were washed thoroughly with tap water followed by distilled water. They were first dried at room temperature by frequent turning over and then quick dried in an oven at 50 °C for 2–3 h. The dried samples were coarsely crushed and powdered using an electric mixer-grinder.

2.1. Hydrothermal liquefaction

The HTL experiments were conducted in a 100 ml high pressure autoclave (Parr reactor) made of hastelloy at different reaction conditions of temperature. In a typical experiment, the reactor was loaded with *S. tenerrimum* with water as solvent (1:6 by weight). The reactor was then purged five times with nitrogen to remove the air inside. Reactants were agitated using a stirrer (~200 rpm). The reaction temperature was then raised to the desired value and maintained for 15 min. The pressure during the process was autogenous and maximum pressure was in the range of 40–83 bar under different reaction conditions. After the reaction, the reactor was left to cool down to room temperature to remove the reaction products. The gaseous products were vented and the liquid portion separated from solid residue using diethyl ether and vacuum filtration. The liquid portion was then extracted with an equal quantity of diethyl ether. The ethereal solution

thus obtained was dried over anhydrous sodium sulfate, filtered and evaporated in a rotary evaporator at room temperature. Upon removal of diethyl ether, this fraction was weighed and designated bio-oil1. The water phase that remained after extraction contained the water-soluble hydrocarbons. Solid products were extracted with acetone in a soxhlet extraction apparatus until the solvent in the thimble became colourless. After removal of the acetone under reduced pressure in a rotary evaporator, this fraction was weighed and designated bio-oil2. The ether soluble combined with the acetone soluble fraction were collectively designated as bio-oil. The acetone insoluble fraction was dried at 80 °C, weighed and termed solid residue (bio-residue). The experiments were repeated several times and the deviation of the liquid yields was always ± 1%. The equations to calculate yield of various fractions are given below:

$$Conversion\ (\%) = \frac{W1-W2}{W1} \times 100$$

$$Bio\ oil\ 1\ yield\ (wt.\ \%) = \frac{W\ ether\ soluble}{W1} \times 100$$

$$Bio\ oil\ 2\ yield\ (wt.\ \%) = \frac{W\ acetone\ soluble}{W1} \times 100$$

$$Total\ bio\ oil\ yield\ (wt.\ \%) = Bio{-}oil1 + Bio{-}oil2$$

$$Solid\ residue\ yield\ (wt.\ \%) = \frac{W\ solid}{W1} \times 100$$

$$Gas\ yield\ (wt.\ \%) = \frac{W\,(vessel + feed + water)\ before\ HTL - W\,(vessel + feed + water)\ after\ HTL}{Amount\ of\ feed\ taken\ (g) + amount\ of\ water\ added\ (g)} \times 100$$

$$Other\ yield\ (wt.\ \%) = 100-(bio{-}oil1 + bio{-}oil2 + solid\ residue + gas)$$

W1 is the weight of *Sargassum tenerrimum* algal feed; *W2* is the weight of bio-residue; $W_{ethersoluble}$ is the weight of ether soluble bio-oil (bio-oil1); $W_{acetonesoluble}$ is the weight of acetone soluble bio-oil (bio-oil2). All yields were calculated on a dry basis of material. Others correspond to the water soluble oxygenated hydrocarbons and some losses.

2.2. Characterization of feedstock and products

Thermogravimetric analysis (TGA) was carried out on a Shimadzu DTG-60 instrument. These tests were conducted using 5–10 mg of *S. tenerrimum* algal biomass at a heating rate of 10 °C/min in a temperature range of 25–900 °C under N_2 atmosphere and a gross calorific value was found using Parr 6300 Bomb Calorimeter. The elemental analysis was carried out in an Elemental vario micro cube unit. Moisture content was obtained using HR-83 Mettler Toledo Halogen Moisture Analyzer. The ^{1}H NMR spectra have been recorded on a Bruker Avance 500 Plus instrument using $CDCl_3$ as solvent. Powder X-ray diffraction patterns were collected on Bruker D8 advance X-ray diffract meter fitted with a Lynx eye high-speed strip detector and a Cu Kα radiation source. Diffraction patterns in the 2°–80° region have been recorded with a 0.04 step size (step time = 4 s). The FT-IR spectra were recorded on a Nicolet 8700 FT-IR spectrometer with the sample powder diluted in KBr. The organic fraction of the bio-oil was analyzed using gas chromatography–mass spectrometry (GC/MS, Agilent 7890B). The carrier gas was He and column flow rate was 1 ml min^{-1}. An HP-1 column (25 m × 0.32 mm × 0.17 μm) was used for the separation. An oven isothermal program was set at 50 °C for 2 min, followed by a heating rate of 5 °C min^{-1} up to 280 °C where it was held for 5 min. The injected volume was 0.4 μL in a split less mode. Volatile matter content has been calculated along the lines of ASTM D3175, by measuring the weight loss in the sample after placing it in a muffle furnace at 950 °C for 2 min.

Table 1
Proximate and ultimate analyses of *Sargassum tenerrimum* algae (%, dry basis).

	Ultimate analysis		Proximate analysis
C	32.1	Moisture	5.7
H	4.7	Ash content	26.5
O	60.72	Volatile matter	61.5
N	0.93	Fixed carbon	6.3
S	1.55		

Volatile matter and ash analyses of the feed were carried out using oven-dried feedstock.

3. Results and discussion

3.1. Characterization of Sargassum tenerrimum feed

The result of the proximate and ultimate analysis of the *S. tenerrimum* sample, including the total content of volatiles, moisture, fixed carbon and ash (i.e., inorganic components of the samples) is summarized in Table 1. Total volatiles collected at 950 °C represent 61.5% of total product. The moisture, ash and fixed carbon represent 5.7%, 26.5% and 6.3%, respectively, of total product. Ultimate analysis showed composition of the key element as 32.1% C, 4.7% H, 0.9% N, 60.7% O and 1.5% S (calculated by difference). The calorific value of *S. tenerrimum* was 11.96 MJ kg^{-1}.

Thermal behaviour of *S. tenerrimum* was determined by TGA and differential thermogravimetric analysis (DTG), the results being as in Fig. 1. The profile of algal biomass normally presents three steps. The first one at 100 °C is attributed to moisture present in algal biomass [26]. The mass loss between 200 and 327 °C would correspond to decomposition of carbohydrates while the one at higher temperature (350 °C) would indicate decomposition of the protein fraction [27]. The major mass decomposition occurs between 200 and 350 °C, as was observed for other macroalgae also [26,28]. The mass loss at temperatures higher than 600 °C would be related to lipid degradation. Fig. 1 thus shows that the main components of feedstock, hemicelluloses and cellulose of *S. tenerrimum* start decomposing at 200 °C. The maximum decomposition temperature was determined as approximately 264 °C. Hence, from the thermal analysis (TGA/DTG) it has been shown that the temperature range between 200 and 327 °C may be considered as an active pyrolytic zone for *S. tenerrimum* biomass, where maximum decomposition (depolymerization) takes place.

A broad band in the frequency range 3500–3200 cm^{-1} (Fig. 2) corresponds to N–H and O–H stretching vibration of the feed, which indicates the presence of secondary amines that are attributed to proteins & lipids, and phenols & alcohols, respectively. The band at 2800–3000 cm^{-1} was related to =C–H and –C–H stretching vibrations. The peaks in the region 1650–1580 cm^{-1} may be attributed to N–H bending vibration arising from β-unsaturated ketones and amides. The C–H bending vibration was observed at 1435–1405 cm^{-1}, while C–O stretches and O–H bending vibrations were at 1350–1260 cm^{-1}. This vibration can also be attributed to asymmetric C–O–C stretching, which would indicate the presence of esters. Symmetric C–H stretching was observed in the range 1120–1030 cm^{-1}.

3.2. Hydrothermal liquefaction product yields

Hydrothermal liquefaction of *S. tenerrimum* was performed at various temperatures (260, 280 and 300 °C) using distilled water as the solvent, with a residence time of 15 min. Reaction conditions have been selected based on our earlier studies and literature [29] to understand the effect of temperature on bio-oil product yield of *S. tenerrimum* under sub-critical water. The product distribution upon hydrothermal liquefaction of the *S. tenerrimum* sample is presented in Fig. 3 and Table S1.

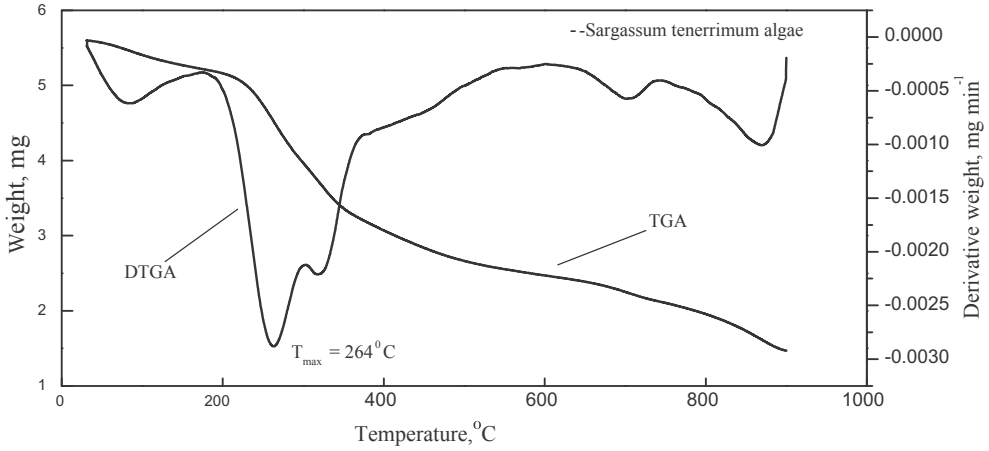

Fig. 1. Thermogravimetric and differential thermal analysis (TGA and DTG) of *Sargassum tenerrimum.*

The total bio-oil yields were 11.5 wt%, 16.3 wt% and 14.7 wt% at 260, 280 and 300 °C, respectively. The maximum total bio-oil yield of 16.33% was thus obtained at 280 °C, further increase of temperature to 300 °C bringing down the yield. The total bio-oil was composed of the ether fraction (bio-oil1) obtained from extraction of liquid portion and the acetone fraction (bio-oil2) obtained from the solid-liquid (acetone) extraction. The solid residue yields also decreased continuously from 61.2 wt% to 24.2 wt% as the temperature increased from 260 to 300 °C. The results indicated that at lower temperature the decomposition of biomass was incomplete and left unreacted biomass which may suppress the bio-oil formation and increase the solid product. Increase in temperature should be able to accelerate the decomposition of the feedstock and benefit bio-oil formation; however, in our experiments an increase in temperature beyond 280 °C, increased the breakdown of biomass as well as the bio-residue to water soluble products and thus led to a decrease in the bio-residue yield and bio-oil yield. The reducing yield of the solid residue suggested an increase of the overall biomass conversion upon increasing the temperature from 260 to 300 °C. The yield of gaseous product initially showed an increase as the temperature was raised from 260 to 280 °C but the yield dropped upon further rise in temperature to 300 °C, whereas as the temperature increased in the range of 260–300 °C, other product yields increased.

The obvious difference in bio-oil yield and optimal conditions

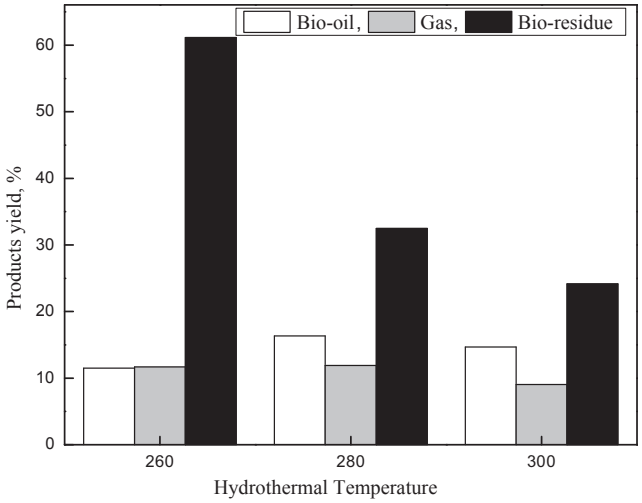

Fig. 3. Product distribution from hydrothermal liquefaction of *Sargassum tenerrimum*. Conversion efficiencies: 260 °C: (38.83%; other yield 15.66%); 280 °C: (67.67%; other yield 39.27%); 300 °C: (75.84%; other yield, 52.11%).

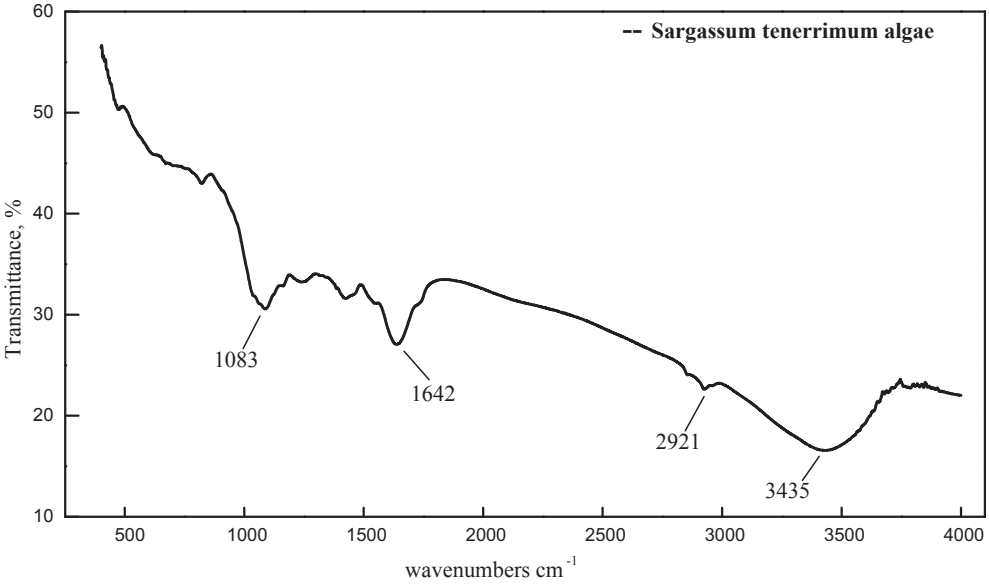

Fig. 2. The FT-IR spectrum of *Sargassum tenerrimum* algae feed.

Table 2
Chemical composition of *Sargassum tenerrimum* bio-oils as obtained from gas chromatography–mass spectrometry (GC/MS).

Compounds identified in bio-oil	Area, %		
	260	280	300
3-Pyridinol	5.50	16.21	9.61
2-Cyclopenten-1-one, 2-methyl-	–	1.48	–
Phenol	–	1.26	–
2-Cyclopenten-1-one, 2,3-dimethyl-	–	1.54	–
p-Cresol	–	1.58	–
3-Pyridinol, 6-methyl-	–	1.24	2.29
Hydroquinone	–	0.98	1.97
2-Cyclohexen-1-one, 4-ethyl-3,4-dimethyl-	–	–	1.53
n-Decanoic acid	1.60	–	–
1,4-Benzenediol, 2-methyl-	–	2.66	2.85
1,3-Benzenediol, 4-ethyl-	–	–	1.03
2,3-Dimethylhydroquinone	–	–	1.07
2-Hydrazino-4-methyl-6-methylthiopyrimidine	3.14	–	–
Phenol, 3,5-bis(1-methylethyl)-, acetate	–	1.68	2.49
7-Ethyl-4,6-heptadecandione	–	–	3.02
Naphthalene, 1,6-dimethyl-	–	3.05	–
d-Proline, N-isobutoxycarbonyl-, isohexyl ester	–	–	4.18
p-Hydroxybiphenyl	–	5.11	–
Dodecanamide	–	–	3.10
Octanamide, N,N-dimethyl-	–	–	2.17
1-Heptadecene	1.12	–	–
2,5-Piperazinedione, 3-benzyl-6-isopropyl-	–	2.13	–
Hexadecanamide	–	4.0	–
Palmitoleic acid	2.90	–	–
n-Hexadecanoic acid	13.85	4.97	1.53
2-Myristynoyl-glycinamide	–	–	2.30
2(1H)-Naphthalenone, octahydro-4a-methyl-7-(1-methylethyl)-, (4a.alpha.,7.beta.,8a.beta.)-	1.51	–	–
26,27-Dinorergosta-5,23-dien-3-ol, (3.beta.)-	–	–	2.86
trans-13-Octadecenoic acid	2.92	–	–
cis-13-Octadecenoic acid	2.16	–	–
9-Octadecenamide, (Z)-	1.21	–	–
Cyclo-(l-leucyl-l-phenylalanyl)	1.57	–	–
2-Propenoic acid, 2-methyl-, 1-methylethyl ester	–	3.28	–
Bis(2-ethylhexyl) phthalate	–	15.05	13.40
Vitamin E	–	3.64	2.22
Adipic acid, isohexyl trans-2-methylcyclohexyl ester	1.0	–	–
Phthalic acid, di(2-propylpentyl) ester	6.46	–	–
1-Nonadecene	0.01	–	–
9-Tricosene, (Z)-	6.38	–	–
(Z)-14-Tricosenyl formate	2.22	–	–
1,9-Tetradecadiene	1.08	–	–
9,12-Octadecadienoic acid (Z,Z)-	4.80	2.72	–
Benzene, 1,2-bis(1-buten-3-yl)-	3.25	–	–
Stigmastan-3,5-diene	8.48	4.41	–
Stigmasta-5,24(28)-dien-3-ol, (3.beta.,24Z)-	6.48	12.31	4.37
Stigmast-4-en-3-one	–	–	5.80
13-Tetradecen-1-ol acetate	1.27	–	–
Pentadecanal-	1.18	–	–

between the feedstock and temperature can be ascribed to that *S. tenerrimum* biomass with different temperature had, leading to the different performance of the product yield.

3.3. Characterization of bio-oils

3.3.1. Gas chromatography-mass spectrometry (GC-MS) of bio-oil

From GC-MS analysis data (Table 2) it was obvious that liquefaction temperature affected the components of the bio-oils produced. As the HTL temperature varied from 260 to 300 °C, production of different compounds as well as different percentages of compounds had been observed. Identification of the main peaks of compounds was performed using NIST mass spectral database. The components of the bio-oils were identified as phenols, ketones, and aldehydes, acid, esters, alcohols, nitrogen-containing compounds (including amides and N-heterocyclic compounds), hydrocarbons, etc [24]. A semi-quantitative analysis was performed by calculating the relative percentage of area of the chromatographic peaks (Table 2). The main compounds obtained by HTL of *S. tenerrimum* were methyl-3-pyridinol, 6-methyl-3-pyridinol, 2-methyl-1,4-benzenediol, *p*-hydroxybiphenyl, *n*-hexadecanoic acid, stigmastan-3,5-diene and bis (2-ethylhexyl) phthalate. Hexadecanoic acid is one of the components most frequently found in bio-oil obtained from algae [30]. Organic acid content in the bio-oils was observed to decrease with increasing temperature from 260 to 300 °C. Phenolic compounds such as phenol, *p*-cresol and 2-methyl-1, 4-benzenediol was observed in bio-oil obtained at the optimum temperature of 280 °C. The phenolics in *S. tenerrimum* bio-oil are likely produced from the carbohydrate and crude fibre of the algal biomass [8,31,25]. Nitrogenated compounds are formed by decarboxylation, deamination, dehydration, depolymerization and decomposition reactions of proteins [3,32]. The Higher percentage area of 3-pyrindiol (16.21 area %) was observed at the optimum temperature of 280 °C but further increase in temperature to 300 °C caused a significant decrease (9.61 area %). The increased percentage of branched amides may be due to the dehydration reactions of amines and carboxylic acids to form amides at higher temperatures. This can also be justified by the decrease in organic acid content with increase of temperature. Also, higher area percentage of other compounds such as Bis(2-ethylhexyl) phthalate (15.05), Stigmast-4-en-3-one (13.40 area %) at 280 and 300 °C and Stigmastan-3,5-diene (8.48 area %) at 260 °C were observed in the bio-oil. As the composition of the liquid product is so complex, further upgrading such as denitrogenation and deoxygenation would be necessary to make the bio-oil suitable as engine fuel.

3.3.2. Fourier Transform-Infrared (FT-IR) spectroscopy of bio-oil

FT-IR spectra of the *S. tenerrimum* feed and bio-oil obtained from liquefaction of the alga with water at 260, 280 and 300 °C are shown in Fig. 4. The broad band at around 3200–3405 cm^{-1} is attributed to the O–H or N–H stretching vibration caused by water, O–H groups or N–H groups present in bio-oil [33,25]. A broad absorbance was displayed at around 3314 cm^{-1} for the raw material, which indicated a high content of carbohydrates and proteins [34,35]. The bio-oils showed a weaker absorbance at the wave number region of 3200–3405 cm^{-1}, suggesting that both carbohydrates and proteins were decomposed in the HTL process. The band at 2854–2950 cm^{-1} in the bio-oil obtained by liquefaction of *S. tenerrimum* and the absorbance of these peaks in all the bio-oils were stronger due to the C–H stretching vibrations, indicating the presence of alkyl C–H groups [8,35]. The C=O stretching vibrations at around 1645–1720 cm^{-1} in the bio-oils indicate the presence of ketones, aldehydes, esters or acids [33]. 260 °C bio-oil showed slightly stronger absorbance in the C=O stretching region (1645–1720 cm^{-1}) than 280 °C and 300 °C bio-oils, suggesting a greater abundance of unsaturated carboxylic acids [36]. The bending vibrations bands at around 1580–1650 cm^{-1} indicate the presence of N–H groups of amines. The bands in the region 1430–1480 cm^{-1} were attributed to α-CH_2 bending vibrations present in the bio-oils. The presence of C-N stretching bands at around 1266–1342 cm^{-1} in the bio-oils was due to aromatic amines. The stretching band at 1266–1342 cm^{-1} shoewd higher intensity in the 280 °C bio-oil than the other temperature bio-oils, suggesting a greater abundance of N-contains compound in 280 °C bio-oil than other bio-oils (Table 2). In addition, some other absorbance peaks appearing in the range of 780–850 cm^{-1} are ascribed to the C–H out of plane bending vibrations which may be from aromatics [33]. The band at 1083 cm^{-1} only appeared in the absorption profile of *S. tenerrimum* feed, which could be C-O connected with hydroxyl groups and were dehydrated after liquefaction. The FT-IR spectrum of different bio-oils from HTL of *S. tenerrimum* at different temperatures has shown majorly the same peaks, indicating the presence of the same functional groups in all bio-oils. The bands that evidence the presence of alcohols, phenols, esters, ethers and alkanes were more prominent in the bio-oil than in the raw *S. tenerrimum* feed.

3.3.3. ^1H Nuclear magnetic resonance (NMR) of bio-oil

NMR analysis of the bio-oil1 samples had been carried out to

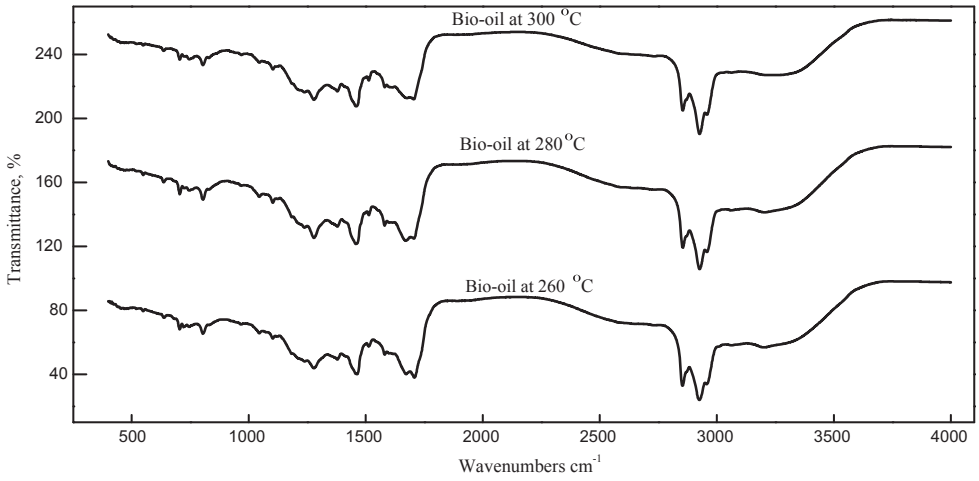

Fig. 4. The FT-IR spectra of *Sargassum tenerrimum* bio-oil at different temperatures.

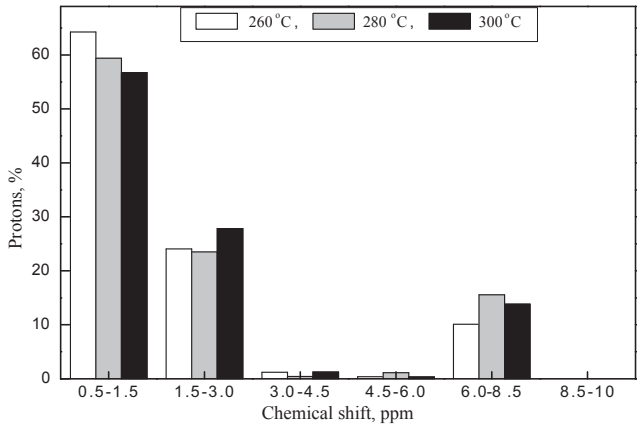

Fig. 5. ^{1}H Nuclear magnetic resonance (NMR) spectra of *Sargassum tenerrimum* bio-oil at different temperatures.

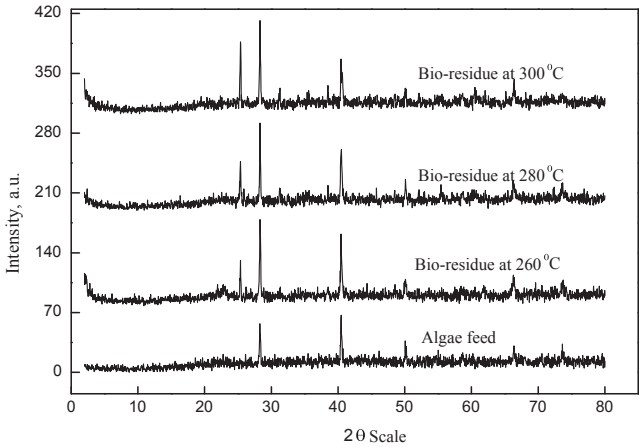

Fig. 6. XRD of *Sargassum tenerrimum* bio-residue obtained at 260, 280 and 300 °C.

understand the ratios of chemical environments of the protons. NMR spectra provided complementary functional group information to FT-IR spectra and the ability to quantify and compare integration areas between spectra. The FT-IR spectral data were in accordance with the various peaks obtained in the NMR spectra of the bio-oils (Fig. 5). Similar to FT-IR, ^{1}H NMR spectra showed a high percentage of aliphatic functional groups for all bio-oils and a summary of integrated peak area regions assigned to different functional group classes is provided in Fig. 6. The most upfield region of the spectra, from 0.5 to 1.5 ppm, represents aliphatic protons that are attached to carbon atoms at least two bonds away from a C=C or heteroatom (O or N). The next integral region from 1.5 to 3.0 ppm represents protons on aliphatic carbon atoms that may be bonded to a C=C double bond [36]. All the bio-oils have higher percentages of protons in the spectral region from 0.5 to 3.0 ppm. The bio-oil samples have higher percentage (56.73–64.26%) of protons in the region from 0.5 to 1.5 than in the region from 1.5 to 3.0 (24.06–27.84). The difference of proton percentages, possibly due to a large number of nitrogenous and oxygenated compounds derived from the feedstock's high protein that has been shown to resonate in this area [33,37]. The next portion of the ^{1}H NMR spectrum at 3.0–4.5 ppm represents methoxyl protons [38] or the methylene group that joins two aromatic rings. In this region very low proton percentages are observed, perhaps due to the methylene group that joins two aromatics rings not being observed (Table 2). All bio-oils displayed a low percentage of methoxy/carbohydrate functionality (4.5–6.0 ppm). The maximum percentage of the proton (1.13%) was observed at 280 °C liquefied bio-oil while the minimum percentage of the proton (0.37 and 0.34%) was observed at 260 and 300 °C liquefied bio-oil at 4.5–6.0 ppm. The section of the spectrum between 6.0 and 8.5 ppm corresponds to the aromatic region [36]. Maximum proton content of bio-oil was obtained at 280 °C at around 15.54% in this region. Aromatic/heteroaromatic functionality was also observed in all bio-oils (6.0–8.5 ppm) in agreement with the findings from FT-IR. The downfield spectral regions (8.5–10 ppm) of the bio-oils arise from the aldehydes. Aldehyde functionality (9.5–10.0 ppm) was absent from all bio-oils despite the observed C=O functional groups (1645–1720 cm^{-1}) in FT-IR. The appearance of such FT-IR bands could also be due to other carbonyl-bearing groups such as protonated carboxylic acids, carboxylic acid esters, amides or ketones.

3.3.4. FT-IR and XRD analyses of bio-residue

Fig. S1 shows the FT-IR spectra of *S. tenerrimum* feed and the bio-residues. The broad bands at 3200–3500 cm^{-1} are assigned to the stretching vibrations of hydrogen-bonded O–H groups and N–H groups and these bands indicate the presence of polysaccharides, carbohydrates and proteins in the *S. tenerrimum* feed. This feed has strong stretching vibration peaks corresponding to the O–H and N–H groups but these transmittances decrease in the bio-residue. The peak at 1083 cm^{-1} disappeared in the bio-residue. The peak around 1600–1620 cm^{-1} corresponding to the N–H bending vibration was present in the *S. tenerrimum* feed as well as bio-residue. The peaks between 2800 and 2930 cm^{-1} in the spectra of residues were much weaker than those of the raw feed. The presence of a single peak at 1590–1630 cm^{-1} attributed to the C=C stretching indicates the formation of aromatic bio-residue [39]. The XRD spectra of *S. tenerrimum*

feed and bio-residues (Fig. 6) at different temperatures showed no significant differences in the powder X-ray diffract gram. Normally peaks at the 2θ values around 20° and 22° were assigned to the crystalline region of cellulose in biomass [40]. The biomass was decomposed partially at 260 °C, the crystalline structure of cellulose at 22.65° remained due to the thermal stability of cellulose at low temperatures. However, this peak were invisible in the XRD spectra for Bio-residue-280 °C and 300 °C indicating that crystalline cellulose molecule was destroyed. However, upon liquefaction new XRD signals were detected at 2θ = 25.32° in all bio-residues (260, 280 and 300 °C), which indicated that coke/char occurred. The chemical crystal structure of the algae was destroyed and coke/char was formed during the liquefaction process due to decomposition of the *S. tenerrimum* macromolecular matrix [41]. These are in good agreement with the results of FT-IR, which indicates the conversion of cellulose present in *S. tenerrimum* into products. The analysis of bio-residue obtained at various temperatures showed typical amorphous nature indicating the rich carbon content of the residue.

4. Conclusion

S. tenerrimum algal biomass is a potential feedstock for renewable fuels/chemicals production owing to its wide availability and non-competitiveness to food/fodder and land issues. Hydrothermal liquefaction is the most promising technique for producing biofuels from wet biomass, has lower reaction temperature and higher energy efficiency than that of pyrolysis process because energy intensive drying and dewatering steps are not imperative. A type of bio-oil directly useable as biofuels and more commercially viable could be obtained from *S. tenerrimum* feedstock by the process of hydrothermal liquefaction. The maximum total bio-oil yield of 16.33% was thus obtained at 280 °C, further increase of temperature to 300 °C bringing down the yield. The analysis of bio-oil by GC-MS, ^{1}H NMR, and FT-IR spectra showed that the presence of alcohols, phenols, esters, ethers and alkanes was more prominent in the bio-oil. The peaks between 2800 and 2930 cm^{-1} in the spectra of bio-residues were much weaker than of the raw feed. The presence of a single peak at 1590–1630 cm^{-1} attributed to the C=C stretching indicates the formation of aromatic in the bio-residue. The chemical crystal structure of the algae was destroyed and coke/char was formed during the liquefaction process due to decomposition of the *S. tenerrimum* macromolecular matrix. Analysis of the bio-residue obtained at various temperatures showed typical amorphous nature and higher content of carbon.

Acknowledgements

The authors thank the Director, CSIR-Indian Institute of Petroleum, Dehradun for his constant encouragement and support and AcSIR for granting permission to conduct this research work at CSIR IIP. They thank the Analytical Science Division (ASD) of CSIR-IIP for NMR, FT-IR, and XRD analyses. The authors thank CSIR in the form of XII Five Year Plan project (CSC0116/BioEn) and Ministry of New and Renewable Energy for providing financial support. AF is grateful to the UGC (Govt. of India) for the MANSF award that has facilitated her contribution to this study which forms part of her Ph.D. research work at the Dept. of Biotechnology, Goa University.

Appendix A. Supplementary data

Supplementary data associated with this article can be found, in the online version, at http://dx.doi.org/10.1016/j.fuel.2018.02.153.

References

[1] Marcilla A, Catalá L, García-Quesada JC, Valdés FJ, Hernández MR. A review of thermochemical conversion of microalgae. Renew Sustain Energy Rev 2013;27:11–9.
[2] Anastasakis K, Ross AB. Hydrothermal liquefaction of four brown macro-algae commonly found on the UK coasts: an energetic analysis of the process and comparison with bio-chemical conversion methods. Fuel 2015;139:546–53.
[3] Ross AB, Biller P, Kubacki ML, Li H, Lea-Langton A, Jones JM. Hydrothermal processing of microalgae using alkali and organic acids. Fuel 2010;89:2234–43.
[4] Wu K-T, Tsai C-J, Chen C-S, Chen H-W. The characteristics of torrefied microalgae. Appl Energy 2012;100:52–7.
[5] De Caprariis B, De Filippis P, Petrullo A, Scarsella M. Hydrothermal liquefaction of biomass: influence of temperature and biomass composition on the bio-oil production. Fuel 2017;208:618–25.
[6] Chen W-H, Lin B-J, Huang M-Y, Chang J-S. Thermochemical conversion of microalgal biomass into biofuels: a review. Bioresour Technol 2015;184:314–27.
[7] Vardon DR, Sharma BK, Blazina GV, Rajagopalan K, Strathmann TJ. Thermochemical conversion of raw and defatted algal biomass via hydrothermal liquefaction and slow pyrolysis. Bioresour Technol 2012;109:178–87.
[8] Huang Y, Chen Y, Xie J, Liu H, Yin X, Wu C. Bio-oil production from hydrothermal liquefaction of high-protein high-ash microalgae including wild Cyanobacteria sp. and cultivated *Bacillariophyta* sp. Fuel 2017;197:138–44.
[9] Huber GW, Iborra S, Corma A. Synthesis of transportation fuels from biomass: chemistry, catalysts, and engineering. Chem Rev 2006;106:4044–98.
[10] Peterson AA, Vogel F, Lachance RP, Froling M, Antal Jr MJ, Tester JW. Thermochemical biofuel production in hydrothermal media: a review of sub- and supercritical water technologies. Energy Environ Sci 2008;1:32–65.
[11] Chumpoo J, Prasassarakich P. Bio-oil from hydro-liquefaction of bagasse in supercritical ethanol. Energy Fuels 2010;24:2071–7.
[12] Kruse A, Dinjus E. Hot compressed water as reaction medium and reactant properties and synthesis reactions. J Supercrit Fluids 2007;39:362–80.
[13] Krammer P, Vogel H. Hydrolysis of esters in subcritical and supercritical water. J Supercrit Fluids 2000;16:189–206.
[14] Uematsu M, Franck EU. Static dielectric constant of water and steam. J Phys Chem Ref Data 1980;9:1291–306.
[15] King JW, Holliday RL, List GR. Hydrolysis of soybean oil in a subcritical waterflow reactor. Green Chem 1999;1:261–4.
[16] Akiya N, Savage PE. Roles of water for chemical reactions in high-temperature water. Chem Rev 2002;102:2725–50.
[17] Hu Y, Gong M, Xu C (C), Bassi A. Investigation of an alternative cell disruption approach for improving hydrothermal liquefaction of microalgae. Fuel 2017;197:138–44.
[18] Valdez PJ, Nelson MC, Wang HY, Lin XX, Savage PE. Hydrothermal liquefaction of *Nannochloropsis* sp: Systematic study of process variables andanalysis of the product fractions. Biomass Bioenergy 2012;46:317–31.
[19] Jena U, Das KC. Comparative evaluation of thermochemical liquefaction and pyrolysis for bio-oil production from microalgae. Energy Fuels 2011;25:5472–82.
[20] BillerP RoB. Potential yields and properties of oil from the hydrothermal liquefaction of microalgae with different biochemical content. Bioresour Technol 2011;102:215–25.
[21] Shaobo L, Liqing W, Maxine LP, Kevin F, Armando GM. Hydrothermal liquefaction of laboratory cultivated and commercial algal biomass into crude bio-oil 2017;36:781–7.
[22] Barreiro DL, Samorì C, Terranella G, Hornung U, Kruse A, Prins W. Assessing microalgae biorefinery routes for the production of biofuels via hydrothermal liquefaction. Bioresour Technol 2014;174:256–65.
[23] Raikova S, Le CD, Beacham TA, Jenkins RW, Allen MJ, Chuck CJ. Towards a marine biorefinery through the hydrothermal liquefaction of macroalgae native to the United Kingdom. Biomass Bioenergy 2017;107:244–53.
[24] Parsa M, Jalilzadeh H, Pazoki M, Ghasemzadeh R, Abduli MA. Hydrothermal liquefaction of *Gracilaria gracilis* and *Cladophora glomerata* macro-algae for biocrude production. Bioresour Technol 2018;250:26–34.
[25] Shakya R, Adhikari S, Mahadevan R, Shanmugam RS, Nam H, Hassan BE, et al. Influence of biochemical composition during hydrothermal liquefaction of algae on product yields and fuel properties. Bioresour Technol 2017;243:1112–20.
[26] Kim SS, Ly HV, Kim J, Choi JH, Woo HC. Thermogravimetric characteristics and pyrolysis kinetics of alga Sargassumsp. biomass. Bioresour Technol 2013;139:242–8.
[27] Ross AB, Jones JM, Kubacki ML, Bridgeman T. Classification of macroalgae as fuel and its thermochemical behavior. Bioresour Technol 2008;99:6494–504.
[28] Li D, Chen L, Zhang X, Ye N, Xing F. Pyrolytic characteristics and kinetics studies of three kinds of red algae. Biomass Bioenergy 2011;35:1765–72.
[29] Singh R, Balagurumurthy B, Bhaskar T. Hydrothermal liquefaction of macroalgae: effect of feedstock composition. Fuel 2015;146:69–74.
[30] Chen Y, Wu Y, Zhang P, Hua D, Yang MD, Li C, et al. Direct liquefaction of *Dunaliella tertiolecta* for bio-oil in sub/supercritical ethanol-water. Bioresour Technol 2012;124:190–8.
[31] Brown TM, Duan P, Savage PE. Hydrothermal liquefaction and gasification of *Nannochloropsis* sp. Energy Fuels 2010;24:3639–46.
[32] Toor SS, Rosendahl L, Rudolf A. Hydrothermal liquefaction of biomass: a review of subcritical water technologies. Energy 2011;36:2328–42.
[33] Zhou D, Zhang L, Zhang S, Fu H, Chen J. Hydrothermal liquefaction of macroalgae *Enteromorpha prolifera* to bio-oil. Energy Fuels 2010;24:4054–61.
[34] Wang F, Chang Z, Duan P, Yan W, Xu Y, Zhang L, et al. Hydrothermal liquefaction of Litseacubeba seed to produce bio-oils. Bioresour Technol 2013;149:509–15.
[35] Arun J, Shreekanth SJ, Sahana R, Raghavi MS, Gopinath KP, Gnanaprakash D. Studies on influence of process parameters on hydrothermal catalytic liquefaction of microalgae (*Chlorella vulgaris*) biomass grown in wastewater. Bioresour Technol 2017;244:963–8.

[36] Cheng F, Cui Z, Chen L, Jarvis J, Paz N, Schau T, et al. Hydrothermal liquefaction of high- and low-lipid algae: bio-crude oil chemistry. Appl Energy 2017;206:278–92.
[37] Mullen CA, Strahan GD, Boateng AA. Characterization of various fast pyrolysis bio-oils by NMR spectroscopy. Energy Fuels 2009;23:2707–18.
[38] Kosa M, Ben H, Theliander H, Ragauskas AJ. Pyrolysis oils from CO_2 precipitated kraft lignin. Green Chem 2011;13:3196–202.
[39] Uchimiya M, Orlov A, Ramakrishnan G, Sistani K. *In situ* and *ex situ* spectroscopic monitoring of biochar's surface functional groups. J Anal Appl Pyrolysis 2013;102:53–9.
[40] Yang H, Yan R, Chen H, Lee DH, Zheng CG. Characteristics of hemicellulose, cellulose, and lignin pyrolysis. Fuel 2007;86:1781–8.
[41] Xu Y, Hu X, Yu H, Wang K, Cui Z. Hydrothermal catalytic liquefaction mechanisms of algal biomass to bio-oil. Energy Sources Part A 2016;38:1478–84.

Bioresource Technology 307 (2020) 123232

Contents lists available at ScienceDirect

Bioresource Technology

journal homepage: www.elsevier.com/locate/biortech

Solid base catalytic hydrothermal liquefaction of macroalgae: Effects of process parameter on product yield and characterization

Bijoy Biswas[a,b], Avnish Kumar[a,b], Alisha C. Fernandes[c], Komal Saini[a,b], Shweta Negi[a], Usha D. Muraleedharan[c], Thallada Bhaskar[a,b,*]

[a] Biomass Conversion Area (BCA), Material Resource Efficiency Division (MRED), CSIR-Indian Institute of Petroleum (IIP), Dehradun 248005, India
[b] Academy of Scientific and Innovative Research (AcSIR), New Delhi, India
[c] Department of Biotechnology, Goa University, Goa 403206, India

GRAPHICAL ABSTRACT

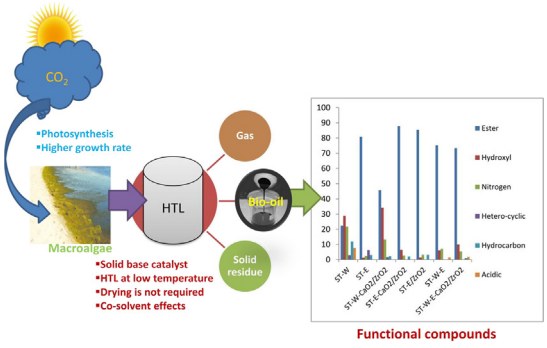

ARTICLE INFO

Keywords:
Catalytic hydrothermal liquefaction
Macroalgae
Bio-oil
Ester compounds

ABSTRACT

The hydrothermal liquefaction (HTL) of *Sargassum tenerrimum* (ST) macroalgae was carried out for 15 min, over various solid base catalysts (CaO supported on CeO_2, Al_2O_3, and ZrO_2) at different reaction temperatures (260–300 °C), different catalyst quantities (5–25 wt%) and using different solvent systems. Maximum bio-oil (BO) yields for the non-catalytic HTL with single solvent water, ethanol, and water-ethanol co-solvent were 3.3 wt%, 23.3 wt%, and 32.0 wt%, respectively, at 280 °C. Ethanol as single solvent elicited highest BO yield of 25.2 wt% with CaO/ZrO_2 (10.0 wt%) catalyst. However, the highest BO yield (33.0 wt%) accompanied by higher conversion (70.5%) was obtained with CaO/ZrO_2 (10.0 wt%) under water-ethanol co-solvent. The selectively higher percentage of ester functional compounds (87.8%) was found with CaO/ZrO_2 catalyst under water-ethanol co-solvent. Also, the bio-oil obtained from catalytic liquefaction showed a higher high heating value (HHV) compared to that from the non-catalytic HTL reaction.

1. Introduction

Worldwide, there has been increased use of non-renewable fossil fuel resources for economic development, for which reason they have been found continuously depleting (Zhang et al., 2019; Xu et al., 2011). It is thus essential to look at alternatives to fossil resources (Yan et al.,

* Corresponding author at: Biomass Conversion Area (BCA), Material Resource Efficiency Division (MRED), CSIR-Indian Institute of Petroleum (IIP), Dehradun 248005, India.
E-mail address: tbhaskar@iip.res.in (T. Bhaskar).

https://doi.org/10.1016/j.biortech.2020.123232
Received 30 January 2020; Received in revised form 17 March 2020; Accepted 20 March 2020
Available online 25 March 2020
0960-8524/

2019; Zhang et al., 2019). Biomass such as agricultural, forest, municipal solid waste, animal wastes, waste from food processing and aquatic residues are promising alternatives to fossil resources because biomass is renewable and can be used for both energy and chemicals production (Raikova et al., 2019b; Aysu and Sanna, 2015). Many different technologies have been used for biomass utilization which could be biological, physical or thermochemical conversion. Among the thermochemical processes such as pyrolysis, hydrothermal liquefaction (HTL) and gasification, the hydrothermal method is most widely used for aquatic biomass conversion into useful products as it does not require feed drying process and can be commercialized in industrial perspectives (Ma et al., 2019; Raikova et al., 2019a). The process parameter is an important factor during biomass conversion into products (Xue et al., 2016: Guo et al., 2015). Researchers have been using various parameters such as temperature, reaction environment, reaction holding time, catalyst, reaction heating rate, etc., for the optimization and to produce higher yields of bio-oil (Yuan et al., 2019; Kandasamy et al., 2020, Ma et al., 2019).

While HTL of macroalgae has been carried out over various homogeneous catalysts such as KOH, K_2CO_3, NaOH, Na_2CO_3, H_2SO_4, HCl etc., (Shakya et al., 2015; Yan et al., 2019; Kandasamy et al., 2020; Egesa et al., 2018; Yang et al., 2014), the use of homogeneous catalyst might not be useful for industrial applications as it is hard to separate and reuse (Ma et al., 2019; Wang et al., 2018). Hence the need to initiate use of solid catalyst for the liquefaction process. Wang et al. (2018) investigated HTL of the microalgae *Nannochloropsis* over various transition metals M/TiO_2 (M = Fe, Co, Ni, Mo, or Mn) as catalysts and showed that Ni/TiO_2 was the most effective for higher bio-oil yield. The maximum bio-oil yield of 48.23% was obtained at 300 °C. They observed that upon addition of a catalyst, the quality and composition of the bio-oil also significantly changed. Another research group (Yuan et al., 2019) carried out a catalytic HTL of macroalgae with the co-solvent system. They observed that with the addition of ZSM-5 catalyst, the bio-oil yields (46.75%) as well as the conversion (95.5%) in the HTL reaction were enhanced significantly. The catalytic bio-oil thus obtained was majorly composed of ester compounds compared to that from the non-catalytic reaction. Kandasamy et al. (2020) examined the catalytic HTL reaction of *Spirulina platensis* macroalgae with nano-catalyst (CeO_2). Maximum bio-oil (26.0%) with higher conversion was observed at 250 °C. The bio-oil being largely composed of amino acids and nitrogen-containing compounds, the need arises to introduce a suitable catalyst which could reduce its nitrogen content. Ma et al. (2019) added zeolite-based catalysts for HTL of macroalgae and found ZSM-5 to be most suitable in terms of bio-oil yield and quality. Maximum bio-oil yield (29.3 wt%) was observed at 280 °C. They found that use of the zeolite catalyst could reduce the oxygen content in the bio-oil. However, the production of selective functional group compounds or quality bio-oil would call for further catalytic screening of algal biomass.

While homogenous base catalytic HTL of macroalgae has been reported by several researchers, the use of solid base catalyst as a more economically viable choice has not been examined. Hence the present study, wherein various solid base catalysts were synthesized for application in HTL of *Sargassum tenerrimum* (ST) at different reaction temperatures, catalyst amounts and involving the use of co-solvent. We examined the catalytic effect on product yield and composition changes in the bio-oil by GC–MS, FT-IR, NMR, and elemental analysis. The prepared catalysts were characterized using various techniques: BET, SEM, TEM, XRD, and CO_2-TPD. The possible reaction mechanism of functional compound formation was also investigated.

2. Materials and methods

Sargassum tenerrimum (ST) was collected from the west coast region of Goa, India. The sun-dried sample was crushed and sieved to a size between 0.5 and 2 mm.

2.1. Characterization methods

Thermogravimetric analysis (TGA) of ST was carried out in a DTG-60 unit (Shimadzu, Japan). Biomass sample (2–5 mg) was placed in a sample pan and heated from ambient temperature to 900 °C under N_2 flow at a heating rate of 10 °C/min. Elementarvario micro cube unit was used for the analysis of elements (C, H, N, S) present in the biomass feed and bio-oil. Moisture content of the biomass was analyzed using HR-83 Mettler Toledo Halogen Moisture Analyzer. The types of protons present in the bio-oils obtained were characterized in a Bruker Advance 500 Plus instrument using $CDCl_3$ solvent for dissolving the bio-oil. Gas chromatography-mass spectrometry (GC/MS, Agilent 7890 B) was used for the analysis of bio-oil functional compounds. Helium (He) was used as a carrier gas, at a flow rate of 1 mL min^{-1}; An HP-1 column (25 m × 0.32 mm × 0.17 μm) was heated from 50 °C to 280 °C, at a heating rate of 5 °C min^{-1} and it was held for 5 min. Bio-oil (0.4 μL) was injected in a splitless mode. Nicolet 8700 FT-IR spectrometer was used for the analysis of functional groups present in the raw biomass and bio-oil. Scanning Electron Microscopy (SEM) was carried out on the instrument FEI Quanta 200F for obtaining surface morphology images of the catalysts. An X-ray source fitted with an ETD (Everhart Thornley Detector) was used for SEM analysis. XRD analysis of the catalyst was done on a Bruker D8 advance X-ray diffractometer fitted with a Lynx eye high-speed strip detector and Cu Kα radiation source with a 0.04 step size (step time = 4 s). Brunauer- Emmett-Teller (BET) method was applied to calculate the total surface area, and the Barrett-Joyner-Halenda (BJH) method was used to calculate the average pore size and pore volume on BELSORP max instrument at 77 K. The basic sites were identified using temperature-programmed desorption of carbon dioxide (CO_2-TPD) of the catalyst (BELCAT-B temperature programming unit BELCAT, Osaka, Japan) coupled with thermal conductivity detector (TCD). The proximate analysis, *i.e.*, ash, volatile and fixed carbon content, was carried out by placing the sample in a muffle furnace, analogous to the ASTM D3175 method. Dry biomass feed was used for ultimate and proximate analyses.

2.2. Experimental procedure

The HTL experiments on ST were performed in a high-pressure (100 mL, 4560 micro reactor, Parr Instrument Company, USA) autoclave reactor. In every experiment, 6 g biomass feed was taken in the reactor and heated up to the desired temperature (260, 280 and 300 °C) for a 15 min reaction holding time. Nitrogen (N_2) was used as a purging gas to evacuate the inside air of the autoclave reactor. The autogenous pressure was generated during the reaction and the pressure range was 45 to 120 bar. The liquefaction products consisted of gases, aqueous phase, organic phase (bio-oil), and the solid residue. The gases were vented out after the reaction system cooled. The organic phase was then separated from the aqueous phase by using an organic solvent (diethyl ether) where water was the solvent used during HTL, whereas for alcoholic solvents (ethanol and methanol), the respective alcoholic solvent was used. Thereafter the organic solvent was removed using a rotary evaporator at 50 °C and the organic fraction (bio-oil) kept in an oven at 80 °C for removing any remaining solvent. The solid residue was dried at 100 °C for 12 h. The reactions were carried out in duplicate, and the average values have been reported. The equations for the calculation of product yields are given below:

$$\text{Bio}-\text{oil yield, wt\%} = \frac{\text{Dry weight of bio}-\text{oil}}{\text{Weight of feed}} \times 100$$

$$\text{Bio}-\text{char yield, wt\%} = \frac{\text{Dry weight of bio}-\text{char}}{\text{Weight of feed}} \times 100$$

$$\text{Gas yield, wt\%} = 100 - (\text{Bio}-\text{oil yield, wt\%} + \text{Bio}-\text{char yield, wt\%})$$

Table 1
Proximate and ultimate analyses of *Sargassum tenerrimum* algae (%, dry basis).*

	Ultimate analysis		Proximate analysis
C	32.1	Moisture	5.7
H	4.7	Ash content	26.5
O	60.72	Volatile matter	61.5
N	0.93	Fixed carbon	6.3
S	1.55		

* From Biswas et al. (2018).

Conversion, % = 100 − (Bio − char yield, wt%)

2.3. Catalyst preparation

Catalysts CaO/CeO_2, CaO/Al_2O_3, and CaO/ZrO_2 were prepared by an incipient wetness impregnation process. Initially, the supported oxides CeO_2, Al_2O_3, and ZrO_2 were calcined in air at 550 °C for 3 h. The CeO_2 was dissolved in water (20 mL) for 30 min at room temperature under continuous stirring, and then CaO (10 wt%) was added slowly into it (Mondal et al., 2007; Liu et al., 2019). The solution was stirred at 40 °C for 2 h, following which it was oven-dried for 12 h at 110 °C. The same procedure was followed for preparation of the other two catalysts. All the catalysts were calcined in the presence of air at 550 °C for 3 h, with a heating rate of 5 °C/min. The prepared catalysts have been characterized using BET, SEM, TEM, XRD, and CO_2-TPD techniques.

3. Results and discussion

3.1. Feed characterizations

Table 1 depicts the proximate and ultimate analyses as well as higher heating value (HHV) of ST macroalgae. The ST biomass composition showed the presence of volatile matter (61.5%), fixed carbon (6.3%), and highest ash content (26.5%). Elemental analysis indicated that 32.0% carbon, 4.7% hydrogen, 0.93% nitrogen, 1.55% sulfur, and a higher amount of 60.7% oxygen were present in the ST biomass. The stretching of functional groups such as O—H, C—H, C═C, C═O, and C—O was most abundant in ST biomass. The band at around 1320–1480 cm^{-1} is associated with crystalline cellulose content. The stretching vibration at 3200–3500 cm^{-1} of N—H confirmed that ST biomass contained protein components. The band at ~1262 cm^{-1} is assigned to C—H stretching which may be attributed to double-bonded C—H stretching or aromatic C—H stretching present in the biomass. The C—O stretching vibrations that peak at around 1033–1067 cm^{-1} confirmed that the ST biomass holds a massive carbohydrate content, detailed characterization of which has been discussed earlier (Biswas et al., 2018).

3.2. Catalyst characterization

BET surface area, pore diameter, and pore volume of catalysts (CaO, CaO/CeO_2, CaO/Al_2O_3, and CaO/ZrO_2) are given in Table 2. All catalysts showed the IV type of adsorption isotherm corresponding to their mesoporosity. Supported metal oxide catalysts CeO_2, Al_2O_3, and ZrO_2 have been reported with a surface area of 18.1, 87.0 and 88.0 m^2/g, respectively (Thitsartarn and Kawi, 2011; Marinkovic et al., 2017). While the CaO acquired surface area and pore diameter as 12.2 m^2/g and 59.6 nm, respectively, synthesized catalysts suppress surface area: CaO/CeO_2 (16.0 m^2/g), CaO/Al_2O_3 (17 m^2/g) and CaO/ZrO_2 (17.3 m^2/g). The decreased surface area observed has been attributed to CaO agglomeration on the supported oxide (Zhang et al., 2013). Among all the synthesized catalysts, maximum surface area (17.3 m^2/g) and pore-diameter (59.7 nm) were observed for CaO/ZrO_2. This could be due to the formation of new pores upon addition of CaO to ZrO_2. The pore volumes were 0.04, 0.04, 0.02 and 0.06 $cm^3\ g^{-1}$, respectively, for CaO, CaO/CeO_2, CaO/Al_2O_3, and CaO/ZrO_2. The diffraction patterns of various diffraction planes of CaO impregnated on CeO_2, Al_2O_3 and ZrO_2 catalysts were characterized. The catalysts showed the peak of their respective support, along with the diffraction plane of CaO. In case of CaO/CeO_2 catalyst, the XRD pattern found at 2θ of 48, 56, 59, 69, and 77° was ascribed to the peak pattern of CeO_2 (JCPDS # 34-0394) (Kumar et al., 2012). The CaO/Al_2O_3 catalyst indicated the peak of Al_2O_3 at 43, 67, and 70° 2θ value (JCPDS # 04-0878). However, CaO/ZrO_2 catalysts showed the peak pattern of ZrO_2 support at 2θ of 28, 32, 41, 50, 54, and 56° (JCPDS # 37-1487) (Mondal et al., 2007; Tsoncheva et al., 2009). The presence of CaO impregnated on supported metal oxide was confirmed by the peak pattern of 2θ at 24, 34, 47, 53, and 63°.

Table 2
BET and CO_2-TPD characterizations of the catalysts.

Catalyst	Surface area (m^2/g)	Pore diameter (nm)	Pore volume (cm^3/g)	Basicity (μmol/g)
CaO	12.2	59.6	0.04	599
CaO/CeO_2	16.0	44.0	0.04	58
CaO/Al_2O_3	17.0	44.1	0.02	21
CaO/ZrO_2	17.3	59.7	0.06	183

Catalyst morphology was analyzed by SEM and TEM (Transmission Electron Microscopy). The SEM image of CaO exhibited flake-like morphology, while all the synthesized catalysts showed a different type of structural morphology. In case of CaO/CeO_2, spherical shaped particles were accumulated, forming a bunch of sheet-like structures (Yen et al., 2016). The CaO/Al_2O_3 catalyst showed a distribution of flakes on the sheet-like surface which may be due to the presence of Al_2O_3 while the CaO/ZrO_2 catalyst showed agglomerated morphology of irregular shaped particles (Pradhan et al., 2016). The bunch of irregular shaped particles looked like a portion of the sheet. It was well in agreement with the high-resolution TEM image. The SAED (Selected Area Electron Diffraction) of CaO/ZrO_2 catalyst confirmed that it possessed high crystalline character compared to the other catalyst. The distribution of CaO on the surface of ZrO_2 was confirmed by the elemental mapping analysis. The CO_2-TPD (Temperature Programmed Desorption) of all catalysts was analyzed to understand their basic character and the catalyst acidic-base nature was observed to significantly influence the liquefaction. The total desorbed CO_2 data with respect to each catalyst is given in Table 2. The TPD experimental results of CaO showed the highest desorption of CO_2, 208 μmol/g of CO_2 being desorbed between 300 and 400 °C temperature and 391 μmol/g CO_2 desorption above 500 °C, indicating the strong basic site of CaO. This basic character decreased in CaO impregnated on metal oxide catalyst. Of all the synthesized catalysts, higher basicity (183 μmol/g) was found for CaO/ZrO_2 catalyst by the desorption of 114 μmol/g of CO_2 from 300 to 400 °C, and 69 μmol/g above 500 °C. Other catalysts such as CaO/CeO_2 and CaO/Al_2O_3 showed lower basic character (57 μmol/g and 21 μmol/g, respectively).

3.3. Product yield

3.3.1. Effects of synthesized catalysts and metal oxide supports

Fig. 1a shows the product yield distribution obtained from the HTL of ST in presence of catalysts (10 wt%) at 280 °C with ethanol as a solvent for a reaction holding time of 15 min. It can be seen that conversion, as well as bio-oil content, were affected by catalyst addition. Only the CaO/ZrO_2 catalyst improved both conversion (61.8 wt%) and bio-oil yield (25.2 wt%). Although other catalysts such as CaO/Al_2O_3, CaO/CeO_2, and CaO increased the liquefaction conversion, the bio-oil yield was adversely affected. The probable reason could be that CaO/ZrO_2 with higher surface area (17.3 m^2/g) and moderate basicity (183 μmol/g) provoked the decomposition of macroalgae. All catalysts

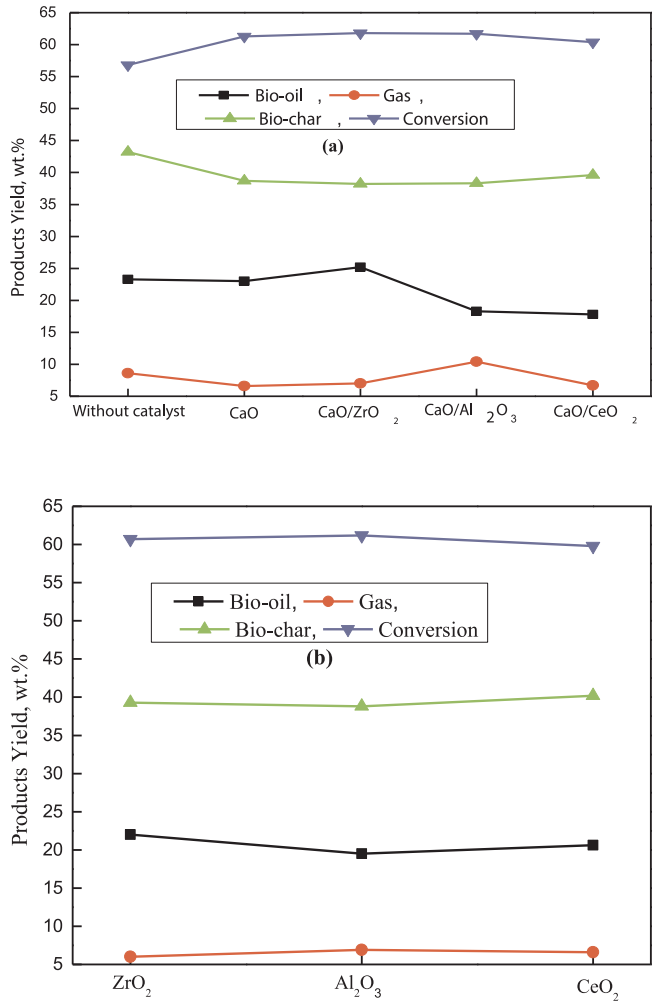

Fig. 1. Product distribution of (a) non-catalytic and synthesized catalytic HTL reaction and (b) supported metal oxide catalyst HTL reaction.

showed lower bio-char yield compared to the non-catalytic experiment, implying that they effectively decomposed the macroalgal composition (carbohydrates, lipids and proteins). The bio-char yield was found minimum (38.2 wt%) in presence of CaO/ZrO_2 catalyst. It may be due to the acceleration of the secondary reaction by CaO/ZrO_2 and increased bio-oil yield and conversion (Liu et al., 2019). However in case of the non-catalytic process, rearrangement and condensation reaction occurred, which decreased the bio-oil yield (Shakya et al., 2015). The maximum gas yield (10.4 wt%) observed with CaO/Al_2O_3 catalyst was attributed to the lower basicity or higher acidic character (21 μmol/g) of the CaO/Al_2O_3 catalyst, which provoked the secondary reaction between the volatile molecules and increased non-condensable gas (Yan et al., 2019).

The effect of support metal oxide catalyst on the HTL of ST macroalgae was examined. Maximum bio-oil yield (22.0 wt%) was obtained in presence of the ZrO_2 catalyst, the same trend also being observed with CaO/ZrO_2 catalyst, with 19.5 and 20.6 wt% bio-oil being obtained using Al_2O_3 and CeO_2 catalysts (Fig. 1b). Maximum gas yield of 6.9 wt % with lower bio-char yield (38.8 wt%) was obtained with Al_2O_3 metal oxide support catalyst. Hence, the overall conversion of ST macroalgae in the presence of metal oxide support was found to be 60.7 wt% for ZrO_2, 61.2 wt% for Al_2O_3, and 59.8 wt% for CeO_2. The decomposition of macroalgal components such as carbohydrates and proteins influenced the bio-oil yield. Since the conversion of carbohydrates and protein require higher activation energy, the introduction of CaO/ZrO_2 catalyst could reduce the activation energy and effect better conversion

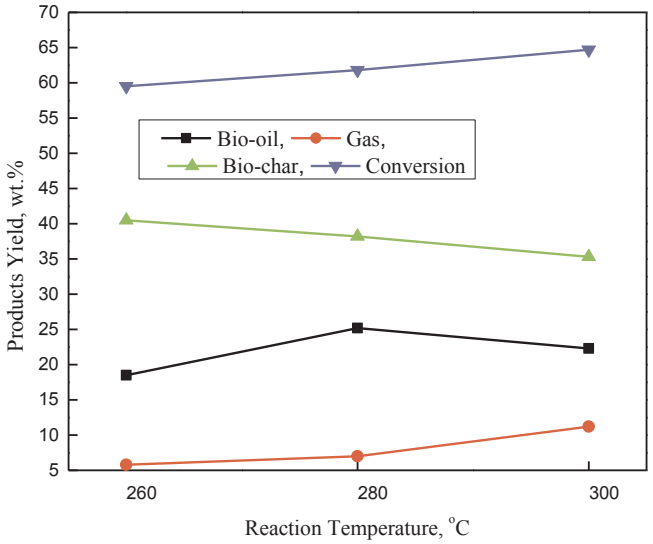

Fig. 2. Effect of reaction temperatures (260, 280 and 300 °C) on product yields.

into bio-oil (Wang et al., 2018). Although the support metal oxide and CaO impregnated on Al_2O_3, ZrO_2, and CeO_2 oxide catalyst did not show a remarkable change in bio-oil yield or conversion, significant changes in bio-oil composition were observed, as discussed in Section 3.4 below.

3.3.2. *Effect of reaction temperature*

Three different temperatures 260, 280, and 300 °C, were tested for the production of bio-oil through HTL. The reaction was carried out with CaO/ZrO_2 (10 wt%) under ethanol solvent for a 15 min reaction time. Reaction temperature has been reported to significantly influence product yield and bio-oil composition (Wang et al., 2018). Our results too clearly demonstrated increased bio-oil yield from 18.5 to 25.2 wt% as the temperature was raised from 260 to 280 °C, while the yield of bio-char product decreased from 40.5 to 38.2 wt% (Fig. 2). This might be due to the endothermic nature of the depolymerization reaction, which would, therefore, be favored at a higher temperature (Yuan et al., 2019; Xu et al., 2018). However, when the temperature was further increased to 300 °C, the bio-oil yield decreased to 22.3 wt%, accompanied by increased bio-char and gaseous product yield. This might be due to enhanced condensation reactions at a higher temperature. When the HTL reaction was carried out at the lower temperature of 260 °C, the bio-oil yield was lowest while bio-char yield was highest (Fig. 2). Similar observations were made by other research groups (Yan et al., 2019; Wang et al., 2018). The decreased bio-oil yield at higher temperatures might be due to the higher cracking of its compounds into small molecules (non-condensable gas), as indicated by Wang et al. (2018). A reaction temperature of 280 °C was thus optimum for HTL of ST macroalgae over CaO/ZrO_2 catalyst.

3.3.3. *Effect of amount of CaO/ZrO_2 catalyst*

The distribution of HTL products with varying quantities of CaO/ZrO_2 catalyst was investigated. Maximum bio-oil yield of 25.2 wt% was obtained with 10 wt% CaO/ZrO_2, while with an increasing amount of catalyst from 10 to 25 wt%, the bio-oil yield decreased to 18.3 wt% (Fig. 3). However, the gas yield was enhanced from 5.2 to 9.1 wt%, the opposite trend being observed for bio-char yield, which decreased from 43.3 to 34.2 wt% with an increase in the amount of catalyst from 5 to 25 wt%. Maximum conversion was found with 25 wt% of catalyst, compared to the non-catalytic experiment. A lower amount of catalyst at 5 wt% was not capable of eliciting higher bio-oil yield, probably due to insufficient active sites to break the macroalgal macromolecule (Xu et al., 2018). On the other hand, a high amount of catalyst (25 wt%) with a greater number of active sites enhanced the cracking of bio-oil,

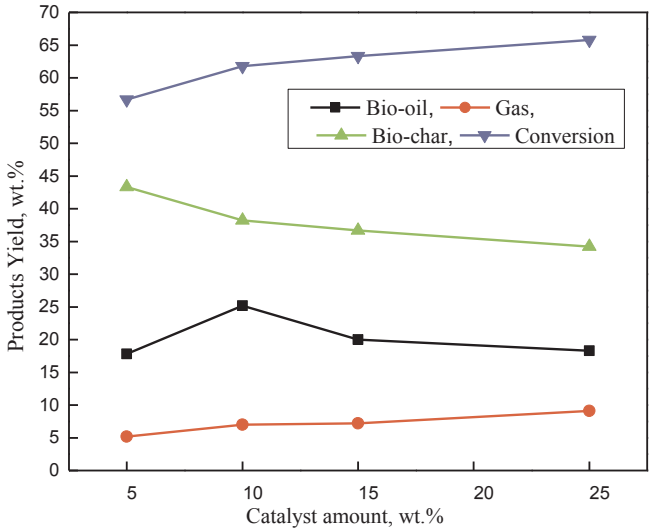

Fig. 3. Effect of CaO/ZrO_2 catalyst amount on product yields.

resulting in lower yield and higher gas production. During the liquefaction reaction, the macroalgal components decomposed into amino acids, glucose, fatty acids, etc., which further participated in various reactions such as decarboxylation, dehydration, hydroxylation, condensation, polymerization, and cyclization, to form bio-oil, gas, and bio-char (Yuan et al., 2019).

3.3.4. Effect of solvent mixtures

The HTL reaction was carried out in water-ethanol co-solvent (50:50 v/v), with and without a catalyst. The reaction was performed for 15 min at 280 °C with CaO/ZrO_2 (10 wt%) catalyst. From Fig. 4, it is clear that for the uncatalyzed reaction with water-ethanol co-solvent, the bio-oil yield significantly increased to 32.0 wt% compared to when water (3.3 wt%) or ethanol (23.3 wt%) was used as a liquefaction solvent. Interesting results were obtained upon the addition of CaO/ZrO_2 catalyst with the water solvent, the bio-oil yield decreasing from 3.3 to 2.5 wt%. In water-ethanol co-solvent, the bio-oil yield improved only by 1% in comparison with the uncatalyzed HTL reaction, while solid bio-char yield reduced from 30.0 to 29.5 wt%. Compared to the use of individual solvents, the co-solvent system accelerated the hydrolysis reaction, and the bio-oil yield showed a synergistic effect on ST macroalgae depolymerization. A similar result was recorded by Hafez and Hassan (2015), who found that HTL of *Magnolia macrophylla* algae

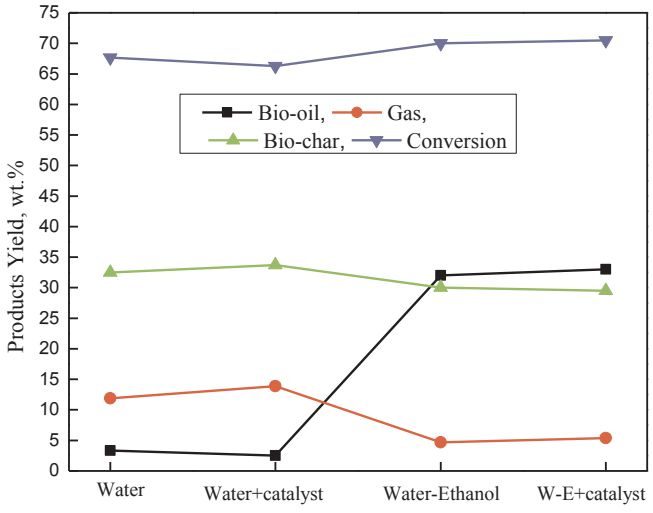

Fig. 4. Effects of solvent mixture on product yields.

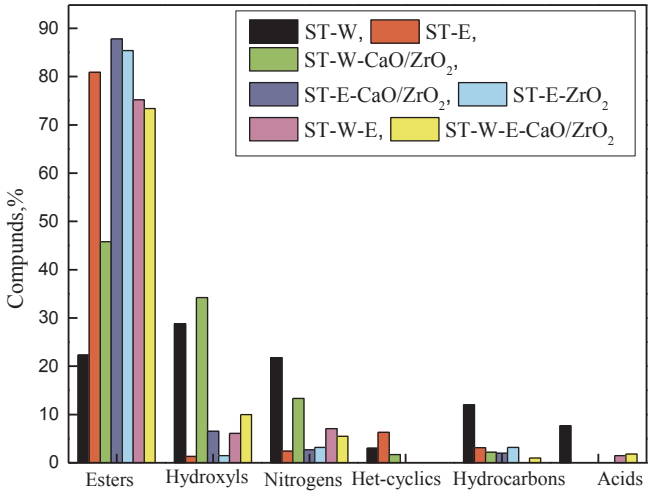

Fig. 5. Major chemical compositions of bio-oil obtained from best HTL conditions.

with water-ethanol (1:1) co-solvent system produced more bio-oil.

3.4. Functional group analysis of the bio-oils

Gas chromatography-Mass spectrometry (GC–MS) spectra of the bio-oil products were analyzed to quantify the peak areas of the compound and classify them into esters, hydroxyls, nitrogens, heterocyclics, hydrocarbons, and acids (Raikova et al., 2019a). Fig. 5 display the area percentage of different types of functional compounds. The use of different catalysts and solvent systems had an important effect on the area percentage of the various types of compounds. During the HTL process, carbohydrate, amino acids, and fatty acids are subjected to a series of reactions such as hydrolysis, decarbonylation, decarboxylation, dehydration, and cleavage of C-O and C–C bonds (Wang et al., 2018). Bio-oil derived from the non-catalytic reaction with water solvent was majorly composed of ester (22.3%), hydroxyl (28.8%), and hydrocarbon (12.0%), with higher nitrogen (21.8%) and acidic (7.7%) compounds. The liquefaction experiment with a catalyst in water solvent minimized acidic and nitrogen compounds to 0% and 13.3%, respectively. With ethanol as solvent, the main components in the bio-oil were esters (80.9%) and heterocyclic compounds (6.3%) with very small amounts of other compounds. Besides, the selectivity of the ester compounds increased from 80.9% to 87.8% upon the addition of CaO/ZrO_2 as catalyst. It is also worth noting that the heterocyclic compound content decreased from 6.3% to 0%.

When water-ethanol co-solvent was used, the main components in the bio-oil were ester (75.2%), hydroxyl (6.1%), and nitrogen (7.1%). Inclusion of CaO/ZrO_2 as catalyst in the co-solvent system did not significantly change the bio-oil components. The ester and nitrogen compounds decreased to 73.4% and 5.5%, respectively, while heterocyclic compound content increased to 10.0%. These results indicate that the liquefaction of ST macroalgae with a solid base catalyst in an alcoholic solvent encouraged the esterification reaction. Higher percentage of ethyl ester hexadecanoic acid was observed in the liquefaction reaction with ethanol solvent, indicating that the solvent participated in the reaction. Higher area percentage of ethyl ester hexadecanoic acid (59.8%) was observed in the case of catalytic (CaO/ZrO_2) liquefaction reaction compared to the other reaction conditions. In addition, the negligible presence of acidic compounds in the bio-oil might show higher stability (Yuan et al., 2019). Liquefaction reaction with the catalysts increased the denitrification reaction and thus decreased the nitrogenous elements in the bio-oil, resulting in enhanced bio-oil quality (Yan et al., 2019).

The presence of various types of protons in the bio-oil obtained after

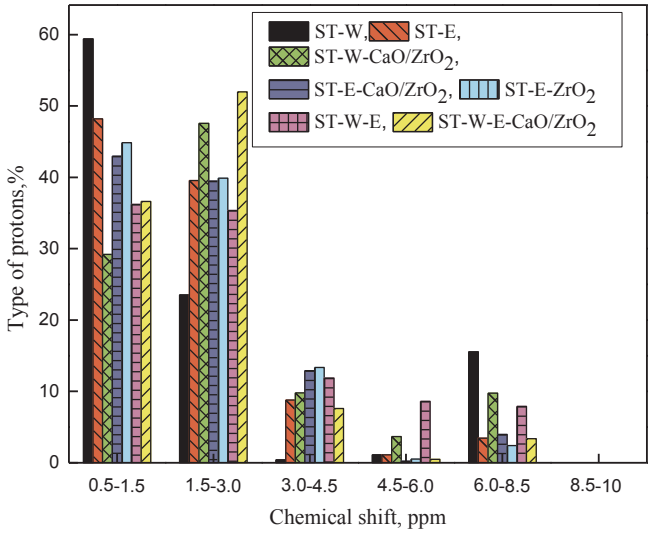

Fig. 6. ^{1}H NMR analysis of the bio-oil obtained from best HTL conditions.

HTL was established through NMR spectra. Fig. 6 showcases the distribution of the integrated peak area corresponding to different types of protons into numerous classes, which is also established (Aysu and Sanna, 2015). The protons in small chain aliphatic compounds were identified from the highly upfield region, *i.e.*, 0.5–1.5 ppm. The bio-oil obtained after the liquefaction in water as a solvent showed the highest area percentage in this region. The protons attached to sp^3 hybridized carbon, which is further directly attached to sp^2 carbon of aromatics or olefins, were identified from the region of 1.5–3.0 ppm. The bio-oil obtained after liquefaction using a metal-based catalyst, CaO/ZrO_2 in water-ethanol co-solvent showed the highest area percentage of 52%, for these types of protons. All the bio-oils had a very high occurrence of protons from 0.5 to 1.5 and 1.5–3.0 ppm regions. The region from 3.0 to 4.5 ppm corresponds to methylene group proton and methoxy carbon proton (Biswas et al., 2017). The highest number of these types of protons was found in bio-oil obtained through liquefaction in the presence of ethanol solvent and ZrO_2 catalyst. The region from 6.0 to 8.5 ppm showcases the aromatic proton found in bio-oil. There was no proton found in the very highly deshielded region of 8.0–10.0 ppm, which indicated the absence of aldehydic proton. Analysis of NMR data of the bio-oils points to a higher percentage of aliphatic compounds in all the bio-oils investigated.

The FT-IR spectra of bio-oils obtained after HTL of *Sargassum tenerrimum* (ST) showed different functionality present in the bio-oil. The hydroxyl and N—H groups in the bio-oil were confirmed by the presence of a band at 3316 cm^{-1}. The band at 2924 and 2845 cm^{-1} established C—H asymmetric and symmetric vibrations. The absorption band in the 1688–1735 cm^{-1} range corresponds to the C=O functionality of amide, ester/ketone, and acids (Yan et al., 2019). The aromatic C=C symmetric and asymmetric vibrations were confirmed from the band in the range 1598-1468 cm^{-1}. The absorption band between 1269 and 1018 corresponds to C-O ether linkages, pointing to the presence of ester functional compounds being present in the bio-oil. (Yan et al., 2019). Higher intensity of ester C-O stretching was observed in case of liquefaction with ethanol solvent compared to that with water solvent (Biswas et al., 2017). The nitrogen functional group stretching was ascribed at 1200–1270 cm^{-1}. N—H bond stretching with higher intensity was observed in case of bio-oil resulting from liquefaction with water solvent, which was also confirmed from the GC–MS analysis of the bio-oil. In addition, C—H vibrations of the aromatic functional groups were confirmed by the bands at 822 and 854 cm^{-1}. The FT-IR analysis thus indicates the presence of nitrogen-containing, esters, ketones compounds with an aromatic functional group in the bio-oils.

Table 3
Elemental analysis of bio-oil obtained from non-catalytic and catalytic HTL reaction.

Reaction conditions*	C (%)	H (%)	N (%)	S (%)	O (%)	HHV (MJ/kg)
ST-W	53.7	6.3	5.6	0.4	33.3	22.4
ST-E	55.6	7.5	4.2	0.3	32.2	25.6
ST-W-CaO/ZrO_2	56.2	7.2	5.1	0.2	32.1	22.8
ST-E-CaO/ZrO_2	58.7	8.1	3.1	0.3	26.6	27.9
ST-E-ZrO_2	58.1	8.2	3.0	0.3	27.1	26.4
ST-W-E	56.2	7.4	4.1	0.4	27.1	24.5
ST-W-E-CaO/ZrO_2	58.9	6.7	3.6	0.2	27.0	24.2

* ST = *Sargassum tenerrimum*, W = water, E = ethanol, W-E = water-ethanol co-solvent.

3.5. Elemental analysis of bio-oil

The elemental analysis of bio-oil was carried out to gauge the energy value of the bio-oils (Table 3). Catalytic liquefaction improved the bio-oil quality to a higher extent. Maximum carbon percentage of 58.9% was obtained with CaO/ZrO_2 catalyst under ethanol-water mixture solvent. Lower carbon (53.7% and 55.6%) and higher oxygen (33.3% and 32.2%) content was observed in case of non-catalytic experiments with water and ethanol solvent. All catalytic reactions improved the bio-oil quality, with decreased oxygen and nitrogen content (Yan et al., 2019). The effect of catalyst on liquefaction with ethanol solvent showed higher hydrogen content in the bio-oil, indicating that more saturated aliphatic compounds were produced during the liquefaction. Lower oxygen content (26.6%) bio-oil was found with catalytic liquefaction in ethanol solvent. Higher HHV (27.9 MJ/kg) was found with CaO/ZrO_2 catalyst due to the higher carbon content with lower oxygen in bio-oil obtained with ethanol as solvent. As is known, higher the carbon content, higher the HHV value (Raikova et al., 2019a). The ethanol solvent with catalyst enhanced the hydrogen production, ethanol acting as a hydrogen donor solvent (Wu et al., 2019). This hydrogen is involved in the chemical reaction promoting dehydrogenation of bio-oil compounds, which reduced the oxygen content in the bio-oil. It can be seen that the nitrogen content in the bio-oil decreased while using the catalyst, confirming that the catalyst had an effect on denitrogenation, which also concurred with the results of GC–MS analysis.

3.6. Possible formation pathway of ester compounds

The possible reaction pathways during the non-catalytic and catalytic HTL of *Sargassum tenerrimum* macroalgae have been discussed on the basis of previous literature from other research groups (Kandasamy et al., 2020; Yan et al., 2019; Yuan et al., 2019; Wang et al., 2018). During the liquefaction reaction, components such as carbohydrates, lipids, and proteins of the macroalgae are at first decomposed into monomers (monosaccharides, fatty acids, and amino acids). The monomers are then involved in a series of reactions such as hydrolysis, decarboxylation, hydrogenation, amination, cyclization, Maillard reaction, etc. In the bio-oil, the ester compounds are formed by the transesterification reaction of long-chain lipids in ethanol. Also, some fatty acid and ethanol components participated in the esterification reaction and formed ester compounds. It is well known that macroalgae possess a lower amount of lipid compared to microalgae, but as observed by Zhou et al. (2012), carbohydrates are converted into acid compounds, which then react with alcohol to form ester compounds. In our study the use of the catalyst CaO/ZrO_2 promoted the transesterification or esterification reaction. In addition, some nitrogen-containing ester compounds observed in the bio-oil might be due to compounds other than lipid, *viz.*, carbohydrates and proteins that contributed to their formation (Zhou et al., 2012; Yan et al., 2019).

4. Conclusions

In this study, choice of catalyst, catalyst amount, reaction temperature and solvent system have been investigated while using solid based catalysts for HTL of *ST*. The HTL reaction using CaO/ZrO_2 catalyst in a water-ethanol co-solvent system produced maximum bio-oil yield of 33.0 wt%. Higher percentages of ester functional compounds were obtained with CaO/ZrO_2 catalyst in ethanol solvent. Catalytic liquefaction reaction reduced the nitrogen and oxygen content in the bio-oil, thereby enhancing its quality. Maximum HHV (27.9 MJ/kg) was obtained with CaO/ZrO_2 catalyzed liquefaction bio-oil. Addition of the catalyst in the HTL reaction enhanced the transesterification as well as esterification reactions.

CRediT authorship contribution statement

Bijoy Biswas: Conceptualization, Investigation, Methodology, Writing - original draft. **Avnish Kumar:** Data curation, Methodology. **Alisha C. Fernandes:** Procurement of algal biomass, Investigation, Formal analysis. **Komal Saini:** Formal analysis, Resources. **Shweta Negi:** Investigation. **Usha D. Muraleedharan:** Writing - review & editing. **Thallada Bhaskar:** Supervision, Writing - review & editing.

Declaration of Competing Interest

The authors declare that they have no known competing financial interests or personal relationships that could have appeared to influence the work reported in this paper.

Acknowledgements

The authors thank the Director, CSIR-Indian Institute of Petroleum, Dehradun for his constant encouragement and support and AcSIR for granting permission to conduct this research work at CSIR-IIP. Bijoy Biswas thanks CSIR, New Delhi, India, for his Senior Research Fellowship (SRF). Authors also thank the Analytical Science Division (ASD) of CSIR-IIP.

Appendix A. Supplementary data

Supplementary data to this article can be found online at https://doi.org/10.1016/j.biortech.2020.123232.

References

Aysu, T., Sanna, A., 2015. Nannochloropsis algae pyrolysis with ceria-based catalysts for production of high-quality bio-oils. Bioresour. Technol. 194, 108–116.
Biswas, B., Fernandes, A.C., Kumar, J., Muraleedharan, U.D., Bhaskar, T., 2018. Valorization of Sargassum tenerrimum: value addition using hydrothermal liquefaction. Fuel 222, 394–401.
Biswas, B., Kumar, A.A., Bisht, Y., Singh, R., Kumar, J., Bhaskar, T., 2017. Effects of temperature and solvents on hydrothermal liquefaction of Sargassum tenerrimum algae. Bioresour. Technol. 242, 344–350.
Egesa, D., Chuck, C.J., Plucinski, P., 2018. Multifunctional role of magnetic nanoparticles in efficient microalgae separation and catalytic hydrothermal liquefaction. ACS Sustainable Chem. Eng. 6, 991–999.
Guo, Y., Yeh, T., Song, W., Xu, D., Wang, S., 2015. A review of bio-oil production from hydrothermal liquefaction of algae. Renew. Sustain. Energy Rev. 48, 776–790.
Hafez, I., Hassan, E.B., 2015. Rapid liquefaction of giant miscanthus feedstock in ethanol-water system for production of biofuels. Energy Conver Manage. 91, 219–224.
Kandasamy, S., Zhang, B., He, Z., Chen, H., Feng, H., Wang, Q., 2020. Effect of low-temperature catalytic hydrothermal liquefaction of Spirulina platensis. Energy 190, 116236.
Kumar, P.A., Tanwar, M.D., Russo, N., Pirone, R., Fino, D., 2012. Synthesis and catalytic properties of CeO_2 and Co/CeO_2 nanofibres for diesel soot combustion. Catal. Today 184, 279–287.
Liu, F., Xiao, Y., Sun, X., Qin, G., Song, X., Liu, Y., 2019. Synergistic catalysis over hollow CeO_2-CaO-ZrO_2 nanostructure for polycarbonate methanolysis with methanol. Chem. Eng. J. 369, 205–214.
Ma, C., Geng, J., Zhang, D., Ning, X., 2019. Hydrothermal liquefaction of macroalgae: Influence of zeolites based catalyst on products. J. Energy Inst. https://doi.org/10.1016/j.joei.2019.06.007.
Marinkovic, D.M., Avramovic, J.M., Stankovic, M.V., Stamenkovic, O.S., Jovanovic, D.M., Veljkovic, V.B., 2017. Synthesis and characterization of spherically-shaped CaO/c-Al_2O_3 catalyst and its application in biodiesel production. Energy Convers. Manage. 144, 399–413.
Mondal, K.C., Choudhary, V.R., Joshi, U.A., 2007. CO_2 reforming of methane to syngas over highly active and stable supported CoO_x (accompanied with MgO, ZrO_2 or CeO_2) catalysts. Appl. Catal. A 316, 47–52.
Pradhan, S., Sahu, V., Mishra, B.G., 2016. CaO-ZrO2 nanocomposite oxide prepared by urea hydrolysis method as heterogeneous base catalyst for synthesis of chromene analogues. J. Mol. Catal. A: Chem. 425, 297–309.
Raikova, S., Allen, M.J., Chuck, C.J., 2019a. Hydrothermal liquefaction of macroalgae for the production of renewable biofuels. Biofuels Bioprod. Bioref. 13, 1483–1504.
Raikova, S., Knowles, T.D.J., Allen, M.J., Chuck, C.J., 2019b. Co-liquefaction of macroalgae with common marine plastic pollutants. ACS Sustainable Chem. Eng. 7, 6769–6781.
Shakya, R., Whelen, J., Adhikari, S., Mahadevan, R., Neupane, S., 2015. Effect of temperature and Na_2CO_3 catalyst on hydrothermal liquefaction of algae. Algal Res. 12, 80–90.
Thitsartarn, W., Kawi, S., 2011. An active and stable CaO–CeO_2 catalyst for transesterification of oil to biodiesel. Green Chem. 13, 3423.
Tsoncheva, T., Ivanova, L., Minchev, C., Froba, M., 2009. Cobalt-modified mesoporous MgO, ZrO_2, and CeO_2 oxides as catalysts for methanol decomposition. J. Colloid Interface Sci. 333, 277–284.
Wang, W., Xu, Y., Wang, X., Zhang, B., Tian, W., Zhang, J., 2018. Hydrothermal liquefaction of microalgae over transition metal supported TiO_2 catalyst. Bioresour. Technol. 250, 474–480.
Wu, X.F., Zhang, J.J., Huang, Y.H., Li, M.F., Bain, J., Peng, F., 2019. Comparative investigation on bio-oil production from eucalyptus via liquefaction in subcritical water and supercritical ethanol. Ind. Crops Prod. 140, 111695.
Xu, D., Lin, G., Guo, S., Wang, S., Guo, Y., Jing, Z., 2018. Catalytic hydrothermal liquefaction of algae and upgrading of biocrude: A critical review. Renew. Sustain. Energy Rev. 97, 103–118.
Xu, J., Wang, Z., Cheng, J.J., 2011. Bermuda grass as feedstock for biofuel production: a review. Bioresour. Technol. 102, 7613–7620.
Xue, Y., Chen, H., Zhao, W., Yang, C., Ma, P., Han, S., 2016. A review on the operating conditions of producing bio-oil from hydrothermal liquefaction of biomass. Int. J. Energy Res. 40, 865–877.
Yan, L., Wang, Y., Li, J., Zhang, Y., Ma, L., Fu, F., et al., 2019. Hydrothermal liquefaction of Ulva prolifera macroalgae and the influence of base catalysts on products. Bioresour. Technol. 292, 121286.
Yang, W., Li, X., Liu, S., Feng, L., 2014. Direct hydrothermal liquefaction of undriedmacroalgae Enteromorpha prolifera using acid catalysts. Energy Convers Manag. 87, 938–945.
Yen, B., Zhang, Y., Chen, G., Shan, R., Ma, W., Liu, C., 2016. The utilization of hydroxyapatite-supported CaO-CeO2 catalyst for biodiesel production. Energy Convers. Manage. 130, 156–164.
Yuan, C., Wang, S., Qian, L., Barati, B., Gong, X., Abomohra, A.E.F., et al., 2019. Effect of cosolvent and addition of catalyst (HZSM-5) on hydrothermal liquefaction of macroalgae. Int J Energy Res. 43, 8841–8851.
Zhang, M., Peng, Y., Sun, Y., Li, P., Yu, J., 2013. Preparation of CaO–Al_2O_3 sorbent and CO_2 capture performance at hightemperature. Fuel 111, 636–642.
Zhang, Z., Li, K., Ma, S.W., Cui, M.S., Lu, Q., Yang, Y.P., 2019. Fast pyrolysis of biomass catalyzed by magnetic solid base catalyst in a hydrogen atmosphere for selective production of phenol. Ind. Crops Prod. 137, 495–500.
Zhou, D., Zhang, S., Fu, H., Chen, J., 2012. Liquefaction of macroalgae enteromorpha prolifera in sub-/supercritical alcohols: direct production of ester compounds. Energy Fuels 26, 2342–2351.